

**A combined structural and sedimentological study
of the Inner Carpathians at the northern rim of the
Transylvanian basin (N. Romania)**

Inauguraldissertation

zur

Erlangung der Würde eines Doktors der Philosophie

vorgelegt der

Philosophisch-Naturwissenschaftlichen Fakultät

der Universität Basel

von

Matthias Tischler

aus

Giessen (Deutschland)

Basel, 2005

Genehmigt von der Philosophisch-Naturwissenschaftlichen Fakultät

auf Antrag von:

Prof. L. Csontos

Institute of Geology

Eötvös Loránd University

Budapest

PD.Dr. B. Fügenschuh

Institut für Geologie-Paläontologie

Universität Basel

Prof. A. Wetzel

Institut für Geologie-Paläontologie

Universität Basel

Prof. S.M. Schmid

Institut für Geologie-Paläontologie

Universität Basel



(Fakultätsverantwortlicher)

Basel, den 05.07.2005

Prof. H.J. Wirz

(Dekan der Philosophisch-

Naturwissenschaftlichen Fakultät)

Abstract

By integrating detailed structural and sedimentological field-work with paleomagnetic data, this thesis provides constraints for the reconstruction of the Late Tertiary tectonic history of the Inner Carpathians in Northern Romania. Central for the understanding of the formation of the Carpathians is the emplacement history of crustal blocks into the so-called 'Carpathian embayment'. This large-scale bight in the European continental margin is situated between the Bohemian and Moesian promontories.

Roll - back of the (partly?) oceanic crust formerly occupying the Carpathian embayment, combined with lateral escape due to indentation in the Eastern Alps are thought to be the driving forces for this emplacement. The irregular shape of the European continental margin ultimately led to the formation of a highly bent orogen, the Carpathians. The study area is a key area for the understanding of the tectonic processes during this emplacement, since it is situated at a triple point where three of the major continental blocks (ALCAPA, Tisza and Dacia) meet.

During the time interval covered by this study, the Tisza and Dacia blocks are considered firmly attached to each other, representing one single block. A large fault zone between the ALCAPA block and the Tisza-Dacia block, termed Mid-Hungarian fault zone, accommodated most of the complex deformation caused by their contemporaneous invasion into the Carpathian embayment. During emplacement corner effects at the Bohemian and Moesian promontories resulted in large differential rotations of the invading blocks.

The juxtaposition of the Tisza-Dacia block and the ALCAPA block along the Mid-Hungarian fault zone resulted in the formation of a flexural basin on the northern part of Tisza-Dacia. The filling of this basin started in Oligocene times, developing from flysch units into Burdigalian-age molasse-type deposits. The last moment of thrusting of ALCAPA related units onto Tisza-Dacia is reflected by the Early Burdigalian SE - directed emplacement of unmetamorphic flysch nappes (Pienides) onto the autochthonous cover of Tisza-Dacia. Back-arc type extension leading to the formation of the Pannonian basin is in the study area only weakly documented as SW-NE extension.

Roughly perpendicular 'soft collision' of Tisza-Dacia with the European margin leads to transpressional deformation in the study area after 16 Ma. Due to migration of slab retreat, the convergence direction of Tisza-Dacia becomes more oblique, initiating a deformation stage characterized by transtension (NW – SE extension). The northern rim of Tisza-Dacia is 'fitted' to the European continental margin by E-W trending, sinistral strike slip faults coupled to SW – NE trending normal faults. This process leads to a weak (~20°-30°) counterclockwise rotation as well as accelerated uplift of the northern part of Tisza-Dacia. After 16 Ma deformation in the study area is located within the Tisza-Dacia block, but most likely connected to the Mid-Hungarian fault zone.

Organisation of this thesis

The presented thesis is organised into six chapters, two of which have been submitted to scientific journals as papers. An outline of each of these chapters and the contributions of the various authors to them is provided below.

Chapter 1:

Introduction

Aside from providing an overview of the geological setting, this chapter outlines the scope and aims of this study.

Chapter 2:

Miocene tectonics of the Maramures area (Northern Romania) – implications for the Mid-Hungarian fault zone

Tischler, M., Gröger, H.R., Fügenschuh, B., Schmid, S.M.

published 2006: *International Journal of Earth Sciences*

This study focuses on the Late Tertiary tectonic history of the study area. Based mainly on structural fieldwork and the kinematic analysis of mesoscale structures and incorporating fission track ages, a succession of tectonic phases is elaborated.

In close collaboration with H.R. Gröger, M. Tischler has performed the fieldwork and collection of structural and fault slip data for the kinematic analysis. He wrote a first draft of the manuscript, which was significantly improved by the collaboration with H.R. Gröger. H.R. Gröger additionally provided fission track data, critically improving constraints for the exhumation history. B. Fügenschuh contributed during fieldwork, structural and fission track data analysis and by correction of the manuscript. S.M. Schmid also contributed by providing guidance during field work as well as during structural data analysis and significantly improved the quality of the resulting manuscript.

Chapter 3:

Sedimentological constraints derived from syntectonic deposits regarding the Tertiary emplacement of ALCAPA and Tisza-Dacia (N. Romania)

This chapter is a survey of the sedimentological features of deposits syntectonic to the emplacement of Alcapa and Tisza-Dacia. By combination of traditional sedimentological approaches with subsurface data, the depositional setting for these sediments is constrained, providing implications for the tectonic history of aforementioned crustal units. In collaboration with H.R. Gröger, M. Tischler collected the field data and samples necessary for facies analysis and sedimentary petrography. M. Marin (University of Bucharest / University of Basel) provided the interpretation of subsurface data. Mikropaleontological data have been provided by Prof. Sorin Filipescu, Cluj University.

Chapter 4:**The contact zone between the ALCAPA and Tisza-Dacia mega-tectonic units of Northern Romania in the light of new paleomagnetic data**

Márton, E., Tischler, M., Csontos, L., Fügenschuh, B., Schmid, S.M.

submitted to: *Ecolgae Geologicae Helvetiae*

In this paper new paleomagnetic data from the study area are presented and discussed. The data provide an important reference for the integration of the findings of this thesis into the existing datasets. The paleomagnetic data in this chapter have been processed and analysed by Emő Márton (Paleomagnetic Laboratory of the Eötvös Loránd Geophysical Institute of Hungary). The samples were collected during a joint excursion of Emő Márton, László Csontos, Gabor Imre, H.R. Gröger and M. Tischler in 2004. Emő Márton provided a first version of the text, subsequently edited by S.M. Schmid and M. Tischler. The text has been significantly improved by constructive revisions of László Csontos and Emő Márton.

Chapter 5:**A contribution to the reconstruction of the Late Tertiary tectonic history of Tisza-Dacia – Constraints from a palinspastic reconstruction of the study area**

The data evaluated in chapter 2 - 4 are combined to arrive at a palinspastic reconstruction of the study area. The aim of this reconstruction is to integrate the findings of this thesis into the regional framework. The palinspastic reconstructions have been prepared by M. Tischler, their integration into the regional framework is based on an unpublished compilation of the major tectonic units of the Alps, Carpathians and Dinarides by S.M. Schmid, B. Fügenschuh, L. Matenco, R. Schuster, M. Tischler and K. Ustaszewski as well as Fügenschuh and Schmid (2005).

Chapter 6:**Summary**

A chapter summarising the results of the presented thesis

Appendix:

Detailed lithostratigraphic logs

Acknowledgements

First of all I would like to thank my supervisors, Stefan Schmid, Andreas Wetzel and Bernhard Fügenschuh for initiating a project in a region of Europe I should come to lose my heart to: The Maramures in Northern Romania.

The constant interest and thirst for knowledge of Stefan Schmid was a major driving force and motivation during my studies in Basel. This, together with highly constructive discussions and a huge amount of patience Stefan mustered in revising my garbled manuscripts led to a massive improvement of this thesis. But above all I am glad that I have been able to profit from his experience in the “traditional” work of a geologist. Among many other things, my skills regarding field-work, the reading of maps and profiles were vastly improved here in Basel.

All of the above also holds true for Bernhard Fügenschuh, though I not only have to thank him for his significant scientific input, but also for his open ear regarding all of the scientific and general problems one has during a PhD-thesis. By not only stating, but really living an “open door” policy Fügen has been the central point in our working group. On many occasions only a “cigarette break” with Fügen helped me to absorb the wealth of information generated by the Schmid / Fügenschuh team.

I especially thank Andreas Wetzel for providing and supporting the opportunity to broaden my “structural geologist’s” field of view to include sedimentology – to not only look at the nice folds, but actually at what is folded.

I would like to thank Laszlo Csontos for all the time he invested, since I started this PhD. His always optimistic and constructive way helped to shape and improve this thesis. Additionally I am indebted that he accepted the role as reviewer on a very short notice.

The work in the Maramures led to many contacts, not only in Romania, but also in Hungary. Without these people, this thesis would not have been possible. L. Matenco has been an invaluable source of regional knowledge, scientific input as well as logistical help. I especially want to thank him for helping me to access and understand the data on my study area. I would like to thank M. Marin for our collaboration and the good times we had during our work.

All of my work is building up on the work of M. Săndulescu. His special interest in the Maramures area led to an exceptionally good data and map base of my study area, which he shared with us. M. Săndulescu and D. Badescu are thanked for the introduction into the geology of the Maramures and fruitful discussions. For sharing their data as well as many discussions D. Radu, C. Krezsek, S. Filipescu, L. Fodor and E. Marton are gratefully acknowledged.

Numerous people from the institute in Basel significantly improved this thesis by providing ideas, the possibility for discussions and constructive criticism. Well aware of the danger of forgetting someone, I would like to thank L. Hottinger, (also for dating and introducing me to Foraminifera), D. Bernoulli, P. Ziegler and H. Stüniz.

Special thanks go to Bernhard Schneider, for many nice discussions, and an often very helpful Geographers view of geological problems.

Well, even the most intelligent head would not be able to work if not for the body it is resting on. By this I mean the big number of students, PhD-students and Post-Docs who make Basel a productive, but more importantly a nice place to work in. I would like to thank all of you for support and fun during and after work. While I would like to include a sentence for each of my colleagues, I feel that the acknowledgements should be shorter than my list of references...

However, it has been a special pleasure for me to share the ups and downs of the final sprint for the finishing line with my time-schedule-partner, Katy Waite.

Additionally, even when trying to be brief, I do have to especially thank Kamil Ustaszewski, who opened my eyes to the wonders of brittle deformation and helped in a lot of different ways.

I also enjoyed the extremely good working climate in “Room 21”. I especially thank my box-mates James MacKenzie and Christian Seiler for lively discussions across most geological disciplines as well as – a good time.

This leads to the people who keep everything running and fix the real problems, while we wonder about the age of a piece of mud in Romania: H.R. Ruegg, S. Lauer, W. Tschudin, K. Leu, J. Glanzmann and V. Scheuring are thanked for repeatedly making the impossible possible.

I am very indebted to Mioara and Luci Lungulescu. They provided a secure and cozy base in the Marmures, and helped wherever they could – which was a lot. During the long field summers, I really felt like part of the family. Without their support, my field-work would not have been as successful.

Naturally, I thank my parents for their support, and making my studies possible in the first place.

Last, and most definitely not least the most important support during my PhD-studies: I thank Heike Gröger for her love and support in all parts of my life – be it private or scientific, in Basel or in the field.

Table of contents

Abstract	I
Organisation of this thesis	II
Acknowledgements	IV
Table of contents	VI
Chapter 1: Introduction.....	1
1.1 General geological overview	1
1.2 Outline of the projects incorporating this thesis	2
1.3 Aims and approach of this thesis	3
1.4 Stratigraphic correlation used	3
Chapter 2: Miocene tectonics of the Maramures area (Northern Romania) - implications for the Mid-Hungarian fault zone	5
<i>Tischler, M., Gröger, H.R., Fügenschuh, B., Schmid, S.M.</i>	
<i>International Journal of Earth Sciences (2006)</i>	
2.1 Abstract.....	5
2.2 Introduction	6
2.3 Geological Setting	9
2.4 Methods	10
2.4.1 Derivation of kinematic axes.....	10
2.4.2 Fission track analysis.....	11
2.5 Structural analysis.....	12
2.5.1 Early Burdigalian top-SE thrusting of the Pienides.....	12
2.5.2 Late Burdigalian NE-SW extension	13
2.5.3 Post-Burdigalian structures	14
2.5.4 Stratigraphical timing constraints regarding post-Burdigalian deformation	16
2.6 Constraints from fission track data	17
2.7 Synthesis of data	18
2.7.1 Burdigalian thrusting of the Pienides followed by NE-SW extension	18
2.7.2 Post-Burdigalian faulting along the Bogdan- and Dragos-Voda faults	18
2.7.3 Estimates of horizontal and vertical components of displacement across the Bogdan-Voda and Dragos-Voda faults.....	19
2.8 Discussion of earlier work in the working area and large-scale correlations	20
2.8.1 Comparison with previous data from the working area	20
2.8.2 Burdigalian top-SE thrusting of the Pienides followed by NE-SW extension in the larger scale context	21
2.8.3 Post-Burdigalian activity along the Bogdan- Dragos-Voda fault system in the larger scale context	21
2.9 Conclusions	22
2.10 Acknowledgements	23
2.11 References	24
2.12 Appendix	28

Chapter 3: Sedimentological constraints on the Tertiary emplacement of ALCAPA and Tisza-Dacia (N. Romania)	35
3.1 Abstract.....	35
3.2 Introduction.....	36
3.3 Geological Setting.....	37
3.4 Evaluation of the effect of eustatic sea-level variations.....	41
3.5 Data.....	42
3.5.1 Sub-surface data.....	42
3.5.1.1 Sub-surface data.....	42
3.5.1.2 Interpretation of the sub-surface data.....	42
3.5.2 Facies analysis	45
3.5.2.1 Introduction.....	45
3.5.2.2 Facies associations of the lithostratigraphic logs	49
3.5.2.3 Facies analysis summary.....	57
3.5.3 Paleocurrent measurements	60
3.5.4 Petrographic overview of the studied flysch units.....	61
3.5.5 Micropaleontological data	63
3.6 Summary.....	65
Chapter 4: The contact zone between the ALCAPA and Tisza-Dacia mega-tectonic units of Northern Romania in the light of new paleomagnetic data.....	67
<i>Márton, E., Tischler, M., Csontos, L., Fügenschuh, B., Schmid, S.M.</i>	
<i>Eclogae Geologicae Helveticae (accepted)</i>	
4.1 Abstract.....	67
4.2 Zusammenfassung.....	68
4.3 Introduction.....	69
4.4 Geological setting	70
4.5 Paleomagnetic sampling	72
4.6 Laboratory measurements and results.....	73
4.7 Discussion of paleomagnetic results.....	78
4.7.1 Mid-Miocene localities: Dej tuff and related sediments.....	78
4.7.2 Late Cretaceous localities: red marls.....	79
4.7.3 Eocene to Oligocene localities: flysch samples.....	80
4.8 Discussion and tectonic interpretation of the results.....	81
4.8.1 Inferences regarding post-12 Ma counter-clockwise rotations (Mid-Miocene and Late Cretaceous localities).....	81
4.8.2 Inferences regarding pre-12 Ma clockwise rotations (Eocene to Oligocene localities)	83
4.8.3 Disintegration of the ALCAPA mega-tectonic unit starting at 18.5 Ma ago.....	84
4.8.4 Tentative model for the tectonic evolution	84
4.9 Conclusions.....	86
4.10 Acknowledgements.....	86
4.11 References.....	87

Chapter 5: A contribution to the reconstruction of the Late Tertiary tectonic history of Tisza-Dacia – Constraints from a palinspastic reconstruction of the study area	91
5.1 Introduction	91
5.2 Summary of Late Tertiary tectonic phases and available constraints	93
5.2.1 Early Burdigalian emplacement of the Pienides	93
5.2.2 Late Burdigalian SW-NE extension	93
5.2.3 Post Burdigalian structures – ‘soft collision’	96
5.3 The 12 Ma time-slice: retro-deformation of post-Burdigalian transtension	98
5.4 The 16 Ma time slice: retro-deformation of post-Burdigalian transpression	102
5.5 The 20 Ma time slice: retro-deformation of the Early Burdigalian emplacement of the Pienides	104
5.6 The 34 Ma time slice: reconstruction of the situation before the onset of lateral extrusion of ALCAPA and clockwise rotation of Tisza-Dacia	106
5.7 Conclusions	108
Chapter 6: Summary	109
6.1 Chapter 2: Tectonic constraints	110
6.2 Chapter 3: Sedimentological constraints	112
6.3 Chapter 4: Paleomagnetic constraints	112
6.4 Integration of the results into the regional setting	112
References	117
Appendix	On CD

Chapter 1:

Introduction

1.1 General geological overview

A central part for the understanding of the formation of the Carpathian orogen is the Late Tertiary tectonic history of the crustal blocks which are juxtaposed against the highly irregular European continental margin (e.g. Royden 1988). The European continental margin features a large-scale bight (“Carpathian embayment”) between the Bohemian and Moesian promontories (Fig. 1.1), thought to have been formerly occupied by (partly?) oceanic crust by many authors (e.g. Balla 1982; Mason et al. 1998).

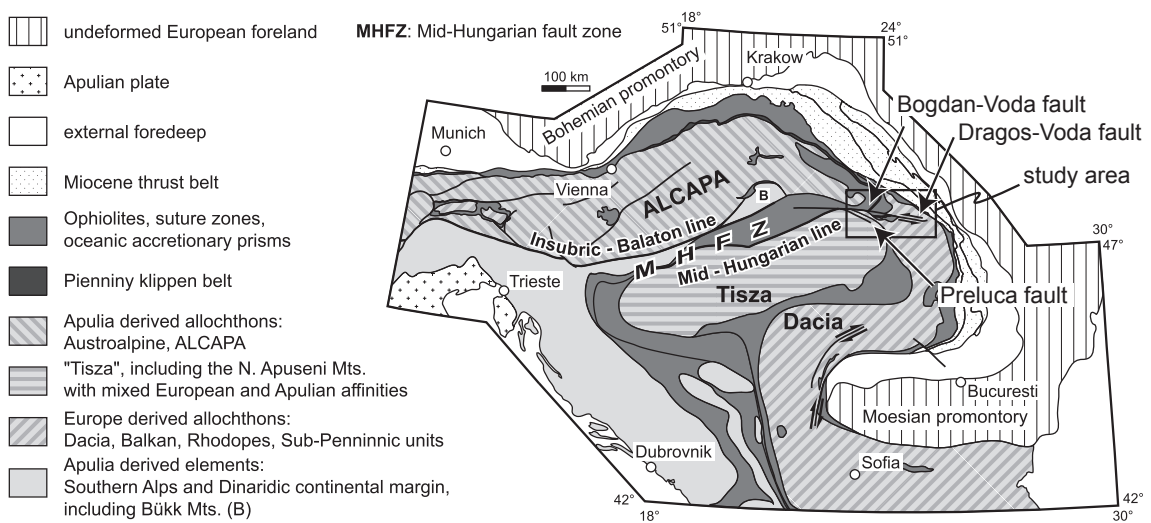


Fig. 1.1: Major tectonic units of the Alps, Carpathians and Dinarides, simplified after an unpublished compilation by S. Schmid, B. Fügenschuh, K. Ustaszewski, L. Matenco, R. Schuster and M. Tischler.

The continental units found within this embayment show marked differences in character and inferred provenance. Apart from contrasting Triassic and Jurassic sedimentary facies (e.g. Csontos and Vörös 2004 and references therein), these continental blocks also show different rotational histories, established by numerous paleomagnetic studies (e.g. Patrascu et al. 1994, Marton et al. 2002, Marton and Fodor 2003). The main focus of this thesis is on the ALCAPA and Tisza-Dacia blocks. For a definition of the continental blocks within the Carpathian embayment see chapter 2.

Slab retreat of the subducting former fill of the Carpathian embayment (e.g. Royden 1988; Wortel and Spakman 2000; Sperner et al. 2005) is thought to have been the main driving force during emplacement of these continental blocks, coupled to eastward translation of parts of the Eastern Alps by lateral escape (e.g. Ratschbacher et al. 1991a, b). Space problems and corner effects at the promontories led to extensive deformation accompanied by opposed rotations of the invading blocks (e.g. Fodor et al. 1999). The ALCAPA and Tisza-Dacia blocks are juxtaposed along a broad zone of deformation, termed the Mid-Hungarian fault zone. Unravelling the tectonic history of this fault zone can provide crucial constraints for the tectonic development of the intra-Carpathian area.

Unfortunately, most of the Mid-Hungarian fault zone is covered by the Neogene sediments of the Pannonian basin, restricting field-work to small areas at the basin borders. The study area of this thesis is located in one of these areas, in northern Romania.

1.2 Outline of the projects incorporating this thesis

The project providing the framework for the presented study are mainly the NF-project “The Dragos Voda fault in northern Romania – the eastern termination of the Mid-Hungarian Line fault system?” (Nr. 21-64979.01), and its follow-up project (Nr. 200020-105136/1). Initiated by Bernhard Fügenschuh and supported by Andreas Wetzel and Stefan Schmid, this project is designed to obtain field-based and geochronological evidence to augment the existing geophysical dataset concerning the tectonic history of the Mid-Hungarian fault zone.

Since most of the Mid-Hungarian fault zone is covered by the young sediments of the Pannonian basin, the focus of this project lies on the basin border (Northern Romania), where outcrops permit field-based studies. Within the study area, several map scale faults are first order candidates for representing the continuation of the Mid-Hungarian fault zone (Fig. 1.1): The Bogdan-Voda fault, Dragos-Voda fault and the Preluca fault.

Another NF-project granted to Stefan Schmid (Nr. 200021-101882/1) aims at continuing the work and expanding the scope towards the Dinarides. The long term aim of all of the above-mentioned projects is the improvement of the general tectonic map presented in Fig. 1.1, together with the better understanding of the Late Tertiary emplacement of the crustal blocks into the Carpathian embayment. The ultimate goal is a palinspastic restoration of the Late Tertiary tectonic history of the Carpathian embayment.

In order to reconstruct the Late Tertiary tectonic history of the study area, the following approach was chosen:

- Detailed structural fieldwork focussing on Late Tertiary structures in crystalline as well as sedimentary units of the study area.
- Extensive geochronology on the crystalline units utilising fission track dating on apatite and zircon in order to constrain the uplift history of the study area.
- Detailed sedimentological fieldwork on Late Tertiary strata, in order to reconstruct their depositional setting and thus obtain constraints for synsedimentary tectonics.
- Paleomagnetic analysis of selected sites within the study area in order to provide the link to already existing paleomagnetic databases.

Within the larger framework of the original project, two complementary PhD-theses are situated, each concentrating on different aspects of the approaches mentioned above. While the PhD thesis of H. R. Gröger focussed on the structural geology and uplift of the crystalline units, this thesis concentrates on structural and sedimentological field-work.

1.3 Aims and approach of this thesis

This study addresses the interplay between tectonic activity and sedimentation in northern Romania. Located at the triple point where three major continental blocks that invaded the Carpathian embayment meet, the study area represents a key area for the understanding of the tectonic history of these continental blocks. The main goal of this thesis is to provide a sound field-based dataset providing constraints for the Late Tertiary tectonic history of the study area. Since tectonic activity is not only recorded by corresponding structures but also in the sedimentary record, this thesis also integrates sedimentological constraints.

Due to the different approaches taken, each chapter includes an individual introduction into the general and regional geological frame – focussing on the information relevant to the respective chapter. The presented thesis has significantly profited from the integration into the aforementioned larger project. Most notably, close collaboration with the author of the parallel thesis, H.R. Gröger, especially during common field-work proved very fruitful. A brief description of the aim and approach of each chapter, including the various authors' contributions, is presented in the section "Organisation of this thesis" above.

1.4 Stratigraphic correlation used

The correlation chart used throughout this thesis is presented in Fig. 1.2. For the temporal correlation of Mediterranean and Paratethys stages, the correlation chart of Steininger and Wessely (2000) has been used. Respective ages of stratigraphic intervals (Fig. 1.2) refer to the Geologic Time Scale of Gradstein et al (2004).

Geologic Time Scale Gradstein et al. 2004				Cenozoic Mediterranean / Paratethys Correlation Chart F.F.Steininger and G.Wessely, 2000		
TIME In Ma	SYSTEM	SERIES	MEDITERRANIAN STAGES	Med. Stages	Central Paratethys Stages	Eastern Paratethys Stages
0	Q.	PLIO-CENE			shaded: no information	
			U	1.81 GELASIAN		
			2.59 PIAZENZIAN			
5		L	3.60 ZANCLEAN		DACIAN	KIMMERIAN
		UPPER	5.33 MESSINIAN		PONTIAN	PONTIAN
			7.25 TORTONIAN		PANNONIAN	MAEOTIAN
10		MIDDLE	11.61 SERRAVALLIAN		SARMATIAN	Khersonian Bessarabian Volhynian
			13.65 LANGHIAN		BADENIAN	Konkian Karaganian Ishokranian
15			15.97 BURDIGALIAN		KARPATIAN OTTNANGIAN	TARKHANIAN
20		LOWER	20.43 AQUITANIAN		EGGERBURGIAN	KOTSAKHURIAN
			23.03 CHATTIAN		EGERIAN	SAKARAULIAN
25		UPPER				KARADZHALGAN- IAN
		LOWER	28.40 RUPELIAN		KISCELLIAN	KALMYKIAN
30			33.9 PRIABONIAN			SOLENOVIAN
		UPPER	37.2		PRIABONIAN	PSHEKIAN
35						BELOGLINIAN

Fig. 1.2: Stratigraphical correlation chart used in this thesis.

Chapter 2:

Miocene tectonics of the Maramures area (Northern Romania) - implications for the Mid-Hungarian fault zone

Tischler, M., Gröger, H.R., Fügenschuh, B., Schmid, S.M.

International Journal of Earth Sciences (2006)

Geologisch - Paläontologisches Institut, Bernoullistr. 32, CH-4056 Basel, Switzerland

2.1 Abstract

The interplay of emplacement of crustal blocks (eg. “ALCAPA”, “Tisza”, “Dacia”) and subduction retreat is a key issue for understanding the Miocene tectonic history of the Carpathians. Coeval thrusting and basin formation is linked by transfer zones, like the Mid-Hungarian fault zone, which separates ALCAPA from Tisza-Dacia. The presented study provides new kinematic data from this transfer zone.

Early Burdigalian (20.5–18.5 Ma) SE- directed thrusting of the easternmost tip of ALCAPA (Pienides), over Tisza-Dacia is linked to movements along the Mid-Hungarian fault zone (and Periadriatic line), accommodating the lateral extrusion of ALCAPA. Minor Late Burdigalian (~18.5–16 Ma) NE-SW directed extension is interpreted as related to back-arc extension.

Post Burdigalian (post- 16 Ma) NE-SW-directed compression and NW-SE-oriented extension correlates with “soft collision” of Tisza-Dacia with the European foreland coupled with southward migration of active subduction. During this stage the Bogdan-Voda and Dragos-Voda faults were kinematically linked to the Mid-Hungarian fault zone. Sinistral transpression (16–12 Ma) at the Bogdan-Voda fault was followed by sinistral transtension (12–10 Ma) along the coupled Bogdan- Dragos-Voda fault system. During the transtensional stage, left-lateral offset was reduced eastwards by SW-NE trending normal faults until terminating in an extensional horse-tail splay.

Keywords: Kinematic analysis, Eastern Carpathians, Mid-Hungarian fault zone, Pienides, Miocene tectonics

2.2 Introduction

Miocene tectonics in the Carpathian region is characterised by the formation of an arcuate fold-and-thrust-belt and contemporaneous back arc extension in the Pannonian basin (e.g. Royden 1988). The European margin features a large-scale bight between the Moesian and Bohemian promontories (Fig. 2.1). According to most authors (e.g. Balla 1982; Mason et al. 1998) this Carpathian “embayment” was at least partly floored by oceanic crust. Slab retreat (e.g. Royden 1988; Wortel and Spakman 2000; Sperner et al. 2005) created the necessary space that allowed for the invasion of large continental blocks (ALCAPA, Tisza and Dacia; Balla 1987) and smaller displaced terranes (Fig. 2.1).

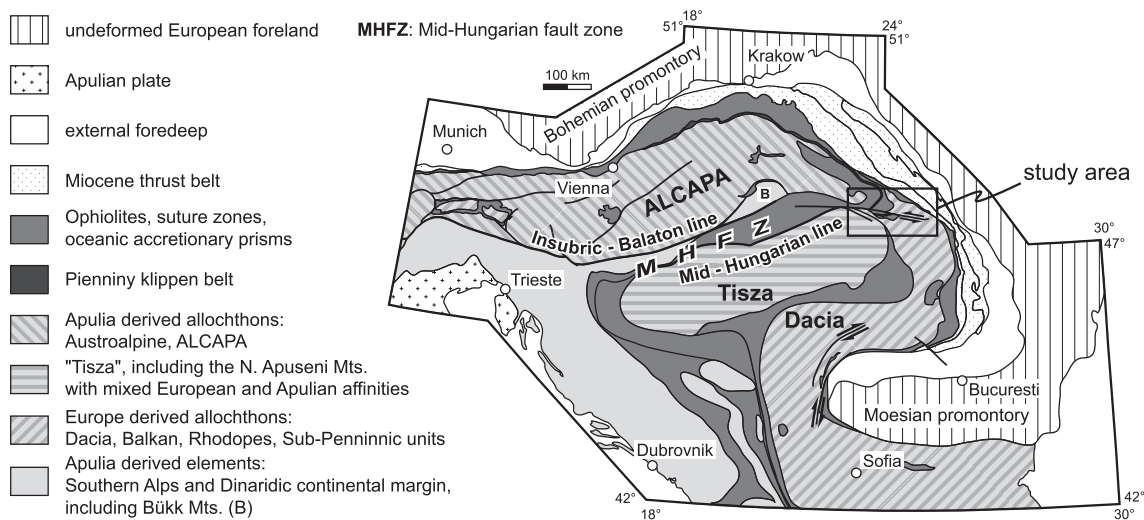


Fig. 2.1: Major tectonic units of the Alps, Carpathians and Dinarides, simplified after an unpublished compilation by S.M. Schmid, B. Fügenschuh, K. Ustaszewski, L. Matenco, R. Schuster and M. Tischler.

Invasion of the ALCAPA block lasted from the Late Oligocene to the Middle Miocene (Fodor et al. 1999), but initiated earlier in case of the Tisza and Dacia blocks (Fügenschuh and Schmid 2005). Emplacement was accompanied by substantial strike-slip movements, together with extension, shortening and rotations of rigid blocks (Ratschbacher et al. 1993; Fodor et al. 1999; Márton 2000; Márton and Fodor 2003; Csontos and Vörös 2004; Horváth et al. 2005). The major displaced units are, from NW to SE (Fig. 2.1):

- 1) Apulia-derived allochthons, such as the Austroalpine nappes of the Eastern Alps, that extend into the Central and Inner West-Carpathians (ALCAPA, e.g. Plasienska et al. 1997a,b).
- 2) A small stripe of units situated within the intensely deformed belt of the Mid-Hungarian fault zone (Fig. 2.1), whose Late Paleozoic and Mesozoic cover (outcropping in the Bükk Mountains) has a marked affinity to the internal Dinarides (Kovács et al. 2000; Haas et al. 2000). These Dinaridic units also contain remnants of obducted ophiolites and oceanic accretionary prisms.
- 3) The Tisza block, located SE of the Mid-Hungarian fault zone and largely covered by the Neogene fill of the Pannonian basin, crops out in the North Apuseni mountains, as well as in a series of Hungarian and Croatian inselbergs. The paleogeographic position of the Tisza unit is much debated (e.g. Burchfiel 1980; Săndulescu 1984, 1994; Csontos et al. 1992; Balintoni 1995; Fodor et al. 1999; Haas and Pero 2004).

Its Mesozoic cover with European as well as Apulian affinities suggests that it broke off Europe along an eastern extension of the Piedmont-Liguria basin in Mid-Jurassic times (Haas and Pero 2004; Stampfli and Borel 2004).

4) The Dacia block is a Europe-derived allochthon (or “Rhodopian” allochthon, Burchfiel 1980; Schmid et al. 1998; Fügenschuh and Schmid 2005), comprising the Balkan mountains, the Getides of the Southern Carpathians, as well as the Eastern Carpathian Bucovinian nappe system (Median Dacides of Săndulescu et al. 1981; Săndulescu 1994). Some authors consider Tisza and Dacia as representing one single block (e.g. “Tisza-Dacia terrane” of Csontos and Vörös 2004) since the Late Cretaceous, but it is not yet sure as to how firmly Dacia remained attached to Tisza since the Mid-Cretaceous orogeny.

The development of the Carpathian orogen is also highly influenced by tectonic events within the Alps (Schmid et al. 2004a, b) and the Dinarides (Pamic 2000, Dimitrijevic 2001). Particularly the onset of “lateral extrusion”, a mechanism defined by Ratschbacher et al. (1991a, b) in the Eastern Alps, is of major importance: Indentation by the South Alpine block, coupled to retreat of the descending European lithosphere (Royden 1988; Wortel and Spakman 2000), led to the ENE-ward translation of the ALCAPA block along the Insubric-Balaton line.

However, since the emplacement of Tisza and Dacia is unrelated to indentation in the Alps, subduction retreat is considered to provide the principal driving force for the invasion of the various blocks into the Carpathian embayment (Royden 1988; Wortel and Spakman 2000; Sperner et al. 2005). Furthermore subduction and retreat of the European plate beneath the inner Carpathians led to the formation of a back-arc-type basin: the Pannonian basin (i.e. Horváth et al. 2005; Cloetingh et al. 2005). Net east-west extension in the Pannonian basin is realized by normal faulting connected via conjugate strike-slip dominated systems. These strike-slip systems are also kinematically linked to synchronous thrusting in the external Miocene thrust belt (Royden 1988).

Field-based studies in the West Carpathians shed light on the interplay between subduction retreat and “lateral extrusion” (e.g. Nemčok 1993; Ratschbacher et al. 1993; Sperner et al. 2002). These authors documented NE-ward displacement and counter-clockwise rotation of the ALCAPA block, guided by strike-slip zones oriented sub-parallel to the collision suture. NNE-SSW shortening and ESE-WNW extension were the dominant modes of deformation during Late Oligocene to Mid-Miocene NE-ward movement of ALCAPA. After soft collision of ALCAPA with the European margin in the Western Carpathians at around 13 Ma ago, active subduction continued only further to the southeast, inducing NW-SE extension in the area of the Western Carpathians (Sperner et al. 2002).

The Mid-Hungarian fault zone played a key role during the emplacement of the various blocks in the Carpathian embayment. This major NE- trending strike-slip zone is thought to accommodate differential movements between ALCAPA and Tisza-Dacia. (Fig. 2.1). It is bounded to the north by the Balaton line, the NE-wards continuation of the Periadriatic line (Fodor et al. 1998). The southern boundary of the Mid-Hungarian fault zone is termed Mid-Hungarian line, defined as “a major strike-slip fault along which the ALCAPA and Tisza–Dacia units of different provenance were juxtaposed” by Csontos and Nagymarosy (1998).

ALCAPA, Tisza and Dacia feature contrasting Triassic and Jurassic sedimentary facies and fossil assemblages (Csontos and Vörös 2004, and references therein). The first important activity within the Mid-Hungarian fault zone occurred during the Oligocene (or earlier) (Csontos et al. 1992; Csontos and Nagymarosy 1998; Fodor et al. 1999). Thereby collision led to thrusting of the ALCAPA block over Tisza and Dacia in Late Oligocene times (Csontos and Nagymarosy 1998).

Corner effects at the Bohemian (Sperner et al. 2002) and Moesian (Ratschbacher et al. 1993; Schmid et al. 1998) promontories, respectively, led to opposed rotations well established by paleomagnetic studies (e.g. Márton and Fodor 1995, 2003; Márton 2000). While the timing of the emplacement of the ALCAPA block is fairly well constrained to have occurred between Late Oligocene and Middle Miocene times (Fodor et al. 1999, Sperner et al. 2002), emplacement of the Dacia (and Tisza?) block commenced earlier (during the Eocene according to Fügenschuh and Schmid 2005), and ended later (in post-Middle Miocene times, e.g. Matenco et al. 2003). During Mid - to Late Miocene times (i.e. after 16 Ma) strike-slip deformation and extension dominated within the Mid-Hungarian fault zone, allowing for ongoing differential movements of the ALCAPA and Tisza-Dacia blocks (Csontos and Nagymarosy 1998). During this late stage the Mid-Hungarian fault zone may also have served as a transfer zone between the foreland thrust belt and the back-arc extension domain. In conclusion, diverging movement vectors as well as large opposed rotations call for important and complex tectonic movements within the Mid-Hungarian fault zone all the way from Oligocene to Miocene times.

This study covers the outcropping parts of the Mid-Hungarian fault zone at its NE termination in northern Romania (Fig. 2.1). The thrust contact of the so-called “Pienides” (Săndulescu et al. 1981), flysch nappes situated at the contact of the easternmost tip of ALCAPA with Tisza-Dacia, represents the Early Miocene Mid-Hungarian line sensu Csontos and Nagymarosy (1998) and is exposed in the study area. The Bogdan-Voda and Dragos-Voda strike-slip faults, as well as the Preluca fault near the northeastern rim of the Tisza block (Fig. 2.2), are first order candidates for representing surface exposures of the Mid-Hungarian fault zone that were active during Mid- to Late Miocene times.

This study aims to provide further constraints on the timing and kinematics of movement along the Mid-Hungarian fault zone during back-arc extension and final emplacement of the ALCAPA, Tisza and Dacia blocks. With the aid of published and unpublished (Săndulescu pers. com.) maps of the Geological Survey of Romania, our field-work focussed on the analysis of kinematic data and was assisted by apatite fission track analyses. Stratigraphic ages are after Gradstein et al. (2004), Mediterranean and Parathetys stages are correlated according to Steininger and Wessely (2000).

2.3 Geological Setting

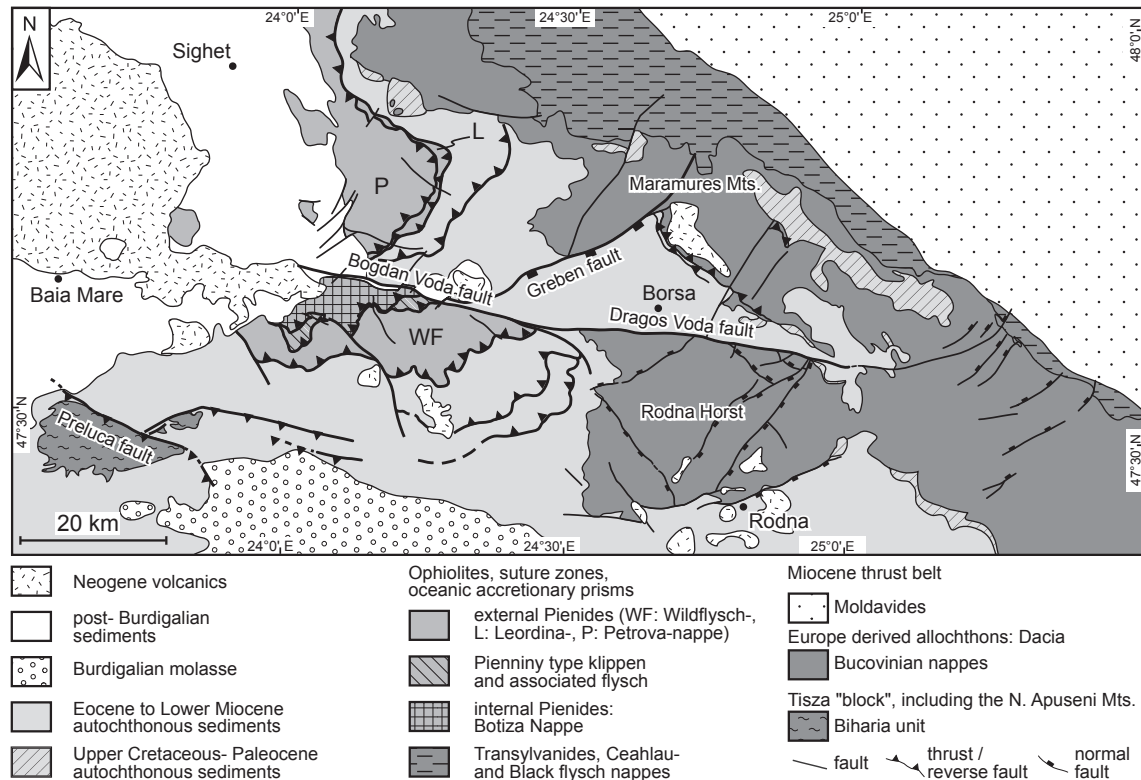


Fig. 2.2: Tectonic map of the study area based on published geological maps (1:50.000 and 1: 200.000) of the Geological Survey of Romania, Dicea et al. (1980), Săndulescu (1980), Săndulescu et al. (1981) and Aroldi (2001).

The study area, located in the internal East Carpathians (Northern Romania) near the transition to the Western Carpathians (Fig. 2.1), comprises the northeastern tip of the Tisza block (Biharia unit) and the northernmost part of Dacia (Bucovinian nappes). Alpine-age deformation within the Bucovinian nappes and the Biharia unit started in Mid-Cretaceous times ("Austrian" phase) and continued until Late Cretaceous times ("Laramide" phase, Săndulescu et al. 1981, Săndulescu 1994). Upper Cretaceous to Paleocene sediments unconformably cover these Mid- and Late Cretaceous tectonic contacts, as well as contacts between Tisza, Dacia and intervening oceanic remnants (Fig. 2.1). Eocene to Burdigalian strata were deposited above a second unconformity. This mainly Tertiary cover is referred to as "autochthonous cover of Tisza-Dacia" in the following. During final closure of the Carpathian embayment the Bucovinian nappes were emplaced onto Cretaceous to Miocene flysch deposits now forming the Miocene fold-and-thrust-belt of the East Carpathians.

Tisza and Dacia, together with their autochthonous cover, were overthrust by the Pienides during Burdigalian times (Săndulescu et al. 1981). According to Săndulescu et al. (1993) the Pienides, situated at the easternmost tip of ALCAPA, comprise an external (Petrova, Leordina and Wildflysch nappes) and an internal thrust sheet (Botiza nappe). Internal and external Pienides, mainly consisting of Eocene to Oligocene non-metamorphic flysch units, can be correlated with the Ivancovce-Krichevo units and the Magura flysch of the Western Carpathians, respectively (Săndulescu et al. 1981, Săndulescu 1994). Furthermore the internal Pienides feature frontal imbricates containing phacoids of Pieniny Klippen type material embedded in Eocene flysch (Săndulescu et al. 1993).

Note that these units and their equivalents form the innermost part of the Outer West Carpathians (Plasienska 1997 a, b), while they take a more internal position in our working area.

The post-Burdigalian infill of the Pannonian- and Transylvanian basins in the working area starts with the deposition of the Mid-Miocene (Badenian) Dej tuff during a period of mainly acidic volcanism (Mason et al. 1998). Subduction-related calc-alkaline magmatism (Mason et al. 1998) started during Middle Miocene times in the working area (13.5 Ma, Pécskay et al. 1995). Magmatic activity led to the formation of a linear chain along the inner side of the East Carpathians decreasing in age from 12 Ma in the NW to 0.2 Ma in the SE.

From a tectonic point of view the most obvious structure is the E-striking, predominantly left-lateral, Bogdan- Dragos-Voda fault system. The Bogdan-Voda fault to the west offsets the autochthonous cover of Tisza-Dacia, as well as the nappe pile of the Pienides, and is sealed by Mid-Miocene volcanics. The Dragos-Voda fault to the east forms the northern boundary of a horst-like crystalline body (“Rodna horst”, Fig. 2.2), built up by the Bucovinian nappe stack. Possible linkage of and mutual relationships between these two fault segments have been a point of discussion in the Romanian literature. While Săndulescu et al. (1981) interpreted the two faults as separate, Dicea et al. (1980) mapped a single continuous fault. Other authors (e.g. Huismanns et al. 1997, Györfi et al. 1999) mapped one single fault termed “Dragos-Voda fault”.

2.4 Methods

2.4.1 Derivation of kinematic axes

Kinematic axes (principal shortening and extension directions) were derived from meso-scale structures in order to analyse the regional tectonic history. For this purpose, fault-slip sets (orientation of fault plane, sense and direction of movement) were analysed. Fieldwork focussed on correlation of the kinematic data with large-scale structures.

The direction of movement being given by a lineation (mechanical striation or slicko-fibre orientation), the sense of movement was determined by criteria such as slicko-fibre growth direction, orientation of Riedel shears or offset of marker horizons. Inhomogeneous fault data sets were separated into homogenous subsets based on field observations, and their kinematic compatibility.

Kinematic axes were computed with the right dihedron method described by Angelier and Mechler (1977). Applicable to newly formed, as well as to reactivated pre-existing fractures, this simple graphical method reflects the bulk finite strain state (Pfiffner and Burkhard 1987). Eigenvectors and Eigenvalues (Bingham 1964) have been used to determine mean axes of shortening and extension (Fig 2.3). A tabular overview on the analysed stations is found in Appendix 1.

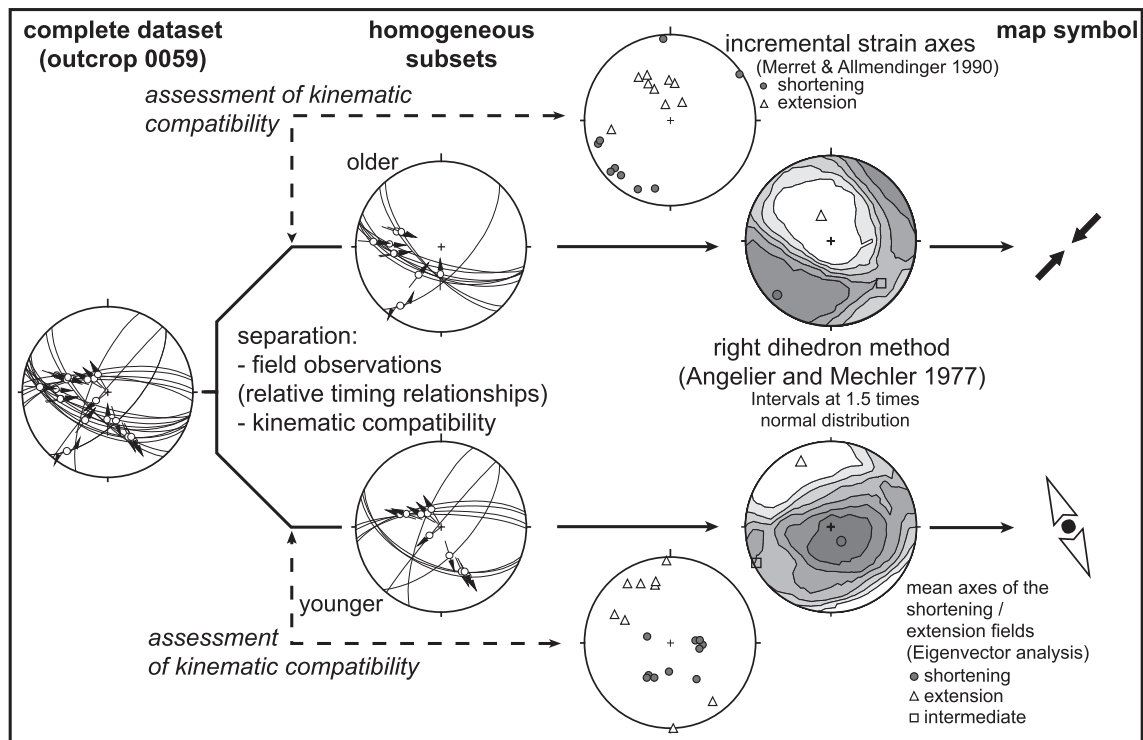


Fig. 2.3: Flow chart for the analysis of fault-slip data. For the separation of homogenous subsets field observations as well as kinematic compatibility have been used. Kinematic compatibility has been assessed using plots of the fault sets and correspondent incremental strain axes (Marret and Allmendinger 1990). For map display mean axes of shortening and extension are used. Intersection relationships in the analysed outcrop show exemplarily, that transpression was followed by transtension during the post Burdigalian stages.

For calculation of kinematic axes and visualisation of fault sets we used the software TectonicsFP (Franz Reiter and Peter Acs © 1996-2000: <http://go.to/TectonicsFP>; based on TectonicVB by Hugo Ortner).

2.4.2 Fission track analysis

Apatite mineral concentrates were prepared by conventional crushing, sieving, magnetic and heavy liquid separation. The grains were mounted in epoxy resin, polished and etched for 40 sec at room temperature in 6.5 % HNO₃. Samples were analysed using the external detector method (Gleadow 1981), with muscovite as an external detector. Irradiation was carried out at the High Flux Australian Reactor (HIFAR) with neutron fluxes monitored in CN5. Muscovite was etched 40 min at room temperature in 40% HF.

Fission tracks were counted on a computer-controlled Zeiss microscope at magnifications of X1250 (dry). Ages were calculated using the zeta-calibration method (Hurford and Green 1983) with a zeta-value of 355.96 ± 9.39 (CN5, Durango). For data processing the windows software TRACKKEY (Dunkl 2002) was used. All ages are central ages (Galbraith and Laslett 1993), with errors quoted as 1s. Closure temperatures for apatite are $90 \pm 30^\circ \text{C}$, the uncertainty being given by the lower and upper limits of the apatite fission track partial annealing zone (Gleadow and Duddy 1981, Gallagher et al. 1998).

2.5 Structural analysis

2.5.1 Early Burdigalian top-SE thrusting of the Pienides

The emplacement of the Pienides during Burdigalian times (Fig. 2.2) also led to the imbrication of the autochthonous cover of Tisza-Dacia. Deformation related to the emplacement of the Pienides is primarily controlled by the more incompetent silty-marly flysch units, which are serving as detachment horizons. The more massive sandy layers only display moderate brittle deformation, even close to nappe contacts. Cataclastic shear zones related to nappe emplacement are the predominant deformation features, while folding is only locally developed. Within marly layers shear-bands and/or SC-type fabrics can locally be observed. The shortening direction related to the emplacement of the Pienides was evaluated by kinematic analysis of mesoscale faulting found near major cataclastic shear zones.

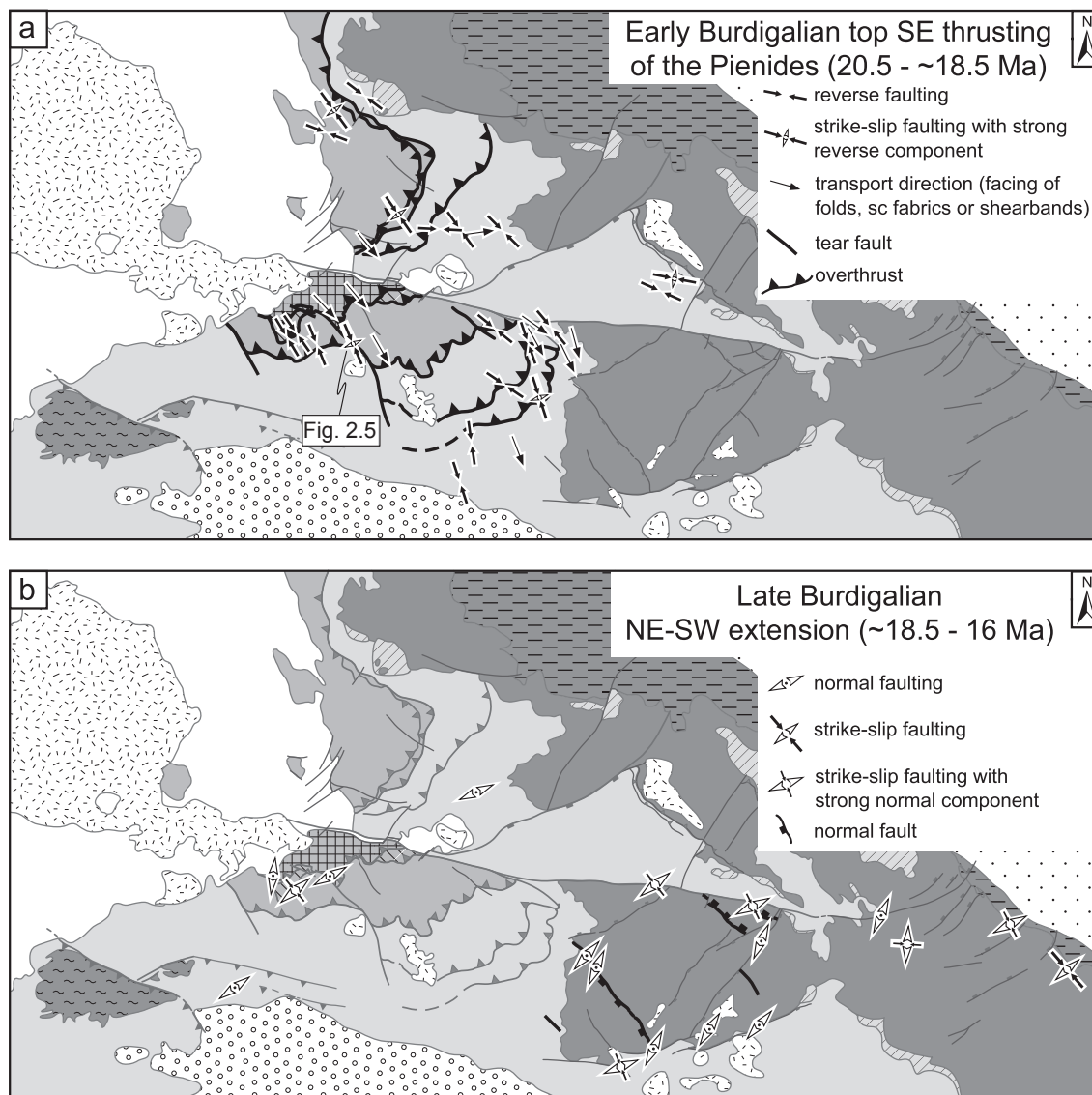
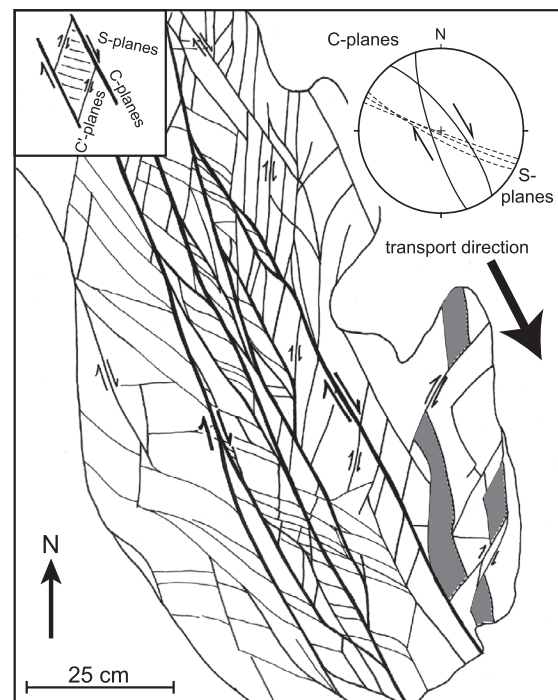


Fig. 2.4: Kinematics and structures related to the Burdigalian deformation phases. a: Early Burdigalian emplacement of the Pienides shows consistent top-to-SE thrusting. The pronounced bends in the nappe front are interpreted as a result of a change in thrust geometry featuring frontal and lateral ramps as well as tear faults (see text). b: Subordinate NE-SW extension, related to SE-striking normal faults of Late Burdigalian age.

Transport direction was inferred from the facing direction of outcrop-scale folds and/or SC-type fabrics and shear-bands. The deduced kinematic directions (Fig. 2.4a) reveal a consistent displacement direction towards the SE (Appendix 2), both for the Pienides as well as for the imbricates of the autochthonous cover of Tisza-Dacia. The relative timing of fault sets found in two outcrops (Appendix 2, Stations 0639, 0584) suggests a possible minor change in transport direction from top-SE towards top-ESE.

The frontal thrust of the Pienides has an extremely variable trace in map view (Fig. 2.4a), showing alternating SW- and SE-striking segments. Outcrops along the northernmost SE-striking thrust segment (Fig. 2.4a) expose SSE-striking strike-slip fault zones with a significant reverse component. The predominantly transpressional deformation encountered along this segment (Appendix 2; Station 0639), suggests a lateral ramp geometry. The thrust front of the Pienides south of the Bogdan-Voda fault shows three major sharp bends in map view (Fig. 2.4a). At one of the bends a steeply dipping dextral strike-slip fault zone, sub-parallel to the transport direction (Fig. 2.5), is interpreted as a tear fault. The increase of shortening within the autochthonous cover of Tisza-Dacia, observed in front of the Pienides towards the northeast, is a map-scale argument in favour of this interpretation.

Fig. 2.5: Outcrop sketch (map view) of a cataclastically deformed fault zone at the NW-SE striking nappe contact of the Pienides against the autochthonous cover of Tisza-Dacia (see Fig. 2.4a). The fine-grained siliciclastics (homogenous clay rich silts) are dissected by anastomosing shear zones featuring shear band geometries. Shaded areas indicate offset of silty marker horizons. The strike-slip dominated kinematics confirm the interpretation of the NW-SE striking contacts as tear faults.



The timing of Pienide nappe emplacement and related structures is constrained by stratigraphic arguments. The youngest thrust strata are Aquitanian in age (Dicea 1980), and thrust contacts are sealed by Badenian-age (16- ~13 Ma) sediments. Hence, an intra-Burdigalian activity can be inferred. The fact, that structures related to Late Burdigalian extensional deformation (see below) overprint nappe emplacement features, allows us to suggest an Early Burdigalian (20.5-~18.5 Ma) age for the emplacement of the Pienides.

2.5.2 Late Burdigalian NE-SW extension

While SE-trending normal faults are rarely observed in the sedimentary cover, they are more abundant within the basement units of the study area. The most prominent of these SE-striking faults are found within the SW part of the Rodna massif (Fig. 2.4b), where they offset Bucovinian-type basement as well as Oligocene strata.

Kinematic analysis of these faults yielded NE-SW to NNE-SSW extension, i.e. normal faulting with a minor strike-slip component (Fig. 2.4b; Appendix 3). Field evidence clearly suggests that these normal faults overprint structures related to the emplacement of the Pienides (e.g. Station 0236, Appendix 2, 3). Since structures of this phase are cut by the Dragos-Voda fault while Badenian (16 - ~13 Ma) strata are unaffected, we assume a pre-Badenian (18.5 - 16 Ma) age for this extensional deformation.

2.5.3 Post-Burdigalian structures

Emplacement of the Pienides was post-dated by extensive faulting. Strike-slip activity along the Bogdan-Dragos-Voda fault system can be subdivided into an earlier transpressional stage followed by transtension (Fig. 2.6).

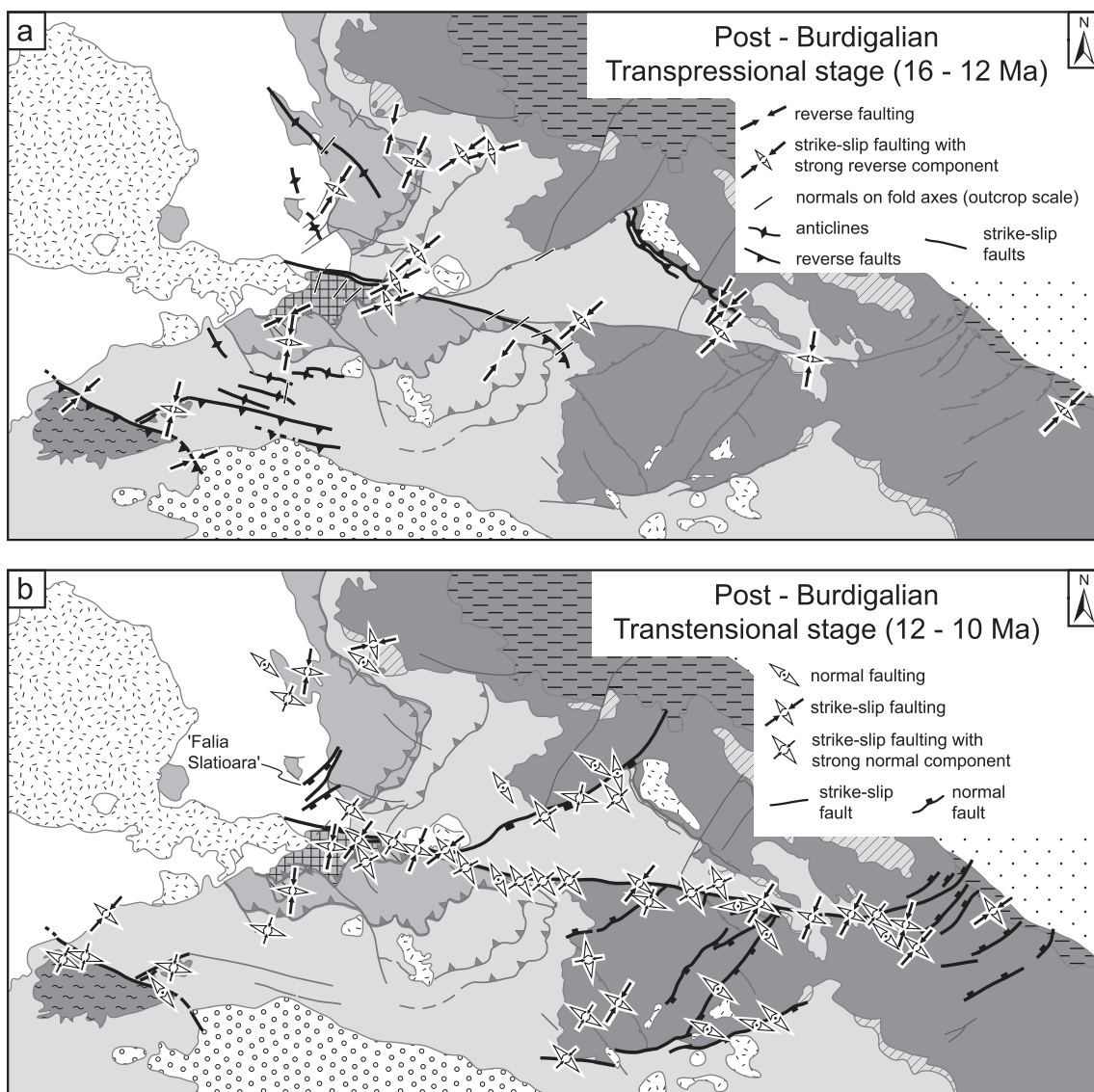


Fig. 2.6: Kinematics and structures related to the post-Burdigalian (16 – 10 Ma) activity of the Bogdan- and Dragos-Voda faults. Transpression (a) precedes transtension (b). Shortening is SW-NE during both phases. Note the linked Bogdan-Voda and Dragos-Voda fault activity during the transtensional stage.

Transpressional stage

Open folds with SE- to ESE-striking fold axes (Fig. 2.6a) evidence post-Burdigalian shortening in the sedimentary units of the study area. Wavelengths of these folds range between outcrop-scale up to several hundreds of meters. While fold limbs are only weakly inclined south of the Bogdan-Voda fault, they reach dip angles of up to 50° in the north. These SE- to ESE-striking folds overprint earlier nappe emplacement structures (Fig. 2.7). Approaching the fault trace of the Bogdan-Voda fault, this late-stage folding locally intensifies, which leads to isoclinal folding around steeply inclined fold axes.

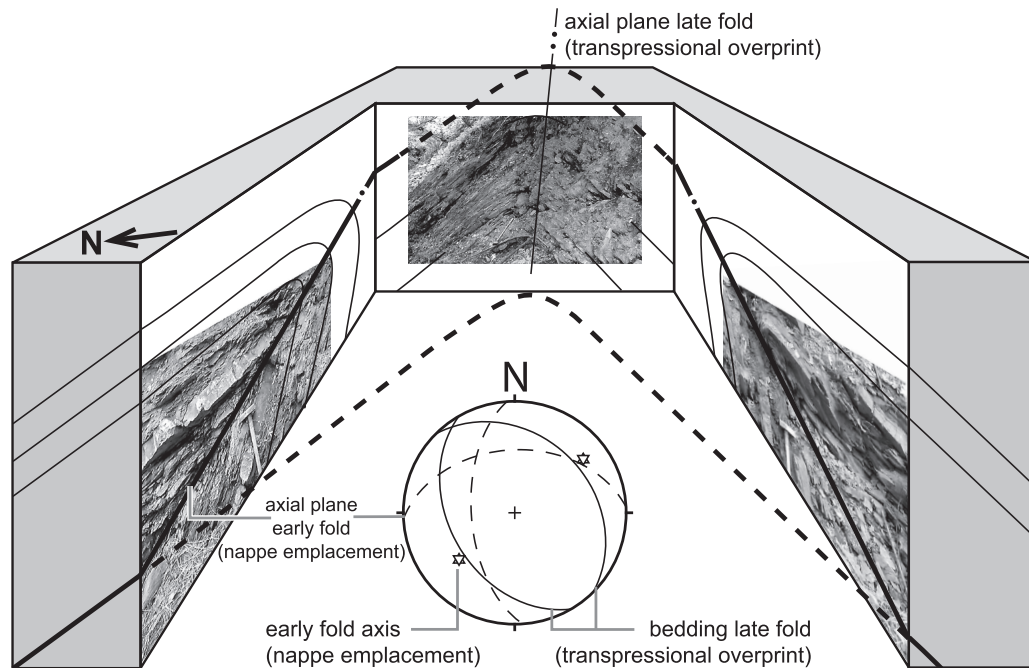


Fig. 2.7: Schematic block diagram of an outcrop showing the overprinting of nappe emplacement structures. The tight asymmetric folds developed during nappe emplacement (left and right) are refolded by an upright open fold with SE-trending fold axis. Such folds are related to the post Burdigalian transpressional stage and can be found throughout the study area.

Faulting with a strong reverse component is found throughout the study area and is documented in map scale (Fig. 2.6a), as well as in outcrop scale (Appendix 4). The most dominant types of structures are SE-striking reverse faults (e.g. back-thrust E of Borsa, Appendix 4, Station 0809; Preluca fault, Appendix 4, Station 0259), as well as E-striking transpressional faults (e.g. Bogdan-Voda fault Appendix 4, Stations 0682, 0675). During this transpressional phase the Bogdan-Voda fault terminates at the Rodna horst in a thrust splay geometry. In summary, the kinematic analysis yields transpression with NE-SW shortening and minor NW-SE extension.

Transtensional stage

E-trending strike slip faults (e.g. Bogdan- Dragos-Voda fault system) as well as SW-striking normal faults (e.g. Greben fault) can be attributed to the transtensional stage (Fig. 2.2). Deformation found along and associated with the Bogdan-Voda and Dragos-Voda faults is dominated by sinistral strike-slip faulting often featuring a normal component. Striations plunge about 5 to 15 degrees to the west along the Bogdan-Voda fault and up to 20 degrees along the Dragos-Voda fault (Appendix 5, 6). These strike-slip faults are commonly accompanied by sets of SW-striking normal faults (Appendix 5, 6).

The E-trending strike slip faults as well as SW-striking normal faults yield regionally consistent kinematic axes. The extensional axes are oriented sub-horizontally NW-SE. Shortening axes strike SW, with dip angles depending on the relative amount of the normal and strike-slip components respectively.

Near its eastern termination, the Bogdan- Dragos-Voda fault system splays into an array of SW-trending normal faults with a left-lateral component. These "horsetails", which accommodated only minor displacements, allowed for "distributed" sinistral offset. This is reflected by the lack of a map-scale discrete offset of major pre-existing tectonic boundaries, such as the front of the Bucovinian nappes (Fig. 2.2). Kinematic axes derived for these SW-NE trending normal faults are compatible with those derived for the Bogdan-Dragos-Voda fault system (Fig. 2.6b, Appendix 5).

Sinistral transtension is further documented along the Preluca fault, where it overprints a preceding phase of top NE thrusting (Fig. 2.6b, Appendix 6).

2.5.4 Stratigraphical timing constraints regarding post-Burdigalian deformation

The formation containing the Early Badenian Dej tuff represents an ideal marker horizon in the northern part of the study area. Post-dating Burdigalian age deformation, it is affected by both the transpressive and transtensive stages along the Bogdan-Voda and the Dragos-Voda fault and hence provides a lower time bracket of 16 Ma (i.e. onset of the Badenian). The Preluca fault also shows post 16 Ma activity, indicated by Burdigalian strata affected by NE-SW shortening (Appendix 4, Station 0260).

The upper time bracket of post-Burdigalian deformation is well defined by the Neogene volcanic body near Baia Mare (Fig. 2.2). The 10 Ma old volcanics constituting the main body (Pécskay et al. 1995) seal the Bogdan-Voda fault (Fig. 2.2).

Overprinting criteria observed at outcrop and map scales indicate that transpression was followed by transtension. For example the SE-striking back-thrust east of Borsa is cut by the younger Greben normal fault (Fig. 2.6). The timing of the change from transpression to transtension is derived from Antonescu et al. (1981). These authors map SW-trending faults (e.g. "Falia Slatioara", Fig. 2.6b) which are cutting strata younger than ~12,2 Ma (Early Bessarabian in Antonescu et al. 1981). Since the strike of the faults mapped by Antonescu et al. (1981) is compatible with normal faults related to the transtensional stage, we infer the onset of transtension to have commenced at around 12 Ma ago.

2.6 Constraints from fission track data

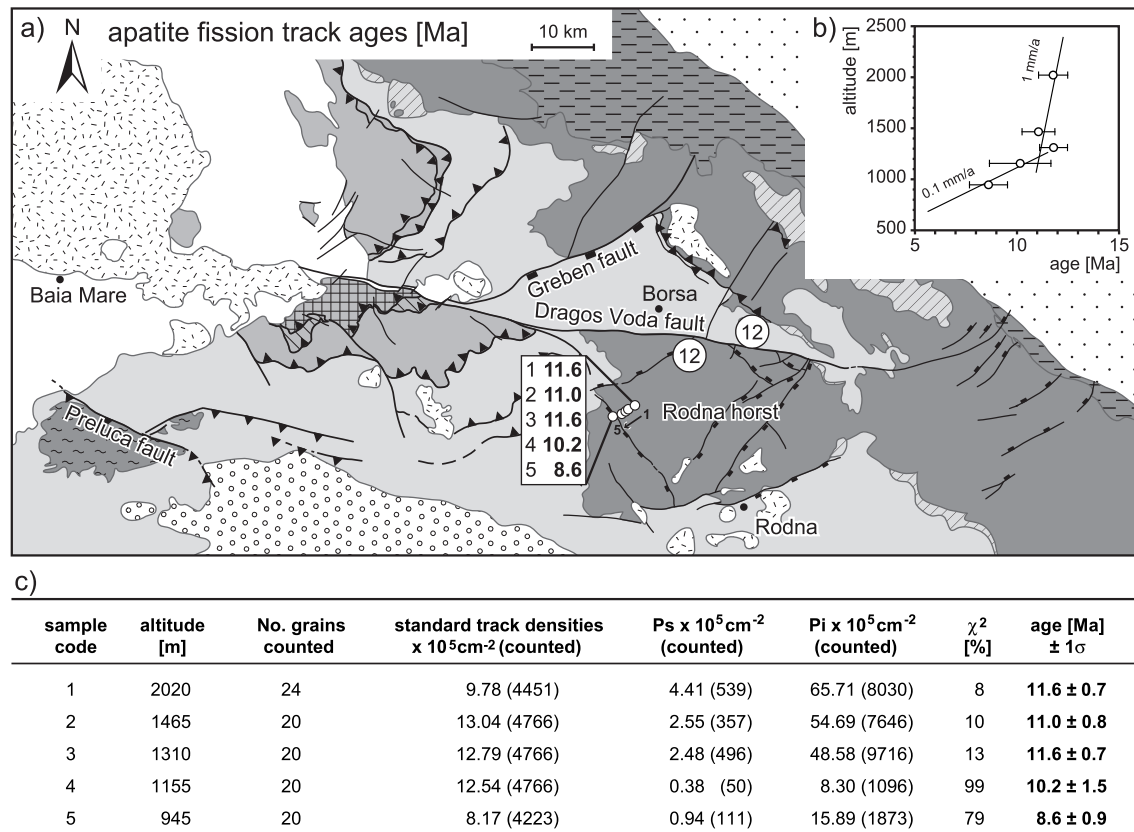


Fig. 2.8: Results of apatite fission track analyses. All samples were analysed using the external detector method (Gleadow 1981) and ages were calculated using the zeta-calibration method (Hurford and Green 1983) on the base of the Durango standard with a zeta value of 355.96 ± 9.39 .

a) Tectonic map showing apatite fission track data. Samples labelled with circles are from Sanders (1998).
 b) Altitude vs. age diagram of the apatite fission track ages. The ages show relatively fast exhumation (at least 1mm/a) between 12-11 Ma followed by slow exhumation (around 0.1 mm/a) after 10 Ma.

c) Table regarding the apatite fission track data. Column 1 gives the sample code, column 2 the altitude above sea level, column 3 the number of dated grains. Columns 4, 5 and 6 show standard, spontaneous and induced track densities, respectively, and the number of counted tracks in brackets. Column 7 gives Chi-square probability (Galbraith 1981) and column 8 apatite fission track central ages (Galbraith and Laslett 1993), which are the weighted mean of the single grain ages.

Due to the lack of stratigraphical timing constraints along the Dragos-Voda fault, its activity was indirectly dated by inferences from the cooling history of the syn-kinematically exhumed Rodna horst (Fig. 2.8). A vertical profile covering about 1000 m of altitude difference has been sampled for apatite fission-track analysis (5 samples). The uppermost sample is taken close to the projected basal unconformity of the overlying Tertiary sediments. The presented samples have been selected from a larger set of data that will be discussed in more detail elsewhere (Gröger 2006).

Burial by Eocene to Lower Miocene sediments led to total annealing of fission tracks in all samples, as evidenced by the fact that all samples passed the Chi-square test (Fig. 2.8c; $\chi^2 > 5\%$). Subsequent cooling through the apatite fission track annealing zone yielded Middle to Late Miocene cooling ages (11.6 to 8.6 Ma, Fig. 8), where the youngest ages are found at the lowest altitudes of the profile. The three uppermost samples span 710 m, but yield similar ages (11.6, 11.0 and 11.6 Ma). A significant decrease in age can only be observed in the two lowermost samples (10.2 and 8.6 Ma).

The altitude vs. age relationship thus suggests enhanced exhumation between 12-11 Ma with exhumation rates of at least 1 mm/a. After 10 Ma the rate of exhumation decelerates to around 0.1 mm/a (Fig. 2.8b). Our data are in agreement with data by Sanders (1998), also depicted in Fig. 2.8a.

The enhanced cooling of the Rodna horst through the apatite partial annealing zone between 12-11 Ma is interpreted to be caused by fault-bounded exhumation in the footwall of the sinistral transtensive Dragos-Voda fault. This indirect dating of the transtensional stage based on apatite fission track analysis is consistent with stratigraphical timing constraints (12-10 Ma, see above) for transtension along the Bogdan-Voda fault. The concurrent time constraints, independently derived, support the conclusion that the Bogdan-Voda and Dragos-Voda faults acted as a single continuous fault during this second transtensional stage. Additionally, the apatite fission track data corroborate that the transtensional stage between 12-10 Ma represents the main phase of activity along the Dragos-Voda fault.

2.7 Synthesis of data

2.7.1 Burdigalian thrusting of the Pienides followed by NE-SW extension

Analysis of the structures related to the Burdigalian-age emplacement of the Pienides consistently yielded top-SE transport (Fig. 2.4a). Thrusting of the Pienides and within the autochthonous cover of Tisza-Dacia was coeval, as indicated by stratigraphic timing criteria corroborated by our kinematic analyses. A change from top-SE to top-ESE transport, as suggested by two of the studied outcrops, could not be consistently documented for the study area.

At first sight, the constant displacement directions inferred for the thrusting of the Pienides is in contradiction to the extremely variable trace of the frontal thrust in map view. The most likely explanation for the arcuate shape of the Pienide nappe contact is a laterally changing thrust plane geometry, with SW striking frontal ramps alternating with SE-striking tear faults and/or lateral ramps.

Although SE-striking normal faults, generated by a phase of SW-NE extension, are found throughout the study area, they are more abundant in the basement rocks of the Rodna horst (Fig. 2.4b) than in the Oligocene sediments. The age of this normal faulting is inferred as Late Burdigalian.

2.7.2 Post-Burdigalian faulting along the Bogdan- and Dragos-Voda faults

Our observations indicate a significant component of shortening during the earlier stage of left-lateral strike-slip movements along the Bogdan-Voda fault, which terminated towards the east along a SE striking thrust-splay, as mapped by Săndulescu (1994) and Dicea et al. (1980). Due to the scarcity of evidence for coeval transpressive deformation along the Dragos-Voda fault, we regard its role during this earlier stage of the post-Burdigalian deformation as subordinate.

Hence, the two fault segments were not yet linked, much of the offset along the Bogdan-Voda fault being taken up by thrusting along its eastern termination.

In the eastern part of the study area (near Borsa), a SE-trending back-thrust represents the major feature formed during this transpressive post-Burdigalian stage (Fig. 2.6a). The differences in deformational style between west and east may be due to earlier structures, particularly to the presence of a basement high in the area of the Rodna horst. This horst already existed during the Eocene. While the shallow marine Iza limestone formed on the Rodna horst, the pelagic sediments of the Vaser Formation were deposited north of it (Săndulescu et al. 1991, Kräutner et al. 1982). During the subsequent sinistral-transpressive stage the Bogdan-Voda and Dragos-Voda faults were kinematically linked; they acted as a single Bogdan- Dragos-Voda fault system, as mapped by Dicea et al. (1980). This is confirmed by structural and kinematic data and is also very evident from map-view. Additionally, intensely faulted outcrops situated at the junction between the two segments yield similar kinematics (Appendix 5, 6, Stations 0462, 0481, 0079) further corroborate this interpretation.

Since the major SW-trending normal faults within the Rodna horst and in the Maramures Mountains (i.e. the Greben fault) are kinematically compatible with this sinistral-transpressive activity along the Bogdan- Dragos-Voda fault system, we regard their activity as contemporaneous. The transtension along the Bogdan- Dragos-Voda fault system led to final cooling and exhumation of the Rodna horst from 12 Ma onwards, as indicated by apatite fission track data. Towards the east, the net left-lateral offset along the Bogdan- Dragos-Voda fault system decreases due to the distribution of deformation into a horse-tail like array of SW-trending normal faults. At the contact of the inner East Carpathians with the Miocene thrust belt of the Moldavides the localised offset diminishes to almost zero. Transtension also affected the southeastern part of the study area, where the entire Rodna horst is affected and partly bounded by SW-striking normal faults (Fig.6b, Appendix 5). Subordinate reactivation by transtension is also observed along the Preluca fault.

2.7.3 Estimates of horizontal and vertical components of displacement across the Bogdan-Voda and Dragos-Voda faults

Since movement along the Bogdan-Voda fault segment accumulated during two stages, we first evaluate the offsets along the Dragos-Voda fault, which was essentially active only during the later transpressive stage.

Based on published maps (Geological Survey of Romania) and stratigraphic logs of the sediments juxtaposed against the crystalline basement units (Dicea et al. 1980) the south-side-up vertical offset across the Dragos-Voda fault south of Borsa (Fig. 2.2) can be estimated to reach 2km. Assuming that the average measured pitch of striations at the Dragos-Voda fault of 15° (Appendix 5, 6) indicates the movement vector during transtension, the horizontal displacement had to be in the order of 7km.

Since offset along the Dragos-Voda fault continuously decreases from west to east due to coevally active SW-trending normal faults, the offset for a specific point can be estimated by a simple linear interpolation using the previously mentioned displacement estimates

together with the horizontal distance between Borsa and the point of negligible offset at the horsetail splay. Thus the maximum offset of the Dragos-Voda fault segment, accumulated in its westernmost part, can be estimated to reach values in the order of 11km (horizontal) and 3km (vertical), respectively. For the eastern part of the Rodna horst our linear approach predicts a vertical offset in the order of 1km. Apatite fission-track ages from this region (Sanders, 1998) are identical on either side of the Dragos-Voda fault (Fig. 2.8), thus also indicating minor (i.e. <1km) vertical displacement below data resolution.

A total lateral offset of about 25km for the Bogdan-Voda fault can be deduced from the left-lateral offset of the Pienide thrust front (Fig. 2.2). The north side down component is evidenced by the relative offset of the post-Burdigalian strata (Fig. 2.2). From the shallow plunge of lineations observed at the Bogdan-Voda fault (5° west), a total vertical offset of about 2.5km is obtained. Using the estimate of total lateral offset along the Dragos-Voda fault (see above), we infer that at least 11km lateral and 1km vertical offset were produced during the transtensional stage.

It should be noted, that the marked difference in vertical offsets between the Bogdan-Voda fault segment (1km) and Dragos-Voda fault segment (3km) during the transtensional stage is accommodated by the SW-trending Greben fault. Based on published geological maps (Geological Survey of Romania), the vertical offset at the Greben fault is estimated to reach about 2km.

2.8 Discussion of earlier work and large-scale correlations

2.8.1 Comparison with previous data from the working area

Our observations and conclusions are largely comparable to a previous study in this area carried out by Györfi et al. (1999). However, we consider SW-NE shortening to be post-Burdigalian rather than Oligocene in age. Györfi et al. (1999) correlated the Late Miocene activity of the Bogdan- Dragos-Voda fault system with extensional features of Early Pannonian (~9-11.8 Ma) age described in seismic studies from the Pannonian basin. This time frame is compatible with our timing estimates for the transtensional stage (12-10 Ma).

The conclusions of Huisman et al. (1997) strongly differ from our interpretation. The major difference to our study is that we regard the Early Burdigalian emplacement of the Pienides as top-SE directed rather than due to NNE-SSW compression. We partly disagree with Ciulavu (1999), who argued that extensional veins filled by hydrothermal ore deposits, dated to 8.7 ± 0.4 Ma (Pécskay et al. 1994) and found within the volcanic body of Baia Mare, point towards a post-10 Ma activity of the Bogdan-Voda fault. On the available maps the pyroxene andesites (10.1 – 10.9 Ma, Pécskay et al. 1994), constituting most of the volcanic body of Baia Mare, are not crosscut by the Bogdan-Voda fault. Hence we conclude, that major activity along the Bogdan- Dragos-Voda fault system ceased at some 10 Ma ago, while the mineralized veins indicate partial reactivation of minor importance only.

2.8.2 Burdigalian top-SE thrusting of the Pienides followed by NE-SW extension in the larger scale context

Based on seismic studies located in central Hungary Csontos and Nagymarosy (1998) report Oligocene to early Miocene-age thrusting of ALCAPA onto Tisza-Dacia along the Mid-Hungarian line. In agreement with Csontos and Nagymarosy (1998) and Csontos and Vörös (2004) we consider the Pienide nappe contact as representing the eastward continuation of the Mid-Hungarian fault zone during Burdigalian times. Since the Pienides are correlated with parts of the Western Carpathians (Săndulescu et al. 1981, Săndulescu 1994), i.e. with units that are clearly part of what is commonly referred to as “ALCAPA”, they are considered to represent the easternmost tip of ALCAPA.

Many authors postulate a significant (in the order of 90°) clockwise rotation of Tisza-Dacia during its mid-Miocene emplacement (e.g. Fodor et al. 1999, Márton and Fodor 2003). Such rotations should cause progressive reorientation of earlier formed structures (i.e. our nappe emplacement structures) as they are passively rotated together with the Tisza-Dacia block. However, we observed no regionally consistent evidence for such a change in transport directions. Thus we conclude that a major part of the rotation commenced earlier, possibly in the Early Oligocene, as is discussed in Györfi et al. (1999). This would imply that shortening across the Mid-Hungarian fault zone (Csontos and Nagymarosy 1998) and the emplacement of the Pienides in northern Romania only reflect the last stage of the juxtaposition of the ALCAPA and Tisza-Dacia blocks, a process that initiated much earlier (Csontos and Nagymarosy 1998). Comparable to the Late Burdigalian (~18.5 – 16 Ma) NE-SW extension documented in this study, Csontos and Nagymarosy (1998) report Early to Mid- Miocene extension within the Pannonian basin i.e. also along the Mid-Hungarian fault. Fodor et al. (1999) interpret NE-SW extension (17-15 Ma) within the Pannonian basin system as being related to back arc extension in the context of subduction roll-back in the Carpathians.

In conclusion, we regard Early Burdigalian top-SE thrusting of the Pienides, i.e. the easternmost tip of ALCAPA, to be related to transpression along the Mid-Hungarian fault zone in the context of lateral extrusion of ALCAPA. Subsequent Late Burdigalian NE-SW-directed extension marks the extensional overprint of the Tisza-Dacia block due to ongoing roll-back in the northernmost East Carpathians.

2.8.3 Post-Burdigalian activity along the Bogdan- Dragos-Voda fault system in the larger scale context

While subduction rollback migrates eastwards due to propagating slab detachment (Wortel and Spakman 2000) convergence in the western Carpathians comes to a halt and most likely leads to a pronounced change in deformational style along the Mid-Hungarian fault zone (Fodor et al. 1999). Late Badenian to Sarmatian (14-11 Ma) NW-SE extension in the Pannonian basin (Fodor et al. 1999) is interpreted as a period of left lateral transtension along the Mid-Hungarian fault zone (Csontos and Nagymarosy 1998).

The left-lateral activity of the Bogdan-Voda and Dragos-Voda faults (16–10 Ma) coincides with this phase of sinistral transtension along the Mid-Hungarian fault zone and suggests a direct kinematic link between all these faults during this time interval. We suggest that the differing kinematics in our working area – transpression followed by transtension – may be explained by the “docking” of Tisza-Dacia with the European foreland. Starting in Late Burdigalian times, NE-directed thrusting of the Miocene thrust belt (Matenco and Bertotti 2000) led to “soft collision” of Tisza-Dacia with the European foreland in the East Carpathians between some 16 to 10 Ma ago. This scenario is comparable to the Western Carpathians, where Sperner et al. (2002) correlate NNE-SSW compression (dated by these authors as Oligocene (?) to Mid-Miocene) with “soft collision” between ALCAPA and the European continent. Final emplacement of the northern part of Tisza-Dacia induces the change towards the transtensional activity along the Bogdan- Dragos-Voda fault system. This transtensional stage is coeval to Late Sarmatian strike-slip activity in the external Miocene thrust belt of the East Carpathians (Matenco and Bertotti, 2000).

Our data indicate a direct kinematic link between the Mid-Hungarian fault zone, the Bogdan-Voda fault and the Bogdan-Dragos-Voda fault system since post-Burdigalian times. However, since the Bogdan-Voda and Dragos-Voda faults are located within the Bucovinian basement (i.e. within the Dacia Block) they should not be considered as representing the continuation of the Mid-Hungarian Line as defined by Csontos and Nagymarosy (1998). Moreover, the amount of displacement documented for the Bogdan-Dragos-Voda fault system (~26km) rapidly diminishes towards the east. Its termination before reaching the foreland fold-and-thrust-belt, as well as the coeval activity at the Preluca fault and faulting south of the Rodna horst, suggests a rather distributed linkage of the foreland fold-and-thrust-belt with the extensional back-arc domain in post-Burdigalian times. This is in agreement with the interpretation of Matenco and Bertotti (2000), who demonstrated that deformation caused by the final ESE-ward emplacement (Latest Sarmatian-Early Meotian, ~10 – 8 Ma) was distributed over large parts of the East Carpathians. According to these authors the ESE movement of the central sectors of the Eastern Carpathians was accommodated by numerous E-W trending sinistral faults located east of our study area, rather than by one major strike-slip fault such as the Bogdan- Dragos-Voda fault system.

2.9 Conclusions

1. Early Burdigalian (20.5 - ~18.5 Ma) SE- directed emplacement of the Pienides, i.e. the eastern tip of ALCAPA, onto Tisza-Dacia is correlated with the thrusting of ALCAPA over Tisza-Dacia along the Mid-Hungarian line observed in the subsurface of the Pannonian basin (Csontos and Nagymarosy 1998). The Pienide nappe front in Maramures is kinematically linked to dextrally transpressive movements along the Mid-Hungarian fault zone that, together with the Periadriatic line, accommodates the lateral extrusion of ALCAPA.
2. Minor Late Burdigalian (18.5-16 Ma) NE-SW extension is interpreted as due to back-arc extension related to subduction roll back in the northernmost East Carpathians.

3. In post-Burdigalian (post-16 Ma) times a pronounced change in the tectonic regime led to NE-SW shortening and NW-SE extension. This change correlates with “soft collision” of Tisza-Dacia with the European foreland and the migration of active subduction from N to S along the Miocene foredeep of the Eastern Carpathians. Post-Burdigalian deformation was concentrated along the Bogdan-Voda and Dragos-Voda faults. Sinistral transpression (16 - 12 Ma) was mainly restricted to the Bogdan-Voda fault, which terminated eastwards in a thrust splay geometry. Sinistral transtension (12 – 10 Ma) was kinematically linked along the Bogdan- and Dragos-Voda fault segments (Bogdan- Dragos-Voda fault system). During this transtensional stage, coevally active SW-NE trending normal faults reduced the left-lateral offset towards the east, where the fault system terminates in an extensional horse - tail splay. The Bogdan- Dragos-Voda fault system is kinematically linked to the Mid-Hungarian fault zone during the post-Burdigalian stages, albeit deformation is distributed over large parts of the East Carpathians.

2.10 Acknowledgements

We are very grateful for an excellent introduction into the geology of the area by M. Săndulescu and L. Matenco and for all the discussions we had with them and with all the other Romanian colleagues. We would also like to particularly mention the fruitful interactions with L. Csontos, L. Fodor, S. Kovács, M. Marin, E. Márton, C. Pero, D. Radu, D. Badescu and C. Krezsek during our study. M. Marin is gratefully acknowledged for providing additional data from the eastern part of the study area. The careful and constructive review by L. Ratschbacher significantly improved a first version of the text. This work was financed by NF-projects Nr. 21-64979.01, Nr. 200020-105136/1 and Nr. 200021-101882/1, granted to B.F. and S.Sch., respectively.

2.11 References

- Angelier J, Mechler P (1977) Sur une méthode graphique de recherche des contraintes principales également utilisable en tectonique et enséismologie: la methode des diédres droits. Bull Soc Géol France VII 19: 1309-1318
- Antonescu F, Mitrea G, Popescu A (1981) Contributii la cunoasterea stratigrafiei si tectonicii miocenului din regiunea Vadu Izei-Birsan-Botiza (Maramures). D.S. Inst Geol Geofiz LXVI: 5-23
- Aroldi C (2001) The Pienides in Maramures – Sedimentation, tectonics and paleogeography. PhD Thesis, Cluj, pp 1-156
- Balintoni I (1995) Alpine structural outline of the Pannonian Carpathian realm. Studia Universitates Babes - Bolyai, Geologia XL(2): 3 – 16
- Balla Z (1982) Development of the Pannonian Basin basement through the Cretaceous-Cenozoic collision; a new synthesis. Tectonophysics 88: 61-102
- Balla Z (1987) Tertiary paleomagnetic data for the Carpatho-Pannonian region in the light of Miocene rotation kinematics. Tectonophysics 139: 67-98
- Bingham C (1964) Distributions on a sphere and the projective plane. PhD. diss. Yale University, New Haven, pp 1-93
- Burchfiel BC (1980) Eastern European Alpine system and the Carpathian orocline as an example of collision tectonics. Tectonophysics 63: 31–61
- Ciulavu D (1999) Tertiary tectonics of the Transylvanian Basin. PhD. diss. Vrije Universiteit Amsterdam, Amsterdam, pp 1-154
- Cloetingh S, Bada G, Matenco L, Lankreijer A, Horváth F, Dinu C (2005) Thermo-mechanical modelling of the Pannonian-Carpathian system: Modes of tectonic deformation, lithospheric strength and vertical motions. Geol. Soc. London Spec. Publ., in press.
- Csontos L, Nagymarosy A, Horváth F, Kováč M (1992) Cenozoic evolution of the Intra-Carpathian area: a model. Tectonophysics 208: 221–241
- Csontos L, Nagymarosy A (1998) The Mid-Hungarian line: a zone of repeated tectonic inversions. Tectonophysics 297: 51-71
- Csontos L, Vörös A (2004) Mesozoic plate tectonic reconstruction of the Carpathian region. Paleogeography, Paleoclimatology, Paleoecology 210: 1-56
- Dicea O, Dușescu P, Antonescu F, Mitrea G, Botez R, Donos I, Lungu V, Moroșanu I (1980) Contributii la cunoasterea stratigrafiei zonei transcarpatice din maramures. D. S. Inst geol geofiz LXV, 4: 21- 85
- Dimitrijevic MD (2001) Dinarides and the Vardar Zone: a short review of the geology. Acta Vulcanologica 13: 1-8.
- Dunkl I (2002) Trackkey: a Windows program for calculation and graphical presentation of fission track data. Computers & Geosciences 28: 3-12
- Fodor L, Jelen B, Márton M, Skaberne D, Car J, Vrabec M (1998) Miocene-Pliocene tectonic evolution of the Slovenian Periadriatic fault: Implications for Alpine-Carpathian extrusion models. Tectonics 17: 690-709

- Fodor L, Csontos L, Bada G, Györfi I, Benkovics L (1999) Cenozoic tectonic evolution of the Pannonian basin system and neighbouring orogens: a new synthesis of paleostress data. In: Durand B, Jolivet L, Horváth F, Séranne M (eds). *The Mediterranean basins: Cenozoic Extension within the Alpine Orogen*. Geol Soc Spec Publ 156: 295–334
- Fügenschuh B, Schmid SM (2005) Age and significance of core complex formation in a highly bent orogen: evidence from fission track studies in the South Carpathians (Romania). *Tectonophysics* in press
- Galbraith RF (1981) On statistical models for fission track counts. *Math Geol* 13: 471-488.
- Galbraith RF, Laslett GM (1993) Statistical models for mixed fission track ages. *Nucl Tracks Radiat Meas* 21: 450-470
- Gallagher K, Brown R, Johnson C. (1998) Fission track analysis and its applications to geological problems. *Annu Rev Earth Planet Sci* 26: 519-571
- Gleadow AJW (1981) Fission track dating methods: what are the real alternatives ? *Nucl Tracks* 5: 3-14
- Gleadow AJW, Duddy IR (1981) A natural long-term track annealing experiment for apatite. *Nucl Tracks* 5(1/2): 169-174
- Gradstein F, Ogg J, Smith A (2004) *A Geologic Time Scale*. Cambridge University Press, Cambridge, pp 1 – 589
- Gröger HR (2006) Thermal and structural evolution of the East Carpathians in northern Romania: from Cretaceous orogeny to final exhumation during Miocene collision. Published PhD-Thesis, Basel, Switzerland pp. 1 - 111
- Györfi I, Csontos L, Nagymarosy A, (1999) Early Cenozoic structural evolution of the border zone between the Pannonian and Transylvanian basins. In: Durand B, Jolivet L, Horváth F, Séranne M (eds). *The Mediterranean Basins: Cenozoic Extension within the Alpine Orogen*. Geol Soc Spec Publ 156: 251– 267
- Haas J, Pero S (2004) Mesozoic evolution of the Tisza Mega-unit. *Int J Earth Sci* 93: 297-313
- Haas J, Mioč P, Pamić J, Tomljenović B, Árkai P, Bérczi-Makk A, Koroknai B, Kovács S, Rálich-Felgenhauer E (2000). Complex structural pattern of the Alpine-Dinaridic-Pannonian triple junction. *Int J Earth Sci* 89: 377-389
- Horváth F, Bada G, Szafián P, Tari G, Ádám A, Cloetingh S (2005) Formation and deformation of the Pannonian basin: constraints from observational data. *Geol Soc London Spec Publ*, in press.
- Huisman RS, Bertotti G, Ciulavu D, Sanders CAE, Cloetingh S, Dinu C (1997) Structural evolution of the Transylvanian Basin (Romania): a sedimentary basin in the bend zone of the Carpathians. *Tectonophysics* 272: 249-268
- Hurford AJ, Green PF (1983) The zeta age calibration of fission track dating. *Isotope Geoscience* 1: 185-317
- Kovács S, Haas S, Csazar G, Szederkenyi T, Buda G, Nagymarosy A (2000) Tectonostratigraphic terranes in the pre-Neogene basement of the Hungarian part of the Pannonian area. *Acta Geol Hung* 43/3: 225-328
- Kräutner HG, Kräutner F, Szasz L (1982): *Geological Map 1:50.000 No 20a Pietrosul Rodnei*. Institutul de Geologie si Geofizica, Bucharest.
- Marret R, Allmendinger RW (1990) Kinematic analysis of fault slip-data. *J Struct Geol* 12: 973-986

- Márton E, (2000) The Tisza Megatectonic Unit in the light of paleomagnetic data. *Acta Geol Hung* 43/3: 329–343
- Márton E, Fodor L (1995) Combination of palaeomagnetic and stress data - a case study from North Hungary. *Tectonophysics* 242: 99–114
- Márton E, Fodor L (2003) Tertiary paleomagnetic results and structural analysis from the Transdanubian Range (Hungary): rotational disintegration of the ALCAPA unit. *Tectonophysics* 363: 201-224
- Mason PRD, Seghedi I, Szákasc A, Downes H (1998) Magmatic constraints on geodynamic models of subduction in the Eastern Carpathians, Romania. *Tectonophysics* 297: 157-176
- Matenco L, Bertotti G (2000) Tertiary tectonic evolution of the external East Carpathians (Romania). *Tectonophysics* 316: 255-286
- Matenco L, Bertotti G, Cloetingh S, Dinu C (2003) Subsidence analysis and tectonic evolution of the external Carpathian-Moesian Platform during Neogene times. *Sediment Geol* 156: 71-94
- Nemčok M (1993) Transition from convergence to escape: field evidence from the West Carpathians. *Tectonophysics* 217: 117-142
- Pamic J (2000) Basic geological features of the Dinarides and South Tisia. In: Pancardi 2000 Fieldtrip Guidebook (eds. Pamic, J. and Tomljenovic, B.). *Vijesti* 37/2: 9-18
- Pécskay Z, Edelstein O, Kovacs M, Bernád A, Crihan M (1994) K/Ar age determination of Neogene volcanic rocks from the Gutai Mts. (Eastern Carpathians, Romania). *Geol Carp* 45(6): 357-363
- Pécskay Z, Edelstein O, Seghedi I, Szakács A, Kovacs M, Crihan M, Bernád A (1995) K-Ar datings of Neogene-Quaternary calc-alkaline volcanic rocks in Romania. In: Downes H, Vaselli O (eds). *Neogene and related magmatism in the Carpatho-Pannonian Region. Acta Vulcanologica* 7: 53-61
- Plasienska D, Grecula P, Mutis M, Kováč M, Hovorca D (1997a) Evolution and structure of the Western Carpathians: an overview. In: (Grecula, P. et al. eds) *Geological Evolution of the Western Carpathians. Mineralia Slovaca Monograph*, Bratislava, pp 1-24
- Plasienska D, Putis M, Kováč M, Sefara J, Hrussecky I (1997b): Zones of Alpidic subduction and crustal underthrusting in the Western Carpathians. In: (Grecula, P. et al. eds) *Geological Evolution of the Western Carpathians, Mineralia Slovaca Monograph*, Bratislava, pp 35-42.
- Pfiffner OA, Burkhard M (1987) Determination of paleo-stress axes orientations from fault, twin and earthquake data. *Annales Tectonicae* 1(1): 48-57
- Ratschbacher L, Linzer HG, Moser F, Strusievicz RO, Bedeleian H, Har N, Mogos PA (1993): Cretaceous to Miocene thrusting and wrenching along the central South Carpathians due to a corner effect during collision and orocline formation. *Tectonics* 12(4): 855-873
- Ratschbacher L, Merle O, Davy P, Cobbold P (1991a) Lateral extrusion in the Eastern Alps; Part 1, Boundary conditions and experiments scaled for gravity. *Tectonics* 10(2): 245–256
- Ratschbacher L, Frisch W, Linzer HG, Merle O, (1991b) Lateral extrusion in the Eastern Alps; Part 2, Structural analysis. *Tectonics* 10(2): 257–271

- Royden LH (1988) Late Cenozoic Tectonics of the Pannonian Basin System In: Royden LH, Horváth F (eds). The Pannonian Basin; a study in basin evolution. AAPG Mem 45: 27-48
- Sanders C (1998) Tectonics and erosion: competitive forces in a compressive orogen. A fission track study of the Romanian Carpathians. Ph.D. thesis, Vrije Universiteit Amsterdam, Amsterdam, pp 1-204
- Săndulescu M (1980) Sur certains problèmes de la corrélation des Carpathes orientales Roumaines avec les Carpathes Ukrainiennes. D. S. Inst geol geofiz LXV(5): 163-180
- Săndulescu M, Krätner HG, Balintoni I, Russo-Săndulescu D, Micu M (1981): The Structure of the East Carpathians. (Guide Book B1), Carp-Balk Geol Assoc 12th Congress, Bucharest, pp 1-92
- Săndulescu M, (1984) Geotectonica Romaniei. Editura Tehnica, Bucharest, pp1 – 450
- Săndulescu M, Szasz L, Balintoni I, Russo-Săndulescu D, Badescu D (1991): Geological Map 1:50.000 No 8d Viseu. Institutul de Geologie si Geofizica, Bucharest.
- Săndulescu M, Visarion M, Stanica D, Stanica M, Atanasiu L (1993) Deep Structure of the inner Carpathians in the Maramures-Tisa zone (East Carpathians). Rom J Geophysics 16: 67-76
- Săndulescu M (1994) Overview of Romanian Geology. In: ALCAPA II field guide book. Romanian J of Tectonics and Reg Geol, 75 suppl. 2: 3-15
- Schmid SM, Berza T, Diaconescu V, Froitzheim N, Fügenschuh B (1998) Orogen-parallel extension in the South Carpathians. Tectonophysics 297: 209-228
- Schmid SM, Fügenschuh B, Kissling E; Schuster R (2004a) Tectonic map and overall architecture of the Alpine orogen. *Eclogae geologicae Helveticae* 97: 93-117
- Schmid SM, Fügenschuh B, Kissling E; Schuster R (2004b) TRANSMED Transects IV, V and VI: Three lithospheric transects across the Alps and their forelands. In: Cavazza W, Roure FM, Spakman W, Stampfli GM, Ziegler PA (eds). The TRANSMED Atlas: The Mediterranean Region from Crust to Mantle. Springer, Berlin Heidelberg, attached CD (version of the explanatory text available from the first author as a pdf-file upon request)
- Sperner B, Ratschbacher L, Nemčok M (2002) Interplay between subduction retreat and lateral extrusion: tectonics of the Western Carpathians. *Tectonics* 21(6): 1051
- Sperner B, CRC 461 Team (2005) Monitoring of Slab Detachment in the Carpathians. In: Wenzel F (ed). *Perspectives in modern Seismology. Lecture Notes in Earth Sciences* 105: 187-202
- Stampfli GM, Borel G (2004) The TRANSMED transects in space and time: constraints on the paleotectonic evolution of the Mediterranean domain. In: Cavazza W, Roure FM, Spakman W, Stampfli GM, Ziegler PA (eds). The TRANSMED Atlas: The Mediterranean Region from Crust to Mantle. Springer, Berlin and Heidelberg, pp 53-80
- Steiniger FF, Wessely G (2000) From the Thethyan Ocean to the Paratethys Sea: Oligocene to Neogene Stratigraphy, Paleogeography and Paleobiogeography of the circum-Mediterranean region and the Oligocene to Neogene Basin evolution in Austria. *Mitt Österr Geol Ges* 92: 95-116
- Wortel MJR, Spakman W (2000) Subduction and slab detachment in the Mediterranean-Carpathian region. *Science* 290: 1910-1917

2.12 Appendix

Appendix 1a: Tabular overview on fault-slip data (for legend see Appendix 1b)

no.	x	y	lithology	rock age	short.	interm.	ext.	r	regime	N D	
data correlated to early Burdigalian nappe emplacement											
0006	24.7279	47.6816	fine flysch	Eocene	101	01	206	57	005 31 1	compressional strike slip	36
0215	24.3295	47.7339	flysch	Oligocene	324	03	233	22	062 68 3	reverse faulting	3
0236	24.0302	47.5991	flysch	Eocene	149	21	054	07	308 66 1	reverse faulting	10
0248	24.0344	47.5970	red marl	Late Cretaceous	145	12	053	08	290 75 2	reverse faulting	6
0272	24.1638	47.9015	conglomerate	L. Alb-Cenomanian	307	14	040	10	164 73 2	reverse faulting	5
0288	24.4847	47.6128	flysch	Rupelian	140	03	050	01	306 87 2	reverse faulting	8
0291	24.4334	47.5459	red marl	Late Cretaceous	124	02	034	21	219 69 2	reverse faulting	5
0314	24.2191	47.7545	flysch	Lutetian-Priabonian	145	00	236	81	055 09 3	compressional strike slip	7
0322	24.4250	47.5912	flysch	Rupelian	129	02	219	15	031 75 1	reverse faulting	6
0326	24.3454	47.4183	sandstone	Oligocene	342	16	072	01	167 74 2	reverse faulting	7
0414	24.3011	47.7350	flysch	Rupelian	093	04	185	32	357 58 1	reverse faulting	6
0453	24.4006	47.7251	flysch	Rupelian	315	02	224	28	049 62 1	reverse faulting	7
0584	24.0641	47.5791	flysch	Priabonian-?Oligocene	158	01	068	07	257 83 1	reverse faulting	18
0639	24.0950	47.8813	red marl	Late Cretaceous	137	09	233	36	035 52 1	compressional strike slip	30
0692	24.0752	47.8488	flysch	Lutetian-Priabonian	111	18	014	22	237 61 3	reverse faulting	6
0743	24.7105	47.6698	marl	Eocene	102	12	354	54	200 33 3	reverse faulting	5
0822	24.3608	47.4721	flysch	Rupelian - Aquitanian	352	05	261	14	100 76 2	reverse faulting	19
0892	24.4782	47.5418	marl	Turonian-Priabonian	162	23	331	67	070 04 1	compressional strike slip	11
1025	24.4616	47.5955	marl	Turonian-Priabonian	341	05	248	28	079 61 1	reverse faulting	14
1056	24.1420	47.5801	flysch	Priabonian-?Oligocene	157	30	037	40	271 35 2	compressional strike slip	5
data correlated to late Burdigalian SW-NE extension											
0236	24.0302	47.5991	flysch	Eocene	148	36	306	51	050 11 1	extensional strike slip	29
0267	23.9266	47.4746	flysch	Chattian-Aquitainian	251	72	145	05	054 17 3	normal faulting	3
0368	24.9089	47.5638	crystalline	basement	285	73	114	17	023 03 1	normal faulting	14
0374	24.6976	47.6213	crystalline	basement	141	12	329	77	232 02 2	extensional strike slip	5
0376	24.8780	47.5983	crystalline	basement	184	58	326	26	064 17 1	extensional strike slip	11
0633	24.3596	47.7297	flysch	Rupelian	114	61	343	20	246 20 2	normal faulting	8
0765	25.1171	47.5908	crystalline	basement	144	78	293	10	024 06 3	normal faulting	5
0792	24.7005	47.4143	crystalline	basement	325	62	109	24	206 15 3	normal faulting	3
0799	24.8962	47.4492	crystalline	basement	037	68	130	01	221 21 1	normal faulting	25
0801	24.8055	47.4421	crystalline	basement	357	56	113	17	212 29 2	normal faulting	9
0802	24.5876	47.5191	crystalline	basement	087	71	297	17	204 09 1	normal faulting	43
0804	24.5811	47.5256	crystalline	basement	100	69	315	17	222 11 1	normal faulting	7
0816	24.6441	47.3919	conglomerate	Eocene	139	36	003	45	248 24 2	extensional strike slip	6
0915	24.0888	47.6218	flysch	Ypresian-Lutetian	128	81	331	08	241 03 3	normal faulting	3
0925	23.9891	47.6164	flysch	Ypresian-Lutetian	161	70	275	08	007 18 2	normal faulting	6
M 30	25.1658	47.5551	crystalline	basement	263	34	116	51	004 16 2	extensional strike slip	11
M 41	25.4644	47.5276	crystalline	basement	139	12	270	72	046 13 2	strike slip	8
M 66	25.3566	47.5826	crystalline	basement	146	19	016	63	243 19 2	extensional strike slip	7
data correlated to post-Burdigalian transpressional stage											
0008	24.2418	47.6984	tuff	Badenian	050	10	298	65	145 22 1	compressional strike slip	13
0059	24.8196	47.6257	conglomerate	Lutetian	225	12	130	23	339 63 2	compressional strike slip	9
0147	24.2452	47.8174	flysch	Lutetian-Priabonian	024	05	284	66	116 23 2	compressional strike slip	16
0237	24.0220	47.5875	flysch	Oligocene-E. Miocene	001	06	298	73	098 16 2	compressional strike slip	11
0259	23.6433	47.5093	crystalline	basement	089	01	139	24	317 66 1	reverse faulting	7
0260	23.8639	47.4366	flysch	Burdigalian	249	06	157	13	006 76 3	reverse faulting	3
0276	24.2015	47.8582	flysch	Oligocene	192	16	101	02	004 74 2	reverse faulting	6
0310	24.1013	47.7794	flysch	Priabonian	212	13	321	55	114 32 1	compressional strike slip	12
0322	24.4274	47.5643	flysch	Rupelian	037	10	305	11	167 76 3	reverse faulting	2
0357	24.8414	47.6499	crystalline	basement	049	03	318	18	147 72 1	reverse faulting	6
0360	24.9921	47.5859	flysch	Lutetian	189	04	094	52	282 38 1	compressional strike slip	13
0462	24.4936	47.6215	limestone	Lutetian-Priabonian	048	05	313	45	143 45 1	compressional strike slip	6
0556	23.8153	47.4966	crystalline	basement	014	08	112	45	276 44 2	compressional strike slip	9
0631	24.3719	47.8333	flysch	Oligocene	255	00	345	61	165 29 1	compressional strike slip	5
0632	24.3395	47.8286	flysch	Oligocene	054	02	323	25	149 65 2	compressional strike slip	7
0675	24.2141	47.6546	flysch	Oligocene	249	03	351	76	159 13 1	compressional strike slip	8
0682	24.2234	47.6636	flysch	Oligocene	063	11	159	29	314 59 3	compressional strike slip	5
0809	24.8339	47.6486	marl/limeston	Lutetian-Priabonian	210	04	119	02	001 86 1	reverse faulting	12
0917	24.0219	47.6177	flysch	Ypresian-Lutetian	245	03	154	17	344 73 2	reverse faulting	13

Appendix 1b: Tabular overview on fault-slip data (continued)

no.	x	y	lithology	rock age	short.	interm.	ext.	r	regime	N D			
data correlated to post-Burdigalian transtensional stage													
0059	24.8196	47.6257	conglomerate	Lutetian	144	72	245	03	336	17	1	extensional strike slip	9
0060	24.7894	47.6107	crystalline	basement	235	38	063	52	328	04	1	extensional strike slip	11
0079	24.4717	47.6215	limestone	Lutetian-Priabonian	223	46	069	41	327	13	1	extensional strike slip	9
0095	24.4103	47.6212	flysch	Lutetian-Priabonian	208	76	066	11	334	08	3	normal faulting	5
0152	24.1337	47.6965	tuff	Badenian	219	27	036	63	128	01	2	extensional strike slip	5
0170	24.1472	47.6656	flysch	Ypresian-Lutetian	037	16	189	72	304	08	2	strike slip	5
0180	24.3487	47.6356	flysch	Lutetian-Priabonian	245	35	058	55	152	03	2	extensional strike slip	11
0236	24.0302	47.5991	flysch/marl	Late Jur.-Eocene	186	11	072	65	281	22	1	strike slip	19
0259	23.6433	47.5093	crystalline	basement	016	44	193	46	285	02	1	extensional strike slip	7
0272	24.1638	47.9015	conglomerate	L. Albian-Cenomanian	077	09	324	67	171	21	2	strike slip	5
0275	24.1536	47.8973	limestone	Lutetian-Priabonian	156	71	038	09	305	16	2	normal faulting	7
0292	24.4926	47.7065	flysch	Rupelian	069	53	229	35	326	10	2	extensional strike slip	7
0297	24.5695	47.7276	flysch	Oligocene	196	24	359	65	103	06	2	extensional strike slip	7
0346	25.1493	47.5659	crystalline	basement	316	61	225	00	135	29	2	normal faulting	6
0360	24.9921	47.5859	sandstone	Lutetian	203	10	060	77	295	08	1	strike slip	18
0363	24.8924	47.6024	crystalline	basement	213	20	021	70	122	04	1	strike slip	14
0368	24.9089	47.5638	crystalline	basement	273	60	043	21	142	21	2	normal faulting	10
0369	24.6908	47.5981	crystalline	basement	131	68	023	07	291	21	2	extensional strike slip	11
0374	24.6976	47.6213	crystalline	basement	219	14	049	75	310	02	2	strike slip	20
0385	24.6186	47.7480	flysch	Oligocene	227	21	055	68	318	03	2	extensional strike slip	4
0386	24.6177	47.7499	crystalline	basement	248	63	080	27	348	05	1	normal faulting	12
0387	24.6069	47.7611	crystalline	basement	161	70	037	12	303	16	1	normal faulting	9
0390	24.0066	47.8386	tuff	Badenian	016	36	213	53	112	08	2	extensional strike slip	7
0413	24.8755	47.5983	crystalline	basement	298	76	178	88	088	12	2	normal faulting	8
0452	24.1424	47.7375	flysch	L. Lutetian/Bartonian	050	73	238	16	147	02	2	normal faulting	8
0462	24.4936	47.6215	limestone	Lutetian-Priabonian	224	66	051	24	320	03	1	extensional strike slip	12
0481	24.5200	47.6219	crystalline	basement	225	51	052	39	319	03	1	extensional strike slip	14
0534	23.6282	47.5041	crystalline	basement	022	45	213	44	117	06	3	extensional strike slip	4
0550	23.8101	47.4680	crystalline	basement	320	81	053	00	143	09	3	normal faulting	6
0556	23.8153	47.4966	crystalline	basement	191	14	055	70	284	13	2	extensional strike slip	9
0588	23.9867	47.5482	flysch	Early Miocene	163	50	032	29	287	25	2	extensional strike slip	11
0625	24.1412	47.6479	tuff	Ypresian-Lutetian	244	52	061	38	152	01	1	extensional strike slip	26
0681	24.2230	47.6629	sandstone	Badenian	213	37	051	51	310	09	1	strike slip	18
0712	23.9619	47.8797	sandstone	Badenian	051	64	218	26	311	05	1	normal faulting	9
0720	24.1340	47.6577	flysch	Ypresian-Lutetian	011	04	116	76	280	14	3	strike slip	8
0733	24.0414	47.8737	tuff	Badenian	009	29	202	61	102	05	1	strike slip	17
0758	25.1234	47.5824	dolomite	basement	038	01	132	82	308	08	1	extensional strike slip	23
0774	24.5453	47.4003	crystalline	basement	030	39	246	45	136	19	2	extensional strike slip	8
0797	24.9295	47.4590	conglomerate	Cretaceous	345	46	228	13	133	23	1	normal faulting	13
0799	24.8962	47.4492	crystalline	basement	021	70	198	20	289	01	2	normal faulting	9
0801	24.8055	47.4421	crystalline	basement	036	61	204	28	296	05	2	normal faulting	11
0804	24.5811	47.5256	crystalline	basement	035	54	272	21	171	27	2	extensional strike slip	8
0807	24.5791	47.4538	crystalline	basement	028	36	219	53	122	05	3	extensional strike slip	4
0814	24.6391	47.4729	crystalline	basement	032	04	203	86	302	01	3	strike slip	10
0818	24.8228	47.4932	crystalline	basement	134	82	037	01	307	08	1	normal faulting	22
0832	24.2835	47.6576	flysch	Rupelian	053	08	180	78	321	10	1	strike slip	21
0838	24.2668	47.6507	sandstone	Badenian	022	05	267	78	113	11	1	strike slip	37
0897	23.6856	47.5602	sandstone	Badenian	042	02	148	82	312	08	2	strike slip	5
M 19	25.0739	47.5916	crystalline	basement	208	03	101	79	299	10	1	strike slip	12
M 27	25.1569	47.5714	crystalline	basement	017	02	162	84	107	05	1	strike slip	9
M 32	25.1724	47.5521	crystalline	basement	041	03	139	73	310	17	1	strike slip	15
M 41	25.4644	47.5276	crystalline	basement	055	01	150	82	324	08	2	strike slip	7

no.: reference number of outcrop, prefix M: data provided by Mihai Marin

X/Y.: coordinates of the outcrops in decimal degrees Lat/Long, WGS 84.

short. / interm. / ext.: orientation of mean kinematic axes (shortening, intermediate, extensional), derived by eigenvector analysis of the shortening/extensional fields obtained by the right dihedral method (Angelier and Mechler 1977).

r: data quality rating: 1: good; 2: moderate; 3: poor.

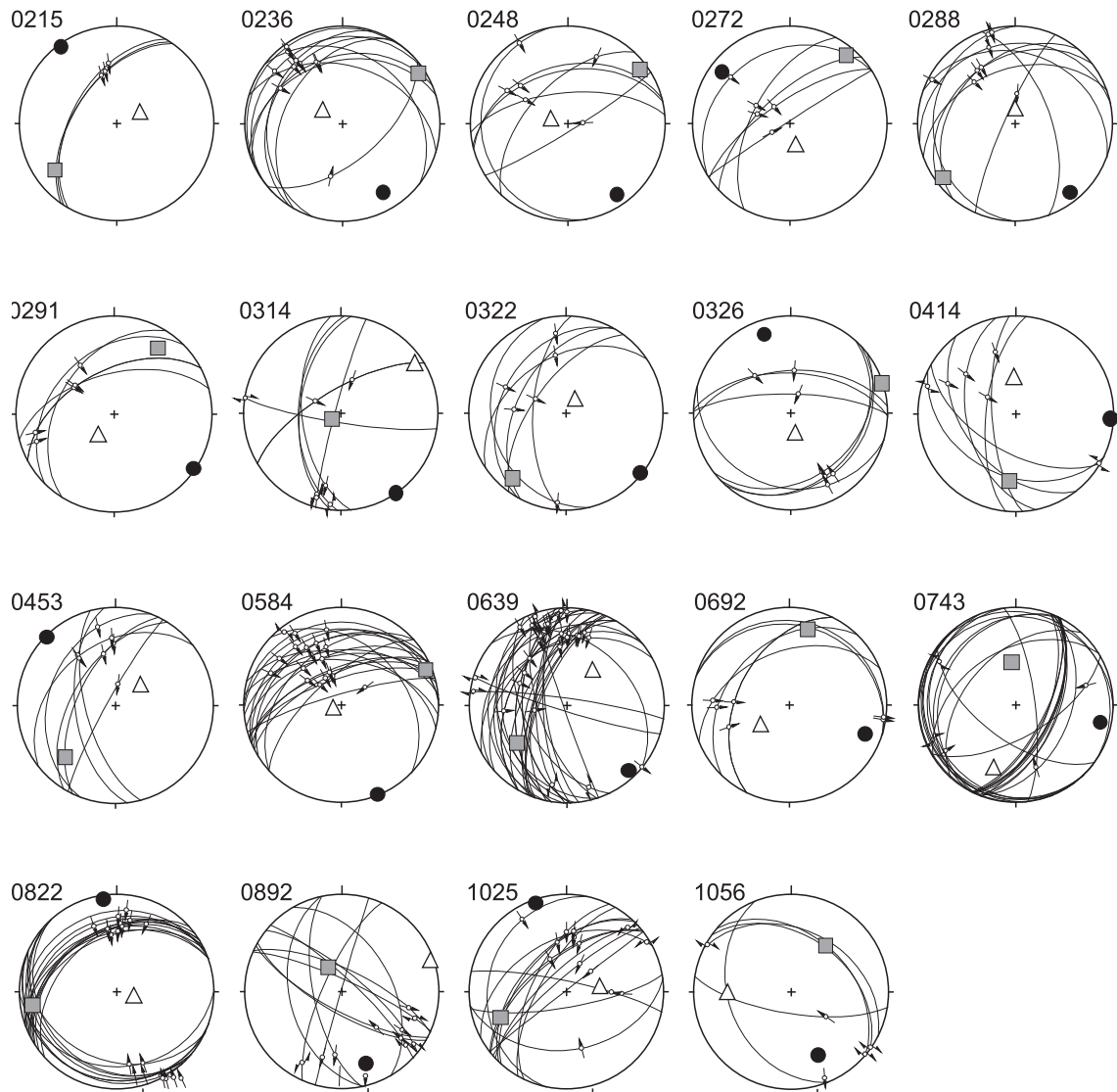
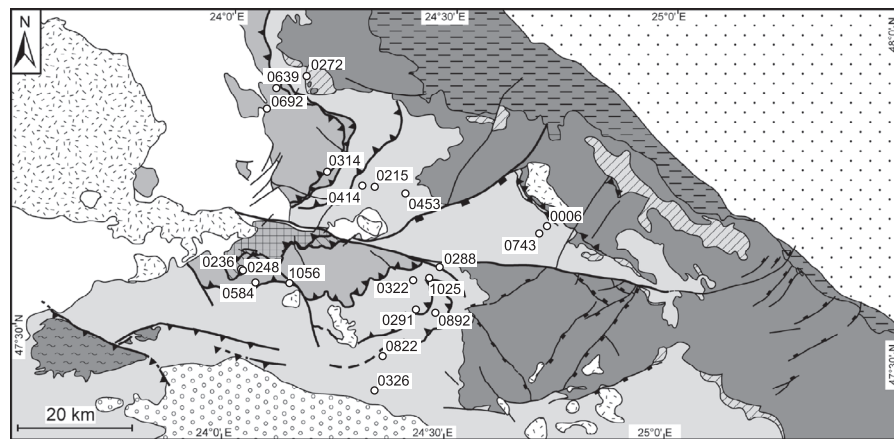
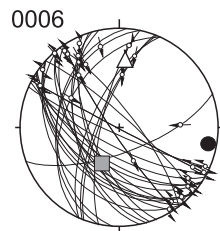
regime: tectonic regime of deformation assessed by the distribution of incremental strain axes (Marret and Almendinger, 1990). Reverse faulting, normal faulting, strike-slip faulting: well-clustered shortening and extension axes; compressional strike-slip: well clustered shortening axes with great circle distribution of extensional axes; extensional strike-slip: well clustered extension axes with great circle distribution of shortening axes.

ND: number of fault-slip sets attributed to respective regime, only fault-slip sets with certain slip sense have been included.

Appendix 2: Fault-slip data (Early Burdigalian top SE-thrusting of the Pienides)

Legend:

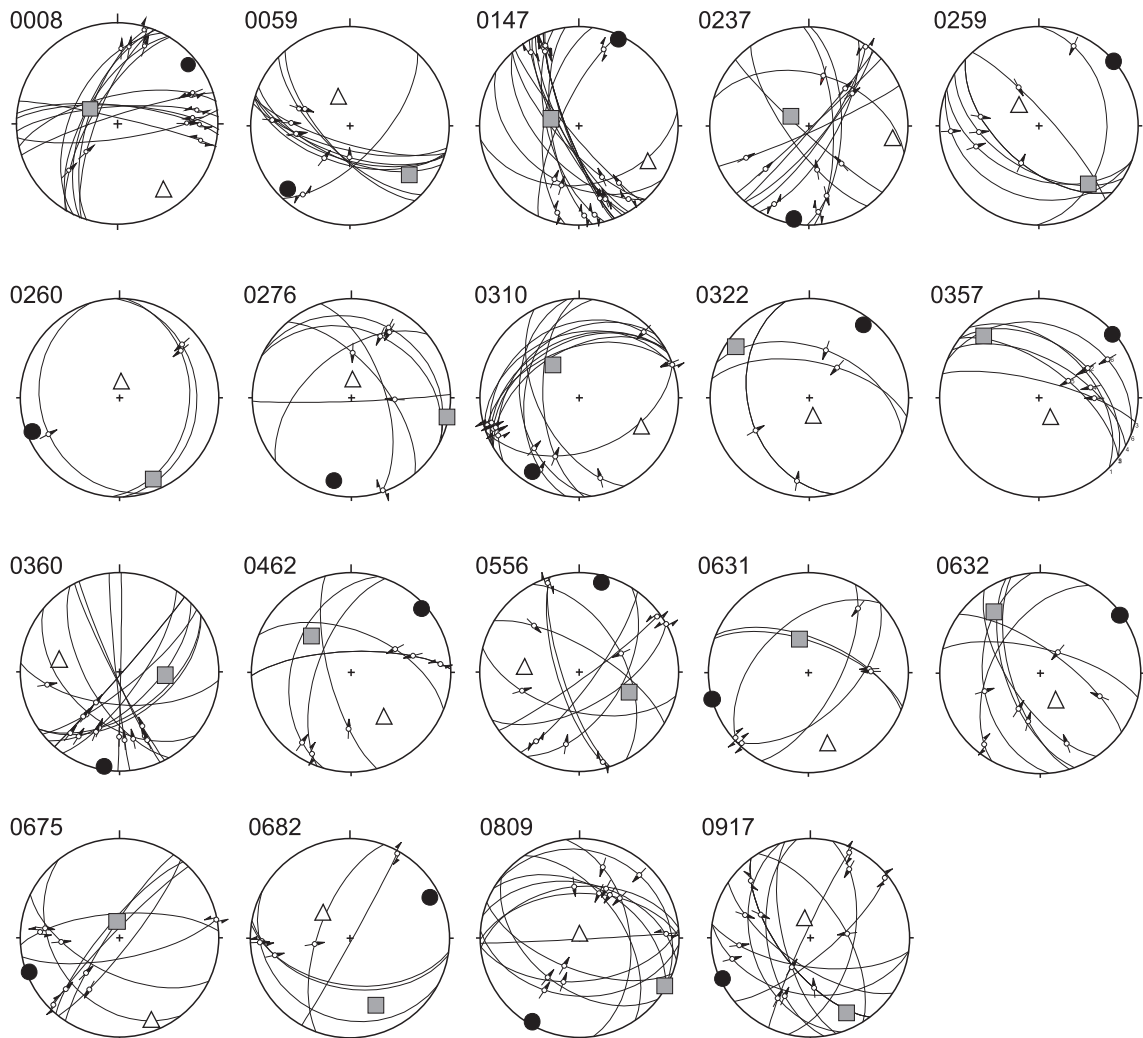
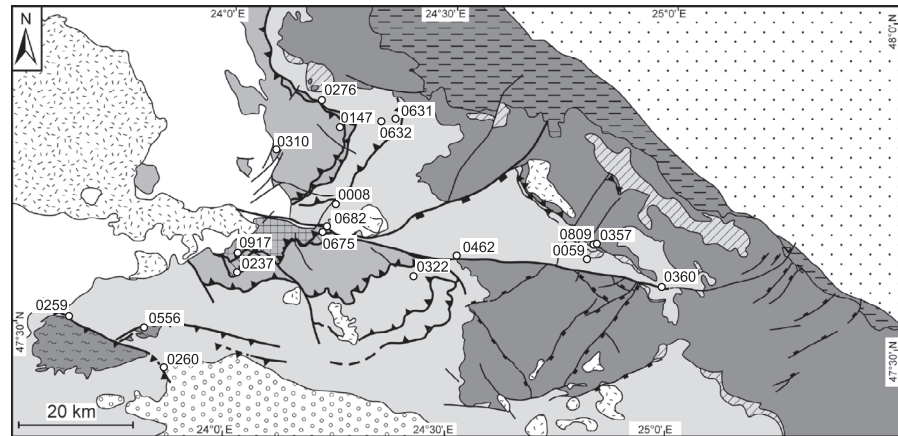
- shortening
- intermediate
- △ extension



Appendix 3: Fault-slip data (Late Burdigalian NE-SW extension)

Legend:

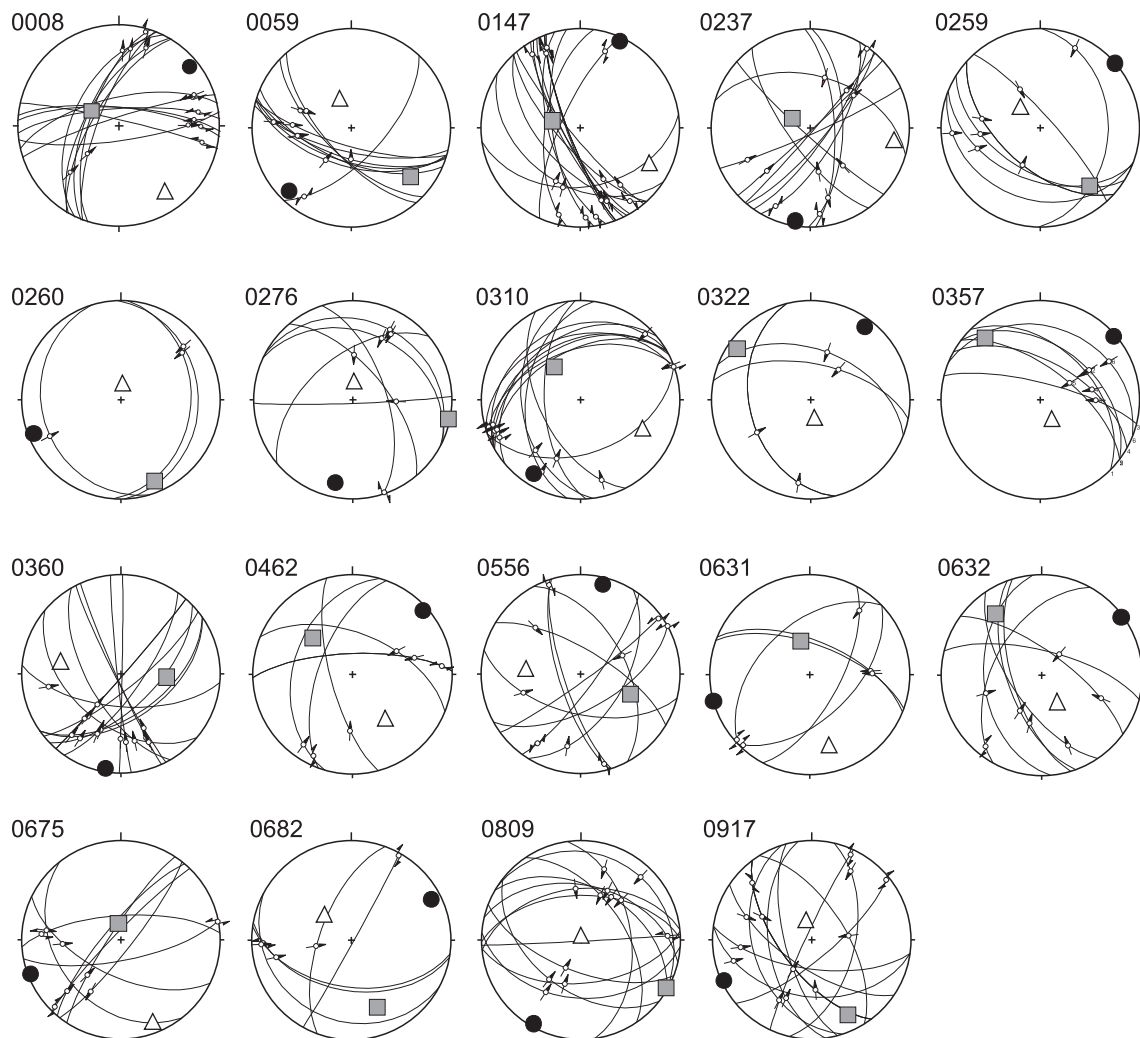
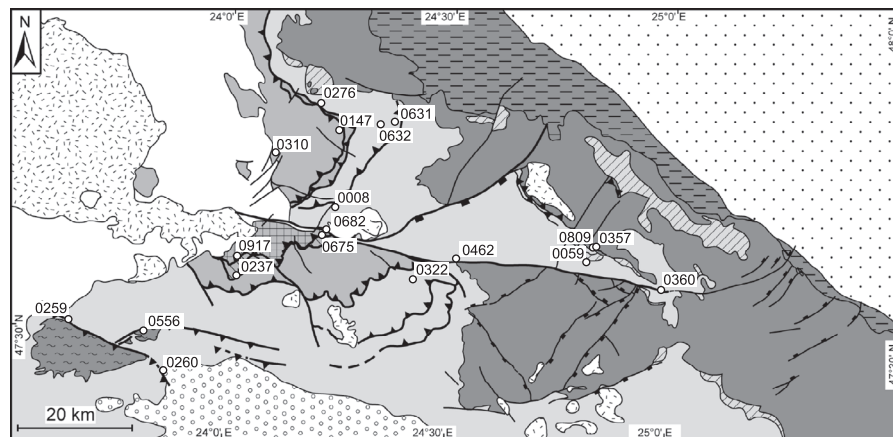
- shortening
- intermediate
- △ extension



Appendix 4: Fault-slip data (post-Burdigalian transpressional stage)

Legend:

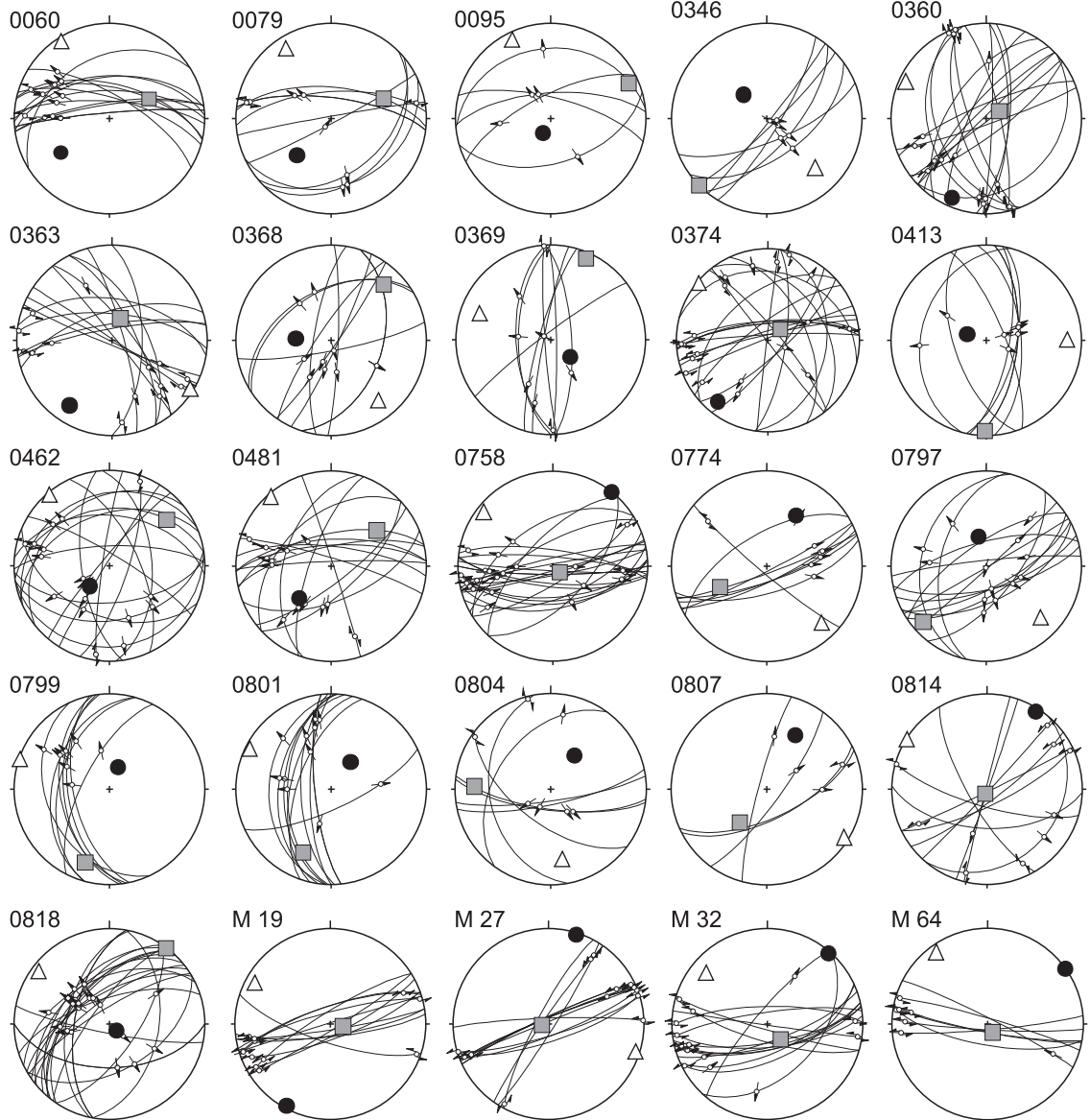
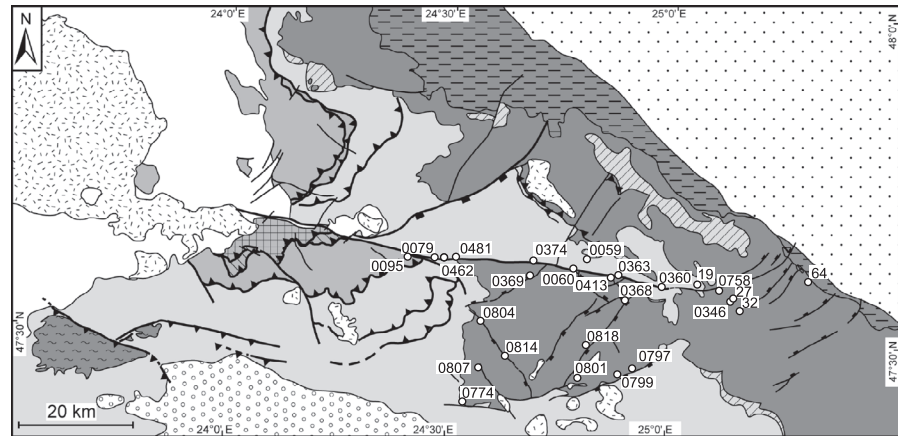
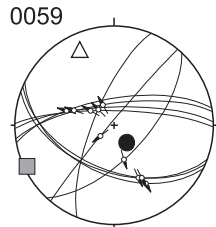
- shortening
- intermediate
- △ extension



Appendix 5: Fault-slip data (post-Burdigalian transtensional stage, eastern stations)

Legend:

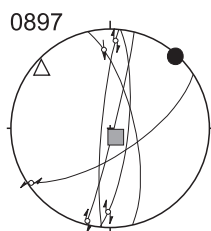
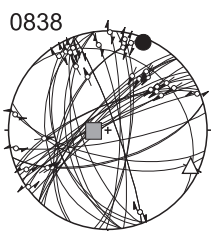
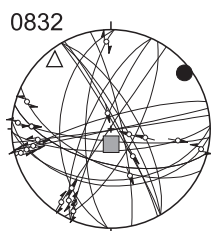
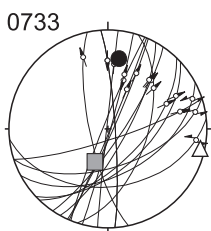
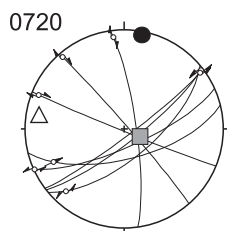
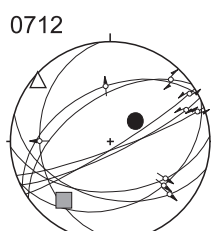
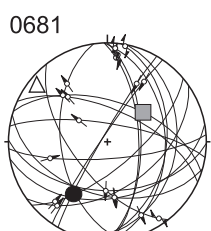
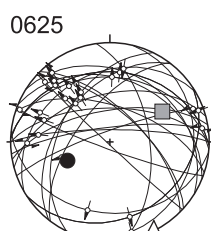
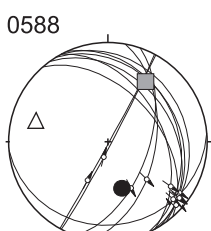
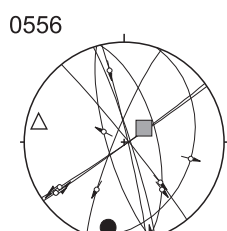
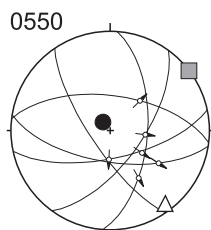
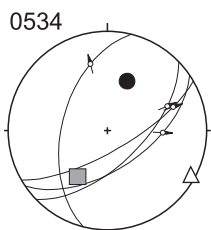
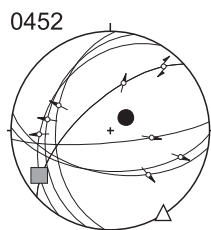
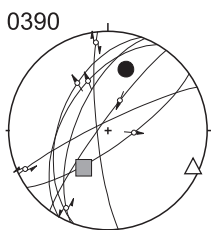
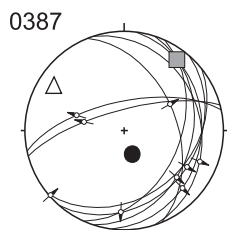
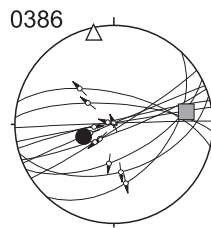
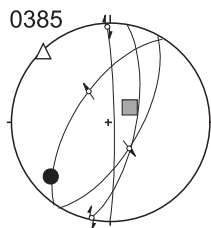
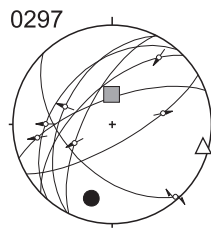
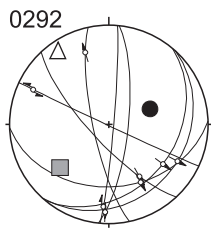
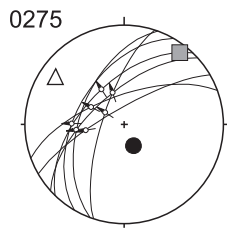
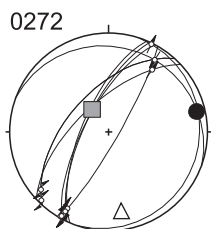
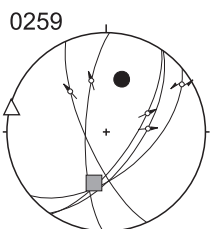
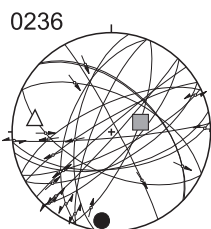
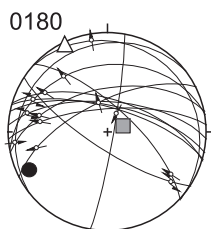
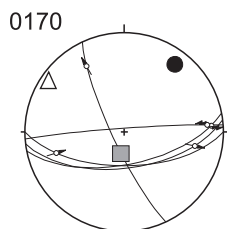
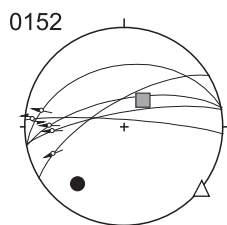
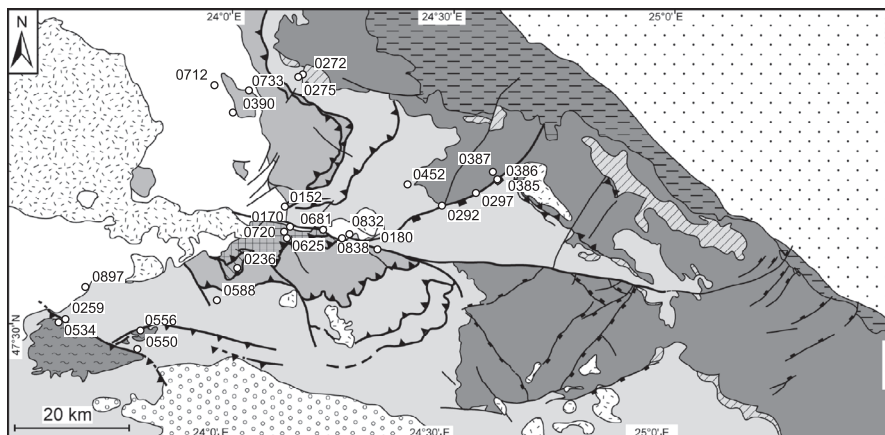
- shortening
- intermediate
- △ extension



Appendix 6: Fault-slip data (post-Burdigalian transtensional stage, western stations)

Legend:

- shortening
- intermediate
- △ extension



Chapter 3:

Sedimentological constraints on the Tertiary emplacement of ALCAPA and Tisza-Dacia (N.Romania)

3.1 Abstract

Starting in Early Oligocene times, marked subsidence and deposition of flysch units migrated S to SE-ward with time in northern Romania. The flysch vertically grades into Burdigalian molasse type sediments, forming a clastic wedge in the Transylvanian basin. The clastics were shed from the NW into a flexural foreland basin that formed in response to the juxtaposition of ALCAPA and Tisza-Dacia, with Tisza-Dacia in the lower plate position. The evolution of the WSW-ENE (present day coordinates) oriented Burdigalian basin out of an E-W to SE-NW (present day coordinates) oriented Oligocene basin is interpreted to result from clockwise rotation of Tisza-Dacia during basin formation. The last stage of the juxtaposition of ALCAPA and Tisza-Dacia is documented by the thrusting of the Pienides onto the autochthonous sedimentary cover of the Tisza-Dacia block. The Burdigalian emplacement of the Pienides is coeval to the deposition of the molasse-type clastic-wedge.

3.2 Introduction

The Miocene geologic history of the Carpathians is dominated by the emplacement of continental blocks during contemporaneous slab retreat of the European lithospheric slab (e.g. Royden 1988). The major continental blocks invading the Carpathian embayment, located between the Moesian and Bohemian promontories, are termed “ALCAPA”, “Tisza” and “Dacia” (Fig. 3.1). The ALCAPA block is separated from the Tisza and Dacia blocks by a broad zone of deformation, the Mid-Hungarian fault zone (e.g. Fodor et al. 1999). These blocks are distinguished by their contrasting Triassic and Jurassic sedimentary facies and fossil assemblages (e.g. Csontos and Vörös 2004 and references therein).

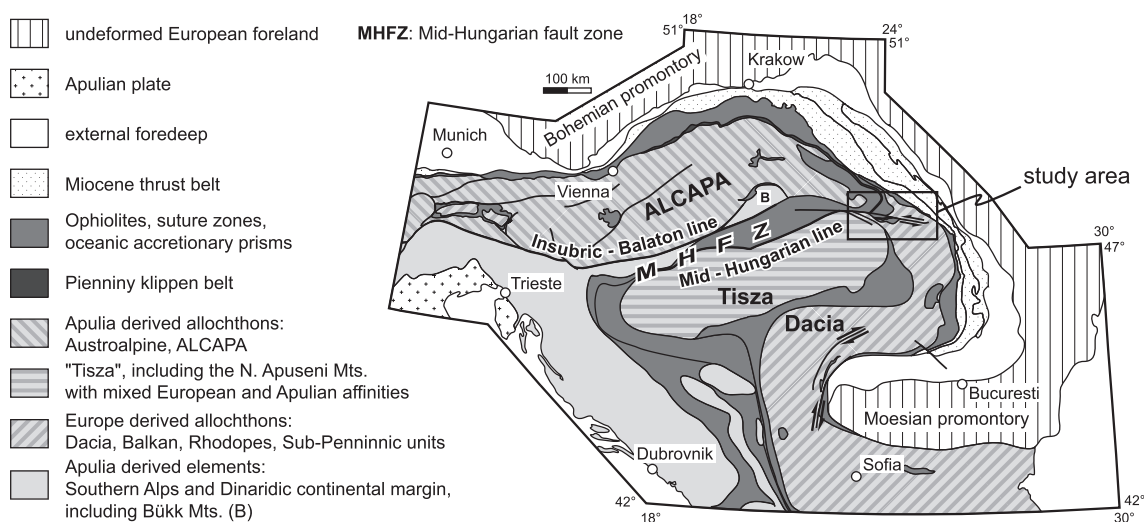


Fig. 3.1: Major tectonic units of the Alps, Carpathians and Dinarides, (simplified after an unpublished compilation by S. Schmid, B. Fügenschuh, K. Ustaszewski, L. Matenco, R. Schuster and M. Tischler.

The emplacement of ALCAPA was affected by the mechanism of lateral extrusion (Ratschbacher 1991a, b), involving eastward escape along conjugate strike-slip faults, coupled to indentation processes in the Eastern Alps. However, it is subduction retreat of the European plate that is thought to be the principal driving force for the final emplacement of the various blocks that build up the internal parts of the Carpathian loop (e.g. Royden 1988, Wortel and Spakman 2000, Sperner et al. 2005).

The emplacement of these continental blocks was accompanied by substantial strike-slip movements, extension and block rotations (Fodor et al. 1999, Márton 2000, Márton and Fodor 2003, Csontos and Vörös 2004, Horváth et al. 2005). Although the final emplacement of ALCAPA and Tisza-Dacia is well documented, the respective onset of their invasion into the Carpathian embayment is less well constrained.

During invasion, the ALCAPA block has been thrust onto Tisza-Dacia along the Mid-Hungarian line (Fig. 3.1; Csontos and Nagymarosy 1998). While the culmination of this thrusting is clearly dated to the Early Miocene, its onset remains rather poorly constrained to probably Late Oligocene (Csontos and Nagymarosy 1998, Fodor et al. 1999, Sperner et al. 2002).

North-eastward movement of ALCAPA was guided by strike slip zones oriented sub-parallel to the collision suture (Nemčok 1993), while corner effects at the Bohemian promontory led to counter-clockwise rotation of the ALCAPA block. Convergence was terminated by “soft-collision” of ALCAPA with the European margin in the Western Carpathians, at around 13 Ma ago (Sperner et al. 2002).

After their amalgamation in Cretaceous times, Tisza and Dacia are considered to represent a single block termed Tisza-Dacia (e.g. “Tisza-Dacia terrane” of Csontos and Vörös 2004). In comparison to ALCAPA, emplacement of Tisza-Dacia into the Carpathian embayment commenced earlier (during the Eocene according to Fügenschuh and Schmid 2005), and ended later (in post-middle Miocene times according to Matenco et al. 2003). Corner effects at the Moesian promontory (e.g. Ratschbacher et al. 1993) led to large clockwise rotations during the emplacement of Tisza-Dacia. The goal of this study is to provide new constraints for the timing of the thrusting of ALCAPA onto Tisza-Dacia, by analysing syntectonic sediments that accumulated on Tisza-Dacia.

3.3 Geological Setting

Situated in northern Romania, the study area lies internally of the main Carpathian chain at the northern border of the Transylvanian basin. The basement units outcropping in the study area belong to Dacia (European affinities, Bucovinian nappes) in the north-eastern part, and to Tisza (Mixed affinities, Bihor unit) in the south-western part (Fig. 3.1). These basement units experienced a polyphase deformation history, their internal nappe stacking occurred during the middle to latest Cretaceous times (Săndulescu et al. 1981). Already in Mid-Cretaceous times the Bucovinian nappes have been thrust onto units constituting the suture zone between Dacia and the European foreland (Fig. 3.1; Săndulescu 1994). During final closure of the Carpathian embayment in Miocene times, this nappe stack has been emplaced onto the Miocene thrust belt, predominantly constituted by Cretaceous to Miocene flysch deposits. During Late Cretaceous to Paleocene times, a sedimentary cover was deposited on Tisza-Dacia (Săndulescu 1994), in turn unconformably overlain by Eocene strata (Fig. 3.2).

During the Eocene, epicontinental deposits formed in the northern part of the study area (Săndulescu et al. 1981). Development of carbonate platforms (Iza limestone, Krätner et al. 1982) indicates relatively shallow environments (Dicea et al. 1980). Conglomerates and sandstones (Prislop Fm., Krätner et al. 1982, Krätner et al. 1983, Săndulescu et al. 1991) prevail along the main Carpathian chain in the study area, grading westwards into marly deposits (Vaser Fm., Săndulescu et al. 1991), developed in a littoral-neritic facies (Dicea et al. 1980). A further deepening towards the west is indicated by “hieroglyphic flyschs” outcropping at the base of the major imbrication of the autochthonous north of the Bogdan Voda fault (Piriul Mocilnei Fm., Săndulescu et al. 1991).

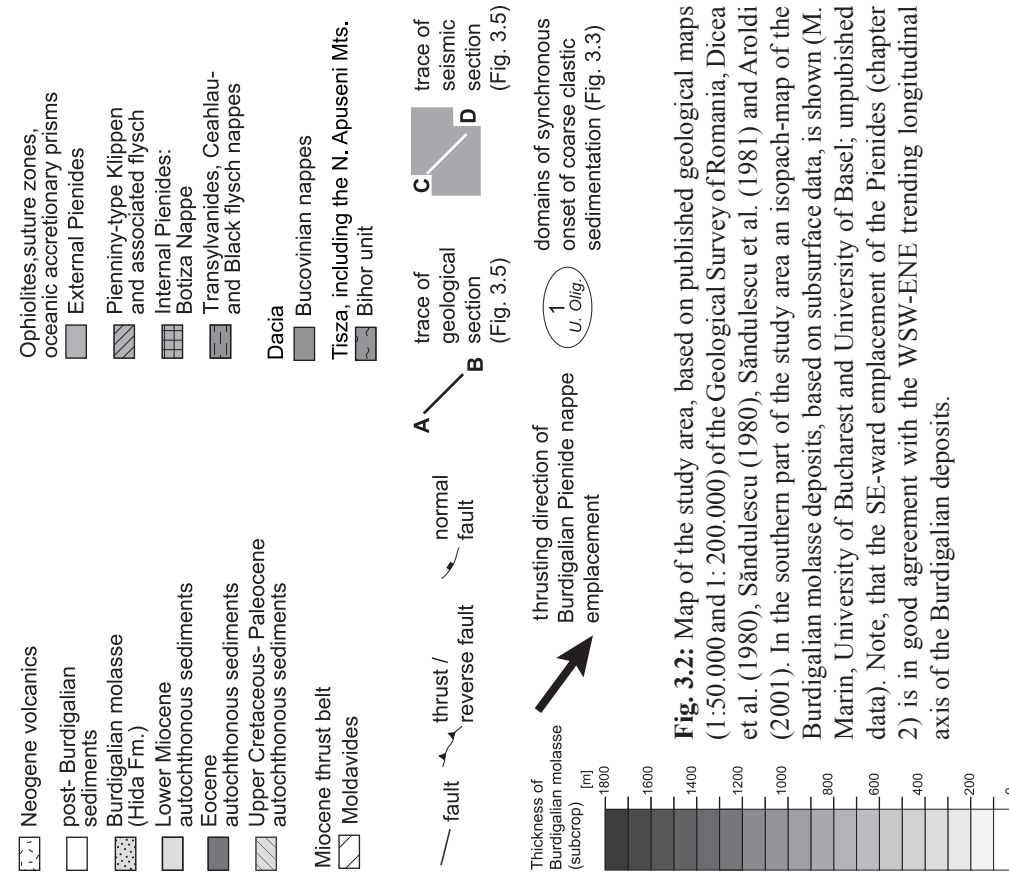


Fig. 3.2: Map of the study area, based on published geological maps (1:50.000 and 1:200.000) of the Geological Survey of Romania, Dicea et al. (1980), Săndulescu (1980), Săndulescu et al. (1981) and Aroldi (2001). In the southern part of the study area an isopach-map of the Burdigalian molasse deposits, based on subsurface data, is shown (M. Marin, University of Bucharest and University of Basel; unpublished data). Note, that the SE-ward emplacement of the Pienides (chapter 2) is in good agreement with the WSW-ENE trending longitudinal axis of the Burdigalian deposits.

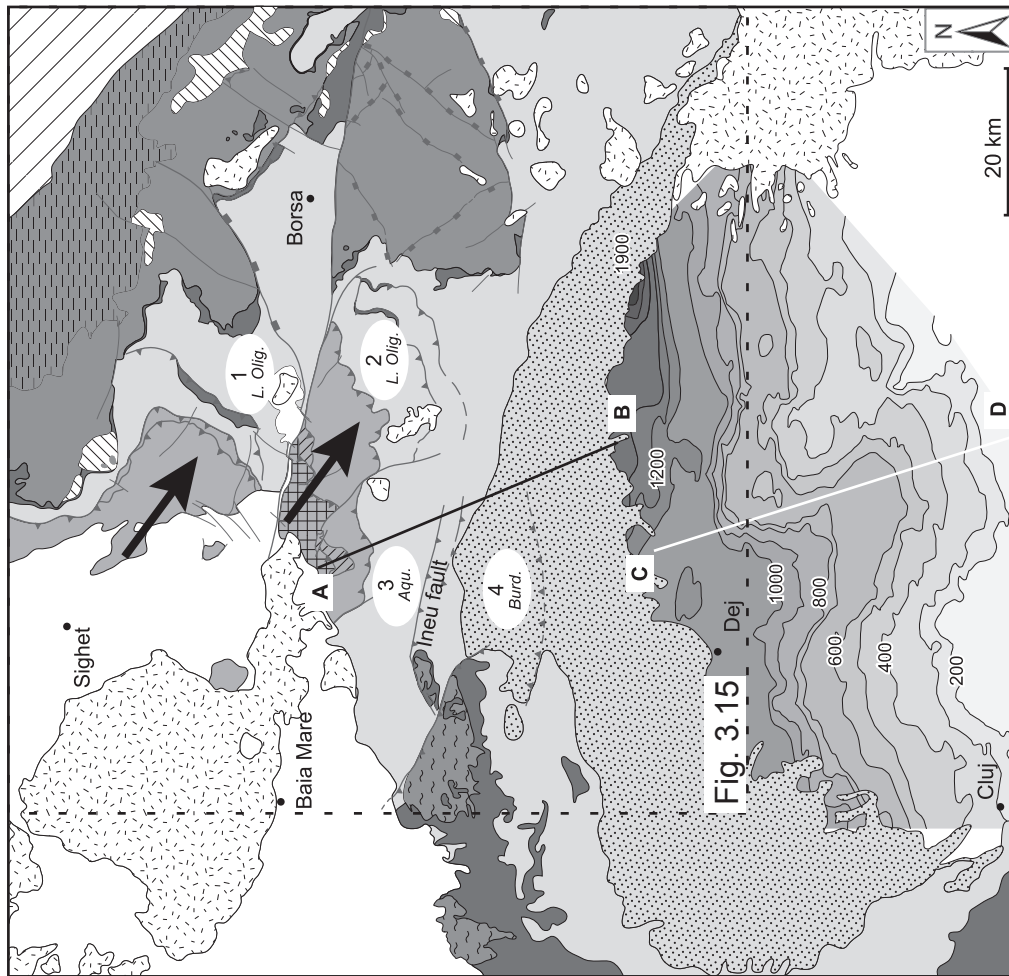


Fig. 3.15

In the southern part of the study area, two sedimentary cycles formed during the Eocene (Popescu 1984). Following a first red-bed type continental basin fill (Early to Mid-Miocene), shallow marine deposits accumulated during two Late Miocene transgressions, separated by continental red-beds and lacustrine sediments (DeBroucker et al. 1998). Like in the north-western part of the study area, an extensive carbonate platform developed during Priabonian times (Culmea Cozlei Fm., DeBroucker et al. 1998, Rusu et al. 1983).

The depositional environment changed significantly around the Eocene-Oligocene boundary, when drowning of the carbonate platforms is documented throughout the study area. Drowning seems to commence slightly earlier in the northern part of the study area (base Oligocene, Kräutner et al. 1982) than in the southern part (Early Oligocene, Györfi et al. 1999). During Oligocene times a E-W to SE-NW (in present coordinates) oriented basin (DeBroucker et al. 1998) developed, starting with the deposition of shale-dominated units throughout the study area.

In the northern part of the study area (Fig. 3.3) the Early Oligocene shale-dominated strata vary considerably in thickness (25 - 1200m), locally slumps and olistoliths are abundant (Dicea et al. 1980). In the southern part of the study area the deposition of shale-dominated units starts with black shales. The shale-dominated-units are overlain by sand-dominated clastics, their base becoming increasingly younger towards the south (Early Oligocene to Mid-Burdigalian, Fig. 3.3).

While in the northern part of the study area (Domain 1 and 2, Fig. 3.3) the deposition of sand-rich flysch starts in Rupelian times (Săndulescu et al. 1991), the onset of coarse clastic input in the central autochthonous Domain (Domain 3, Fig 3.3) starts in the Aquitanian. In the southern part of the area (Domain 4, Fig. 3.3), coarse clastic sedimentation started in Burdigalian times, developing from flysch into molasse deposits (Hida Beds), exhibiting a SW-wards thinning, wedge-shaped geometry (Fig. 3.2, Ciulavu et al. 2002).

Coevally with the deposition of the Burdigalian clastic wedge, the Pienide nappe stack has been emplaced top to SE (Fig. 3.2, chapter 2) onto the autochthonous cover (Săndulescu et al. 1981). The Pienides mainly consist of Eocene to Oligocene flysch, and can be divided into relatively more internal (Botiza nappe and remnants of Pienniny Klippen type units, Săndulescu et al. 1993) and more external units. The first can be correlated with the Inacovce-Krichevo units, the latter with the Magura flysch of the Western Carpathians, (Săndulescu et al. 1981, Săndulescu 1994).

Note, that in the external thrust sheets of the Pienides, sandy flyschs of Oligocene age (Aroldi 2001) i.e. contemporaneous to those in the autochthonous area, suggest a connection of these realms at least during Oligocene times (Săndulescu and Micu 1989). For a detailed sedimentary analysis of the Pienides the reader is referred to Aroldi 2001. The post-Burdigalian fill of the Transylvanian basin starts with the Mid-Miocene Dej tuff unit, unconformably overlying the Hida formation.

Correlation scheme of Oligocene - Lower Miocene units in the study area

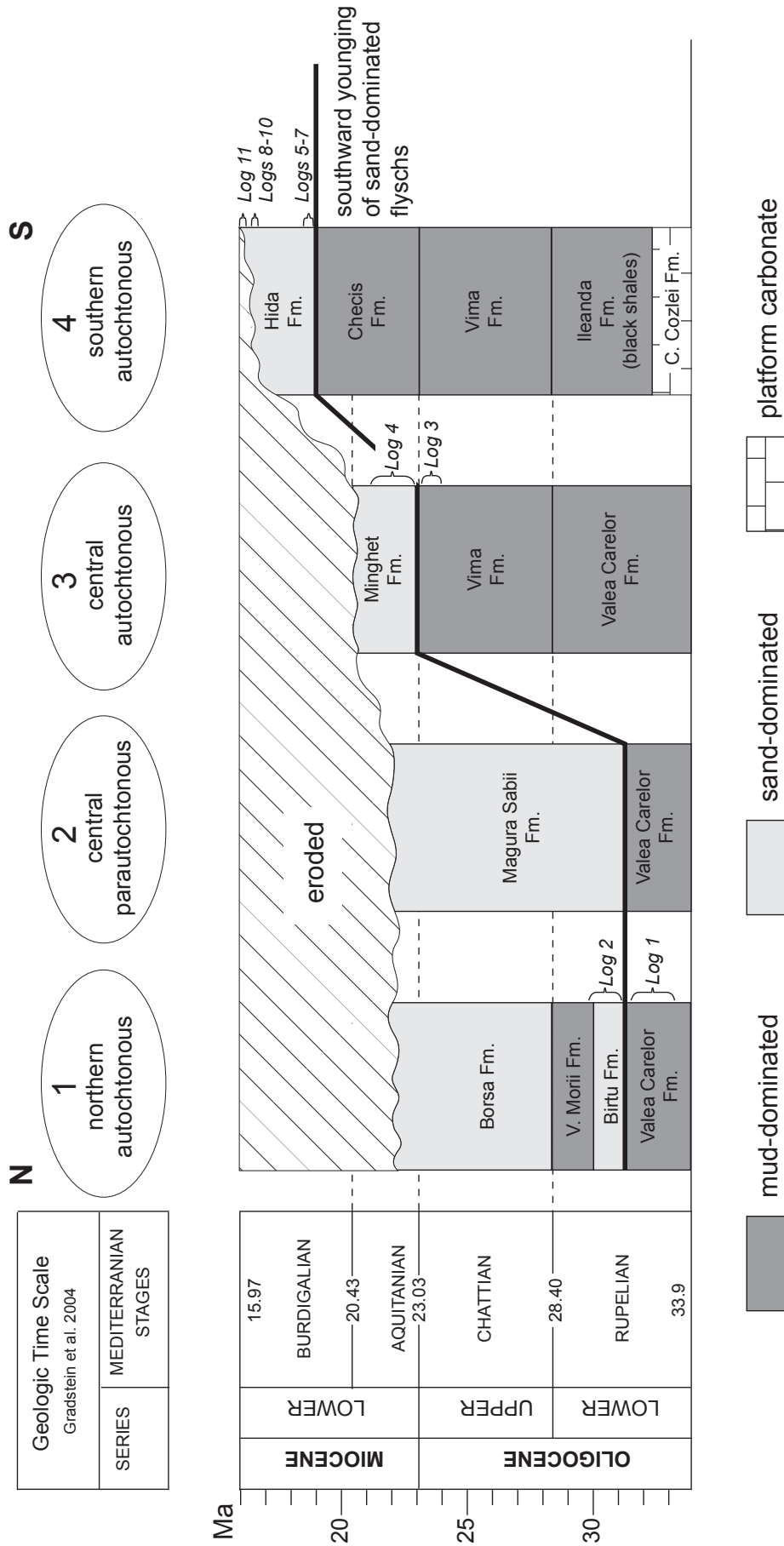


Fig. 3.3: Correlation scheme of Oligocene to Lower Miocene deposits in the study area, illustrating progressive younging of sand-dominated flysch towards the south. Approximate locations of sedimentary logs are indicated, width of the brackets corresponds to the approximate percentage of the unit covered. The number above the columns refers to Domain number in Fig. 2. The ages of the respective units are compiled from official 1:50.000 map sheets (Geological Survey of Romania; Domains 1 and 3), Săndulescu pers. comm. (2002, Domain 2). Ages for Domain 4 are compiled from Rusu (1989), Popescu (1984) and Moiescu (1981) in Györfi et al. (1999) as well as DeBroucker et al. (1998).

3.4 Evaluation of the effect of eustatic sea-level variations

Within the Paratethys the environmental conditions changed intermittently between open marine and restricted conditions. For the time interval considered, a change from reduced salinity, anoxic bottom water and strong endemisms in early Oligocene times towards open marine conditions during middle Oligocene times is postulated by Rögel (1999). Open marine conditions prevailed until Burdigalian times (Rögel 1999). Hence, eustatic sea level changes have to be considered for the development of the Oligocene to Miocene flysch unit in the study area. For this evaluation, the eustatic sea-level curves of Haq et al. (1987) are used (Fig. 3.4).

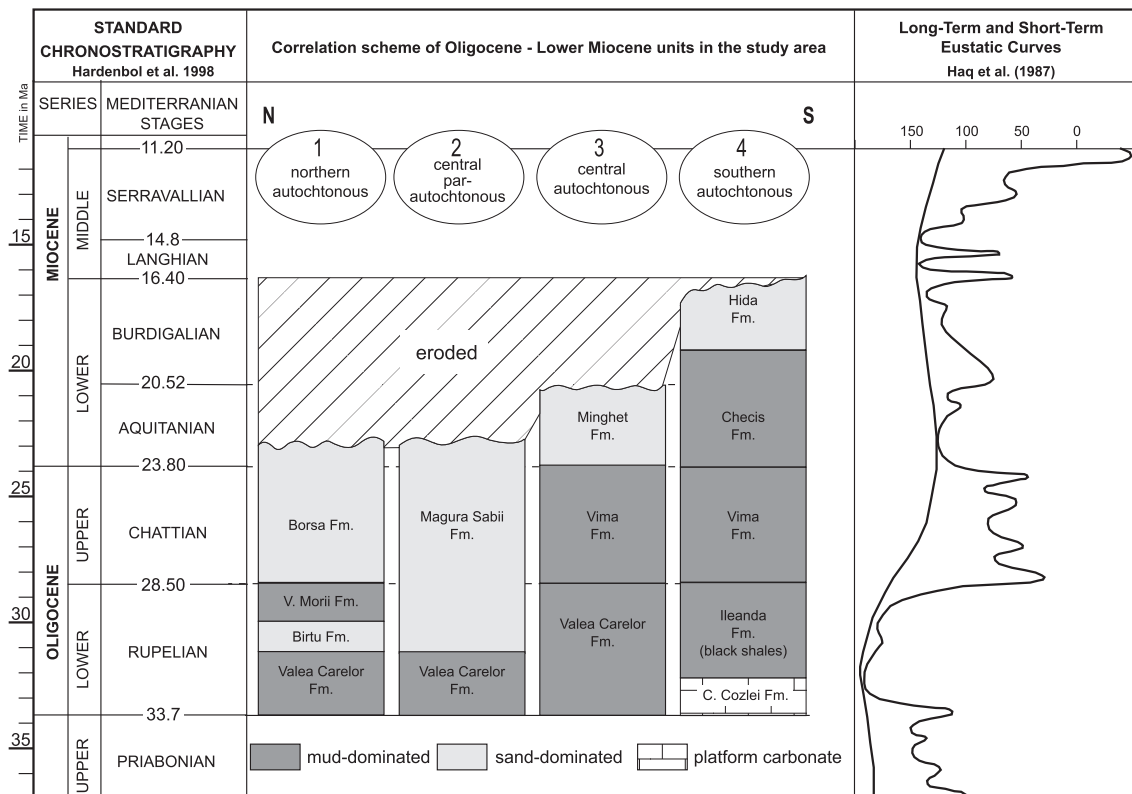


Fig. 3.4: Stratigraphic correlation chart and eustatic sea-level curve. Note that the time scale is from Hardenbol et al. 1988.

At a first glance it can be seen, that the short-term variations in the Oligocene correspond well with the sand-dominated intervals in the northern autochthonous Domain. A minor sea-level fall in Rupelian times coincides with the deposition of the Birtu Sandstone Fm., while a significant fall throughout Chattian times is synchronous to the deposition of the Borsa Sandstone Fm. (Fig 3.4). However, in Aquitanian times the progradation of sand-dominated flysch towards the central autochthonous commenced during a sea-level rise. A marked sea-level fall at the base of the Burdigalian is preceding the deposition of the Hida Formation.

As suggested by the compatibility with the Oligocene development, the eustatic sea-level has an influence by accentuating the flysch sedimentation. However, the effect of sea-level variations did not exclusively account for the overall SE-ward progradation of the sand-dominated flyschs. In the following the governing mechanisms of the SE-migrating deposition of sand-dominated siliciclastics are evaluated.

3.5 Data

3.5.1 Sub-surface data

3.5.1.1 Sub-surface data

The analyzed seismic sections covering the Transylvanian basin reveal a wedge-shaped geometry of the Upper Oligocene to Upper Burdigalian sediments, onlapping on the basement units (Fig. 3.5). For age control, the seismic lines are calibrated by boreholes. The deposition of the sediments constituting the wedge is coeval with the nappe emplacement of the Pienides (chapter 2). The internal structure of these deposits reveals at least three major phases of development, marked by discordances within the wedge.

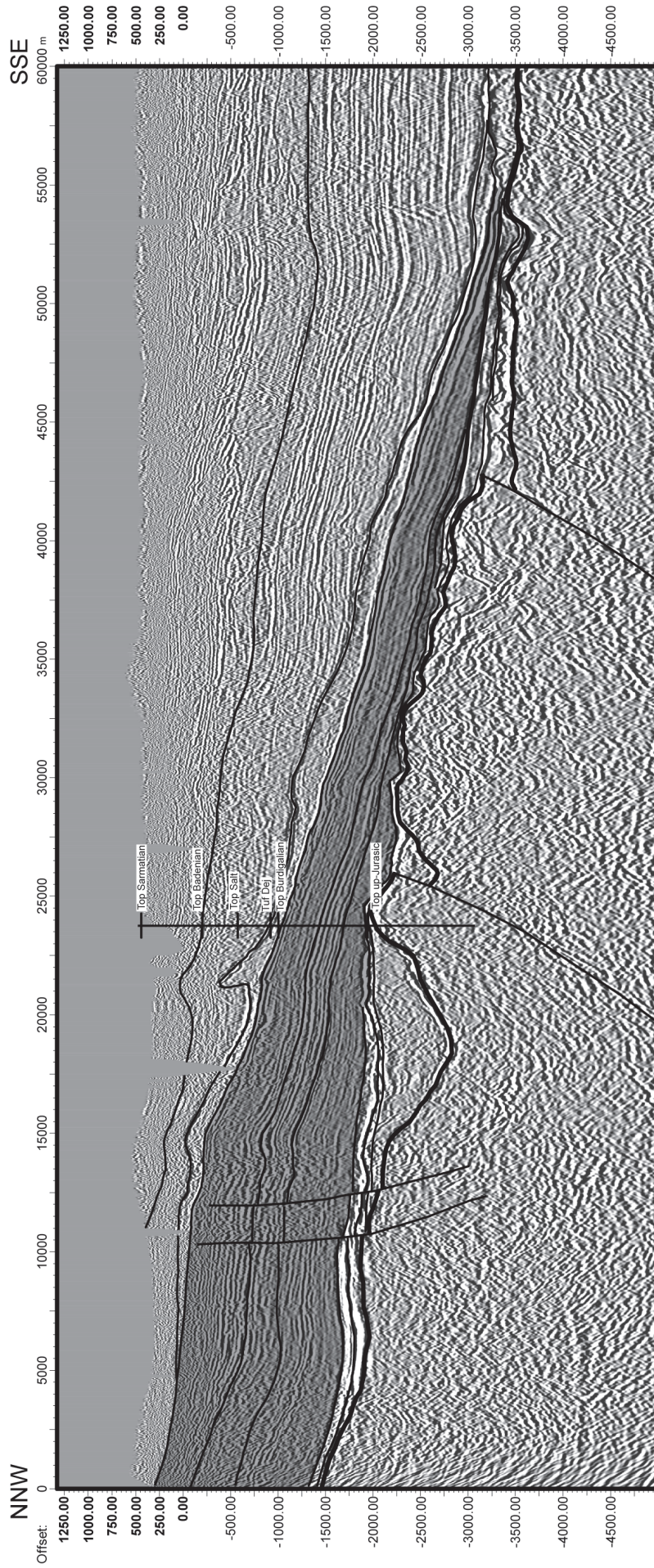
The first stage is characterized by a regional subsidence during Early Oligocene, followed by discordant deposits. These deposits show a coarsening in the upper part of the wedge. The second and third phases of tilting are of intra-Burdigalian age and characterized by onlapping strata forming important unconformities. Featuring a thickness of over 1400m in the northern part of the basin (Figs. 3.2, 3.5), the clastic deposits wedge out to the SE. The sedimentary record within the wedge ends with Mid-Miocene (Early Badenian) sediments, discordantly overlain by the Dej Tuff Formation. The present orientation of the Upper Oligocene - Burdigalian strata is post-depositionally tilted, indicating an uplift of the northern basin border.

3.5.1.2 Interpretation of the sub-surface data

The SE-ward thinning geometry of the clastic deposits and the orientation of onlaps indicate a sediment transport towards the SE. The SE-directed sediment transport within the wedge, as well as the WSW-ENE oriented basin axis (Fig. 3.2) are well compatible with the SE directed emplacement direction (chapter 2) of the Pienides. Conglomeratic deposits in the upper part of the wedge (Hida Fm.) reflect high depositional energy indicating the development of a high topography source area in the NW. The internal unconformities in the wedge are interpreted to reflect successive tilting of the basin floor.

The most likely cause for the formation of this foredeep is the coeval emplacement of the Pienides. Hence following interpretation is put forward: The sedimentary record of the Transylvanian basin reflects the Oligocene – Miocene tectonics of the internal central East Carpathians. The thrusting of the Pienides led to progressive loading and flexure of the northern sector of the Transylvanian basin, acting as a foredeep. Internal unconformities in the architecture of the sedimentary wedge reflect successive tilting due to the flexural response of the loaded plate during SE-ward emplacement of the Pienides (Fig. 3.6).

NNW - SSE depth seismic section in the Transylvanian basin



vertical exaggeration 4x

Fig. 3.5: NNW – SSE interpreted seismic section showing the wedge shaped Burdigalian deposits. The shaded area correlates to the Burdigalian wedge. The two major unconformities within the wedge are interpreted as result of progressive loading and resultant flexure of the northern part of the Transylvanian basin, acting as a foredeep. See Fig. 3.2 for the trace of the section. Interpretation by M. Marin (University of Bucharest and University of Basel; unpublished data)

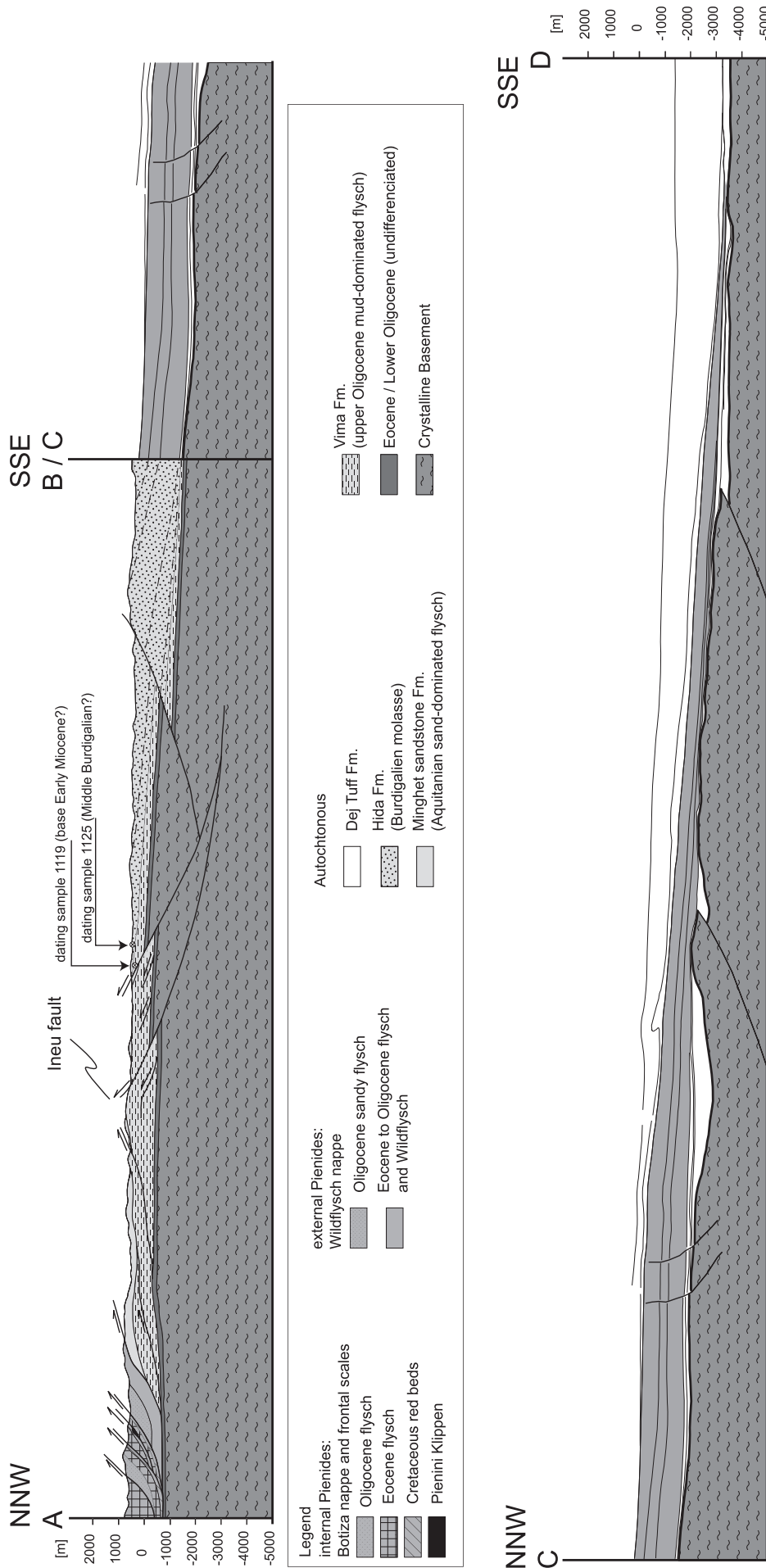


Fig. 3.6: Sketch of the interpreted seismic section (Fig. 3.5) without vertical exaggeration. The section is prolonged towards the north by schematic geological cross-section A-B. The thrust front of the Pienide nappe pile, interpreted to cause the formation of the flexural basin, can be seen in the northernmost part of the section. The reverse faults in the middle of Section A-B (e.g. Ineu fault) are attributed to a later stage of deformation (see chapter 2).

3.5.2 Facies analysis

3.5.2.1 Introduction

Detailed stratigraphic logs have been compiled from outcrop analysis. To subdivide the lithostratigraphic logs on the basis of depositional trends, the hierarchical system of Mutti and Normark (1987) has been used. In this hierarchical system first order features are at the scale of basin fills (turbidite complex), while second order features (turbidite system, ~400m thickness) include depositional sequences, commonly bounded by highstand mud facies. Third order features (turbidite stage, ~250m thickness) are facies associations reflecting different development phases of the system. Fourth order features (turbidite sub stage, ~15m) are characteristic for sub-stages of system development. The smallest, fifth division, is defined by individual lithofacies.

The lithofacies classification is based on Pickering et al. (1989, 1995). This classification scheme aids in the interpretation of the depositional processes, without implying genetic relations between lithofacies. The lithofacies were then grouped into lithofacies associations, which can be interpreted in terms of depositional environments. The various lithofacies are outlined in Table 3.1 and illustrated in Figures 3.7 and 3.8.

The correlation of individual outcrops needs highly detailed observations due to bad exposure conditions and tectonic deformation. Unfortunately, high-resolution age control has not been available. Therefore only continuous sections, individually long enough for a meaningful discussion of the development of the depositional setting, have been included. The logs described below cover the autochthonous Domains (1/3/4, in Figure 3.3), reaching from Early Oligocene to Early Miocene times.

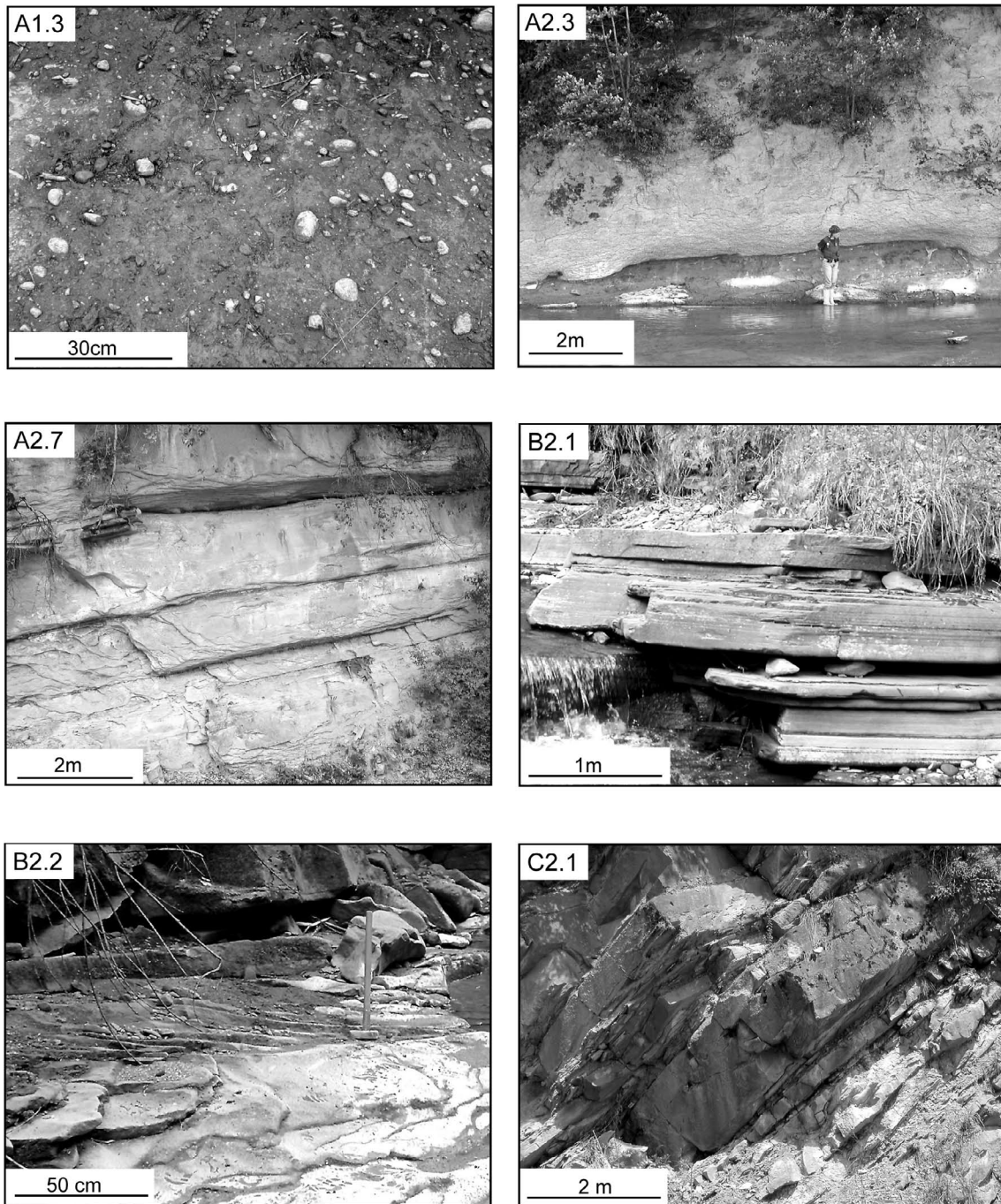


Fig. 3.7: Field examples for facies classes used. The code in the upper left corner of the pictures correlates to the facies codes (See Table 3.1).

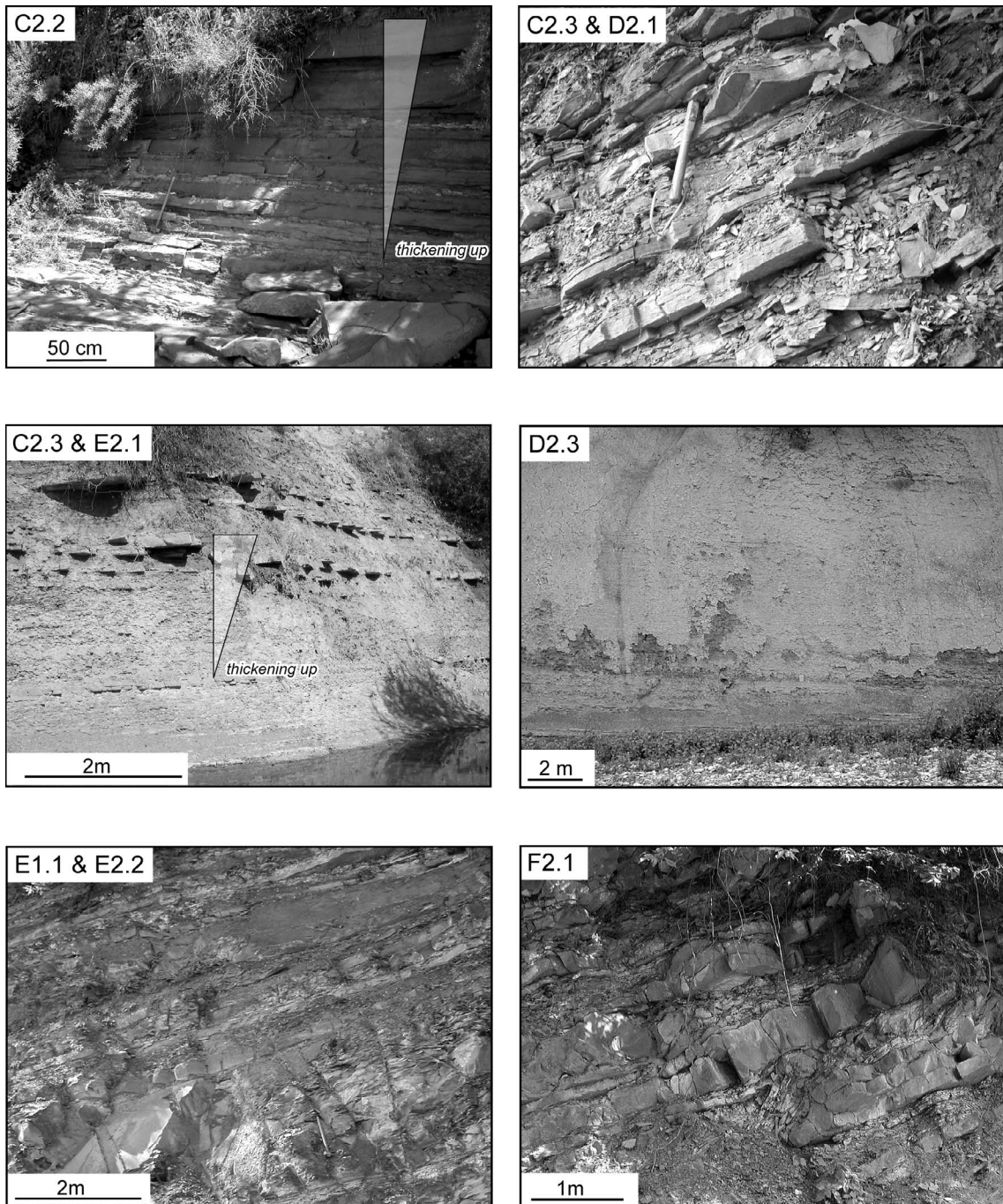


Fig. 3.8: Field examples for facies classes used. The code in the upper left corner of the pictures correlates to the facies codes (See Table 3.1).

Class	Group	Facies	Bed thickness	Bed shape	Internal structures	
A	Gravels, muddy gravels, gravelly muds, pebbly sands, $\geq 5\%$ gravel A1 - Disorganized A2 - Organized	A1.3 Disorganized gravelly mud (Fig. 3.7) A2.3 Normally graded gravel (Fig. 3.7) A2.7 Normally graded pebbly sand (Fig. 3.7)	0.1-several m	irregular, laterally discontinuous	abundant silt/mud clasts	50 - 95% mud - clay
			0.5-several m	irregular (scours)	clast imbrication badly developed	moderately to well sorted
B	Sands, $\geq 80\%$ sand grade, $< 5\%$ pebble grade B2 - Organized	B2.1 Parallel stratified sands (Fig. 3.7) B2.2 Cross-stratified sands (Fig. 3.7)	1-5m	irregular (scours)	distribution and coarse tail grading	
			0.5-3m	moderate lateral continuity	thick parallel lamination in upper third of bed, dish structures, erosional channels, mud clasts	
C	Sand-mud couplets and muddy sands, 20 - 80% sand grade, $< 80\%$ mud grade (mostly silt) C2 - Organized sand-mud couplets	C2.1 thick bedded (Fig. 3.7) C2.2 medium bedded (Fig. 3.8) C2.3 thin bedded (Fig. 3.8)	0.25-2m	irregular, lensing and splitting	tabular to trough shaped cross stratification (10-40 cm set thickness)	coarse grain size for bed thickness, well sorted
			> 30 cm	smooth / planar tops, moderate to good lateral continuity	$T_{ab(c)(d)}$ partly / complete Bouma sequences, (Bouma 1962) $T_{(a)bcd}$ abundant sole marks $T_{(b)cd}$	poorly to moderately sorted sands
			10-30 cm			
D	Silt, silty muds, and silt-mud couplets, $> 80\%$ mud $\geq 40\%$ silt, 0-20 % sand D2 - Organized	D2.1 Graded-stratified silts (Fig. 3.8) D2.3 Thin regular silt and mud laminae (Fig. 3.8)	< 30 cm	marked lateral continuity (several tens of meters)	T_{c-e}	gradational with C2.3
			0.1-1m	good lateral continuity	(lenticular) silt laminae in mud	gradational with E2.1
E	$\geq 95\%$ Mud grade, $< 40\%$ silt grade, $< 5\%$ sand and coarser, $\leq 25\%$ biogenics E1 - Disorganized E2 - Organized	E1.1 Structureless muds (Fig. 3.8) E2.1 Graded muds (Fig. 3.8) E2.2 Laminated muds and clays (Fig. 3.8)	1-tens of m		zones of increased silt content, calcification and nodular, black layers of silicified muds	gradational with E2.; "hemipelagic background sedimentation"
			1-5m		normal grading (silt to mud)	gradational with D2.1
F	Chaotic deposits F - Contorted / disturbed strata	F2.1 Coherent folded / contorted strata (Fig. 3.8)	0.01-0.5m		lamination	partially high content of organic matter (black colour)
			0.01-2m	smooth to planar tops highly irregular lower boundaries	folded and contorted beds	

Table 3.1: Overview on the lithofacies and their most important features (based on Pickering et al. 1989).

3.5.2.2 Facies associations of the lithostratigraphic logs

Log 1

Log 1a (Fig. 3.9) covers approximately 300m of a Early Oligocene mud-dominated unit (Valea Carelor Fm., Fig. 3.3). Structureless muds (E1.1, ~80%) dominate, in which graded muds (E2.1, ~15%) and laminated muds (~5%) are embedded. An overall (3rd order) coarsening-up trend is reflected by an increase in grain size of intercalated turbidites (graded muds, E2.1, towards graded-stratified silts, D2.1) as well as by an increasing amount of sandy turbidites. Depositional coarsening-up trends (4th-order) become more clearly defined towards the top.

Log 1b shows a well-developed 4th-order coarsening-up trend composed of thin-bedded sand-mud couplets (C2.3) and graded-stratified silts (D2.1), confirming the general 3rd-order coarsening-up trend.

Depositional setting:

The occurrence of biogenic oozes and the relative abundance of fine-grained terrigenous material (graded muds, graded-stratified silts) implies a “distal basin” setting (Mutti and Ricci Lucci 1972). The overall, 3rd order coarsening-up organized into 4th order coarsening-up trends are suggestive for a progradation towards a distal lobe environment (Mutti and Normark 1987).

Log 2

Log 2 (Fig. 3.10) covers around 500m of the Early Oligocene sand-dominated deposits (Birtu Sandstone Fm., Fig. 3.3). In the lower 170m a 3rd order coarsening-up trend can be observed. Thin-bedded sand-mud couplets (C2.3), and graded muds (E2.1) grade into thick-bedded sand-mud couplets (C2.1). This overall coarsening-up trend is composed of four 4th-order coarsening-up trends. The lower third of the individual 4th-order trends are dominated by small-scale (2-5m) thickening-up cycles (compensation cycles sensu Mutti and Normark 1987), while the upper part consists of small-scale (2-5m) fining-up cycles. Two 1-2m thick layers of coherent folded and contorted strata occur between meter 130 and 140.

The interval between 170m and 290m is dominated by sand-mud couplets (C) embedded in graded silts (D2.1), lacking clear depositional trends. An abrupt change occurs at meter 250, where normally graded pebbly sands (A2.7) are intercalated into thin-bedded sand-mud couplets.

The interval between 290 and 340m is dominated by very thick- to thick-bedded sand-mud couplets (C2.1) organized in two 4th-order thinning-up sequences. The topmost 130m show an overall 3rd-order fining-up trend organized in 4th-order coarsening-up trends. Very thick/thick bedded sand-mud couplets (C2.1) grade into thin-bedded sand-mud couplets (C2.3) and graded-stratified silts (D2.1) intercalated into structureless muds (E1.1).

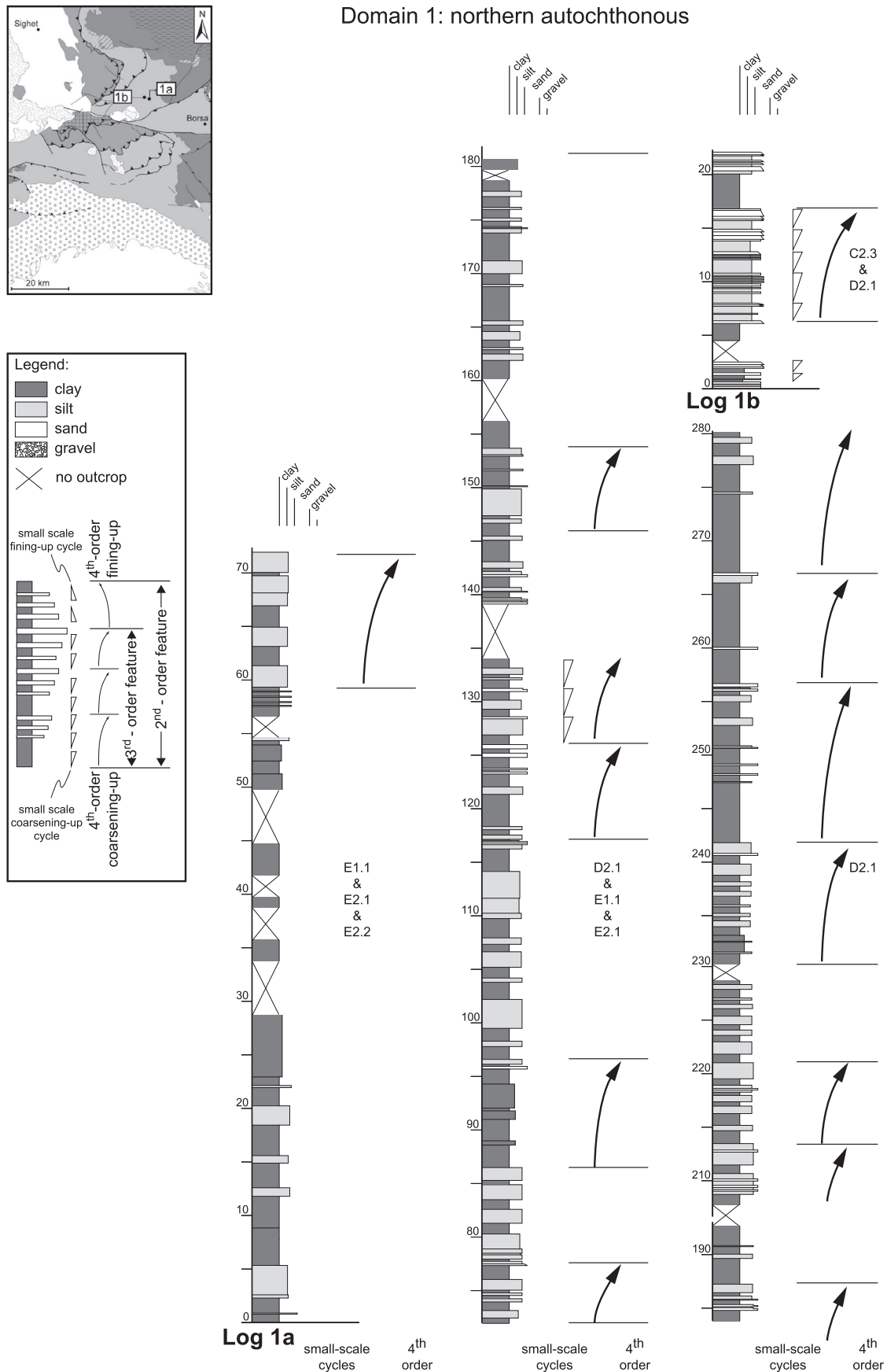


Fig. 3.9: Sedimentary logs 1a and 1b, covering approximately the topmost 70% of the Valea Carelor Fm. A general coarsening-up trend suggests a progradation from basin plain setting towards a distal lobe setting.

Depositional setting:

The clear coarsening-up of the lower 170m, arranged in well-developed 4th-order thickening-up trends (Fig. 3.10), is interpreted to reflect fan progradation. This interval is ascribed to non-channelized deposits of the distal to intermediate lobe setting. Slumped intervals at the top of this interval emphasize the development towards proximal settings.

Rather weakly developed depositional trends and channelized deposits (abrupt vertical facies changes) between 170 and 290m are interpreted to reflect the transition from sheet-like lobe to channelized deposits. The thinning-up sequences of the interval between 290 and 340m are suggestive for channelized deposits in a channel-lobe transitional setting.

The gradual fining-up trend observed within the upper part, accompanied by clear 4th-order thickening up cycles, are explained by a retreat of the system.

Log 3

Location 3 (Fig. 3.11) is situated at the top of the Late Oligocene mud-dominated unit of Domain 3 (Fig. 3.3). Organized sand-mud couplets (C2) are embedded in graded-stratified silts (D2.1) and laminated silts and muds (D2.2). The fine-grained parts of the succession feature intercalations of laminated muds and clays (E2.2). A general (3rd-order) coarsening-up trend is reflected by grading from thin- to thick-bedded organized sand-mud couplets as well as an increase in silt content (~30% to ~60%) of the muddy facies. The overall trend is composed of five 4th-order coarsening-up cycles of 10-20m thickness, comprising small-scale (~2.50m thick), predominantly coarsening-up cycles.

Depositional setting:

The general coarsening-up trend composed of well-defined 4th-order coarsening-up intervals as well as the lithofacies (D2.1 to C2.1) is suggestive of a relatively distal, prograding environment. These facies associations are ascribed to a distal basin to distal lobe setting (Mutti and Ricci Lucci 1972).

Log 4

This log (Fig. 3.11) covers approximately the lower two thirds of the Early Miocene sand-dominated unit of Domain 3 (Fig. 3.3). It is composed of a 3rd-order coarsening-up sequence, followed by a 3rd-order fining-up interval, which in turn is overlain by deposits characterized by facies F2.1.

The basal (0-150m) 3rd-order coarsening-up trend consists of three 4th-order coarsening-up cycles, each approximately 50m thick. The basal 4th-order coarsening-up sequences grades from medium bedded sand-mud couplets (C2.2), intercalated with thin regular silt and mud laminae (D2.2), into normally graded pebbly sand (A2.7; pebble sizes ~1-2cm). The two 4th-order coarsening-up cycles further up-section grade from parallel-stratified sands (B2.1) to normally graded pebbly sand (A2.7), intercalations of cross-stratified sands (B2.2) are abundant. All of the basal coarsening-up cycles display small-scale (2-10 m) fining-upward trends.

The fining- and thinning-up trend at the top of the log is dominated by parallel-stratified sands (B2.1), with intercalations of cross-stratified sands (B2.2). Within this 70m thick 4th-order cycle, small-scale thickening-up sequences are dominant.

At the top, a 5m thick disorganized gravely mud (F1.3, mean 8cm, max pebble size 20cm) is embedded into parallel-stratified sands (B2.1).

Depositional setting:

The coarsening-up trend documented in the lower part is interpreted to reflect a progradation of the system. Since the 4th-order thickening-up cycles within the basal part are characteristic for non-channelized deposits, the depositional setting is interpreted as intermediate to proximal lobe. The upper part, characterized by a thinning-up trend is ascribed to a mid-fan setting, where channelized deposits dominate. The inferred progradation is supported by the occurrence of slump deposits (F1.3) in the topmost part.

Logs 5 and 6

These logs (Fig. 3.12) are situated at the base of the coarse-grained siliciclastics of Domain 4 and show a general (3rd-order) fining-up trend, normally graded gravel (A2.3) and normally graded pebbly sand (A2.7) grading into thick- to medium-bedded sand mud couplets (C2.1/C2.2). The normally graded pebbly sands show thick parallel lamination and occasional cross bedding. The overall (3rd-order) fining-up trend is composed out of three 4th-order cycles.

Depositional setting

The lithofacies and depositional sequences suggest channelized deposits, suggesting a channel-lobe transitional setting (Mutti and Normark 1987). The general fining-up trend might be interpreted as a channel fill.

Log 7

At the locality of log 7, close to the base of the coarse-grained siliciclastics of Domain 4 (Fig. 3.12), sand-mud couplets (C2) are intercalated with thin regular silt and mud laminae (D2.3). Although no general (3rd-order) depositional trend is evident, 4th-order trends are well developed. The log is dominated by six ~15 thick 4th-order coarsening-up cycles, each grading from medium-bedded (C2.2) to thick-bedded (C2.1) sand-mud couplets. At the top a thinning-up cycle is documented, thick bedded (C2.1) grading to medium-bedded (C2.2) sand-mud couplets.

Depositional setting:

The predominantly C and D facies class deposits, together with well developed 4th-order cycles coarsening-up are interpreted as intermediate lobe deposits.

Log 8

Starting approximately 200m below the top coarse-grained siliciclastics of Domain 4, Log 8 is build up by facies Class A deposits (Fig. 3.12), mainly normally graded gravels (A2.3) and pebbly sands (A2.7) dominate. At the top of the log two debris flows (A1.3) occur.

The facies class A deposits form a 3rd-order thinning-up trend. The clast-supported conglomerates show an overall decrease in clast size from 15 to 5cm maximum diameter.

Depositional setting:

The lithofacies and the overall thinning-up trend suggest proximal channelized deposits. The depositional setting is interpreted as a channel.

Logs 9+10

In the upper part of the coarse-grained siliciclastics of Domain 4 (9: 150m below top; 10: 100m below top, Fig. 3.12) homogenous mud-dominated sediments are documented. Logs 9 and 10 feature thin regular silt and mud laminae (D2.3) with few intercalations of graded-stratified silts (D2.1). The mud to silt ratio decreases from 1:1 in log 9 to 1:3 in log 10.

Depositional setting:

The lithofacies of these logs suggests a distal, silt-rich setting, well comparable to the distal basin setting (e.g. Mutti and Ricchi Lucci 1972).

Log 11

Log 11 covers the topmost 70m of the coarse-grained siliciclastics of Domain 4. The top is formed by a reworking horizon, which marks the erosional discordance at the base of the Dej Tuff Formation (Fig. 3.12).

The base of this log shows a rapid 4th-order coarsening-up development from medium (C2.2) over thick (C2.1) bedded sand-mud couplets towards normally graded pebbly sands (A2.7). This trend is followed by a 4th-order thinning-up trend within normally graded pebbly sands. The top of the log consists of graded-stratified silts (D2.1), thin regular silt and mud laminae (D2.3) in which sand-mud couplets are embedded. These intercalated sand-mud couplets define four small-scale coarsening-up trends (~15m thickness), each grading from thin (C2.3) to medium (C2.2) bedded. The mud-silt ratio of the log is approximately 1:10.

Depositional setting:

The lithofacies associations documented at the lower part of the log suggest a proximal setting, possibly developing from intermediate lobe towards channel-lobe transition. Distal lithofacies and consistent coarsening-up trends in the upper part of the log point towards an outer lobe setting.

3.5.2.3 Facies analysis summary

The earliest phase of coarse clastic input (Early Oligocene) is documented in the northern part of the study area (Fig. 3.13). The lithofacies associations documented in Log 1 (Fig. 3.13) suggest a gradual change of the depositional setting from a basin plain towards a distal lobe. The trend towards more and coarser sediment input continues with a gradual progradation from distal, intermediate and proximal lobe towards a channel-lobe transitional setting (Fig. 3.13, log2). After an interval possibly indicating channel facies, the depositional setting steps towards a distal lobe setting.

Since this retreat occurs on a larger scale (it corresponds to the formation mapped as Valea Morii Fm.), it possibly reflects a basinwide decrease in clastic input due to a moment of decreased tectonic activity (Mutti et al. 1999). However, such a retreat is not documented in the central parautochthonous realm (Domain 2, Fig. 3.3), contradicting this interpretation. A higher temporal resolution would be necessary to resolve these contradictory observations.

Approximately 30km further to the south (Domain 3) coarse clastics arrive during Aquitanian times documented by prograding lobe fringes (Fig. 3.14, log 3). Further progradation of the system is recorded by deposits suggesting a channel-lobe transitional setting followed by channelized deposits typical for a middle fan setting (Fig. 3.14, log 4). When comparing the northern and central area, the lobe-dominated sedimentation shifted more than 30km towards the south between Rupelian and Aquitanian times. This significant progradation occurred during a eustatic sea-level rise (Fig. 3.4).

About 10km still further to the south (Domain 4), Burdigalian channel fill deposits (Fig. 3.14, logs 5/6), and intermediate, sand-rich lobes (Fig. 3.14, log 7) confirm the southward migration of proximal depositional settings. The Burdigalian age of these deposits is confirmed by new biostratigraphical data (see below).

In the upper part the coarse-grained siliciclastics of Domain 4 (Fig. 3.14), the transition from channel-fill deposits (Fig. 3.14, log 8) to silt-rich basin plain deposits (Fig. 3.14, logs 9 and 10) suggests a decrease in clastic input. This decrease is followed by a progradational pulse, documented by the development from an intermediate lobe to a channel-lobe transitional setting (Fig. 3.14). The top of the Burdigalian strata is composed of silty distal lobe deposits suggesting a retrogradation. A general decrease in clastic input towards the end of Burdigalian is consistent with a coeval short-term sea-level rise (Fig. 3.4).

The depositional environments are compatible with a foreland basin environment. Significant amounts of sand occur in a laterally relatively continuous geometry, suggestive for elongate foreland basins, where “tectonic activity produces and maintains narrow basins that enhance the distance of transport of the sand” (Mutti and Normark 1987). The generally high sand-mud ratio and the development of well-defined 4th and 3rd order coarsening-up trends typical for lobes, are typical for an active margin setting (Shanmugam and Mojola 1988). Hence, the general development of the depositional environment is interpreted to be dominated by tectonic activity. However, the correspondence between 2nd-order depositional sequences and short-term sea-level changes imply a subordinate influence of eustatic sea-level variations.

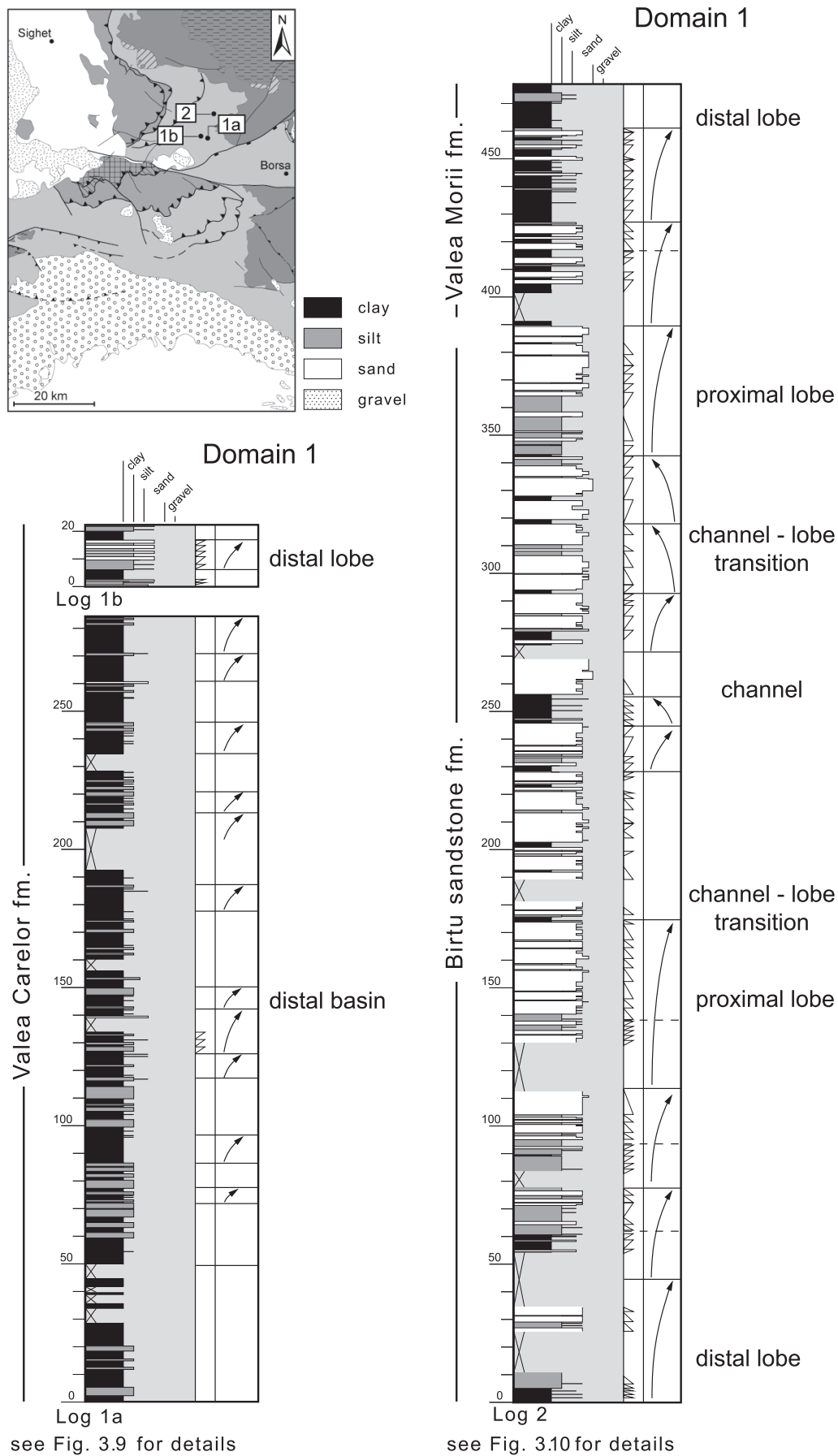


Fig. 3.13: Simplified overview on logs 1 and 2. Following the gradual progradation from basin plain deposits towards a distal lobe setting (log 1a, 1b), a complete 2nd-order depositional sequence (progradation and retrogradation) is documented in log 2 (Lower Oligocene Birtu Sandstone Fm.).

3.5.3 Paleocurrent measurements

Paleocurrent data have been measured focusing on Oligocene to Burdigalian strata throughout the study area (Fig. 3.15). The structures recorded are mainly flute casts and scour marks, subordinately tool marks, groove casts and parting lineations. In the case of coarse grained, conglomeratic layers, long axes of imbricated pebbles have been measured. Where the imbrication of pebbles was used as paleocurrent indicator, the data are presented in form of a rose diagram (Fig. 3.15). Paleocurrent indicators derived from beds with a dip of more than 30° have been backtilted, using the strike and dip of the respective bed.

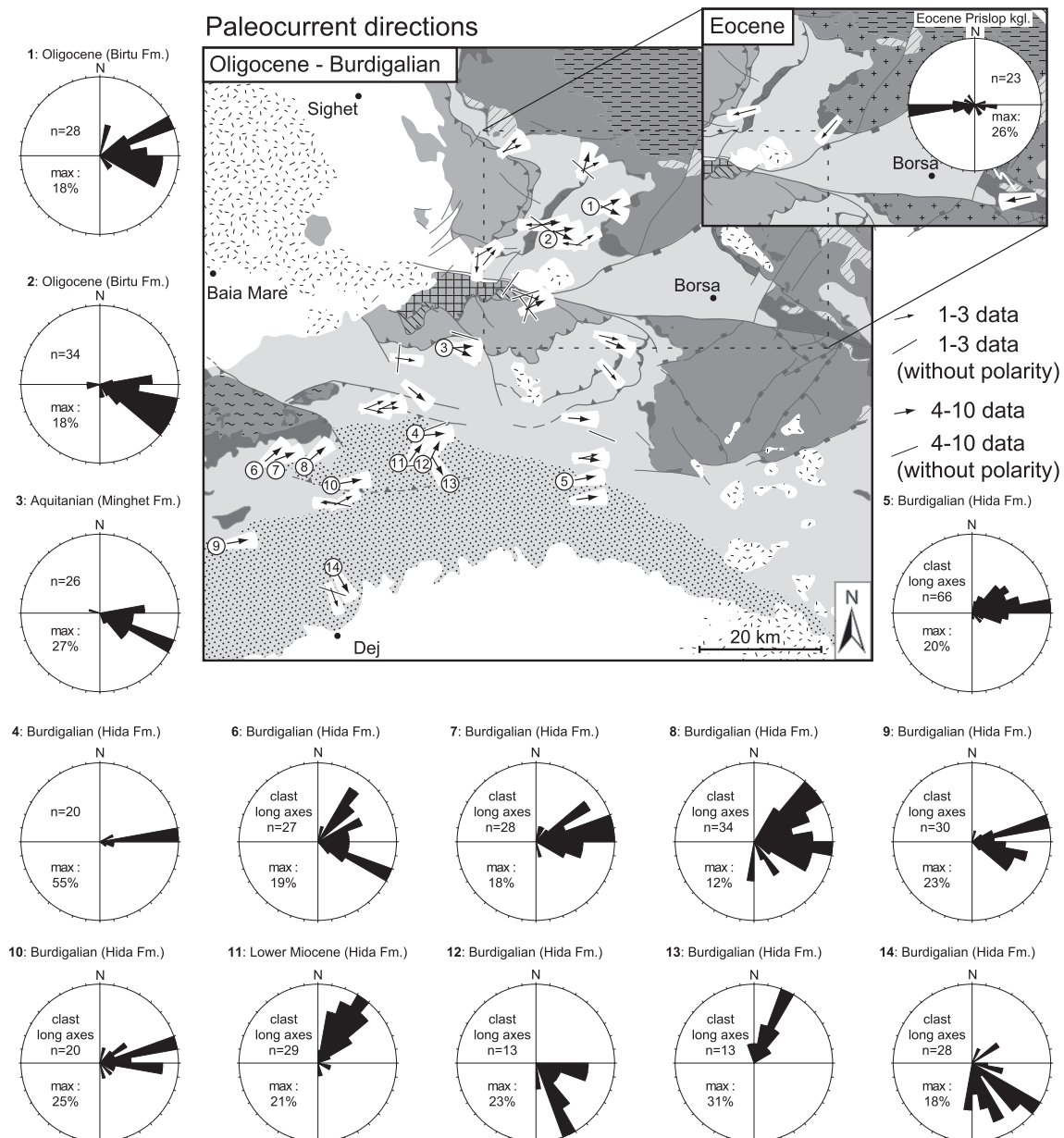


Fig. 3.15: Map showing paleocurrent trends in the study area. Paleocurrent directions change from Eocene W-ward (inset) to Oligocene SE-ward transport. During Oligocene to Burdigalian times NE and ESE-ward directions are dominant. Structures used are flute casts, scour marks, tool marks, groove casts and parting lineations where not specifically noted. Note that Locations 1-4 comprise indicators from logs of 100-400m of sediment thickness. For legend and location of the map compare Fig. 3.2.

Coeval to the change in depositional environment indicated by the drowning of carbonate platforms at the Eocene-Oligocene boundary, a pronounced change in the paleocurrent directions occurred. W-directed transport recorded for Eocene times (Fig. 3.15 inset), switched to NE- to ESE-directed transport in Oligocene to Burdigalian times.

Two directions are dominant (Fig. 3.15): one towards NE and the other towards ESE. This distribution is evident in individual outcrops as well as on the regional scale (Fig. 3.15, locations 1, 2, 3). The observed directions are in good accordance with existing data from Oligocene deposits (Jipa 1962; Mihailescu and Panin 1962). A log in the Oligocene sandy flysch of the most external Pienide nappe (Wildflysch nappe) yielded compatible paleocurrent directions.

The persistence of the observed paleocurrent directions might suggest a similar basin geometry and depositional setting for the Oligocene to Burdigalian strata. The NE-ward directions are subparallel to the thickness maximum visible within the clastic wedge (Fig. 3.2), indicating a longitudinal transport with respect to the basin axis. The SE directed paleocurrent indicators document transversal transport.

3.5.4 Petrographic overview of the studied flysch units

Thirty-two thin sections (sand- grain size interval) from Lower Oligocene to Burdigalian sandstones have been analysed. Between the Lower Oligocene and the Burdigalian samples only minor changes occur in sandstone composition. The sandstones are moderately to well-sorted litharenites (classification of Pettijohn et al. 1987), with a dominantly pseudosparitic matrix. Grains are subangular to subrounded and have a low sphericity. Most samples only show weak signs of compaction, point contacts between grains dominate. Compaction features like bent micas and solution of carbonate grains are common in the Lower Oligocene to Aquitanian strata, while more rare in Burdigalian samples. The lithic clasts are mainly limestone (10-20%) and chert (~5%), subordinately volcanic clasts. Micaschists / gneiss and mud / siltstones occur rarely. An increase in the overall percentage of lithics implies decreasing compositional maturity for the Burdigalian samples. While the average composition of the Oligocene and Aquitanian sands is roughly $Qt_{50}F_{20}L_{30}$ (Total Quartz – Feldspar – Lithics) the average composition of the Burdigalian samples is estimated to about $Qt_{50}F_{15}L_{35}$.

A rough estimation of the modal composition of the samples (Tucker 1981) has been obtained by comparing the sandstone field of view to visual estimation charts (Flügel 1978). These modal compositions have been plotted into standard triangular diagrams for detrital modes (Dickinson 1985) and are compared to the compositional fields indicative for different provenance types (Fig. 3.16). Note, that in the classification after Dickinson (1985), limeclasts are not included into the sedimentary lithics pole.

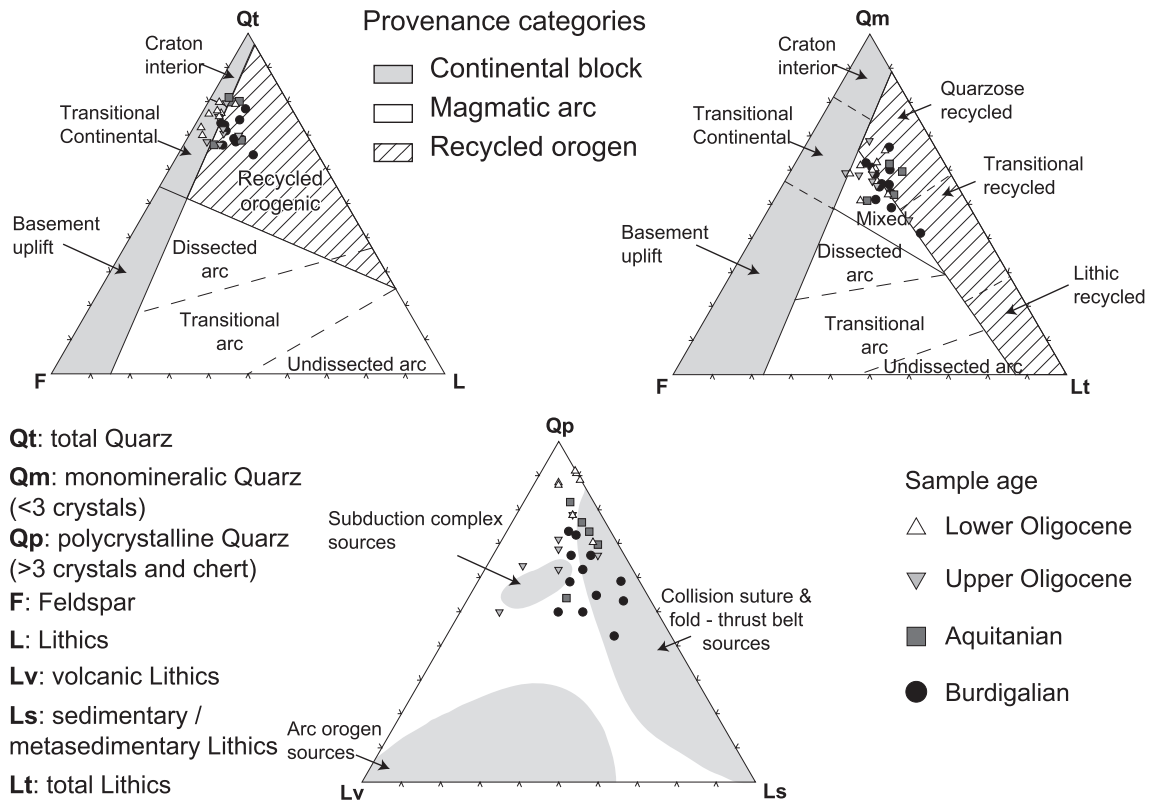


Fig. 3.16: Modal compositions of the analysed samples, based on a rough visual estimate. The compositions and low maturity are suggestive for a foreland basin setting. The Burdigalian samples show a decrease in compositional maturity and an affinity towards fold-and-thrust-belt sources, well comparable to their interpretation as molasse deposits.

The analysed samples plot in the QtFL and QmFLt – Diagrams in the “recycled orogenic” and “continental block” provenance category fields. A trend towards the “recycled orogenic” field with decreasing rock age can be inferred (Fig. 3.16), reflecting the decrease in compositional maturity.

The abundance of sedimentary lithic grains (Ls, QpLvLs – plot), reflecting a relatively short transportation way is suggestive for a fold-and-thrust-belt setting, where detritus from a recycled orogenic source is deposited (Dickinson 1985). The relative proximity to the source area is also reflected by the low degree of rounding of the constituent grains. The abundance of calcareous lithoclasts (not included into the Ls pole, 10 - 25%) also is an important characteristic of foreland sandstone suites (Dickinson 1985).

The analysis of the various types of quartz grains showed a predominance of monocrystalline quartz (up to 70% of total quartz population), with common undulose extinction (half of the monocrystalline population). This observation excludes pure plutonic source areas. The relative abundance of polycrystalline quartz grains with more than 3 crystals (up to 15% of quartz population) points towards a source with a rather low degree of metamorphism.

The rough estimate of modal compositions of the analysed sandstones shows an affinity to recycled orogenic source areas, and decreasing compositional maturity with decreasing rock age. These modal compositions, as well as the abundance of calcareous lithoclasts are well compatible with a foreland basin setting.

3.5.5 Micropaleontological data

Since only few data are available regarding the age of the Hida Formation, samples have been collected for microfossil dating. The preparation of samples followed standard procedures (careful crushing, disaggregation in H₂O₂, sieving, drying at 50°C, picking; Wissing and Herrig 1999). Sample locations are indicated in Figures 3.12 and 3.17. Dating of the mikropaleontological assemblages has been carried out by Prof. Dr. Sorin Filipescu from Cluj University (Table 3.1).

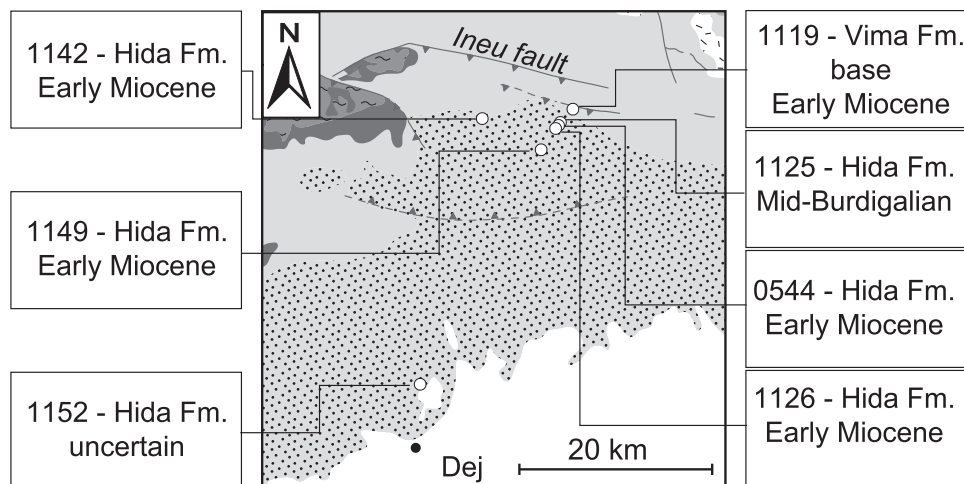


Fig. 3.17: Sample locations and ages of micropaleontological dating samples. Sample 1125 confirms the Burdigalian age of the Hida Fm. The exact location of samples taken in conjunction with a lithostratigraphic log (samples 0544, 1125, 1142, 1126, 1152) is indicated in Fig. 3.12. Samples 1125 and 1119 are also indicated in Fig 3.6.

All analysed samples yielded Early Miocene ages. In two cases a more exact age could be inferred. Sample 1119, collected below the base of the Hida Fm. (Fig. 3.17) yielded a probable base of Early Miocene age, while sample 1125, collected from the basal Hida beds yielded a probable Mid-Burdigalian age.

The suspected earliest Miocene ages of sample 1119 contradict Dicea et al. (1980), assigning a Burdigalian age to the locality in question. This is most likely an effect of the south-side-up offset at the Ineu fault and a similar satellite fault (Fig. 3.6).

The probable middle Burdigalian age from the basal parts of the Hida Fm. (sample 1125) confirms the generally accepted Burdigalian age of the Hida Formation. The micropaleontological assemblage found in this sample, together with the lithofacies associations of this locality (Fig. 3.12) suggest a deep marine turbiditic environment. This observation implies, that the transition from flysch towards molasse commences in Burdigalian times, within the Hida Formation.

Sample 1149 yielded an Early Miocene age slightly older than expected. The species *Pyramidulina latejugata* and *Lenticulina arcuatostrata* are typical for the Chechiş Formation (Early Burdigalian). A possible explanation for this is a heterochronous onset of coarse clastic input within the Hida Fm. The Burdigalian ages of the Hida Fm. clearly show that the onset of coarse clastic input in the southern part of the study area commences later than in the north. The microfossil assemblages indicate a shallowing-up trend for the Hida Formation.

Sample	X	Y	mikropaleontological assemblage	environment	age
0554 Hida Fm.	24.055	47.4374	agglutinated foraminifera (<i>Nothia robusta</i> – very frequent, <i>Rhabdammina discreta</i> , <i>Reticulophragmium rotundidorsatum</i>)	deep marine, turbiditic	probably Early Miocene
1119 Vima Fm.	24.0749	47.4571	flattened planktonic foraminifera (<i>Catapsydrax univavus</i> , <i>Globigerina eurapertura</i> , <i>Globigerina officinalis</i> , <i>Globigerina praebulloides</i> , <i>Globigerina wagneri</i> , and other indeterminate species)	pelagic,	probably base of the Early Miocene
1125 Hida Fm.	24.0582	47.4408	agglutinated foraminifera (<i>Retigulophragmium acutidorsatum</i> , <i>Rhizammina algaeformis</i> , <i>Karrerulina horrida</i>) and rare, poorly preserved, planktonic foraminifera (<i>Globigerinoides trilobus</i> , and other indeterminate species)	deep marine, turbiditic	Early Miocene (probably Middle Burdigalian)
1126 Hida Fm.	24.0558	47.4362	flattened and poorly preserved planktonic foraminifera (<i>Globigerina cf. anguliofficialis</i> , <i>Globigerina cf. falconensis</i> , <i>Globigerinoides cf. trilobus</i> , and other indeterminate species)	pelagic	probably Early Miocene
1142 Hida Fm.	23.9497	47.4434	agglutinated foraminifera (<i>Nothia excelsa</i> , <i>Reophax scorpiurus</i> , <i>Haplophragmoides suborbicularis</i>) together with fish bones and teeth	deep marine, turbiditic	probably Early Miocene
1149 Hida Fm.	24.0303	47.4145	agglutinated foraminifera (<i>Rhizammina algaeformis</i> , <i>Ammodiscus incertus</i> , <i>Glomospira charoides</i>) and calcareous foraminifera (<i>Pyramidulina latejugata</i> , <i>Lenticulina arcuatostrata</i>)	probably continental slope	Early Miocene (not higher than boundary between Chechiş and Hida formations)
1152 Hida Fm.	23.8648	47.197	very rare calcareous foraminifera tolerant to salinity fluctuations (<i>Ammonia</i> div. sp.), reworkings from Cretaceous, fish bones and teeth	sedimentary lobes	uncertain

Table 3.2: Microfossil assemblages of the analysed samples and their probable environment. Compare Figs. 3.6, 3.12 and 3.17 for location of samples. Coordinates are lat/long WGS 84.

3.6 Summary

An overall southward migration of subsidence followed by the deposition of coarse terrigenous clastics, is documented in the study area. The onset of this deposition is of Early Oligocene age in the northern parts of the study area, continuously younging to Burdigalian age at the northern rim of the Transylvanian basin. The facies associations and their depositional trends are suggestive for an active margin setting. The sandstone composition indicates a foreland basin setting. A subdivision into depositional sequences (as documented in Domain 1, Fig. 3.13) possibly documents phases of enhanced tectonic activity. Such a subdivision is consistent with the results from the analysis of seismic lines (Fig. 3.5). Due to bad exposure conditions and insufficient temporal resolution such depositional sequences could not be established for a basin-wide scale, preventing a detailed reconstruction of the tectonic history.

The SE-ward thinning clastic wedge, as seen in seismic records from the Transylvanian basin (Fig. 3.6), shows an internal geometry suggestive for a foreland basin fill. Two important intra-Burdigalian unconformities indicate phases of tectonic activity, forcing the system to further propagate towards the SE. The geometry of the clastic deposits, based on available subsurface data (Fig. 3.2) is suggestive for an elongate basin (WSW-ENE striking axis) with major clastic input derived from provenances from the NW. This observation is confirmed by paleocurrent measurements within the Burdigalian strata, showing a bimodal distribution, where NE directed transport (longitudinal) is more prominent than the SE directed current directions. The Burdigalian deposits show a general development from flysch towards molasse, reflected in the lithofacies as well as petrographical composition of deposits.

The most likely cause for the formation of the flexural basin is the emplacement of the Pienides as already suggested by Ciulavu (1998). Observations confirming this assumption include their position in the probable source area of the clastic deposits as well as their SE-directed emplacement direction, roughly perpendicular to the basin axis. The emplacement of the Pienides is thought to represent the final stages of the juxtaposition of the ALCAPA and Tisza-Dacia blocks. It seems highly likely that the Oligocene to Burdigalian clastic deposits at the northern border of the Transylvanian basin are related to a continuous process which started at the Early Oligocene and led to a S / SE-ward propagating formation of a flexural foreland basin. A change in the basin axis from E-W to SE-NW (DeBroucker et al. 1998) towards WSW-ENE could be related to a clockwise rotation of the Tisza-Dacia Block (compare chapter 4 and 5).

A schematic tectonic model proposing an explanation for the observed change in the basin axes is depicted in Fig. 3.18. In this tectonic model, the change from E-W to SE-NW trending towards a WSW-ENE oriented (in present coordinates) longitudinal axis of the flexural basin is explained by a migration of shortening between Oligocene and Burdigalian times. In the initial stage of thrusting, localised shortening leads to the formation of an Oligocene flexural foredeep. As thrusting continues and migrates to the SW, the old longitudinal basin axes are passively rotated. The last stage of thrusting in Burdigalian times leads to the development of a WSW-ENE oriented flexural basin.

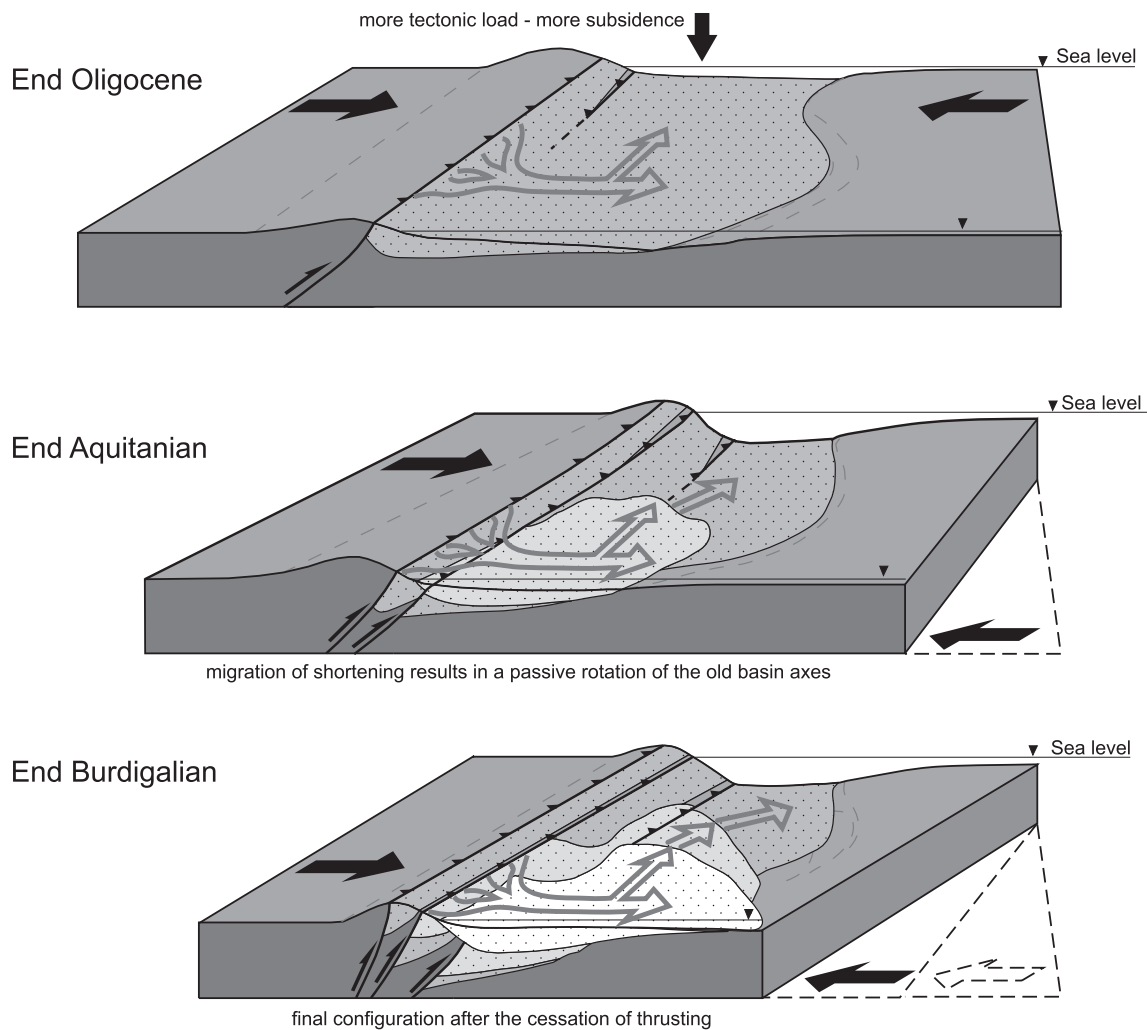


Fig. 3.18: Schematic block diagram of the proposed tectonic setting causing the development from an E-W to NW-SE trending Oligocene basin axis towards a WSW-ENE trending Burdigalian basin axis. A migration of shortening during nappe emplacement leads to a passive rotation of the Oligocene Basin.

In order to reconstruct the basin geometry and development, further studies focussing on sequence-stratigraphic aspects would be necessary. By the correlation of basin-wide data (well logs, seismic records), combined with a high resolution dating, valuable constraints for the Oligocene tectonic history could be obtained.

Chapter 4:

The contact zone between the ALCAPA and Tisza-Dacia mega-tectonic units of Northern Romania in the light of new paleomagnetic data

*Emő Márton¹⁾, Matthias Tischler²⁾, László Csontos³⁾, Bernhard Fügenschuh^{2, 4)},
Stefan M. Schmid²⁾*

Eclogae Geologicae Helveticae (accepted)

¹⁾ Paleomagnetic Laboratory, Eötvös Loránd Geophysical Institute of Hungary, Columbus 17-23, H-1145 Budapest, Hungary

²⁾ Geologisch-Paläontologisches Institut, Basel University, Bernoullistr. 32, CH-4056 Basel, Switzerland

³⁾ Physical and Historical Geology, ELTE University, Pázmány Péter sétány 1/C, H-1117 Budapest, Hungary

⁴⁾ Institute for Geology and Paleontology, Innsbruck University, Innrain 52f, A-6020 Innsbruck, Austria

Keywords: Rotation, Paleomagnetism, Tisza-Dacia, Carpathians, Transcarpathian Depression, Northern Romania

4.1 Abstract

Paleomagnetic analyses were carried out on samples from 19 localities within two different mega-tectonic units in Northern Romania: Tisza-Dacia (11 localities) and ALCAPA (8 localities). The samples cover a range of different lithologies: (1) Late Cretaceous red-coloured marl to marly limestone, (2) Eo- /Oligocene flysch sediments, and (3) Mid-Miocene (Langhian) tuffite (Dej tuff and related sediments). The Late Cretaceous and Mid-Miocene specimens carry secondary paleomagnetic signals exhibiting a counter clockwise deflection of the paleo-declinations by some 30°, while the Eo-/Oligocene localities indicate an overall clockwise deflected (between some 45° and >90°) paleo-declination with respect to present-day north. Clockwise rotation postdates the age of sedimentation (Early Oligocene), as well as (at least partially) thrusting of the Pienides onto the Tisza-Dacia mega-tectonic unit, which occurred between 20.5 and ~18.5 Ma. Clockwise rotation predates post-12 Ma counter clockwise rotations inferred for the Mid-Miocene localities.

Surprisingly, the clockwise rotations of the first rotational stage not only affected the (par-) autochthonous sedimentary cover of the Tisza-Dacia mega-tectonic unit, but also the allochthonous flysch nappes of the Pienides, i.e. the eastern tip of the ALCAPA mega-tectonic unit. Well-documented opposed rotation of the remainder of ALCAPA necessitates a detachment of this eastern tip of ALCAPA after ~18.5 Ma.

The most likely location for this detachment zone is along the margins of the Transcarpathian depression. During a second (post-12 Ma) stage, counter clockwise rotations of up to 30° affected the entire working area. Regarding timing and magnitude, these second stage rotations are similar to rotations documented for the East Slovak basin, but different from those reported from the South Apuseni Mountains and the Central and Inner West Carpathians located west of the East Slovak basin.

4.2 Zusammenfassung

An insgesamt 19 Lokalitäten in Nord-Rumänien wurden paleomagnetische Analysen in zwei grosstektonischen Einheiten durchgeführt: 11 Lokalitäten liegen im Tisza-Dacia Block, 8 sind Teil der ALCAPA-Einheit. Die untersuchten Proben umfassen folgende Lithologien: (1) Oberkretazische rote Kalkmergel, (2) Eo-Oligozäne Flysche und (3) Tuffite (Dej-Tuff und assoziierte Sedimente) des Mittleren Miozäns (Langhian). Die Proben aus der Oberkreide und dem Mittleren Miozän zeigen eine sekundäre Magnetisierung, deren Paläo-Deklination um ca. 30° gegen den Uhrzeigersinn rotiert ist. Die Paläo-Deklinationen der Eo- Oligozänen Proben hingegen weisen Abweichungen zu gegenwärtig Nord mit dem Uhrzeigersinn (45° und >90°) auf.

Die Rotation der Eo-Oligozänen Proben fand nach der Sedimentation der jüngsten Proben (unteres Oligozän), und zumindest teilweise nach dem Deckenschub der Pieniden (20.5 - ~18.5 Ma) auf den Tisza-Dacia Block statt. Diese Rotation mit dem Uhrzeigersinn geht der durch die Mittel- Miozänen Proben dokumentierten gegenläufigen Rotation (ab 12 Ma) voraus.

Die Rotationen der früheren Phase wurden nicht nur in den Sedimenten aus der (par-) autochthonen Bedeckung von Tisza-Dacia, sondern auch in den überschobenen Pieniden nachgewiesen. Dieses Ergebnis ist auf den ersten Blick überraschend, da sie Teil von ALCAPA sind, der Rest von ALCAPA zu dieser Zeit aber in einem gegenläufigen Sinn, also gegen den Uhrzeigersinn, rotierte. Diese gegenläufigen Rotationen erfordern also eine tektonische Ablösung der östlichsten Spitze von ALCAPA vom Rest dieser grosstektonischen Einheit. Der wahrscheinlichste Ort für eine solche Ablösung befindet sich an den Rändern der Transkarpathischen Depression. Die zweite Rotationsphase, ca. 30° gegen den Uhrzeigersinn nach 12 Ma, ist auch aus dem Ost-Slovakischen Becken bekannt. Sowohl die Internen West-Karpathen westlich des Ost-Slovakischen Beckens, als auch das südliche Apuseni Gebirge, zeigen nach 12 Ma ein vom Arbeitsgebiet abweichendes Rotationsverhalten.

4.3 Introduction

Opposed rotations of the two mega-tectonic units building the Carpathians, termed ALCAPA and Tisza-Dacia (Fig. 4.1), are well established by paleomagnetic studies (e.g. Márton and Márton 1978, 1996; Márton and Fodor 1995, 2003; Panaiotu 1998, 1999; Márton 2000) and represent a central issue in the reconstruction of the Tertiary kinematics of these highly mobile units. In several tectonic reconstructions ALCAPA and Tisza-Dacia are treated as two distinct “microplates” or “blocks” (e.g. Fodor et al. 1999, Csontos and Vörös 2004), although both mega-tectonic units were internally deformed. This is particularly true for their contact zone, the Mid-Hungarian fault zone, which continues into Northern Romania (Csontos and Nagymarosy 1998, Fodor et al. 1999, Györfi et al. 1999, Tischler et al. 2006).

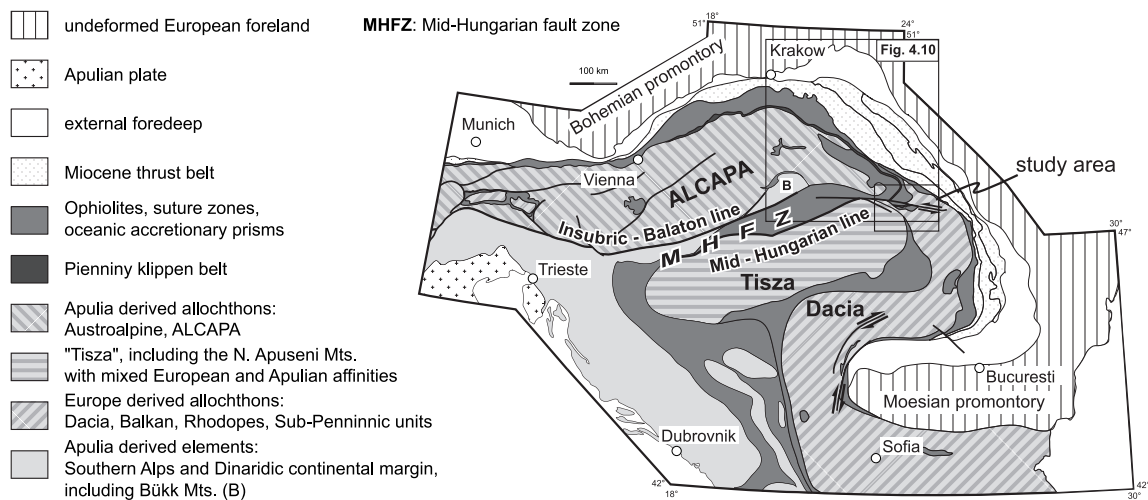


Fig. 4.1: Major tectonic units of the Alps, Carpathians and Dinarides (simplified after an unpublished compilation by S. Schmid, B. Fügenschuh, K. Ustaszewski, M. Tischler and L. Matenco). The boxes mark the outlines of Fig. 4.10 and the study area, respectively.

The invasion of the ALCAPA and Tisza-Dacia mega-tectonic units into the Carpathian embayment is thought to be driven by retreat of the European lithospheric slab (e.g. Royden 1988, Wortel and Spakman 2000) and is coupled to “lateral extrusion” in the Eastern Alps (Ratschbacher 1991 a, b; Sperner et al 2002).

Final emplacement of these mega-tectonic units was accompanied by substantial strike-slip movements, extension and/or block rotations (Fodor et al. 1999, Márton 2000, Csontos et al. 2002, Márton and Fodor 2003, Horváth et al. 2006). Corner effects at the Bohemian (Sperner et al. 2002) and Moesian (Ratschbacher et al. 1993, Schmid et al. 1998, Fügenschuh and Schmid 2005) promontories (Fig. 4.1) are considered as important causes for the opposed rotations of continental units during their Neogene emplacement into the Carpathian embayment. Converging movements partly also accommodated such rotations; they led to the juxtaposition, and finally the thrusting of ALCAPA onto Tisza-Dacia, as is documented by subsurface and outcrop data (e.g. Csontos and Nagymarosy 1998, Györfi et al. 1999, Tischler et al. 2006) along the Mid-Hungarian fault zone. The Mid-Hungarian fault zone shows a poly-phase history, allowing for repeatedly occurring differential movements between the invading mega-tectonic units (e.g. Csontos and Nagymarosy 1998, Fodor et al. 1998, 1999).

Most of the contact zone between the ALCAPA and Tisza-Dacia mega-tectonic units is covered by the Neogene fill of the Pannonian basin, but it is exposed in the Maramures area (Northern Romania).

In this paper two independent methods and studies are combined to better understand the tectonic evolution of the region, namely outcrop-scale structural studies (Huismans et al. 1997, Györfi et al. 1999, Tischler et al. 2006) and paleomagnetic investigations. The latter became possible since the recent regional tectonic study by Tischler et al. (2006) provided suitable outcrops for paleomagnetic sampling, in a generally badly exposed area with friable lithologies. The analysis of structural and paleomagnetic data sets was performed separately and was only combined in a last step. Paleomagnetically registered rotations were robust and extended beyond the study area. This leads us to propose a working hypothesis for the structural and rotational history of the area for the last 30 Ma.

4.4 Geological setting

The study area, located in northern Romania, at the northern margin of the Transylvanian basin, is in an internal position with respect to the main Carpathian chain. The crystalline basement and Mesozoic cover units, which crop out in the study area (Fig. 4.2), belong to the Tisza unit (Bihar unit) and the Dacia-unit (Infra- Sub- and Bucovinian nappes). Both units form a single Tisza-Dacia mega-tectonic unit since Early Tertiary times. These basement units have a poly-phase deformation history; their internal structure was formed during middle to latest Cretaceous times (Săndulescu et al. 1981). During Late Cretaceous and Paleocene times, a common sedimentary cover (“autochthonous cover” of Fig. 4.2) was deposited onto both Tisza and Dacia units, thus sealing all earlier tectonic contacts (Săndulescu 1994).

Eocene strata again unconformably overlay these Upper Cretaceous and Paleocene sediments. In the northern part of the study area a westward deepening of the depositional environment is documented (local carbonate platforms and conglomerates in the east, marly littoral-neritic facies in the west; Dicea et al 1980, Săndulescu et al. 1981). In the southern part of the study area, continental to shallow marine environments prevail during the Eocene (Popescu 1984, DeBroucker et al. 1998).

Following a regional drowning event at around the Eocene/Oligocene boundary terrigenous siliciclastics have been deposited in a E-W to SE-NW oriented basin (DeBroucker et al. 1998). A SE-ward thinning clastic wedge of Burdigalian age (“Burdigalian molasse”, Fig. 4.2), deposited in a WSW-ENE trending basin, is documented at the northern border of the Transylvanian basin (Ciulavu et al. 2002).

Coevally with the deposition of this clastic wedge, flysch nappes (“Pienides”, Fig. 4.2) have been thrust onto the autochthonous cover of the Tisza-Dacia mega-tectonic unit, leading to imbrication of this autochthonous cover in the Early Burdigalian (20.5 – 18.5 Ma; De Broucker et al. 1998, Györfi et al. 1999, Tischler et al. 2006).

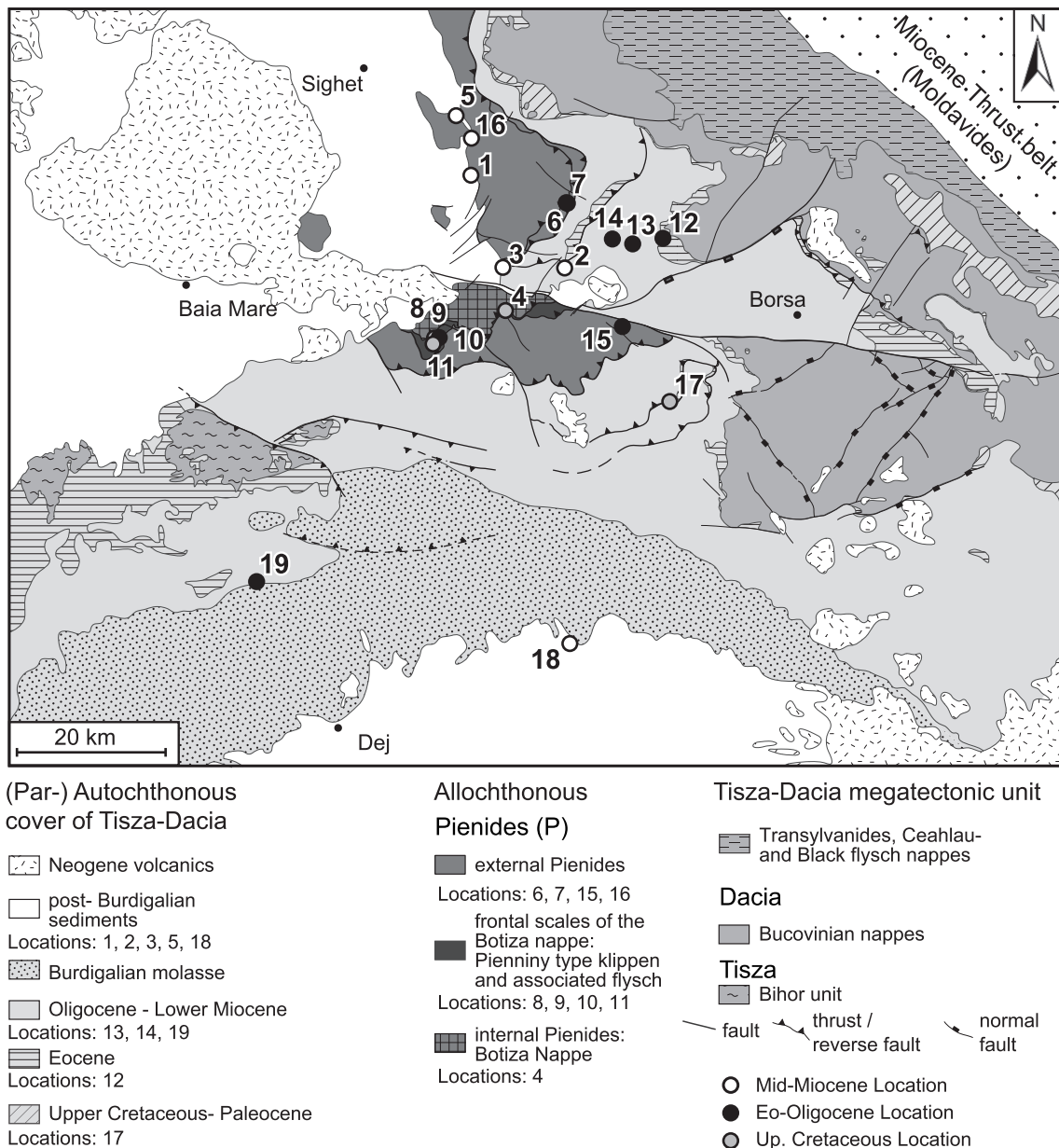


Fig. 4.2: Tectonic map of the study area, based on published geological maps (1:50.000 and 1: 200.000) of the Geological Survey of Romania, Dicea et al. (1980), Săndulescu (1980), Săndulescu et al. (1981), Aroldi (2001) and Tischler et al. (2006). Sampling localities are indicated.

The various units of the Pienides (Săndulescu 1984, 1994; Săndulescu et al. 1993) consist of Eocene and Oligocene flysch units and can be divided, from internal to external, into: Botiza nappe, Pieniny type klippen including associated flysch and external nappes (Petrova, Wildflysch and Leordina nappes). The Pienides represent the eastern continuation of the Pieniny Klippen Belt and the Magura unit of the Western Carpathians (Săndulescu 1980). Hence they are considered as parts of ALCAPA by most authors (e.g. Balla 1984, Csontos 1995, Kováč et al. 1994, Fodor et al. 1999, Tischler et al. 2006).

Their emplacement onto the autochthonous cover of the Tisza-Dacia mega-tectonic unit is thought to represent the last increment of thrusting of the frontal part of ALCAPA onto Tisza-Dacia (see also Györfi et al. 1999). The direction of emplacement (SE-directed in present coordinates) is roughly perpendicular to the long axis of the wedge of the Burdigalian molasse (Fig. 4.2).

This supports the interpretation of the wedge-shaped Burdigalian deposits in terms of a foreland basin fill related to the emplacement of the Pienides, as was previously suggested by De Broucker et al (1998), Györfi et al. (1999) and Ciulavu (1998). During Miocene times the ALCAPA and Tisza-Dacia mega-tectonic units were docked to the European foreland, generating the Miocene thrust belt (Fig. 4.2).

Above a second regional unconformity dacitic tuffs (Dej Tuff) of Langhian (Badenian) age (post-16 Ma; this and all later conversions into an absolute time scale are after Gradstein et al 2004) were deposited onto both the Tisza-Dacia mega-tectonic unit and the Pienides, already thrust onto Tisza-Dacia. The source area of the volcanic activity is thought to be located NW of the study area (Szakács et al. 2000). Andesitic volcanic activity between 14 - 9 Ma (Pécskay et al. 1994) led to the formation of the volcanic body near Baia Mare (Fig. 4.2), which obscures the western continuation of the Pienides.

Starting in Mid-Miocene times, two stages of strike slip dominated brittle deformation indicate ongoing deformation after the amalgamation of Tisza-Dacia with ALCAPA (Tischler et al. 2006). A first transpressional stage (16 – 12 Ma) is dominated by SW-NE compression; active map scale features are the Preluca fault and the Bogdan-Voda fault. This transpressional stage is followed by transtension (SW-NE compression, with dominant NW–SE extension, 12 – 10 Ma), representing the main phase of left lateral movement along the so-called Bogdan- Dragos Voda fault system. These deformations are most probably connected to left lateral transtension along the Mid-Hungarian fault zone (e.g. Csontos and Nagymarosy 1998). Yet substantial relative rotations between the ALCAPA and the Tisza-Dacia mega-tectonic units can be excluded for this late stage of the tectonic evolution (Tischler et al. 2006).

4.5 Paleomagnetic sampling

Samples were collected at 19 localities (Table 4.1 and Fig. 4.2). They cover a range of lithologies and represent different ages and tectonic units. Great care had to be taken to avoid strata, which had been affected by recent gravitational creep or sliding, which is common in the study area. In addition, the need for sufficiently fine-grained and visibly unaltered sediments led to the abandonment of some of the localities visited without sampling. Samples were taken using a portable drill; the cores were oriented with a magnetic compass. The number of independently oriented cores at each locality (Table 4.1) depended on the outcrop conditions in terms of lithology, angle of dip (hence tilt) of the sediments and also on the prospect of obtaining useful paleomagnetic directions. The lithologies included dacite tuffite (“Dej tuff”) and accompanying sediments (e. g. localities 5 and 8), dark grey (silty) marls and red marls (Couches rouges). The age of the sampled rocks ranges from Latest Cretaceous to Langhian (Badenian).

Standard-size specimens were cut from a total of 153 samples drilled at these 19 sites. They were subsequently subjected to paleomagnetic and magnetic susceptibility anisotropy measurements at the Paleomagnetic Laboratory of the Eötvös Loránd Geophysical Institute of Hungary.

Nr	X	Y	Tectonic unit	age	lithology
1	24.0715	47.8040	Dej tuff	Langhian	tuff
2	24.2418	47.6984	Dej tuff	Langhian	tuff
3	24.1337	47.6965	Dej tuff	Langhian	tuff
4	24.1409	47.6456	Botiza nappe	Sennonian (Turonian?)	marly limestone
5	24.0414	47.8737	Dej tuff	Langhian	tuff / marl
6	24.2425	47.7750	Leordina nappe	Ypresian-Low.rupelian	marl
7	24.2407	47.7758	Leordina nappe	Oligocene	marl
8	24.0274	47.6019	Botiza frontal scales	Cenomanian-Sennonian	marly limestone
9	24.0292	47.6011	Botiza frontal scales	Eocene	marl
10	24.0357	47.6026	Botiza frontal scales	Eocene	marl
11	24.0254	47.5947	Botiza frontal scales	Cenomanian-Sennonian	marly limestone
12	24.4124	47.7375	Autochthonous	Priabonian	marl
13	24.3596	47.7297	Autochthonous	Low. Rupelian	menilitic marl
14	24.3238	47.7347	Autochthonous	Low. Rupelian	marl
15	24.3466	47.7347	Wildflysch nappe	Lutetian - Priabonian	marly silt
16	24.0699	47.8477	Petrova nappe	Lutetian - Priabonian	marly silt
17	24.4338	47.5447	Autochthonous	Turonian - Priabonian	marly limestone
18	24.2742	47.2545	Dej tuff	Langhian	tuff / marl
19	23.7255	47.3135	Autochthonous	Low. Oligocene	marl

Table 4.1: List of sampling localities. X/Y coordinates are given in Lat/Long WGS84.

4.6 Laboratory measurements and results

The natural remnant magnetization (NRM) of each specimen was at first measured by using JR-4 and JR-5a spinner magnetometers. This was followed by the measurement of the anisotropy of magnetic susceptibility (on KLY-2). Sister specimens of selected samples were subsequently stepwise demagnetized, by the alternating field (AF) or the thermal method. After each step the remaining NRM was re-measured (also susceptibility in cases where the thermal method was applied). As the NRM was rarely single component, most samples had to be de-magnetized in several, sometimes in a large number of steps (Fig. 4.3).

Demagnetization graphs (examples are shown in Fig. 4.3) were analysed for linear segments (representing components of the NRM; Kirschvink 1980), and the directions of these segments were used for estimating the mean paleomagnetic directions with statistical parameters (Table 4.2).

After removing a small viscous component, NRM sometimes consisted of a single component (Fig. 4.3A, 4.3F); sometimes two components could be separated (Fig. 4.3B, 4.3C, 3D, 3E). Occasionally, the direction of the natural remnant magnetization for some samples moved along a great circle without reaching a stable end point (i.e. the components constraining the great circle were not clearly separable). In such cases (localities 10 and 13, see Table 4.2) the mean paleomagnetic directions for a given locality were determined in three different ways. One was based on linear segments, the second was calculated from the last meaningful demagnetization steps, and the third was based on the combination of stable vectors and remagnetization circles (McFadden 1990). As Table 4.2 documents, the three methods provided the same directions (within the error limit). Unstable behaviour, and consequently failure to determine a mean paleomagnetic direction, only concerned only locality 15, and partly locality 18 (Early Langhian = Lower Badenian sediments). One or more samples from other localities had to be rejected for reasons of instability.

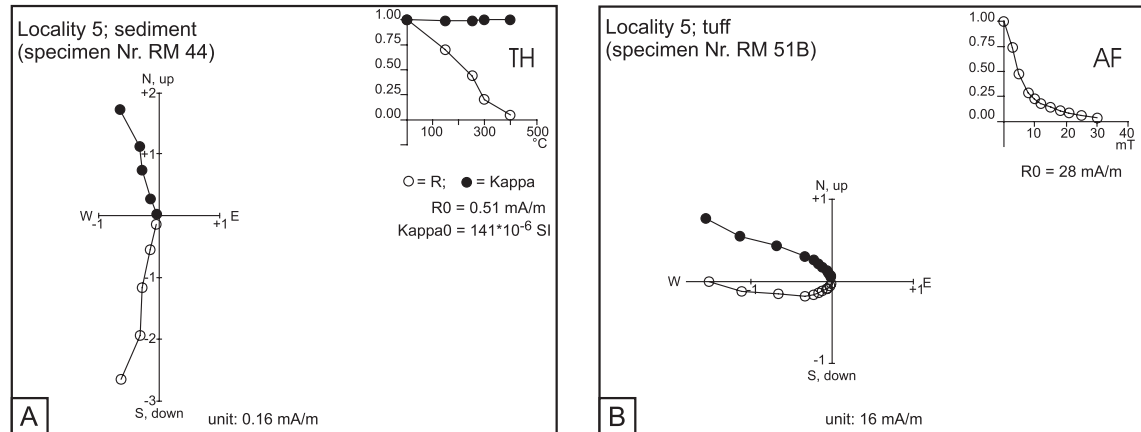
Nr	Locality	n/no	D°	I°	k	α_{95}°	D _c °	I _c °	k	α_{95}°	dip
Dej tuffs and accompanying sediments											
1	Tuff <i>Langhian</i> RM 1-9	4/9	353	+72	212	6	289	75	212	6	224/18
2	Tuff <i>Langhian</i> RM 10-19	4/10	334	+73	151	8	222	78	151	8	181/24
3	Tuff <i>Langhian</i> RM 20-26	7/7	204	-30	104	6	166	-61	104	6	236/45
5a	Sediment <i>Langhian</i> RM 39-47	5/9	339	+57	32	14	3	+14	32	14	28/51
5b	Tuff <i>Langhian</i> RM 48-53	6/6	325	+45	22	14	345	+15	22	14	23/46
18	Dej tuff and accompanying sediment <i>Langhian</i> RM 131-141 (135-137)	3/11	337	+52	159	10	321	+54	159	10	225/10
Autochthonous											
12	Slump? <i>Priabonian</i> RM 97-101	5/5	237	17	13	22	241	2	13	22	238/27
13	<i>lower Rupelian</i> RM 102-107	5/6	330	+26	63	10	324	+8	63	10	280/27
		5/6	328	+10	43	12	329	-8	43	12	
14	<i>lower Rupelian</i> RM 108-114	6/7	264	-26	41	11	274	-57	41	11	251/32
19	Marl <i>Lower Oligocene or</i> <i>Upper Eocene</i> RM 142-153	10/12	256	-49	21	11	276	-43	21	11	157/20
17	red marl <i>Turonian to Priabonian</i> RM 123-130	8/8	188	+18	36	9	173	+66	36	6	20/50 average
Botiza nappe and frontal scales of Botiza nappe (Pienniny type klippen and accompanying sediments)											
9	Flysch <i>Eocene</i> RM 77-79	3/3	351	30	106	12	350	-3	106	12	344/34
10	Flysch <i>Eocene</i> RM 80-88	7/9	294	+27	15	16	295	-13	15	16	312/42
		8/9	298	+14	14	15	296	-26	14	15	
4	red marl <i>Senonian (Turonian?)</i> RM 27-38	8/12	329	+40	24	12	335	+23	7	23	0/28 125/15
8	red marl <i>Cenomanian-Senonian</i> RM 71-76	6/6	321	+51	165	5	321	+21	165	5	300/30
11	red marl <i>Cenomanian-Senonian</i> RM 89-96	8/8	338	+39	29	10	331	+21	12	17	337/30 243/22
External Pienides (Petrova nappe)											
6	Flysch <i>Ypresian - lower Rupelian</i> RM 54-61	5/8	63	+19	8	23	32	+35	8	23	303/57
7	Flysch <i>Ypresian - lower Rupelian</i> RM 62-70,	5/9	269	-3	23	16	249	-41	23	16	311/58
External Pienides (Wildflysch nappe)											
15	Wildflysch <i>Lutetian-Priabonian</i> RM 115-120	0/6	Large scatter, bad demagnetisation behaviour								306/8

* directions calculated from end points of demagnetization

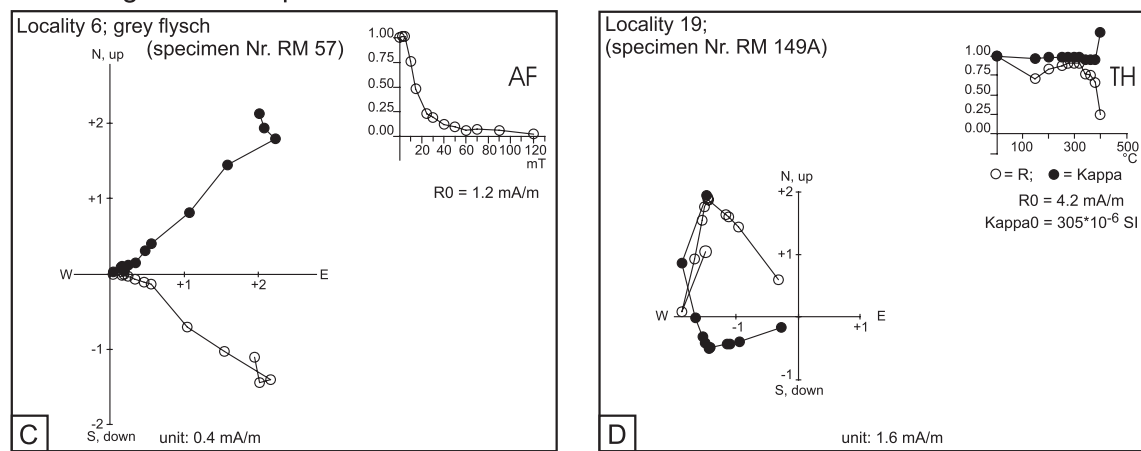
** sediments failed

*** negative within locality fold test

Mid Miocene samples



Eo- / Oligocene samples



Late Cretaceous samples

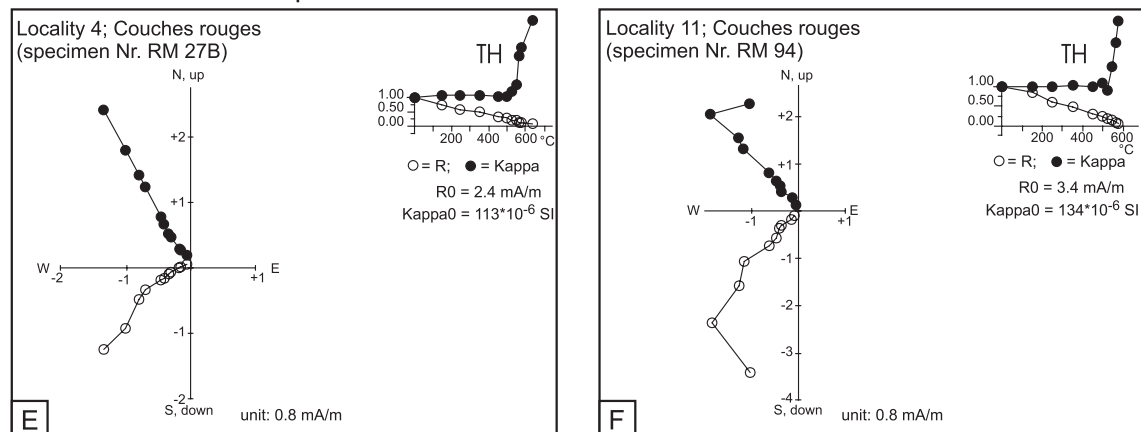


Fig. 4.3: Zijderveld diagrams and intensity/susceptibility versus temperature (TH) or demagnetizing field (AF) curves. Zijderveld diagrams: full/open circles: projection of the natural remnant magnetization in the horizontal and vertical plane, respectively. Other diagrams: dots: susceptibility; circles: intensity of NRM.

Left: Table 4.2: Locality mean paleomagnetic directions with statistical parameters. Key: n/no: number of used / collected samples; D° , I° (Dc° , Ic°): declination, inclination before (after) tilt correction; k and $a95^\circ$: statistical parameters (Fisher 1953). Calculation of directions from least-squares fit of straight line segments after Kirschwink (1980).

From a statistical point of view, the results compiled in Table 4.2 are of different quality. Parameters, k and α are excellent for localities 1, 2, 3, 8 and 17 (k high and α small; Table 4.2); regarding localities: 4, 5, 7, 9, 10, 11, 13, 14, 18 and 19 they are good or acceptable. For localities 6 and 12 the statistical parameters are poor (k lower than 10 or α more than 16° ; Van der Voo 1993). Nevertheless, the tectonic information contained in the result for locality 6 is important. When used in combination with the paleomagnetic direction for locality 7 it provides interesting information about the Pienides. Results for localities 16 and 15 are not tabulated, because too few samples are available and because of the instability of NRM.

Magnetic mineralogy experiments (Lowrie 1990) revealed that the Mid-Miocene samples and the Eo-/Oligocene sediments contain magnetite (Fig 4.4a-c). In the Senonian red marls (Fig. 4.4d) the magnetic mineral is hard and hematite seems to dominate. However, the NRM signal is lost at around 600°C (see Fig. 4.3E). This suggests that slightly oxidized magnetite, rather than hematite, is the actual carrier of the remnant magnetization.

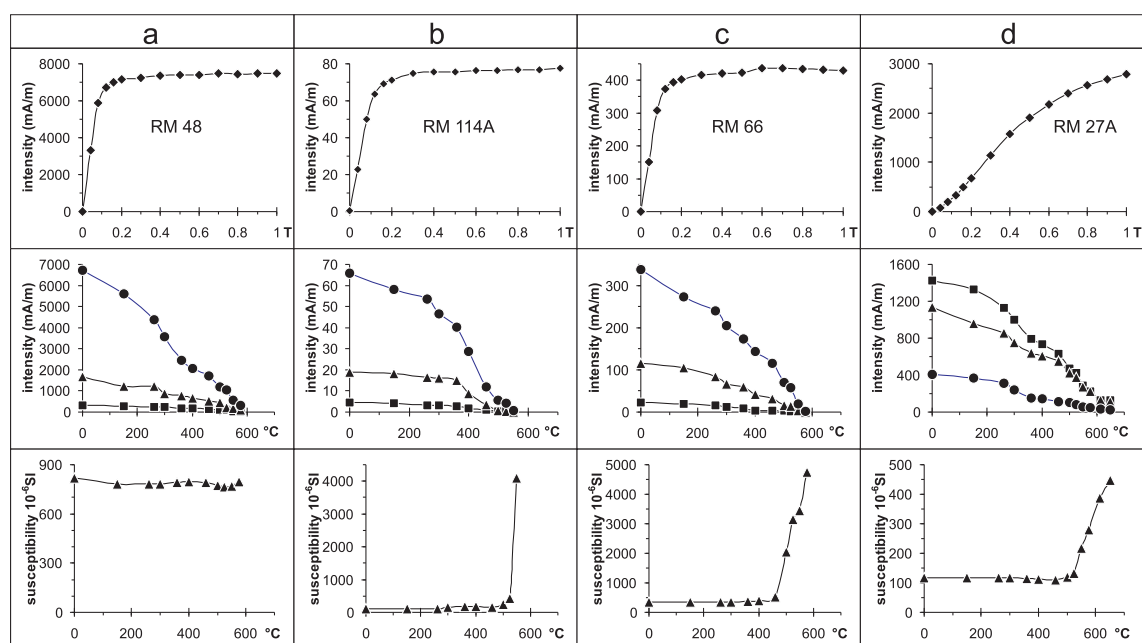


Fig. 4.4: Magnetic minerals, identified by acquisition of isothermal remnant magnetization (IRM, top row), stepwise thermal demagnetization of 3-component IRM (Lowrie 1990), acquired successively in fields of 1.0T (squares), 0.36T (triangles) and 0.12T (circles), respectively, and by the behaviour of the magnetic susceptibility on heating.

Measurements of magnetic susceptibility anisotropy showed that the degree of anisotropy (k_{\max} / k_{\min}) is low in Mid-Miocene samples (between 0.8 and 2.4%), with the exception of locality 18 (as high as 10%). In the remaining samples, the degree of anisotropy lies between 4 and 9%, except for those taken from locality 15, which show a surprisingly low (average 1.4%) degree of anisotropy. This is probably due to the dominance of secondary magnetic minerals, an interpretation corroborated by the failure to obtain a paleomagnetic direction for this locality.

Magnetic fabric is foliated; foliation poles are close to the bedding poles for sedimentary localities, pointing to a dominantly sedimentary origin of the fabric. Magnetic lineation is subordinate (normally less than 1%), yet lineation directions are usually clustered at a given locality (Fig. 4.5).

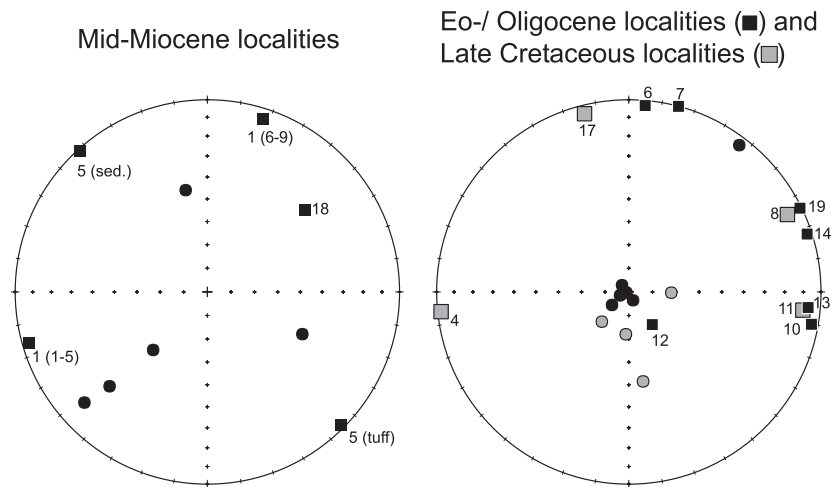


Fig. 4.5: Directions of magnetic lineations (squares; numbered, according to Table 4.1) and foliation poles (dots) in stereographic projection (tectonic system). Note that all magnetic lineations, except 12, are practically horizontal.

There is definitely a small imprint by deformation in case of the sediments that pre-date the Dej tuff, since lineation coincides with the strike of the beds measured in the field. However, a weak lineation suggests weak internal deformation. Consequently, bias of the paleomagnetic vector towards the axis of maximum susceptibility (= "magnetic lineation") is highly unlikely. Concerning the foliation, shallow paleomagnetic inclinations observed for localities 9, 10 and 13 (Table 4.2) are not coupled with a stronger foliation. Therefore inclination shallowing due to compaction is not likely, either.

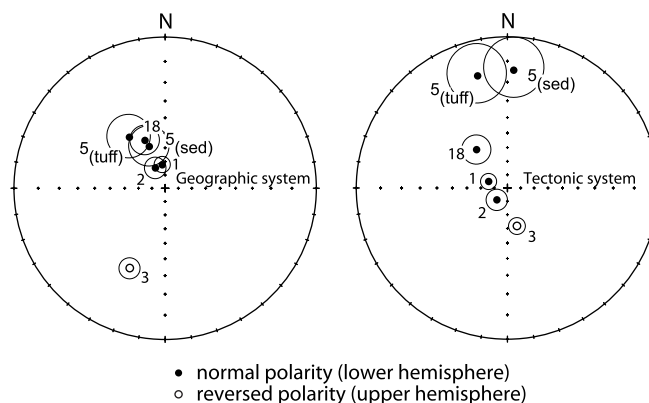
4.7 Discussion of paleomagnetic results

All sampled strata were tilted, occasionally also folded (localities 4 and 11) at the scale of the outcrop. This allowed for fold tests at localities 4 and 11, and for tilt tests on a regional level, thus helping to decide if the paleomagnetic signals were acquired before or after folding/tilting. A positive fold test, characterised by significantly improved clustering of the paleomagnetic directions after application of tilt corrections, suggests acquisition of magnetization before tilting. A negative fold test, with better directional grouping before applying tilt corrections, suggests acquisition of magnetization after tilting. For the test only strata or localities of similar age within the same tectonic unit should be considered. In figures 4.6-4.8 the plots labelled “geographic system” and “tectonic system” show directions before and after tilt corrections (“fold test”), respectively, for the populations of mid-Miocene, Eo-/Oligocene and Late Cretaceous samples.

4.7.1 Mid-Miocene localities: Dej tuff and related sediments

Paleomagnetic directions with normal polarity prevail among the Dej tuff and related sediments. They yield a negative response to tilt corrections (Fig. 4.6, Table 4.2). In our tectonic interpretation we will therefore consider the mean paleomagnetic direction in a geographic coordinate system.

Fig. 4.6: Mean paleomagnetic directions (with confidence circles) for the Mid-Miocene localities. Left: no tilt correction applied; right: tilt correction applied. Tilt test is negative for localities 1, 2, 5 and 18 (Table 4.3), while the mean direction of locality 3 moves towards the rest (with opposite polarity) of the localities after tilt correction.



If we compare the paleomagnetic direction with reversed polarity (locality 3) to this overall mean direction, we can immediately notice that it has a much shallower inclination in geographic coordinates. However, after tilt correction it moves close to the overall mean direction for the normal polarity group (in antipodal position), the latter still in a geographical coordinate system. As the improvement in clustering is basically due to a dramatic improvement in the degree of consistency of inclinations, we interpret the paleomagnetic direction for locality 3 to pre-date tilting (Fig. 4.6). This interpretation implies that number 3 is the only site amongst the Dej tuffs, which preserved the paleomagnetic signal acquired before the tilting event. The overall mean paleomagnetic direction determined this way (Table 4.3, number 3) departs by some 30° from present-day north in a counter-clockwise sense (Fig. 4.6). It is interesting that locality 18, which is situated south of the Dragos-Voda fault, also exhibits counter clockwise rotation.

	N	D°	I°	k	α_{95}°	DC°	IC°	k	α_{95}°	remark
1 Dej tuffs and accompanying sediments localities: 1, 2, 5a, 5b, 18	5	336	+60	38	13	337	+53	4	41	present paper max: -10%
2 Dej tuffs and accompanying sediments localities: 1, 2, 5a, 5b, 18 and 3	6	348	+57	15	18	339	+54	5	32	present paper max: +20%
3 Dej tuffs and accompanying sediments localities: 1, 2, 5a, 5b, 18 before tilt correction and 3 after tilt correction	6	337	+60	46	10	-	-	-	-	present paper
4 Cenomanian-Senonian red marls localities: 4, 8, 11	3	330	+43	81	14	-	-	-	-	present paper
5 Eo/Oligocene autochthonous localities: 14, 19 and Panaiotu RONAP, DS	4	259	-42	37	15	269	-44	60	12	present paper + Panaiotu 1999 max: +60%
6 Eo/Oligocene localities 6,7	2	256	-11	-	-	230	-40	-	-	present paper

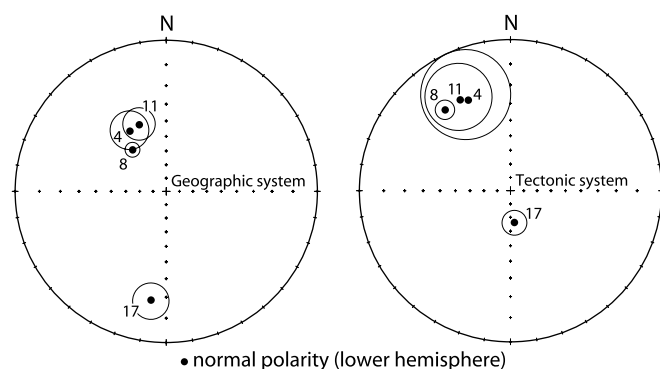
Table 4.3: Overall mean paleomagnetic directions constraining the Tertiary rotations of the Maramures area. Key as for Table 4.2, and N is the number of localities.

This poses a problem in the context of the earlier postulated repeated clockwise rotation of the Tisza-Dacia mega-tectonic unit (Panaiotu 1999); but we have to keep in mind that this result is based on only three samples. Due to the small number of samples, this direction should only be taken into account as an indication, rather than firm evidence, in a tectonic interpretation.

4.7.2 Late Cretaceous localities: red marls

Three out of four Late Cretaceous localities yield good results and are located in allochthonous units (locality 4 at the base of the Botiza nappe; localities 8 and 11 in the Pieniny type klippen and associated flysch). Locality 17 is in the parautochthonous cover of the Tisza-Dacia mega-tectonic unit. At localities 4 and 11 samples were drilled from strata with variable tilts. Within-locality fold tests for these localities yielded negative results (Table 4.2), which indicates re-magnetization. Since the direction of locality 8 groups well with those of 4 and 11 (Fig. 4.7), it is also considered as remagnetized. The most likely explanation for remagnetization after folding is that the red marls originally contained goethite, which became dehydrated and converted into a hematite-like mineral, perhaps under the influence of Neogene volcanism because their paleomagnetic directions show a remarkable similarity to the paleomagnetic directions obtained for the mid-Miocene localities and depart from paleomagnetic directions expected for Cretaceous (Besse and Courtillot 2002).

Fig. 4.7: Mean paleomagnetic directions (with confidence circles) for the Late Cretaceous localities. Note that the data obtained for localities 4 and 11 fail the within-locality fold test (Table 4.2) and thus indicate remagnetization (probably) during Mid-Miocene times.



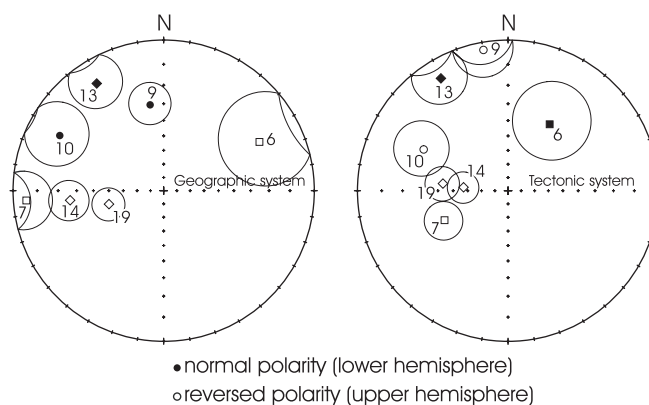
Locality 17 has excellent paleomagnetic properties, but appears as an outlier, both when plotted in the geographic as well as in the tectonic co-ordinate system, respectively (Fig. 4.7). Being collected from the parautochthonous cover of Tisza-Dacia, its unexpected direction is difficult to interpret in terms of tectonics. Quite possibly these strata were also influenced by gravitational movements which were evident nearby but not within the sampled outcrop.

4.7.3 Eocene to Oligocene localities: flysch samples

Seven localities plotted in Fig. 4.8 yielded statistically good or acceptable paleomagnetic directions (see Table 4.2). Three of them (localities 14, 19 and 13) belong to the autochthonous- parautochthonous cover of the Tisza-Dacia mega-tectonic unit. Localities 14 and 19 in both geographic and tectonic co-ordinate systems indicate about 90° clockwise rotation with respect to present north (and also to expected directions for Eocene-Oligocene, Besse and Courtillot 2002), while inclinations are consistent and moderately steep. Locality 13 yields extremely low inclination values, both before and after tilt correction. We suspect that the apparently good magnetic signal still is a composite one, and must be disregarded in tectonic interpretation.

Localities 6, 7 are from the allochthonous external Pienides (Leordina nappe). The mean directions have very shallow inclinations before tilt correction, while after tilt correction (tectonic system in Fig. 4.8), the mean directions become roughly antipodal and inclinations become similar to those obtained for localities 14 and 19 from the autochthonous. We consider these directions as original, pre-folding magnetizations, showing marked clockwise rotation.

Fig. 4.8: Mean paleomagnetic directions for the Eo-Oligocene localities (autochthon: diamond; Leordina nappe: squares; Botiza nappe: circles). Note that the fold test improves the grouping for 6 (normal polarity), 7, 14, 19 (reversed polarities), and that the paleomagnetic direction for locality 10 moves closer to the cluster after tilt correction.



Localities 9 and 10 are from the internal Botiza nappe. Paleomagnetic directions obtained for them are far apart from each other in both co-ordinate systems; inclinations are too shallow in order to represent Paleogene or younger inclinations. Therefore we do not consider them in our tectonic interpretation.

In summary, out of seven tabulated mean paleomagnetic directions for the Eo-/Oligocene, four localities are suitable for an interpretation in terms of regional tectonics: two from the autochthon and two from the Leordina nappe. They have consistent inclinations and all of them exhibit a clockwise deviation of the declination with respect to present-day north. There is, however, a difference in declination between the autochthon and the Leordina nappe, as will be discussed below.

4.8 Discussion and tectonic interpretation of the results

Re-magnetization of the Cretaceous localities led to paleomagnetic directions, which are remarkably similar to those obtained for the mid-Miocene localities (Fig. 4.9). Hence, these two data sets will be discussed together to make inferences about post mid-Miocene counter-clockwise rotations. In a second step we discuss clockwise rotations indicated by the data obtained from the Eo- /Oligocene formations.

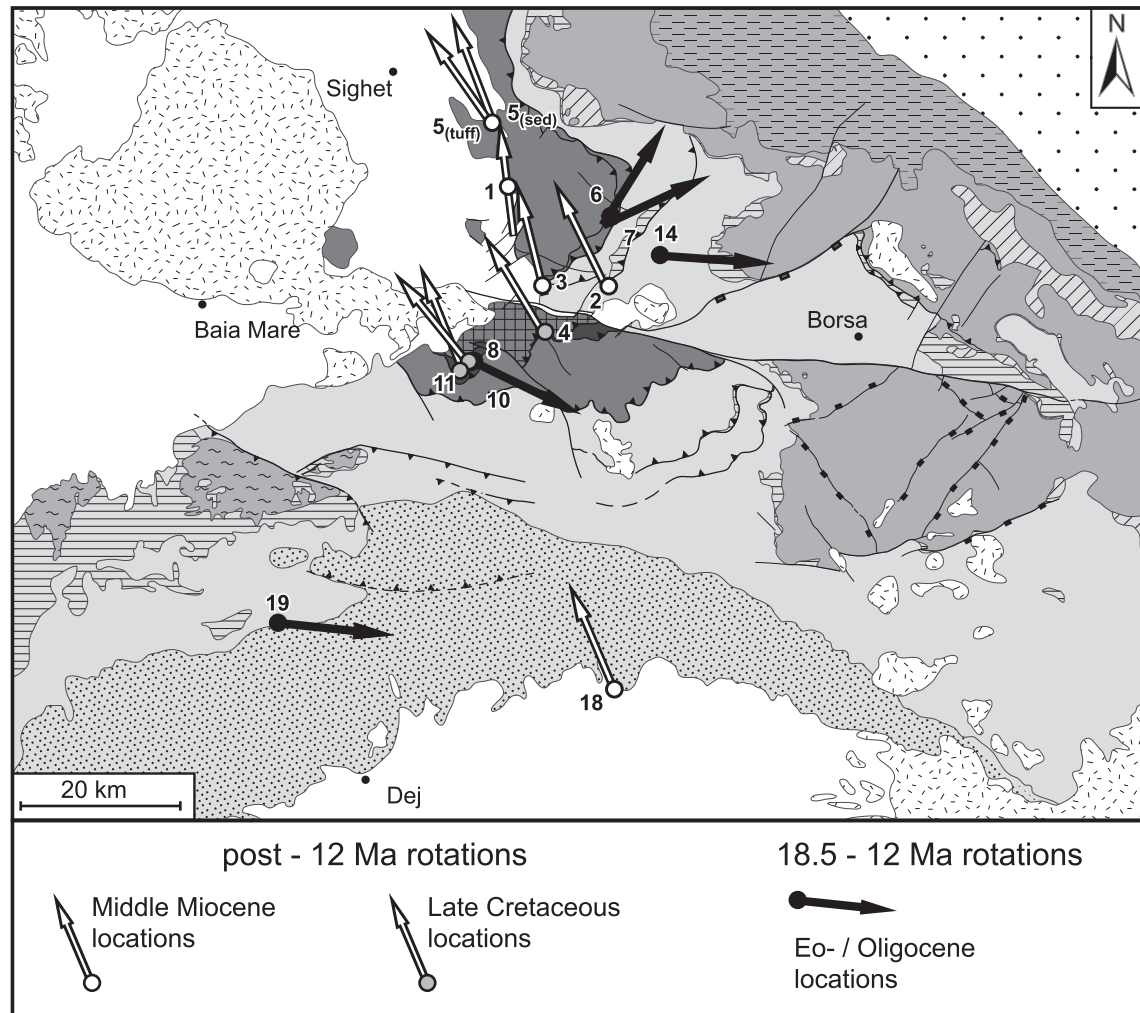


Fig. 4.9: Paleo-declinations, plotted relative to present-day north on a geological map. The secondary magnetizations of Mid-Miocene and Late Cretaceous localities indicate a post-12 Ma (see text) counter clockwise rotation of about 30° (white arrows). The Eo-/Oligocene locations show consistent clockwise rotations that pre-date the counter clockwise rotations (black arrows; see discussion in text).

4.8.1 Inferences regarding post-12 Ma counter-clockwise rotations (Mid-Miocene and Late Cretaceous localities)

The mid-Miocene localities (with the exception of locality 3) and the Late Cretaceous localities carry secondary paleomagnetic signals departing from the direction of the present-day earth magnetic field in the sampling area (Fig 4.9). The deflection indicates counter-clockwise rotations of about 30° (Table 4.3). This rotation must have taken place later than 12 Ma ago, since the negative fold/tilt tests indicate that their characteristic remnant magnetism was acquired after folding, which ended 12 Ma ago (Tischler et al. 2006).

A similar rotation was suggested for the Sarmatian (13 – 11.6 Ma) members of the volcanic body of Baia Mare (Pătrăscu 1993), while the Late Miocene (Pannonian, post-11.6 Ma) members in the same body remained unaffected by this rotation. Thus, the counter-clockwise rotation observed for the Dej tuff and or the Late Cretaceous localities must have occurred immediately after tilting and magnetization, i.e. about 12 Ma ago. Note that this rotation involved the cover of the Tisza-Dacia mega-tectonic unit north, (and possibly south, as our locality 18 suggests) of the Bogdan-Drăgos Voda fault (Fig. 4.9), as well as the Pienides, which were originally part of ALCAPA.

Sense, magnitude and timing of these post-12Ma rotations in the study area are similar to rotations inferred for the East Slovak Basin (Orlicky 1996, Márton et al., 2000), for the Vihorlat Mts (Túnyi et al. 2005) and for the Tokaj area (Márton 2001). Therefore, we think that the East Slovak basin and our working area (Fig 4.10) behaved as a single tectonic unit after some 12 Ma ago.

Rotations, however, are different in those parts of the ALCAPA mega-tectonic unit, which are located west of the Hernád-fault (central W-Carpathians, see Fig. 4.10), where counter clockwise rotation stopped earlier, at around 14.5 Ma (Márton 2001). This different timing of rotations west and east of the Hernád fault calls for a tectonic separation across this fault.

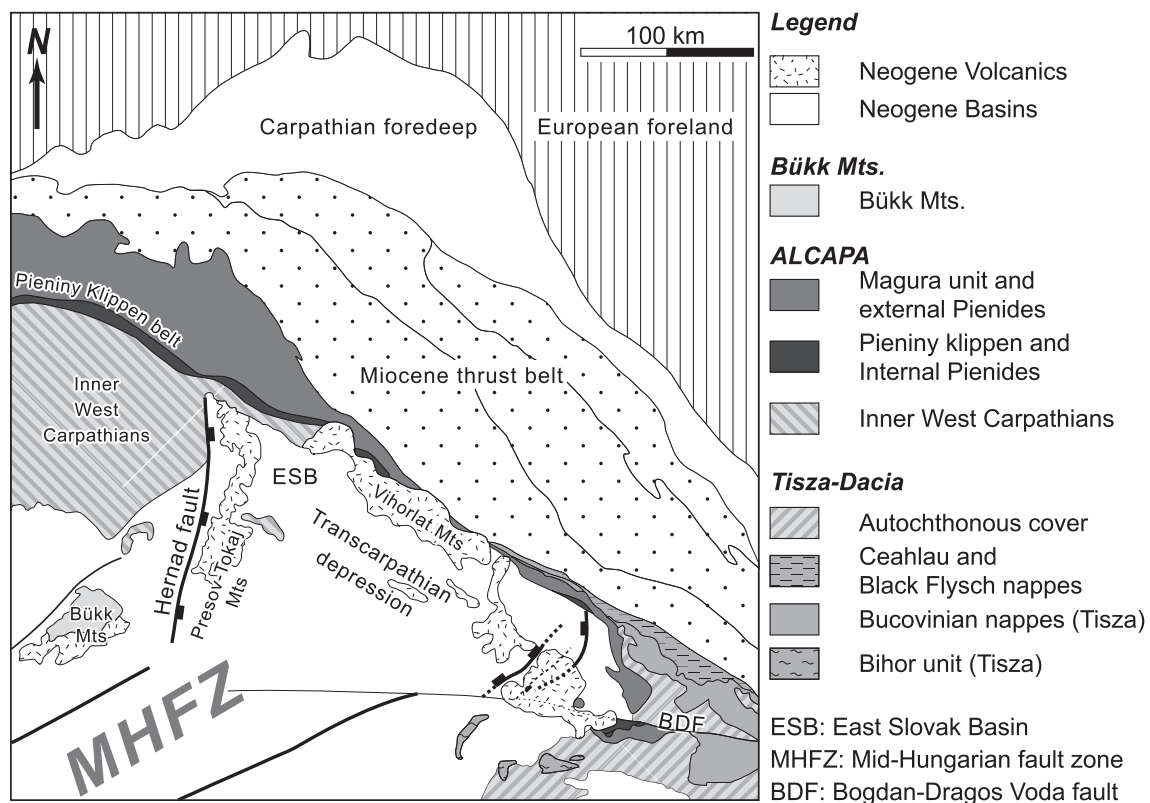


Fig. 4.10: Geological sketch map of the triple junction between ALCAPA, Tisza-Dacia and the European foreland. Map redrawn after Fig. 1, Kováč et al. (1995) and Săndulescu et al (1978). The Hernád fault is interpreted as providing the detachment of the counter clockwise rotating domain of ALCAPA (Inner West Carpathians) and the Transcarpathian depression. The fault pattern of the corresponding eastern detachment fault, between the Transcarpathian depression and the clockwise rotating Tisza-Dacia (including the eastern tip of ALCAPA), follows structures taken from the subcrop map of Săndulescu et al. (1993).

The onset of the post-12 Ma counterclockwise rotations in the study area coincides with a significant change of the tectonic setting. According to Tischler et al. (2006) sinistral transpression (16–12 Ma) changed to sinistral transtension (12–10 Ma), concentrating along the Bogdan-Dragos Voda fault system. This transition is probably due to soft collision of ALCAPA, including the northern parts of the Tisza-Dacia mega-tectonic unit with the European foreland (Tischler et al. 2006). The clockwise rotation documented for the 14.2 – 11 Ma time interval (Panaiotu 1998, 1999), which affected the southern Apuseni Mountains (which are part of Tisza) can also be connected to this event.

4.8.2 Inferences regarding pre-12 Ma clockwise rotations (Eocene to Oligocene localities)

Those four Eo-/Oligocene localities from the study area, which we consider in our tectonic interpretation, exhibit substantial clockwise deflections of paleo-declinations (Fig. 9, Table 4.3), suggesting clockwise rotations which pre-date the counter-clockwise rotations discussed above. Due to the subsequent counter clockwise rotation, the clockwise rotations suggested by the paleo-declinations in Fig. 4.9, and discussed below, represent an under-estimate by some 30°.

The observed pre-12 Ma clockwise rotations for the autochthon (localities 14 and 19) are in line with earlier paleomagnetic results from the Tisza-Dacia mega-tectonic unit (Panaiotu 1998). However, clockwise rotations are unexpected for the Pienides. These are considered as part of the ALCAPA unit, which is known to have suffered counter-clockwise rotations during the Miocene (e.g. Bükk Mts.: Márton and Fodor 1995; Gemer region: Márton et al 1988; Inner West Carpathian flysch basin: Márton et al, 1999).

The following is an important starting point for reconstructing the main rotational events in the Maramures area: localities 14 and 19 of the present study from the (para-) autochthonous sedimentary cover of the Tisza-Dacia mega-tectonic unit, when combined with two earlier published results of the same age from the autochthon (Panaiotu 1998), define a rotation for the autochthon which has good statistical parameters (Table 4.3). The timing of this rotation is not well constrained, except that it must post-date the Eo-/Oligocene ages of deposition of the analysed sediments. Compared to this “reference” direction, localities 6 and 7 from the Pienides (i.e. the easternmost tip of ALCAPA) show less clockwise rotation. This situation suggests that the Pienides and Tisza-Dacia rotated, at least partly, in a different manner and/or at different times.

According to our interpretation Tisza-Dacia started to rotate clockwise before emplacement of the Pienides at around 18.5 Ma. This is supported by independent observations. According to Fügenschuh and Schmid (2005) a substantial clockwise rotation of the Tisza –Dacia mega-tectonic unit predates 18.5 Ma. Also the change in strike of the foredeep of Late Oligocene and Early Miocene age with respect to their earlier orientation (De Broucker et al. 1998, Györfi et al. 1999) suggests clockwise rotation. Since ongoing clockwise rotation affected the Pienides only after emplacement onto and their mechanical coupling with Tisza-Dacia, a smaller angle of rotation is expected for the Pienides.

An alternative to the above interpretation would be that the smaller clockwise rotation of the Pienides resulted from a previous counter-clockwise rotation of the Pienides by about 45° , predating a 90° clockwise rotation (together with the Tisza-Dacia mega-tectonic unit). This possibility is considered, since the Pienides represent the eastern tip of the ALCAPA mega-tectonic unit, which is characterized by counter clockwise rotated Miocene declinations (e.g. Márton 1987, Balla 1987). Fortunately, a paleomagnetic study (Márton and Márton 1996) followed by integrated paleomagnetic measurements and K/Ar isotope age determination (Márton and Pécskay 1998) provided precise time constraints for the rotations of the area W of the Hernád fault. These studies suggest that no Tertiary rotation occurred before 18.5 Ma. The first counter clockwise rotation took place in the 18.5-17.5 Ma time interval, the second from 16 to 14.5 Ma. As both rotation events post-date thrusting of the Pienides, this second alternative interpretation is far less probable compared to the first one.

4.8.3 Disintegration of the ALCAPA mega-tectonic unit starting at 18.5 Ma ago

Our results, in the context of previously published paleomagnetic data, clearly imply that the ALCAPA mega-tectonic unit started to disintegrate during the Miocene. This process started with the decoupling of its northeastern-most tip (Pienides) from the rest of ALCAPA. The decoupling must have occurred somewhere within the Transcarpathian depression (Fig. 4.10), which is an intervening area that strongly subsided since the Middle Miocene, due to transtension (i.e. Kováč et al. 1995). A window of lower structural units (Ináčovce Krichevo unit) in the basement of the East Slovak basin (Soták et al. 1993, 1994) has been interpreted as a metamorphic core (Soták et al. 2000).

We therefore propose that the Transcarpathian depression is the site of major extension. This major NW-SE extension can also be seen in some Slovak seismic lines and is evidenced by thick deposits, tilted beds, syn-rift style geometry, fault offsets (Santavy and Vozár 1999) which occurred there between 17,5 and 11 Ma ago. Major Neogene extension is evident also in our study area. Immediately NW of the internal Pienides a deep Miocene basin (the SE edge of the Transcarpathian depression) is found, featuring thick Langhian (Badenian) salt deposits. Large amounts of buried Middle-Late Miocene volcanites in the area of the Transcarpathian depression (Fig. 4.10) also suggest major extension.

4.8.4 Tentative model for the tectonic evolution

Data and considerations discussed in the previous part of this chapter lead to the following model. The easternmost tip of the ALCAPA mega-tectonic unit (Pienides) was emplaced onto the Tisza-Dacia mega-tectonic unit along the Pienide thrust front between 20.5 Ma and 18.5 Ma. Before this thrusting, Tisza-Dacia underwent some 45° out of its bulk clockwise rotation (Fig. 4.11). After 18.5 Ma both the Pienides and Tisza-Dacia underwent a common clockwise rotation of some 45° (75° if the subsequent counter clockwise rotation is also taken into account), while the rest of the ALCAPA mega-tectonic unit followed a pattern of counter-clockwise rotations (Fig. 4.11b).

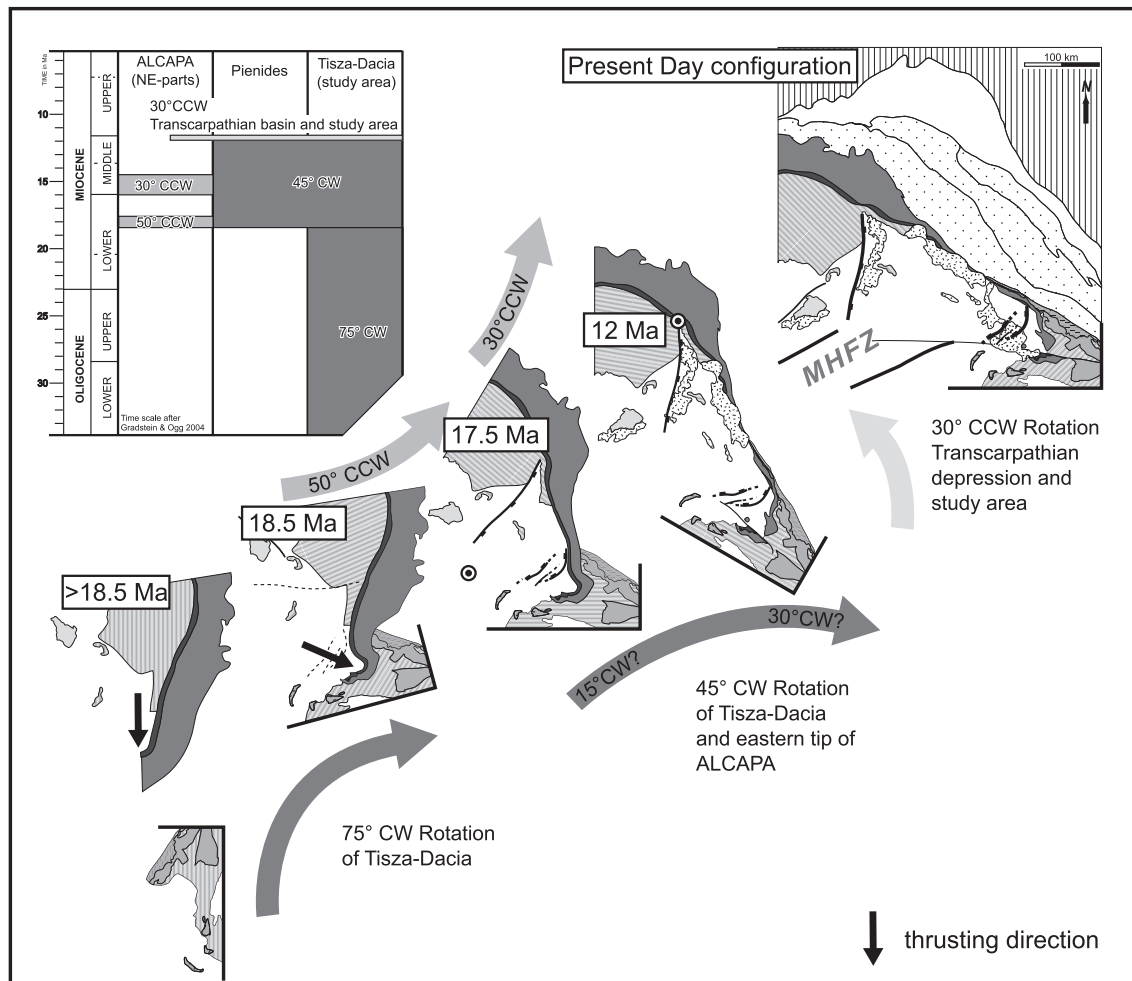


Fig. 4.11: Sketch of the proposed rotational history of the study area and the NE parts of ALCAPA.

This led to the disintegration of ALCAPA, and the decoupling of its easternmost tip (the Pienides), which was previously fixed to Tisza-Dacia. Differential stretching took place across the N-S to NE-SW trending normal faults within the Transcarpathian depression (Fig. 4.10). One of these, the Hernád fault, accounts for decoupling and clockwise rotation of the tip of ALCAPA from the bulk of this mega-tectonic unit. Hence major NW-SE rotational stretching within the Transcarpathian depression, and the East Slovak basin in particular, was driven by differential rotations of the main body of ALCAPA in respect to the thrust tip of ALCAPA (Fig. 4.11). The pole for this rotation is suggested to be located somewhere near the southern termination of the Hernád fault. This implies that the northern rim of the Transcarpathian depression should be stretched and bordered by transfer type faults, as is suggested by the thinning and the NW-SE elongation of the belt of external Carpathian Flysch units.

At around 12-11.5 Ma, when transpression along the Bogdan-Drăgăș Vodă fault system changed to transtension (Tischler et al. 2006), a second differential rotation and decoupling from the main body of ALCAPA occurred at or near the Hernád fault. Syn-rift type Sarmatian beds corroborate this interpretation. The observed 30° counter clockwise rotation in the study area, as well as in the Transcarpathian depression, is modelled as “en block” rotation around a pole at the northern tip of the Hernád fault in Fig. 4.11.

However, rotation of smaller, strike slip fault bound blocks in a deformation corridor cannot entirely be ruled out. Such a rotation would also imply a stretched southern margin, where large subsidence and thick buried Miocene volcanites do occur (Széky-Fux and Pécskay 1991).

4.9 Conclusions

During a main rotational stage, i.e. between 18.5-12 Ma, large clockwise rotations of at least 45° did occur in the study area. These affected the (par-) autochthonous sedimentary cover of the Tisza-Dacia mega-tectonic unit, as well as the allochthonous flysch nappes of the Pienides, representing the easternmost tip of the ALCAPA mega-tectonic unit. Since the Pienides originally belonged to ALCAPA, and because the main body of ALCAPA rotated counter clockwise, our new results from the Maramures area necessitate the disintegration of ALCAPA at around 18.5 Ma ago. The site of disintegration has to be looked for within the Transcarpathian depression (East Slovak basin in particular), located in the NE prolongation of the Mid-Hungarian fault zone, where numerous normal faults account for differential stretching (Fig. 4.10). The opening of the Transcarpathian depression was accompanied by the sedimentation of mid-Miocene and younger sediments of great thickness.

During a second stage, immediately after 12 Ma, counter-clockwise rotations of about 30° are documented in the entire working area. These counter-clockwise rotations are similar in timing and magnitude to rotations observed for the East Slovak basin, for the Tokaj Mts and for the Vihorlat Mts., i.e. areas that are part of the Transcarpathian depression. However, counter-clockwise rotations stopped after 14.5 Ma west of the Hernád-fault, i.e. in the W-Carpathians, as well as in the Bükk Mountains. Hence this second decoupling of the Central W-Carpathians from the Transcarpathian depression occurred along the Hernád fault.

4.10 Acknowledgements

We thank Mircea Săndulescu for introducing two of us (S. Sch, B. F.) into the exciting geology of the Maramures area. We gratefully acknowledge Heike Gröger for useful ideas and permanent support, as well as Gábor Imre for technical assistance in the field and the lab. Comments by Cristian Panaiotu and an anonymous reviewer helped to improve the paper. The present project was granted by NSF 200020-105136/1 („The Dragos-Voda fault in northern Romania: the eastern termination of the Mid-Hungarian Line fault system ?”) and NSF200021-101882/1 (“Tisza and its role in the framework of the tectonic evolution of Alps, Dinarides and Carpathians”) granted to B. F. and S. Sch., respectively.

4.11 References

- Aroldi C (2001) The Pienides in Maramures – Sedimentation, tectonics and paleogeography. PhD Thesis, Cluj, pp 1-156
- Balla Z (1984) The Carpathian loop and the Pannonian basin: a kinematic analysis. *Geophysical Transactions* 30/4: 313-353
- Balla Z (1987) Tertiary paleomagnetic data for the Carpatho-Pannonian region in the light of Miocene rotation kinematics. *Tectonophysics* 139: 67-98
- Besse J, Courtillot V, (2002) Apparent and true polar wander and the geometry of the geomagnetic field over the last 200 Myr. *Journal of Geophysical Research B: Solid Earth* Nov 10; 107 EPM 6-1: 6-31.
- Ciulavu D (1999) Tertiary tectonics of the Transylvanian Basin. PhD. diss. Vrije Universiteit Amsterdam, Amsterdam, pp 1-154
- Ciulavu D, Dinu C, Cloetingh SAPL (2002) Late Cenozoic tectonic evolution of the Transylvanian basin and northeastern part of the Pannonian basin (Romania): Constraints from seismic profiling and numerical modelling. EGU Stephan Mueller Special Publication Series 3: 105-120
- Csontos L (1995) Cenozoic tectonic evolution of the Intra-Carpathian area: a review. *Acta Vulcanologica* 7: 1-13
- Csontos L, Nagymarosy A (1998) The Mid-Hungarian line: a zone of repeated tectonic inversions. *Tectonophysics* 297: 51-71
- Csontos L, Vörös A (2004) Mesozoic plate tectonic reconstruction of the Carpathian region. *Paleogeography, Paleoclimatology, Paleocology* 210: 1-56
- Csontos L, Márton E, Wórum G, Benkovics L (2002) Geodynamics of SW-Pannonian inselbergs (Mecsek and Villány Mts, SW Hungary). EGU Stephan Mueller Special Publication 3: 227-245
- De Broucker G, Mellin A, Duindam P (1998) Tectonostratigraphic evolution of the Transylvanian Basin, Pre-Salt sequence, Romania, In: Dinu C (ed). BGF Special volume 1: 36-70
- Dicea O, Duțescu P, Antonescu F, Mitrea G, Botez R, Donos I, Lungu V, Moroșanu I (1980) Contributii la cunoasterea stratigrafiei zonei transcarpatice din maramures. D. S. Inst geol geofiz LXV, 4: 21- 85
- Fisher R (1953) Dispersion on a sphere. *Proc. Roy. Soc. London Ser. A.* 217, 295–305
- Fodor L, Jelen B, Márton M, Skaberne D, Car J, Vrabc M (1998) Miocene-Pliocene tectonic evolution of the Slovenian Periadriatic fault: Implications for Alpine-Carpathian extrusion models. *Tectonics* 17: 690-709
- Fodor L, Csontos L, Bada G, Györfi I, Benkovics L (1999) Cenozoic tectonic evolution of the Pannonian basin system and neighbouring orogens: a new synthesis of paleostress data. In: Durand B, Jolivet L, Horváth F, Séranne M (eds). *The Mediterranean basins: Cenozoic Extension within the Alpine Orogen.* *Geol Soc Spec Publ* 156: 295–334
- Fügenschuh B, Schmid SM (2005) Age and significance of core complex formation in a highly bent orogen: evidence from fission track studies in the South Carpathians (Romania). *Tectonophysics in press*
- Gradstein F, Ogg J, Smith A (2004) *A Geologic Time Scale.* Cambridge University Press, Cambridge, pp 1 – 589

- Györfi I, Csontos L, Nagymarosy A, (1999) Early Cenozoic structural evolution of the border zone between the Pannonian and Transylvanian basins. In: Durand B, Jolivet L, Horváth F, Séranne M (eds). *The Mediterranean Basins: Cenozoic Extension within the Alpine Orogen*. Geol Soc Spec Publ 156: 251–267
- Horváth F, Bada G, Szafián P, Tari G, Ádám A, Cloetingh S (2006) Formation and deformation of the Pannonian basin: constraints from observational data. *Geol Soc London Spec Publ*, in press.
- Huismanns RS, Bertotti G, Ciulavu D, Sanders CAE, Cloetingh S, Dinu C (1997) Structural evolution of the Transylvanian Basin (Romania): a sedimentary basin in the bend zone of the Carpathians. *Tectonophysics* 272: 249-268
- Kirschvink JL (1980) The least-squares line and plane and the analysis of paleomagnetic data. *Geophysical Journal of the Royal Astronomical Society* 62, 699-718.
- Kovács S, Haas S, Csazar G, Szederkenyi T, Buda G, Nagymarosy A (2000) Tectonostratigraphic terranes in the pre-Neogene basement of the Hungarian part of the Pannonian area. *Acta Geol Hung* 43/3: 225-328
- Kováč M, Král J, Márton E, Plašienka D, Uher P (1994) Alpine uplift history of the Central West Carpathians: geochronological, paleomagnetic, sedimentary and structural data. *Geologica Carpathica* 45: 83-96
- Kováč M, Kováč P, Marko F, Karoli S, Janočko J (1995) The East Slovakian Basin – a complex back arc basin. *Tectonophysics* 252: 453-466.
- Lowrie W (1990) Identification of ferromagnetic minerals in a rock by coercivity and unblocking temperature properties. *Geophysical Research Letters* 17, 159–162
- Marret R, Allmendinger RW (1990) Kinematic analysis of fault slip-data. *J Struct Geol* 12: 973-986
- Márton E (1987) Paleomagnetism and tectonics in the Mediterranean region. *Journal of Geodynamics* 7: 33-57
- Márton E, (2000) The Tisza Megatectonic Unit in the light of paleomagnetic data. *Acta Geol Hung* 43/3: 329–343
- Márton E, (2001): Tectonic implications of Tertiary paleomagnetic results from the PANCARDI area (Hungarian contribution). *Acta Geol Hung* 44: 135-144.
- Márton E, Fodor L (1995) Combination of palaeomagnetic and stress data - a case study from North Hungary. *Tectonophysics* 242: 99–114
- Márton E, Fodor L (2003) Tertiary paleomagnetic results and structural analysis from the Transdanubian Range (Hungary): rotational disintegration of the ALCAPA unit. *Tectonophysics* 363: 201-224
- Márton E, Márton P (1978) On the difference between the palaeomagnetic poles from the Transdanubian Central Mountains and the Villány Mountains respectively (in Hungarian). *Magyar Geofizika* XIX/4: 129-136
- Márton E, Márton P (1996) Large scale rotations in North Hungary during the Neogene as indicated by palaeomagnetic data. In: *Palaeomagnetism and Tectonics of the Mediterranean Region* (edited by Morris, A. & Tarling, D.H.). *Geol. Soc. Spec. Publication* 105: 153-173
- Márton E, Pécskay Z (1998) Correlation and dating of the ignimbritic volcanics in the Bükk foreland, Hungary: complex evaluation of paleomagnetic and K/Ar isotope data. *Acta Geologica Hungarica* 41: 467-476

- Márton E, Márton P, Less G (1988) Paleomagnetic evidence of tectonic rotations in the Southern margin of the Inner West Carpathians. *Physics Earth and Planetary Interiors* 52: 256-266
- Márton E, Mastella L, Tokarski AK (1999) Large counterclockwise rotation of the Inner West Carpathian Paleogene Flysch – evidence from paleomagnetic investigation of the Podhale Flysch (Poland). *Physics and Chemistry of the Earth (A)* 24/8, 645-649
- Márton E, Vass D, Tunyi, I (2000) Counterclockwise rotations of the Neogene rocks in the East Slovak basin. *Geologica Carpathica* 51/3: 159-168
- Matenco L, Bertotti G, Cloetingh S, Dinu C (2003) Subsidence analysis and tectonic evolution of the external Carpathian-Moesian Platform during Neogene times. *Sediment Geol* 156: 71-94
- McFadden PL (1990) A new fold test for palaeomagnetic studies. *Geophysical Journal International* 103: 163-169
- Orlický O (1996) Paleomagnetism of neovolcanics of the East-Slovak Lowlands and Zemplínske Vrchy Mts: A study of the tectonics applying the paleomagnetic data (Western Carpathians). *Geologica Carpathica* 47/1, 12-20
- Pamic J (2000) Basic geological features of the Dinarides and South Tisia. In: Pancardi 2000 Fieldtrip Guidebook (eds. Pamic, J. and Tomljenovic, B.). *Vijesti* 37/2: 9-18
- Panaiotu C (1998) Paleomagnetic constraints on the geodynamic history of Romania. In: *Monograph of Southern Carpathians* (edited by Ioane, D.). *Reports on Geodesy* 7: 205-216
- Panaiotu C (1999) Paleomagnetic studies in Romania; Tectonophysics implications (in Romanian). PhD thesis University of Bucharest, 265 pp
- Pătrăscu S (1993) Paleomagnetic study of some Neogene magmatic rocks from the Oas – Ignis – Varatec – Tibles Mountains (Romania). *Geophys. J. Int.* 113, 215-224.
- Pécskay Z, Edelstein O, Kovacs M, Bernád A, Crihan M (1994) K/Ar age determination of Neogene volcanic rocks from the Gutai Mts. (Eastern Carpathians, Romania). *Geol Carp* 45(6): 357-363
- Popescu BM (1984): Lithostratigraphy of cyclic continental to marine Eocene deposits in NW Transylvania, Romania. In: Popescu BM (ed) *The Transylvanian Paleogene Basin*. Geneva, 37-73
- Ratschbacher L, Merle O, Davy P, Cobbold P (1991a) Lateral extrusion in the Eastern Alps; Part 1, Boundary conditions and experiments scaled for gravity. *Tectonics* 10(2): 245– 256
- Ratschbacher L, Frisch W, Linzer HG, Merle O, (1991b) Lateral extrusion in the Eastern Alps; Part 2, Structural analysis. *Tectonics* 10(2): 257– 271
- Ratschbacher L, Linzer HG, Moser F (1993) Cretaceous to Miocene thrusting and wrenching along the Central South Carpathians due to a corner effect during collision and orocline formation. *Tectonics* 12, 855-873
- Royden LH (1988) Late Cenozoic Tectonics of the Pannonian Basin System In: Royden LH, Horváth F (eds). *The Pannonian Basin; a study in basin evolution*. AAPG Mem 45: 27-48
- Săndulescu M (1980) Sur certains problèmes de la corrélation des Carpathes orientales Roumaines avec les Carpathes Ukrainiennes. *D. S. Inst geol geofiz LXV(5)*: 163-180
- Săndulescu M, (1984) *Geotectonica Romaniei*. Editura Tehnica, Bucharest, pp1 – 450

- Săndulescu M (1994) Overview of Romanian Geology. In: ALCAPA II field guide book. Romanian J of Tectonics and Reg Geol, 75 suppl. 2: 3-15
- Săndulescu M, Kräutner H, Borcos M, Năstăseanu S, Patrulius D, Ștefănescu M, Ghenea C, Lupu M, Savu H, Bercia I, Marinescu F (1978) Geological map of Romania 1:1.000.000. Inst. Geol. Rom., Bucharest
- Săndulescu M, Kräutner HG, Balintoni I, Russo-Săndulescu D, Micu M (1981): The Structure of the East Carpathians. (Guide Book B1), Carp-Balk Geol Assoc 12th Congress, Bucharest, pp 1-92
- Săndulescu M, Visarion M, Stanica D, Stanica M, Atanasiu L (1993) Deep Structure of the inner Carpathians in the Maramures-Tisa zone (East Carpathians). Rom J Geophysics 16: 67-76
- Santavy, Vozár J (1999) Electronical Atlas of Deep Reflection Seismic Profiles of the Western Carpathians. CD ROM, GUDS Bratislava ISBN 80-88974-06-2
- Schmid SM, Berza T, Diaconescu V, Froitzheim N, Fügenschuh B (1998) Orogen-parallel extension in the South Carpathians. Tectonophysics 297: 209-228
- Soták J, Rudinec R, Spišiak J (1993) The Penninic «pull-apart» dome in the pre-Neogene basement of the Transcarpathian depression (Eastern Slovakia). Geol. Carpath. 44/1: 11-16
- Soták J, Spišiak J, Biron A (1994) Metamorphic sequences with Bündnerschiefer lithology in the pre-Neogene basement of the East Slovakian Basin. Mitt. Österr. Geol. Ges. 86: 111-120
- Soták J, Biron A, Prokesova R, Spišiak J (2000) Detachment control of core complex exhumation and back-arc extension in the East Slovakian Basin. In: Environmental, structural and stratigraphical evolution of the Western Carpathians (edited by Kováč, M., Vozár, J., Vozárová, A., Michalik, J.). Slovak Geological Magazine (Geological Survey of Slovak Republic. Bratislava, Slovak Republic) 6: 130-132
- Sperner B, Ratschbacher L, Nemčok M (2002) Interplay between subduction retreat and lateral extrusion: tectonics of the Western Carpathians. Tectonics 21(6): 1051
- Szakács A, Vlad D, Andriessen PAM, Fülöp A, Pécskay Z (2000) Eruption of the “Dej tuff”, Transylvanian Basin: when, where and how many. Vijesti Hrvatskoga geološkog društva, PANCARDI 2000-Special issue, Abstract volume 37/3, 122.
- Széky-Fux V, Pécskay Z (1991) Covered Neogene volcanic rocks at the eastern and northern areas of the Pannonian basin, Hungary. In: Geodynamic evolution of the Pannonian basin (edited by S. Karamata). Serb. Acad. Sci. Arts, Acad. Conf. 62, Dept. Nat. Math. Sci. 4, Belgrade: 275-287pp
- Tischler M, Gröger HR, Fügenschuh B, Schmid SM (2006) Miocene tectonics of the Maramures area (Northern Romania) – implications for the Mid-Hungarian fault zone. Int. J. Earth Sciences
- Túnyi I, Márton E, Žec B, Vass D (2005) Paleomagnetism of Neovolcanics of the Vihorlatské vrchy Mts. Mineralia Slovaca 37, 268-271
- Van der Voo R (1993) Paleomagnetism of the Atlantic, Tethys and Iapetus Oceans. Cambridge University Press, Cambridge
- Wortel MJR, Spakman W (2000) Subduction and slab detachment in the Mediterranean-Carpathian region. Science 290: 1910-1917

Chapter 5:

A contribution to the reconstruction of the Late Tertiary tectonic history of Tisza-Dacia – Constraints from a palinspastic reconstruction of the study area

5.1 Introduction

This chapter evaluates the constraints for a palinspastic reconstruction of the Tisza-Dacia block for Oligocene and Miocene times presented in chapter 2, 3 and 4. A palinspastic reconstruction of the study area, based on the map depicted in Fig. 5.1, is performed and integrated into the regional context. A recent retro-deformation attempted by Fügenschuh and Schmid (2005) for the Southern Carpathians is used as a reference for the integration of the time slices obtained within the working area into the regional setting.

The palinspastic maps of the restored study area show the retrodeformed outlines of the present day map units, and are not intended as paleogeographic maps.

Note, that the reconstructions for the pre-12 Ma time slices are based on structural observations (Fügenschuh and Schmid 2005 and this study) and geometrical constraints. Values of rotations derived by paleomagnetic studies are not included. Hence, these reconstructions allow to compare the rotation values expected from structural observations to the rotation values postulated by paleomagnetic studies.

The major units used in the regional setting are as follows:

ALCAPA:

ALCAPA as used in the restoration comprises Apulia derived allochthons, for simplicity the Bükk mountains are included. The tectonic history of ALCAPA has been included schematically in order to assess the compatibility of the proposed reconstruction for Tisza-Dacia. For detailed paleogeographic reconstructions the reader is referred to e.g. Fodor et al. (1999), Csontos and Vörös (2004).

Tisza-Dacia:

The Tisza-Dacia block is a composite continental block composed of Tisza (Bihor / Mesceek, Codru and Biharia units), including the Apuseni mountains and Dacia (Danubian, external Balkan, Bucovinian, Getic, Sredna Gora, Serbo-Macedonian and Rhodopes). For the time interval considered, Tisza-Dacia is treated as a single block. Also the units of oceanic origin (Ceahlau-Severin, Transylvanian, South Apuseni) are regarded as attached to the Tisza-Dacia block for this reconstruction.

Pienides:

The Pienides are units of oceanic origin, situated between the ALCAPA and the Tisza-Dacia block. They show a strong affinity to the ALCAPA-block. However due to their oceanic origin, they are not included into the continental block ALCAPA.

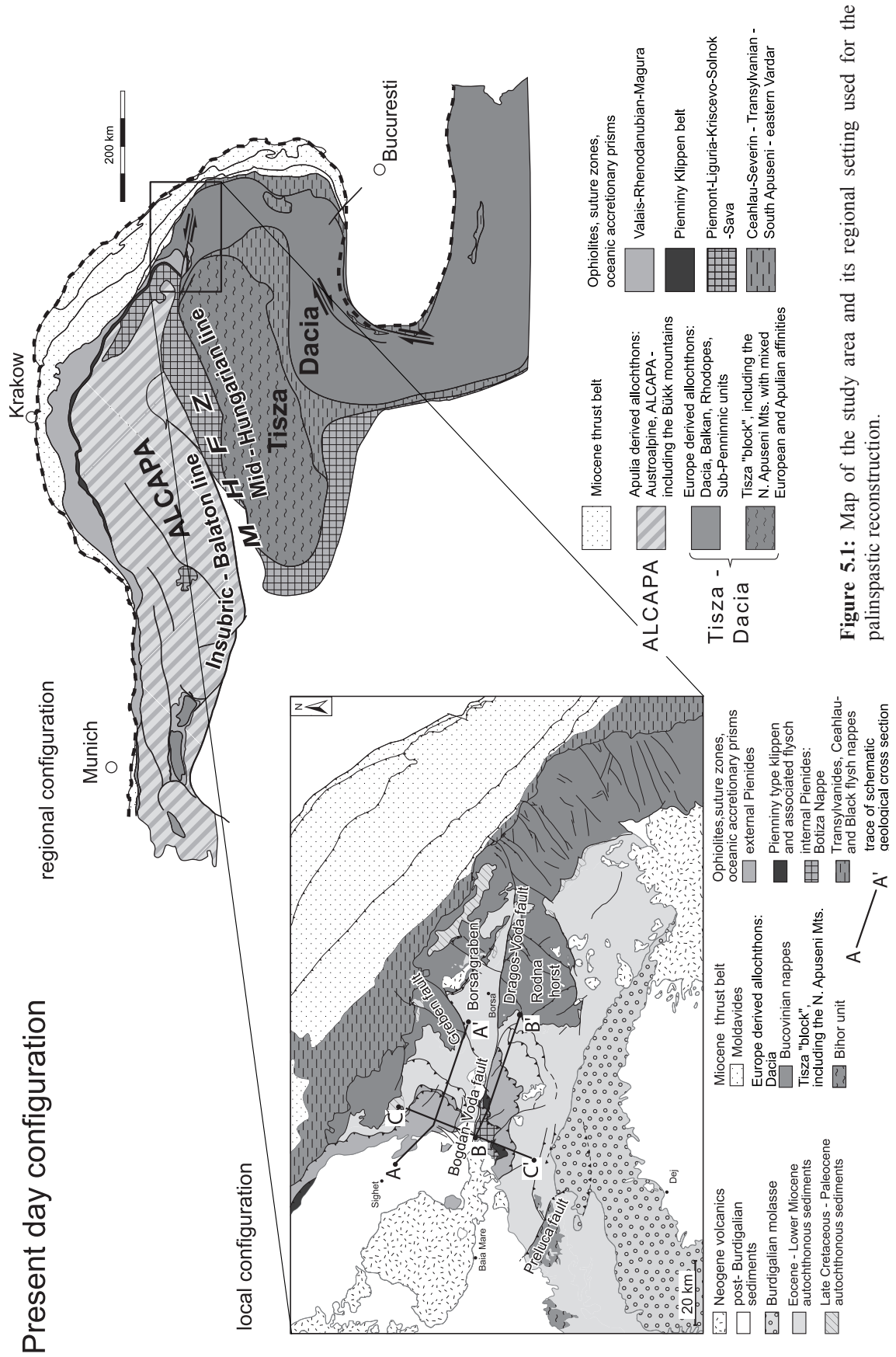


Figure 5.1: Map of the study area and its regional setting used for the palinspastic reconstruction.

5.2 Summary of Late Tertiary tectonic phases and available constraints

In the following an outline of the tectonic stages to be retrodeformed (compare chapter 2), as well as an evaluation of the used constraints is given. In order to estimate the amount of shortening achieved during the respective tectonic phases, schematic geological cross sections were constructed. The construction of the profiles is based on a series of 1 : 50.000 geological maps (Geological survey of Romania, and Săndulescu pers. comm. 2002) and on the geological map by Dicea et al. (1980). In order to provide an overview, the sections have been extrapolated down to the level of the crystalline basement. Deeper structures were included in order to reflect an interpretation of the general geological development of the study area, largely following ideas proposed by Săndulescu (pers. comm. 2002).

5.2.1 Early Burdigalian emplacement of the Pienides

The oldest deformational stage distinguished in the study area is the SE directed emplacement of the Pienides, related to the juxtaposition of ALCAPA and Tisza-Dacia (chapter 2). The thrusting of the unmetamorphic flysch nappes is interpreted as thin-skinned process, where the sand-dominated units are displaced without major internal shortening and the fine-grained flysch series serve as detachment horizons (Figs. 5.2 and 5.3). Sections A (Fig. 5.2) and B (Fig. 5.3) were constructed from WNW to ESE, roughly parallel to the direction of thrusting the Pienides north and south of the E-W trending Bogdan- Dragos-Voda fault system respectively. Based on a qualitative restoration of the northern cross section, the shortening within the imbricates within the autochthonous cover of Tisza-Dacia can be estimated to be in the order of 8km. Due to the lack of cut-off lines within the Pienides, the estimates for the accumulated shortening is restricted to minimum estimates. These minimum estimates are 35 km shortening for the external Pienides and an additional 10 km for the internal Pienides (Fig. 5.2).

5.2.2 Late Burdigalian SW-NE extension

Late Burdigalian SW-NE extension is only weakly expressed within the study area. Therefore this deformational phase is not taken into account in the presented palinspastic restoration. This approach is in good agreement with crustal thinning data presented by Cloetingh et al. 2005. These data show, that the northern part of Tisza-Dacia is only subordinately affected by crustal thinning. The strongly affected part of Tisza-Dacia is not retrodeformed in the following reconstruction and only indicated by dotted lines.

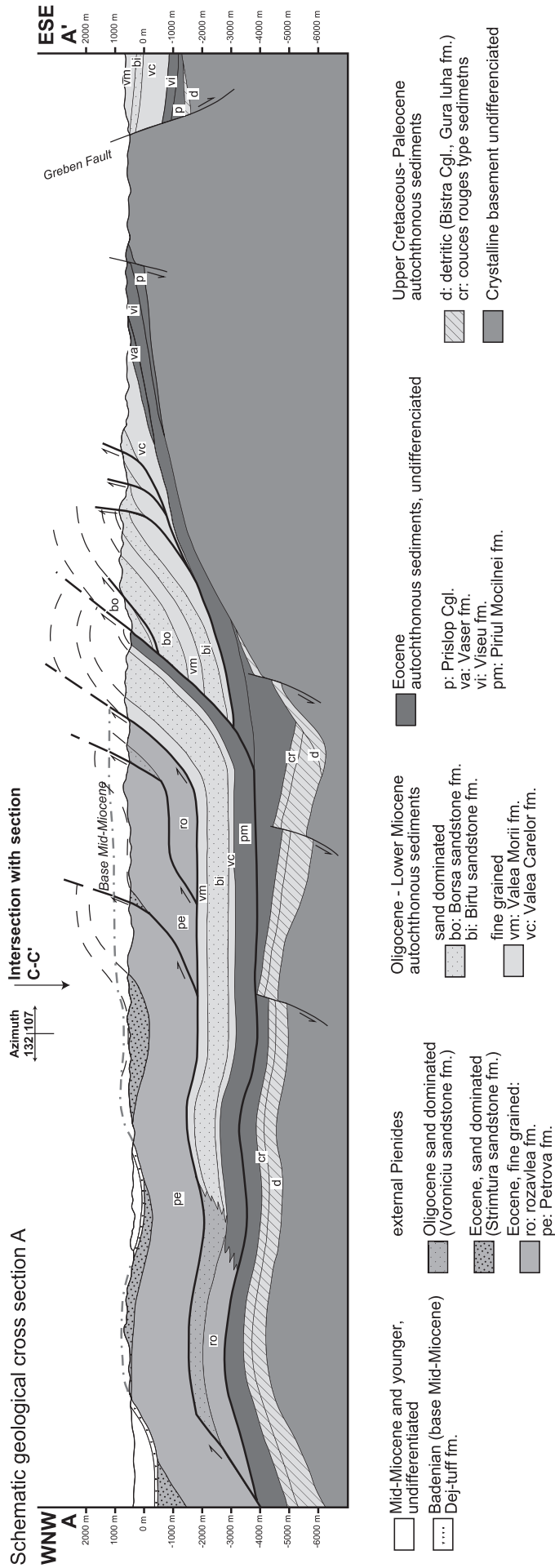


Figure 5.2: Schematic cross section A-A'

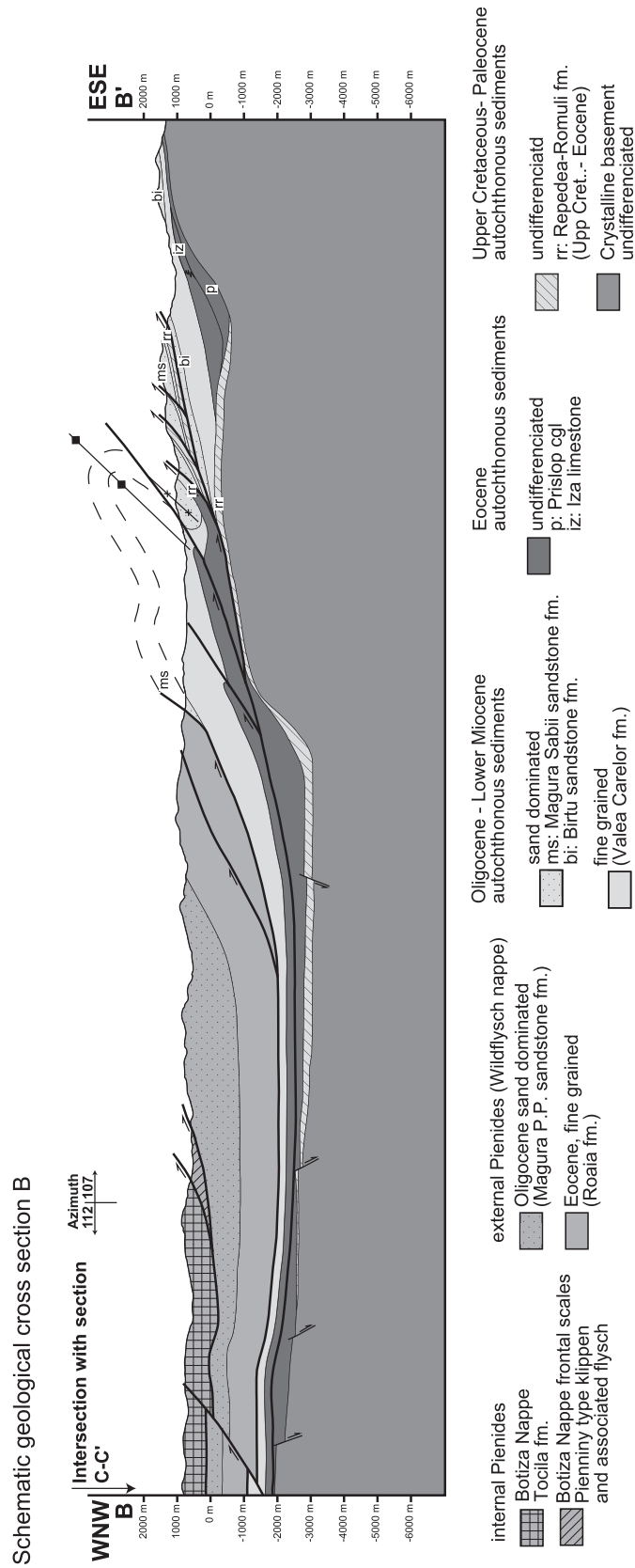


Figure 5.3: Schematic cross section B-B'

5.2.3 Post Burdigalian structures – ‘soft collision’

The post Burdigalian structures are interpreted as the result of the interaction of the northern part of Tisza-Dacia with the European continental margin during ‘soft collision’. The working hypothesis for these two stages is presented in the schematic model of Fig. 5.4. The two sub-stages are interpreted as the result of a change in convergence direction.

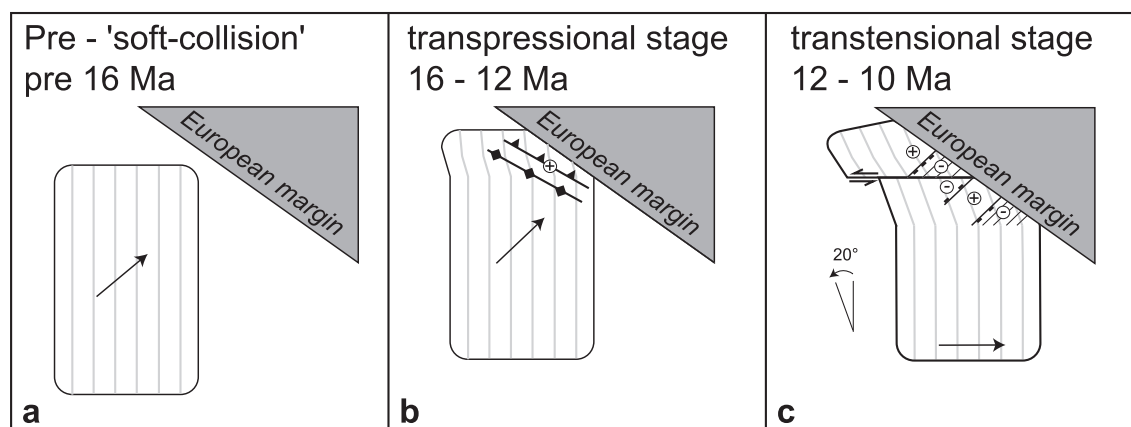


Fig. 5.4: General concept of the deformation processes active during ‘soft collision’ of Tisza-Dacia with the European margin. a: vertical lines represent “passive marker lines”. b: 16-12Ma, roughly perpendicular convergence results in shortening and the formation of backthrusts and open folds. c: 12-10Ma oblique convergence results in strike slip and normal faulting. SW-NE hatched areas indicate areas of distributed normal faulting. + and – denotes areas of relative uplift / subsidence, respectively.

The reconstruction of the late, post-16 Ma, deformations is based on the general concept illustrated in Fig. 5.4 (compare Matenco and Bertotti 2000; chapter 2). In this simplified model, approximately perpendicular convergence of Tisza-Dacia and the European margin leads to shortening and strike slip deformation (16-12 Ma, transpressional post-Burdigalian stage, see chapter 2). During oblique convergence, Tisza-Dacia is ‘fitted’ to the European continental margin by sinistral strike slip faulting along E-W trending faults and NW-SE oriented extension of the contact area by SW-NE trending normal faults (12-10 Ma, transtensional post-Burdigalian stage, see chapter 2). Passive drag during this deformation results in a homogenous counterclockwise rotation of the deformed area. The amount of this rotation is assumed to be in the order of 20°, a minimum estimate in accordance with the paleomagnetic data presented in chapter 4.

transpressional stage

The shortening accumulated during the post-Burdigalian transpressional stage has been assessed on the basis of the schematic geological cross section C (Fig. 5.5) trending subparallel to the shortening direction derived for this stage (see chapter 2). By retrodeforming the Mid-Miocene unconformity (i.e. the base of the Dej tuff), a value of 4% shortening can be derived for the weak folding that developed during this phase.

transtensional stage

Since the exact amount of extension in the contact area of Tisza-Dacia and the European margin is not known, an indirect approach has been chosen for the retrodeformation. The restoration (see below), has been focussed on retrodeforming the paleomagnetically determined counterclockwise rotation discussed in chapter 4.

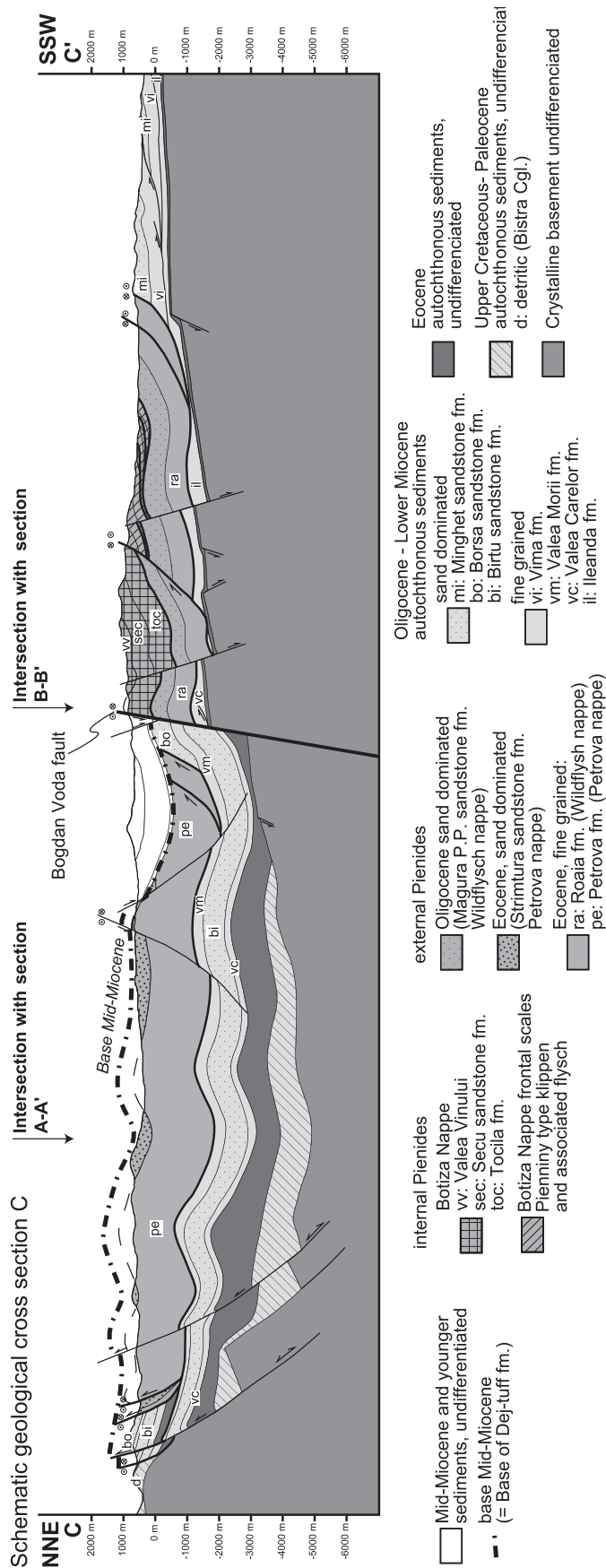


Figure 5.5: Schematic cross section C-C'

5.3 The 12 Ma time-slice: retro-deformation of post-Burdigalian transtension

Reconstruction of post 12 Ma deformations

This part of the reconstruction has been arrived at in the three steps depicted in Fig. 5.6. Although extension, homogeneous simple shear and discrete offset at the E-W trending Bogdan-Voda fault that led to the present-day geometry were most probably coevally active, retrodeformation has been done stepwise. This simplified approach seems reasonable, since the amounts of strain accumulated during the individual steps is relatively small. Hence the influence of the order of the individual retrodeformations has been neglected. Missing exact values for the amount of extension accumulated in the contact area, a rotation of $\sim 20^\circ$ (minimum value indicated by paleomagnetic measurements, chapter 4) has been used as a proxy for the total deformation accumulated.

Step 1: The first step led to the retrodeformation of the extension of the contact area by normal faulting across SW-NE striking normal faults. The shortening in NW-SE direction applied to the working area during retro-deformation progressively decreases towards the SW, i.e. away from the European margin. This retro-deformation step has been applied until 10° (half of the total rotation, compare ‘passive marker lines’ in Fig 5.6) rotation had been restored. This value corresponds to approximately 20% homogenous extension within the contact area.

Step 2: The left lateral strike-slip faulting component of the post-Burdigalian transtensional stage has been retrodeformed by homogeneously simple shearing the study area in a second step. This homogeneous simple shear has been applied until the remaining 10° (compare ‘passive marker lines’ in Fig 5.6) had been retrodeformed.

Step 3: In a third step the left lateral offset along the Bogdan- Dragos-Voda fault system has been retrodeformed. Two thirds of the total left lateral offset evidenced by the offset of the Pienide nappe front (chapter 2) has been restored at the Bogdan-Voda segment, using the Greben fault as a separator between the Bogdan- and Dragos-Voda fault segments. Translation of the crystalline units NW of the Greben fault together with strike slip faulting along the Bogdan-Voda fault segment results in the retrodeformation of the Neogene Borsa graben. This simple retrodeformation correlates to about 8km NW-SE extension in the triangle between the Greben fault and the eastern termination of the Dragos-Voda fault. South of the Rodna horst, no major restoration was performed.

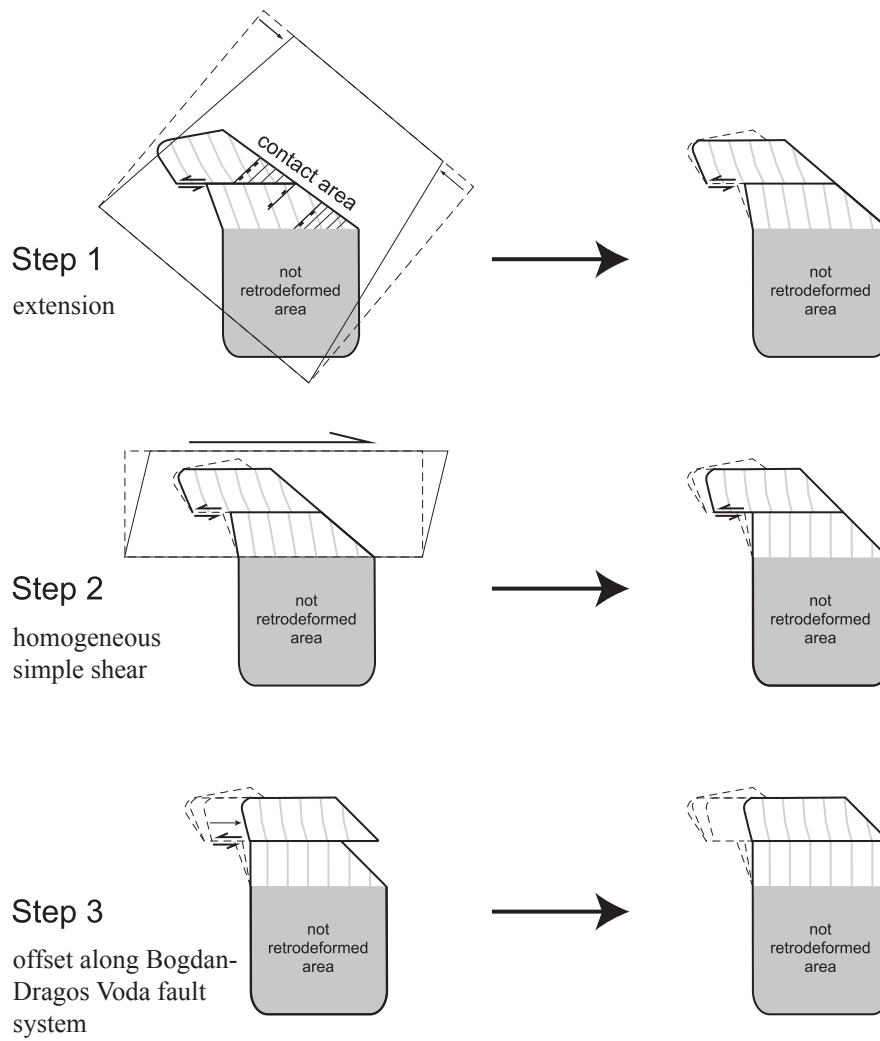


Fig. 5.6: Schematic sketch showing the applied steps for reconstructing the 12Ma time-slice. Note the progressive unroofing of the grey NNW-SSE trending lines, serving as 'passive marker lines'.

Restored 12 Ma time-slice of the Maramures area

After the restoration of the deformations resulting from the transtensional stage, structures formed during the preceding transtensional stage dominate the map view (Fig. 5.7). The map of the study area shows the geometry of the study area after the post Burdigalian transpressional stage (Fig. 5.4b, chapter 2) of 'soft collision' of Tisza-Dacia with the European continental margin. This transpressional stage resulted in shortening of the northern tip of Tisza-Dacia. Corresponding structures are NW-SE trending open folds and backthrusts (Fig. 5.7) as well as E-W striking left lateral strike slip faults (Bogdan-Voda fault). In the transition zone between the Tisza and Dacia blocks an important pop up structure developed (Preluca fault).

Thrusting within the Miocene thrust belt of the Northern East Carpathians, adjacent to our working area starts in Burdigalian times (Săndulescu et al. 1981). The strike of the earlier structures as well as transport directions shown by Matenco and Bertotti 2000 indicate a roughly NE directed emplacement (perpendicular to the European continental margin) during Burdigalian and Langhian times. Since 12 Ma ago (Matenco and Bertotti 2000), however, thrusting continued with a different geometry. The NNW-SSE striking structures of the later stage are consistent with oblique convergence as postulated according to the working hypothesis presented in Fig 5.4.

Integration into the regional setting

Fügenschuh and Schmid 2005 did not provide a time slice for 12 Ma ago, however they inferred a clockwise rotation of 9° between 16 Ma and present day. The best fit of the retrodeformed study area with the orientation of the European margin is reached, when a rotation of 7° is applied to Tisza-Dacia (including the study area). The structures shown in the southern Carpathians (Fig. 5.7) are those presented for the 16 Ma time-slice by Fügenschuh and Schmid (2005).

According to Marton and Fodor (2003) no en-block rotation of the ALCAPA-block is documented after 12 Ma ago. This finding is compatible with the results of Sperner et al. (2002), indicating that soft collision of the ALCAPA block with the European foreland in the Western Carpathians stopped 13 Ma ago. After this soft collision the dominant deformation was extensional, leading to counterclockwise rotations restricted to areas near the European margin (i.e. East Slovak basin; Marton et al. 2000, chapter 4), well comparable to those found within the study area (chapter 4).

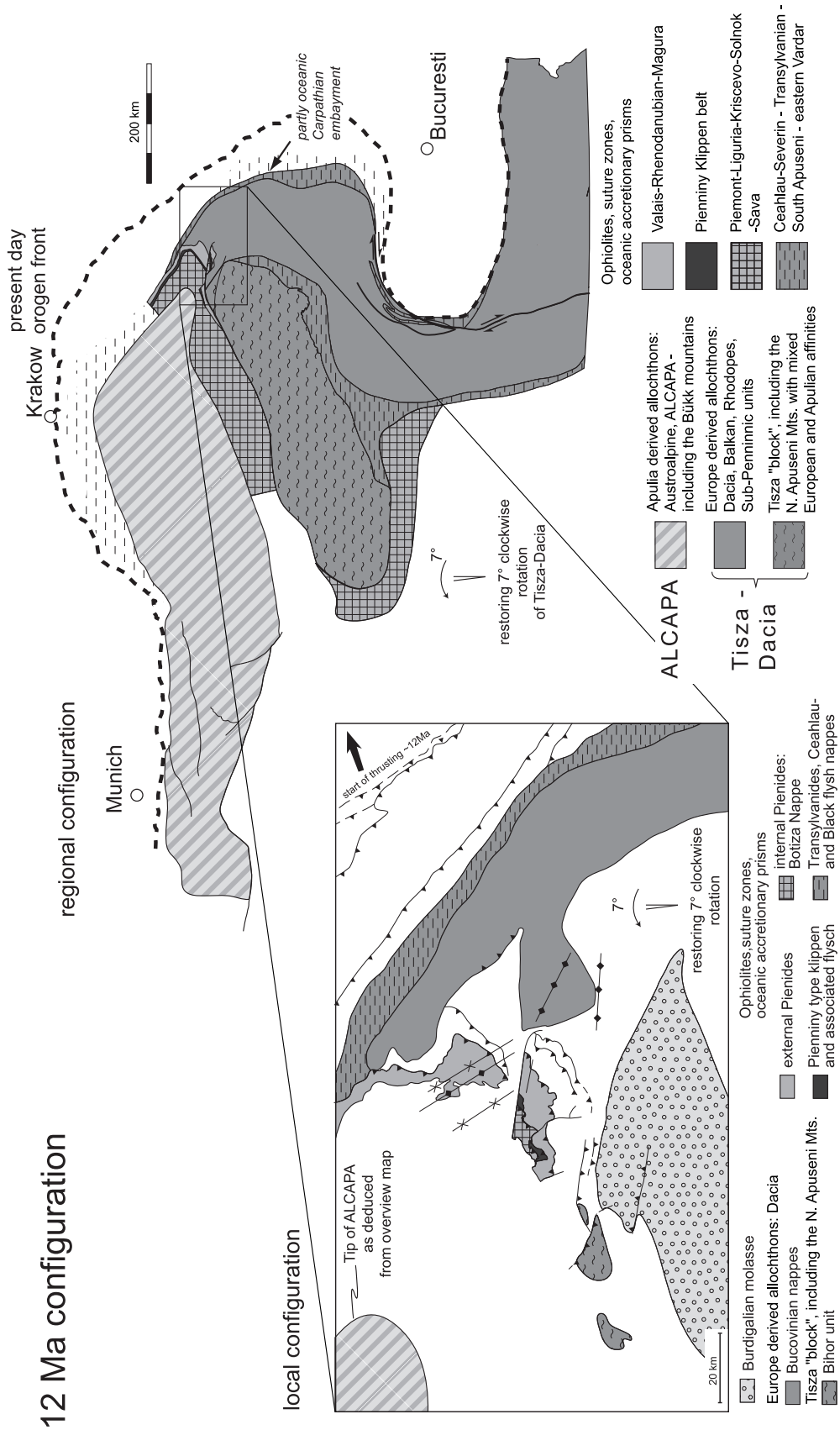


Figure 5.7: Palinspastic map for 12 Ma. Dashed lines in this and subsequent figures denote traces of "future structures"

5.4 The 16 Ma time slice: retro-deformation of post-Burdigalian transpression

Reconstruction of 16 - 12Ma deformations

According to the working hypothesis presented in Fig. 5.4, ‘soft-collision’ of Tisza-Dacia and the European margin led to SW–NE shortening between 16 and 12 Ma ago (‘post-Burdigalian transpression’, chapter 2). Regarding this transpression, a value of 4% shortening has been estimated on the basis of cross section C-C’ (Fig. 5.5) and retrodeformed accordingly. The left lateral strike slip component at the Bogdan-Voda fault segment has been retrodeformed until the SW-NE striking Pienide nappe front was aligned.

Restored 16 Ma time-slice of the Maramures area

The map in Fig. 5.8 shows a retrodeformation of the present-day unit outlines for 16 Ma ago. The onset of soft collision is dated to intra-Burdigalian times by the initiation of thrusting in the most internal units of the Miocene thrust belt (Moldavides, Săndulescu et al. 1981). Thrusting of the more external nappes started in Late Burdigalian (Matenco and Bertotti 2000). The thrusting direction inferred from Matenco and Bertotti (2000) as well as the strike of thrust contacts oriented NW-SE, fit well into the working hypothesis of convergence of Tisza-Dacia approximately perpendicular to the European continental margin (Fig. 5.4). After retrodeformation of the post-Burdigalian transpression, the dominant structure in the map of the study area for the 16 Ma time slice is the Pienide nappe contact, restored to form a continuous SW-NE striking thrust face. This thrust face is dissected by WNW-ESE striking tear faults in the south, the northern bend is due to a change from thrust face to lateral ramp geometry (chapter 2). Also the major imbricates of the autochthonous cover of Tisza-Dacia form a continuous thrust in this restoration.

Integration into the regional setting

For reconstructing the regional configuration the 16 Ma time-slice of Fügenschuh and Schmid (2005) has been used. Retrodeformation of the 9° clockwise rotation of Tisza-Dacia since 16 Ma postulated by these authors leads to a convincing fit of the reconstructed study area in respect to the strike of the European margin (Fig. 5.8).

After 16 Ma ago, opposed rotations are documented for the ALCAPA and Tisza-Dacia block. Aforementioned clockwise rotation of the Tisza-Dacia block (e.g. Fügenschuh and Schmid 2005) is coeval to counterclockwise rotation of ALCAPA (16 – 14.5 Ma, Marton and Fodor 2003). Assuming the pivot-point for the rotation of ALCAPA to be located in the part of the thrust front already locked at 16 Ma, (Fig. 5.8) a minimum of 6° counterclockwise rotation has to be assumed for the ALCAPA block. Such opposed rotations are likely to cause a significant amount of extension. Since the last movements across the contact between the Pienides and Tisza-Dacia are of earlier age (Early Burdigalian, see chapter 2), this extension has to be located further to the west. The minimum of 6° counterclockwise rotation correlates to roughly 20km of NW-SE extension. Note that this minimum value of 6° for the counterclockwise rotation of ALCAPA is drastically lower than the 30° given by Marton and Fodor (2003). This might indicate a higher amount of extension in ALCAPA.

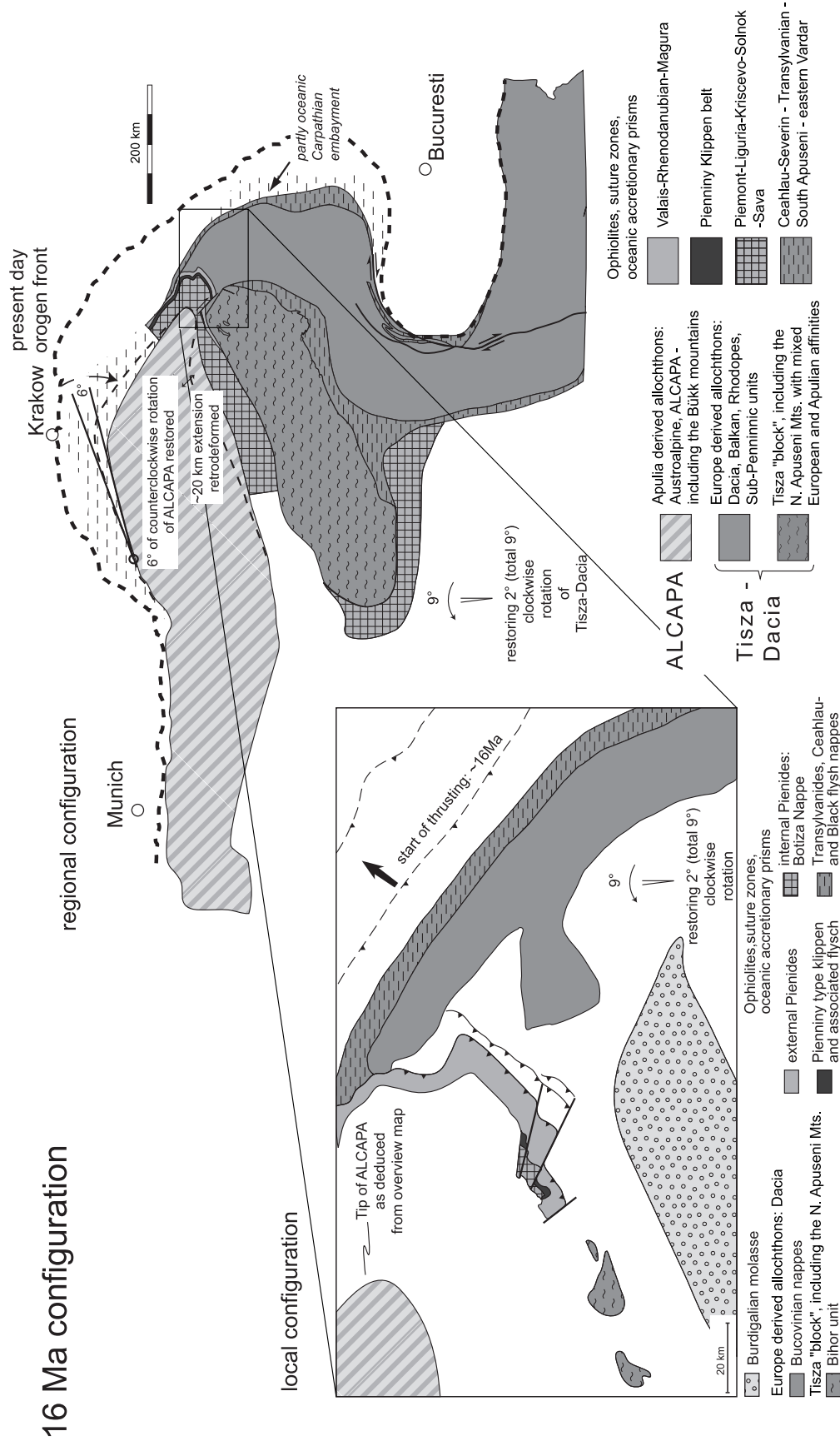


Figure 5.8: Palinspastic map for 16 Ma.

5.5 The 20 Ma time slice: retro-deformation of the Early Burdigalian emplacement of the Pienides

Reconstruction of 20 – 16 Ma deformations

In order to arrive at the 20 Ma time-slice, the nappe emplacement of the Pienides during Early Burdigalian to SE-thrusting had to be retrodeformed. The thrusting distances have been evaluated on the basis of schematic geological cross sections discussed above (Fig. 5.2, 5.3).

Restored 20 Ma time-slice of the Maramures area

The retrodeformed present day outlines of the crystalline basement units are given as reference in the local configuration depicted in Fig. 5.9. The Pienide units have been restored in order to form parallel belts. The 20 Ma time slice shows the configuration before the last major moment of thrusting of the ALCAPA-related units onto the Tisza-Dacia block. The Pienides have been backrotated by the same amount as the rest of the study area. The 38° of clockwise rotation restored in Fig. 5.9 leads to the passive rotation of the emplacement direction (top-SE in present coordinates).

Since the molassic deposits (Hida beds) are interpreted as the fill of the foreland basin that formed during this thrusting (chapter 3), the longitudinal axis of the foreland basin is expected to be oriented roughly parallel to the thrust front of the overriding plate. This strongly suggests that both the Pienides and the Tisza-Dacia block underwent clockwise rotation during 16-20 Ma deformations. This assumption is also supported by the paleomagnetic results from the external Pienides (chapter 4), suggesting post-Oligocene clockwise rotation (~30°-50°). A possible interpretation for these same-sense rotations is, that the Pienide units have already been partially thrust onto the Tisza-Dacia block at 16 Ma, as suggested by Fig 5.9.

Integration into the regional setting

For the integration into the regional setting, the 20 Ma reconstruction of the southern Carpathians by Fügenschuh and Schmid (2005) has been used. The total post-20 Ma clockwise rotation of Tisza-Dacia (38°) proposed by these authors has also been applied to the study area. Since the 20 Ma time slice predates the main phase of basin formation in the Pannonian basin, a significant amount of extension that occurred within the Pannonian basin would have to be retrodeformed. Since the retrodeformation of extension accumulated in the Tisza-Dacia block is beyond the scope of this study, the strongly affected parts of Tisza-Dacia (Clothing et al. 2005) are excluded from further consideration. The not-retrodeformed outlines of the strongly extended parts of Tisza-Dacia are indicated by dotted lines. The approximate position of ALCAPA has been determined by constraints derived from the retrodeformed position of Tisza-Dacia.

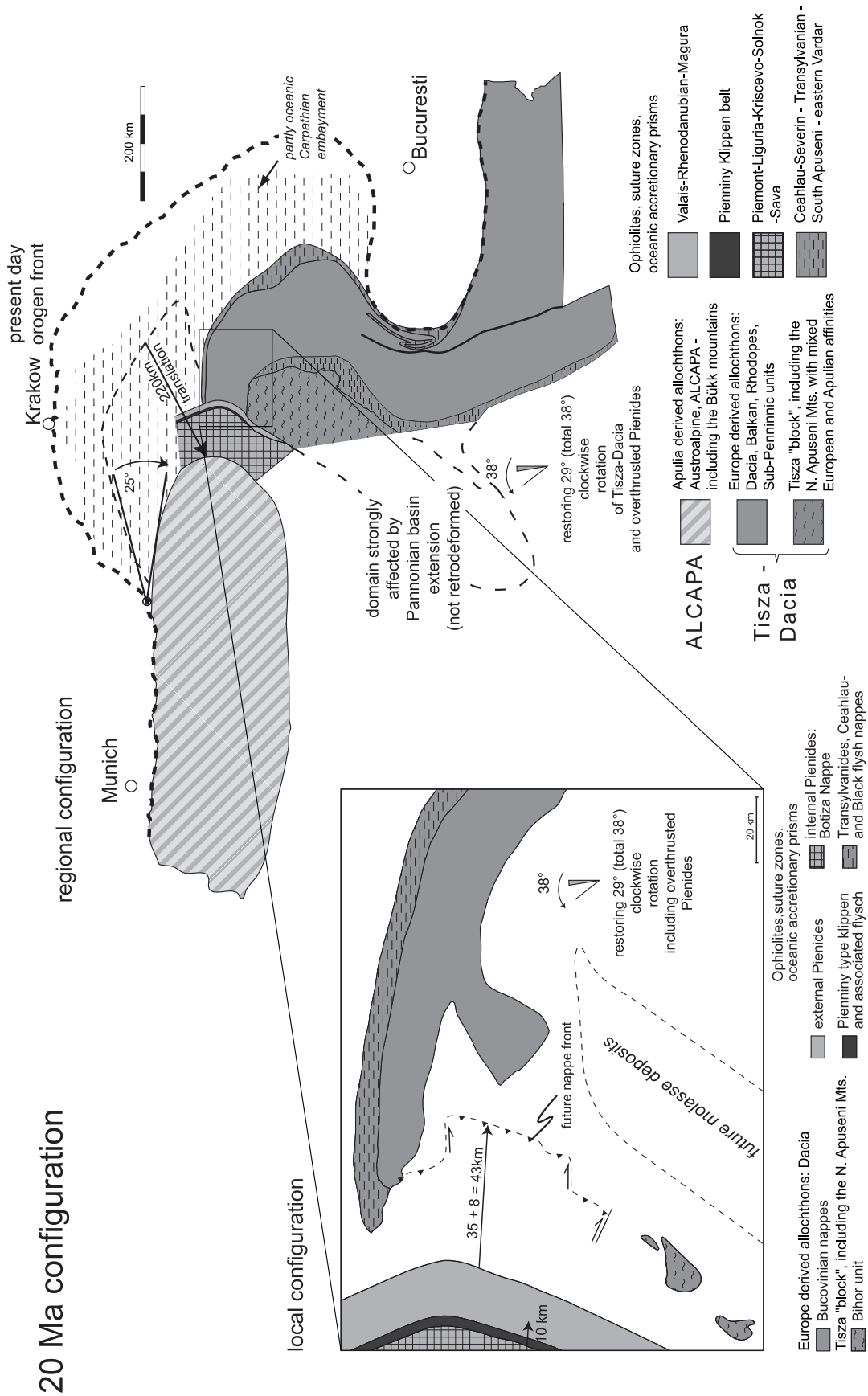


Figure 5.9: Palinspastic map for 20 Ma.

Since it is assumed that thrusting of the Pienide units had already started at 20 Ma, the margin of ALCAPA was placed in relative proximity to the study area, i.e. to the northwestern edge of the Tisza-Dacia block in the reconstruction of Fig. 5.9. All this implies a minimum of 25° post-20 Ma counterclockwise rotation, as well as a restoration of 220km northeast-ward translation of the ALCAPA-block (Fig. 5.9). This rotation (25° counterclockwise, 20-16 Ma) is in good agreement with paleomagnetic data (50° counterclockwise, 18-17 Ma) presented by Marton and Fodor (2003) regarding sense and timing. The significant difference in the amount of rotation might again result from ALCAPA-internal deformation not considered in the presented reconstruction. The 220km eastward translation of the ALCAPA block postulated might represent a combination of lateral extrusion and extension leading to the formation of the Pannonian basin. Note that E-ward lateral extrusion of ALCAPA was roughly parallel to the restored emplacement direction of the Pienides onto the Tisza-Dacia block (Fig. 5.9).

5.6 The 34 Ma time slice: reconstruction of the situation before the onset of lateral extrusion of ALCAPA and clockwise rotation of Tisza-Dacia

Unfortunately, the constraints regarding the 34 Ma time slice are rather poor. However, some constraints are available from the reconstruction of the Southern Carpathians by Fügenschuh and Schmid (2005). A relative proximity of Tisza-Dacia to ALCAPA, as depicted in Fig. 5.10, is suggested by the deposition of Oligocene flysch units onto the northern part of the Tisza-Dacia block. This flysch deposition is possibly related to the onset of juxtaposition of these two blocks whereby the Tisza-Dacia block would be situated in a lower plate position. The axis of this flysch basin (E-W to SE-NW in present day coordinates, DeBroucker et al. 1998) would be oriented roughly WSW-ENE after the retrodeformation presented in Fig. 5.10. This would imply, that ALCAPA was located somewhere NW of the study area at 34 Ma ago. The reconstruction shown in Fig. 5.10 is again partly based on the 34 Ma restoration of the Southern Carpathians of Fügenschuh and Schmid 2005, the total of 52° clockwise rotation postulated by these authors for the Tisza-Dacia block since 34 Ma is also applied to the study area. A roughly NNW - SSE oriented strike of the Pienide realm was arrived at by geometrical considerations taking into account the entire regional picture.

Since the greatest part of lateral extrusion of ALCAPA commenced post 20 Ma (Ratschbacher et al. 1991b, Sperner et al. 2002), no major westward translation of ALCAPA is possible when going from time slice 20 Ma (Fig. 5.9) to 34 Ma (Fig. 5.10). A minor amount of westward translation might be possible assuming, that a subordinate amount of lateral extrusion commenced as early as Late Oligocene times. Such a Late Oligocene E-W extension has been described by Schmid and Froitzheim (1993) for the Engadine line.

When considering the eastern tip of ALCAPA to be relatively fixed between 34 Ma and 20 Ma, space problems occur when retrodeforming the clockwise rotation of Tisza-Dacia. Even when assuming an amount of 30km eastward lateral extrusion of ALCAPA between 34 Ma and 20 Ma, these space problems remain (Fig 5.10).

These space problems could be solved in two ways:

1. By increasing the amount of lateral extrusion commencing pre-20 Ma.
2. By assuming a more southerly position of Tisza-Dacia at 20 Ma ago.

The paleomagnetic data discussed in chapter 4 supports the second solution. While Fügenschuh and Schmid (2005) arrive at a total of 51° clockwise rotation of Tisza-Dacia after 34 Ma ago, greater values (up to 120°) are indicated by the paleomagnetic data presented in chapter 4. A greater amount of rotation of Tisza-Dacia since 34 Ma ago would imply a more southerly position of Tisza-Dacia at 20 Ma, and circumvent the space problems discussed above.

According to the retrodeformation presented in Fig.5.10, a small amount of thrusting of the Pienides onto the Tisza-Dacia block would have had to occur between 34 and 20 Ma. Again, two possible driving-forces can be envisaged for this thrusting. Either the juxtaposition of ALCAPA and Tisza-Dacia in Early Oligocene times is a result of an early stage of lateral extrusion, or related to clockwise rotation of the Tisza-Dacia block.

A build-up of topography, consistent with the small amount of thrusting mentioned above, is indicated by the deposition of extensive Oligocene flysch series onto the autochthonous cover of Tisza-Dacia (chapter 3). When assuming this topography to develop at the edge of the ALCAPA block, this configuration allows for explaining the occurrence of Oligocene turbiditic deposits not only in the autochthonous cover of Tisza-Dacia, but also in the intervening internal Pienides (Secatura Sandstone, frontal scales of the Botiza nappe), external Pienides (Magura Perciu-Pinentul Sandstone, Wildflysh nappe; Voronicu Sandstone, Leordina nappe).

5.7 Conclusions

The palinspastic reconstruction of the study area presented in this chapter has been linked with the reconstruction of the Southern Carpathians presented by Fügenschuh and Schmid (2005). Using the reconstruction of the Southern Carpathians as a starting point for the retrodeformation of the regional settings presented in Figs. 5.7, 5.8, 5.9, 5.10, a generally convincing fit to the observed constraints derived in chapters 2 - 4 is reached. However, the paleomagnetic data presented in chapter 4 indicate a larger value for the clockwise rotation of Tisza-Dacia since 34 Ma ago, than the 51° described by Fügenschuh and Schmid (2005). The more southerly position of Tisza-Dacia at 20 Ma ago (Fig. 5.9) implied by stronger rotations would lead to an optimised fit of the relative positions of ALCAPA and Tisza-Dacia for the 34 Ma and 20 Ma time-slice.

Chapter 6: Summary

In the following, the findings from this thesis are summarised, organized after the respective topics. On the basis of a tectonic map of the study area (Fig. 6.1) a correlation chart of the results of chapters 2 – 4 is presented (Fig. 6.2). In section 6.4 these results are interpretatively integrated into the regional setting.

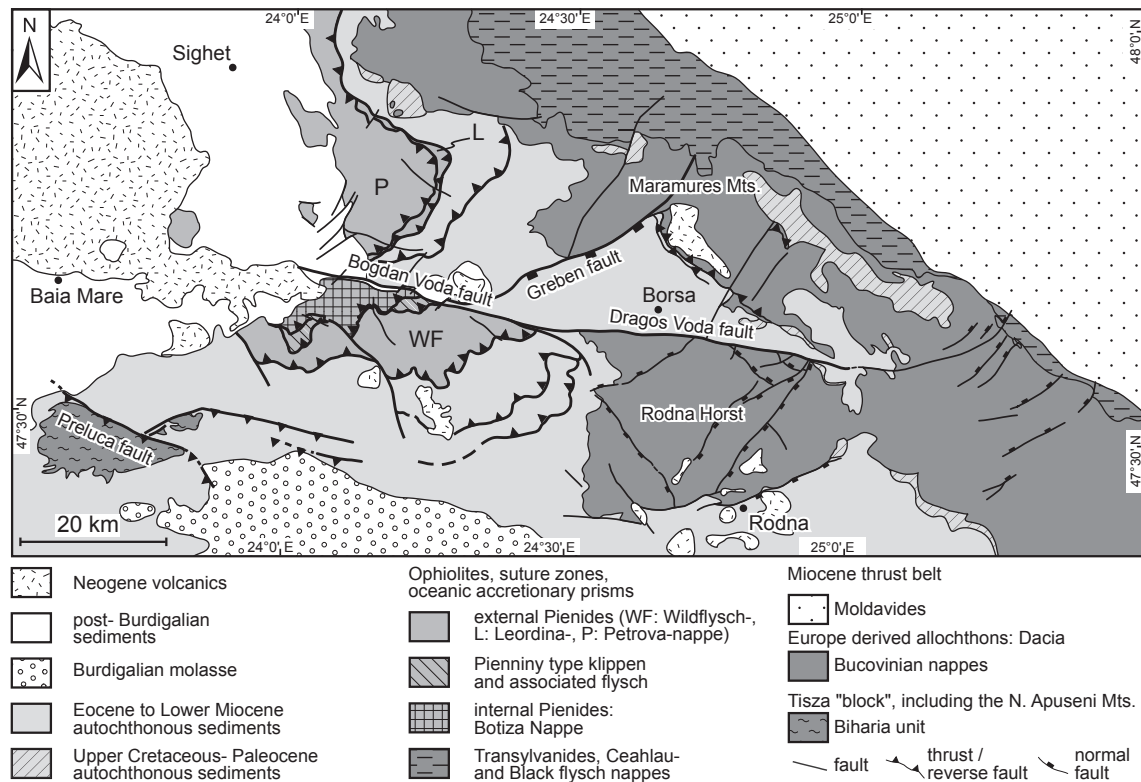


Fig. 6.1: Tectonic map of the study area based on published geological maps (1:50.000 and 1: 200.000) of the Geological Survey of Romania as well as geological maps of Dicea et al. (1980), Săndulescu (1980) Săndulescu et al. (1981) and Aroldi (2001).

6.1 Chapter 2: Tectonic constraints

Detailed structural field-work, based on published (Geological Survey of Romania) and unpublished (Săndulescu pers. com. 2002) geological maps resulted in the separation of four Late Tertiary deformation phases discussed below.

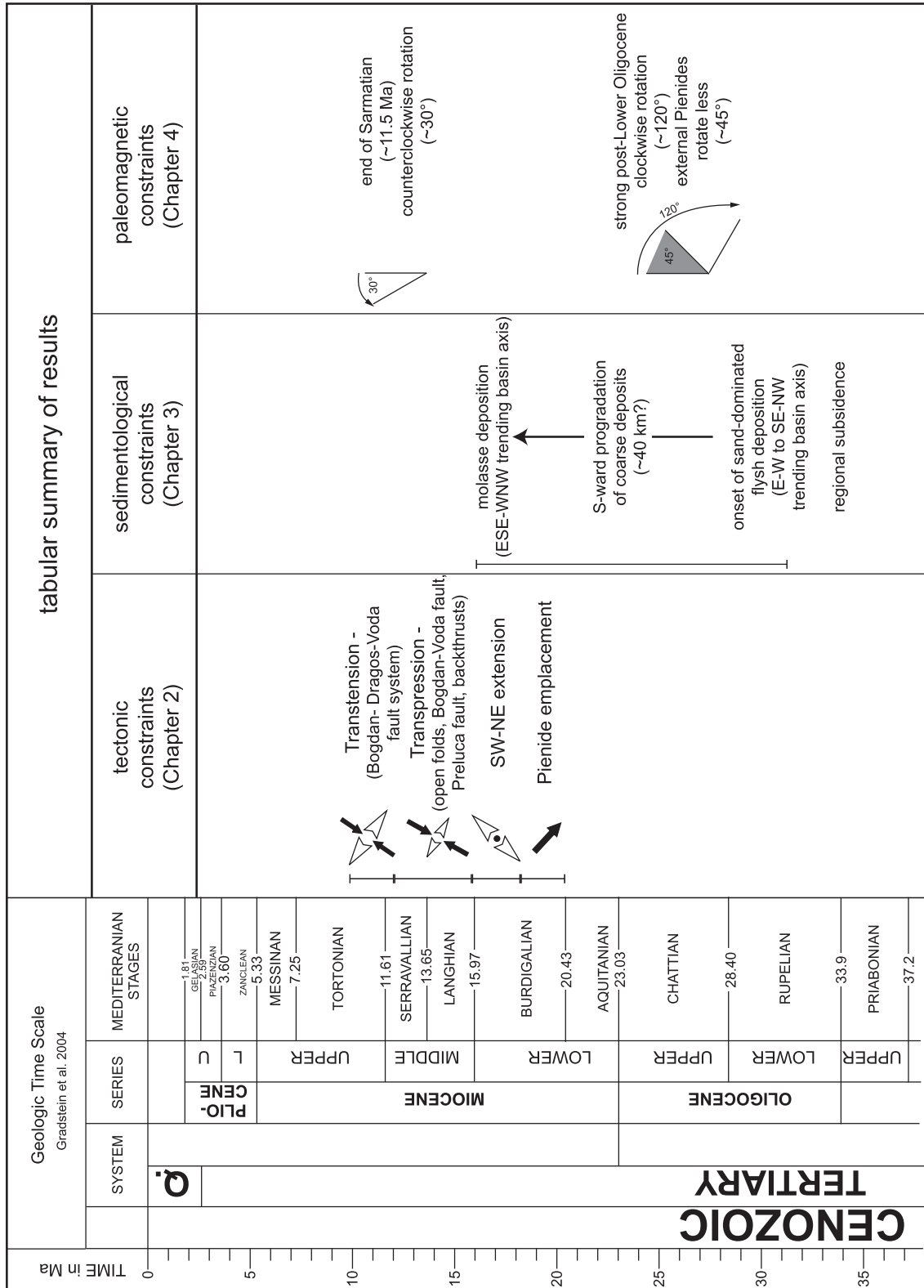


Figure 6.2: Temporal correlation chart of the results of this thesis.

Early Burdigalian top-SE thrusting of the Pienides (20.5 - ~18.5 Ma)

The oldest deformation phase distinguished in the study area is the emplacement of the Pienide nappes. The deformation accompanying the SE-ward thrusting of the unmetamorphic flysch nappes is dominated by cataclastic shear-zones, folding is subordinately developed within the fine grained flysch units serving as detachment horizons. The minimum estimate for shortening in the external Pienides is 35 km, another 10 km are estimated as minimum for the internal Pienides. The curved appearance of the nappe front is due to changing thrust plane geometries: The SW-NE striking thrust face is dissected by tear-faults as well as lateral ramps. Thrusting also led to significant imbrication within the autochthonous units, estimated to accommodate a further 8km of offset.

Late Burdigalian NE – SW extension (~18.5 – 16 Ma)

Overprinting nappe emplacement structures, the 2nd deformation phase is characterised by NE-SW to NNE-SSW extension. The NW-SE striking normal faults formed during this stage are not very pervasively developed, and are more abundant within the crystalline units of the study area.

Post-Burdigalian transpressional stage (16 – 12 Ma)

The first strike-slip dominated deformational phase is characterised by a strong NE-SW oriented compressional component. This compression led to the formation of open folds within the sedimentary units of the study area, in the crystalline units backthrusts have been formed. The major features active during this phase of activity are the Preluca fault (thrust-dominated) and the Bogdan-Voda fault (transpressive deformation prevailing). During this stage the Bogdan-Voda fault accommodated around 14km left lateral offset, and terminated at the (pre-existing) basement high of the present day Rodna horst.

Post Burdigalian transtensional stage (12-10 Ma)

The most prominent strike slip features visible in map view acquired their present day geometry during the second stage of strike-slip deformation, dominated by transtension (NW-SE trending extension). The Bogdan- Dragos-Voda fault system was active as a continuous E-W trending sinistral-transtensive fault, accumulating a lateral offset of about 11km, a maximum vertical offset of 3km is reached at the north-western corner of the Rodna horst. The left lateral offset at the Bogdan- Dragos-Voda fault system diminishes towards the east, until the system ends in an extensional horse tail splay-like geometry before reaching the external Miocene thrust belt. Coevally active structures are SW-NE trending normal faults (Greben fault, faults within the Rodna horst) as well as compatible structures in the south of the Rodna, accentuating the present day map view. Transtensive reactivation is documented at the Preluca fault.

6.2 Chapter 3: Sedimentological constraints

Starting in Early Oligocene times, marked subsidence followed by the deposition of flysch units is documented in Northern Romania. This process shows a S to SE-ward propagation and younging tendency. The deposition of flysch units is grading into molasse type sediments, documented to form a clastic wedge in the Transylvanian basin. The clastic units are deposited within an elongated, flexural foreland basin fed from the NW. The basin axis documented by subsurface data is striking WSW-ENE, but possibly evolved out of a rather E-W to SE-NW trending orientation due to clockwise rotation of Tisza-Dacia.

Formation of the flexural basin may be related to the juxtaposition of ALCAPA and Tisza-Dacia, the last moment of this process being reflected by the thrusting of the Pienides onto the autochthonous sedimentary cover of the Tisza-Dacia block. This last moment of juxtaposition is coeval to the formation of the molassic parts of the clastic wedge. Onset of the flysch deposition in northern Romania, however, points to initiation of these tectonic processes as early as Early Oligocene.

6.3 Chapter 4: Paleomagnetic constraints

Paleomagnetic data from the study area indicate a strong ($\sim 120^\circ$) clockwise rotation of Early Oligocene strata from the autochthonous cover. Samples originating from the cover units of the Tisza block show no differential rotations compared to those from the Dacia block. Interesting to note is, that Eocene and Oligocene units from the external Pienide nappes exhibit same sense rotations, although to a lesser degree ($\sim 75^\circ$).

Mid-Miocene samples indicate a homogenous counterclockwise rotation of the study area ($\sim 30^\circ$) post 12 Ma. These results are consistent with already existing paleomagnetic data.

6.4. Integration of the results into the regional setting

Using the palinspastic restoration of the study area described in chapter 5, the results of this thesis have been integrated into the regional setting (Fig. 6.3). In the following an interpretation of the processes recorded within the study area is given. Descriptive terms used refer to the restored geometries.

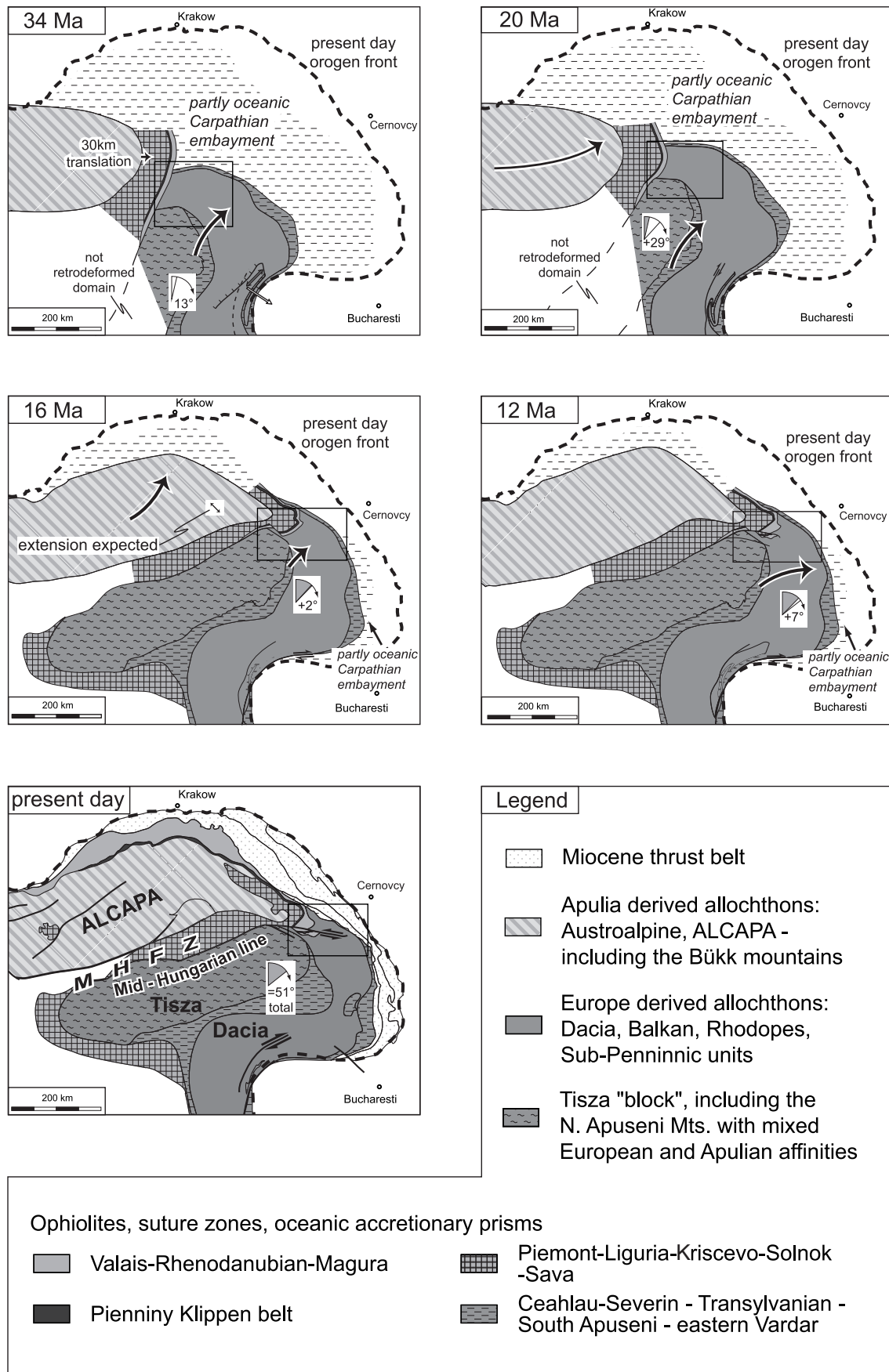


Fig. 6.3: Schematic integration of the results into the regional setting. The maps are based on an unpublished compilation by S.M. Schmid, B. Fügenschuh K., Ustaszewski, L. Matenco, R. Schuster and M. Tischler. Structures and rotations in the Southern Carpathians follow Fügenschuh and Schmid (2005). Arrows and rotations denote movements leading to the next younger time slice. The study area is outlined.

After 34 Ma, tectonic activity, possibly the onset of thrusting of ALCAPA over Tisza-Dacia, is reflected by the deposition of sand-dominated flysch units onto Tisza-Dacia (see chapter 3). The Early Oligocene age of the oldest coarse grained flysch units points towards an initiation of this process possibly as early as Early Oligocene. This suggests relative proximity of ALCAPA and Tisza-Dacia, with Tisza-Dacia in lower plate position during the juxtaposition of the two continental blocks. The then (backrotated) roughly WSW-ENE trending basin axis of the resulting foreland basin implies that ALCAPA was located NW of Tisza-Dacia during these times. The onset of tectonic activity is dated to roughly Late Oligocene by other authors (Csontos and Nagymarosy 1998, Fodor et al. 1999, Sperner et al. 2002). Note, that occurrence of Oligocene sand-dominated flysch units within the external Pienides (Săndulescu and Micu 1989, Aroldi 2001) implies the existence of a continuous water body between the autochthonous realm and (at least) the external Pienides.

Between 34 and 20 Ma, invasion of Tisza-Dacia into the Carpathian embayment is coupled with corner effects at the Moesian promontory. These corner effects lead to strong clockwise rotations of Tisza-Dacia (Patrascu et al. 1994). A small amount of lateral extrusion of ALCAPA may commence in Late Oligocene times (Ratschbacher 1991 b, Schmid and Froitzheim 1993). Converging movement vectors of the two continental blocks may lead to a partial emplacement of the ALCAPA-related Pienides onto Tisza-Dacia.

Between 20 and 16 Ma,

Slab rollback (e.g. Royden 1988, Wortel and Spakman 2000, Sperner et al. 2005) and lateral extrusion (Ratschbacher 1991a, b) lead to the invasion of ALCAPA and Tisza-Dacia into the Carpathian embayment. The clockwise rotation of Tisza-Dacia continues while the last moment of major convergence between ALCAPA and Tisza-Dacia lead to the final emplacement of the Pienides onto Tisza-Dacia (see chapter 2 and references therein). After being thrust onto the clockwise rotating Tisza-Dacia block, the ALCAPA-related Pienides rotate in the same sense – but record only part of the total rotation (chapter 4). While the old basin axis of the foreland basin in the northern part of Tisza-Dacia passively rotates in a clockwise direction, a new basin axis is formed in a WSW-ENE orientation (chapter 3). This basin is filled by flysch deposits evolving into molassic units as the cessation of thrusting results in decreased subsidence. Contemporaneously, ALCAPA starts to rotate into the opposed direction (e.g. Marton and Fodor 2003). Thrusting starts in the external flysch belt (Matenco and Bertotti 2000).

Onset of the main phase of back-arc style rifting in the Pannonian basin causes extension in ALCAPA and Tisza-Dacia blocks (Fodor et al. 1999).

Between 16-12 Ma, ‘soft-collision’ during approximately perpendicular convergence of Tisza-Dacia and the European margin results in shortening and strike slip deformation at the northern tip of Tisza-Dacia. This shortening results in the formation of open folds and transpressional deformation (chapter 2). The amount of shortening is however insufficient to allow the final closure of the remaining partly oceanic crust.

ALCAPA suffers another phase of counterclockwise rotation (e.g. Marton and Fodor 2003) as the remaining gap of oceanic crust between ALCAPA and the European margin is closed. This counterclockwise rotation is likely to result in extension of the transition zone between ALCAPA and Tisza-Dacia.

Between 12 and 10 Ma continuous convergence in the Central East Carpathians results in a change of tectonic setting at the northern tip of Tisza-Dacia. Driven by slab-pull resulting in extension, the contact area of Tisza-Dacia is ‘fitted’ to the European margin. This phase is also the main phase of uplift in the Northern East Carpathians, as documented by fission track studies (Sanders 1998, Gröger 2006). The dominant mechanisms during this process are strike-slip faulting along E-W trending faults, together with normal faulting along SW-NE trending structures. This deformation results in a localized counterclockwise rotation at the northern tip of Tisza-Dacia (chapter 4). Most of the clockwise rotation of Tisza-Dacia is realized until 10 Ma (Patrascu 1993).

References

Following references are a complete list of the citations used in all of the chapters of this thesis

- Angelier J, Mechler P (1977) Sur une méthode graphique de recherche des contraintes principales également utilisable en tectonique et enséismologie: la methode des diédres droits. Bull Soc Géol France VII 19: 1309-1318
- Antonescu F, Mitrea G, Popescu A (1981) Contributii la cunoasterea stratigrafiei si tectonicii miocenului din regiunea Vadu Izei-Birsan-Botiza (Maramures). D.S. Inst Geol Geofiz LXVI: 5-23
- Aroldi C (2001) The Pienides in Maramures – Sedimentation, tectonics and paleogeography. PhD Thesis, Cluj, pp 1-156
- Balintoni I (1995) Alpine structural outline of the Pannonian Carpathian realm. Studia Universitates Babes - Bolyai, Geologia XL(2): 3 – 16
- Balla Z (1982) Development of the Pannonian Basin basement through the Cretaceous-Cenozoic collision; a new synthesis. Tectonophysics 88: 61-102
- Balla Z (1984) The Carpathian loop and the Pannonian basin: a kinematic analysis. Geophysical Transactions 30/4: 313-353
- Balla Z (1987) Tertiary paleomagnetic data for the Carpatho-Pannonian region in the light of Miocene rotation kinematics. Tectonophysics 139: 67-98
- Besse J, Courtillot V, (2002) Apparent and true polar wander and the geometry of the geomagnetic field over the last 200 Myr. Journal of Geophysical Research B: Solid Earth Nov 10; 107 EPM 6-1: 6-31
- Bingham C (1964) Distributions on a sphere and the projective plane. PhD. diss. Yale University, New Haven, pp 1-93
- Bouma AH (1962) Sedimentology of some flysh deposits, a graphic approach to facies interpretation. Elsevier Co. Amsterdam, pp 1-168
- Burchfiel BC (1980) Eastern European Alpine system and the Carpathian orocline as an example of collision tectonics. Tectonophysics 63: 31–61
- Ciulavu D (1998) Tertiary tectonics of the Transylvanian Basin. PhD. diss. Vrije Universiteit Amsterdam, Amsterdam, pp 1-154
- Ciulavu D, Dinu C, Cloetingh SAPL (2002) Late Cenozoic tectonic evolution of the Transylvanian basin and northeastern part of the Pannonian basin (Romania): Constraints from seismic profiling and numerical modelling. EGU Stephan Mueller Special Publication Series 3: 105-120
- Cloetingh S, Bada G, Matenco L, Lankreijer A, Horváth F, Dinu C (2005) Thermo-mechanical modelling of the Pannonian-Carpathian system: Modes of tectonic deformation, lithospheric strength and vertical motions. Geol. Soc. London Spec. Publ., in press.
- Csontos L, Nagymarosy A, Horváth F, Kováč M (1992) Cenozoic evolution of the Intra-Carpathian area: a model. Tectonophysics 208: 221–241

- Csontos L (1995) Cenozoic tectonic evolution of the Intra-Carpathian area: a review. *Acta Vulcanologica* 7: 1-13
- Csontos L, Nagymarosy A (1998) The Mid-Hungarian line: a zone of repeated tectonic inversions. *Tectonophysics* 297: 51-71
- Csontos L, Márton E, Wórum G, Benkovics L (2002) Geodynamics of SW-Pannonian inselbergs (Mecsek and Villány Mts, SW Hungary). *EGU Stephan Mueller Special Publication* 3: 227-245
- Csontos L, Vörös A (2004) Mesozoic plate tectonic reconstruction of the Carpathian region. *Paleogeography, Paleoclimatology, Paleoecology* 210: 1-56
- De Broucker G, Mellin A, Duindam P (1998) Tectonostratigraphic evolution of the Transylvanian Basin, Pre-Salt sequence, Romania, In: Dinu C (ed). *BGF Special volume* 1: 36-70
- Dicea O, Duşescu P, Antonescu F, Mitrea G, Botez R, Donos I, Lungu V, Moroşanu I (1980) Contributii la cunoasterea stratigrafiei zonei transcarpatice din maramures. *D. S. Inst geol geofiz LXX*, 4: 21- 85
- Dickinson WR (1985) Interpreting provenance relations from detrital modes of sandstones. In: Zuffa GG. (ed). *Provenance of arenites*, NATO ASI Series. Series C: Mathematical and Physical Sciences. 148: 333-361
- Dimitrijevic MD (2001) Dinarides and the Vardar Zone: a short review of the geology. *Acta Vulcanologica* 13: 1-8
- Dunkl I (2002) Trackkey: a Windows program for calculation and graphical presentation of fission track data. *Computers & Geosciences* 28: 3-12
- Fisher R (1953) Dispersion on a sphere. *Proc. Roy. Soc. London Ser. A.* 217, 295–305
- Flügel, E. (1978): *Mikrofazielle Untersuchungsmethoden von Kalken*. Springer-Verlag, Berlin Heidelberg New York, pp 1-454
- Fodor L, Jelen B, Márton M, Skaberne D, Car J, Vrabec M (1998) Miocene-Pliocene tectonic evolution of the Slovenian Periadriatic fault: Implications for Alpine-Carpathian extrusion models. *Tectonics* 17: 690-709
- Fodor L, Csontos L, Bada G, Györfi I, Benkovics L (1999) Cenozoic tectonic evolution of the Pannonian basin system and neighbouring orogens: a new synthesis of paleostress data. In: Durand B, Jolivet L, Horváth F, Séranne M (eds). *The Mediterranean basins: Cenozoic Extension within the Alpine Orogen*. *Geol Soc Spec Publ* 156: 295–334
- Fügenschuh B, Schmid SM (2005) Age and significance of core complex formation in a highly bent orogen: evidence from fission track studies in the South Carpathians (Romania). *Tectonophysics* in press
- Galbraith RF (1981) On statistical models for fission track counts. *Math Geol* 13: 471-488.
- Galbraith RF, Laslett GM (1993) Statistical models for mixed fission track ages. *Nucl Tracks Radiat Meas* 21: 450-470
- Gallagher K, Brown R, Johnson C. (1998) Fission track analysis and its applications to geological problems. *Annu Rev Earth Planet Sci* 26: 519-571
- Gleadow AJW (1981) Fission track dating methods: what are the real alternatives ? *Nucl Tracks* 5: 3-14
- Gleadow AJW, Duddy IR (1981) A natural long-term track annealing experiment for apatite. *Nucl Tracks* 5(1/2): 169-174

- Gradstein F, Ogg J, Smith A (2004) A Geologic Time Scale. Cambridge University Press, Cambridge, pp 1 – 589
- Gröger HR (2006) Thermal and structural evolution of the East Carpathians in northern Romania: from Cretaceous orogeny to final exhumation during Miocene collision. Published PhD-Thesis, Basel, Switzerland pp. 1 - 111
- Györfi I, Csontos L, Nagymarosy A, (1999) Early Cenozoic structural evolution of the border zone between the Pannonian and Transylvanian basins. In: Durand B, Jolivet L, Horváth F, Séranne M (eds). The Mediterranean Basins: Cenozoic Extension within the Alpine Orogen. *Geol Soc Spec Publ* 156: 251– 267
- Haas J, Pero S (2004) Mesozoic evolution of the Tisza Mega-unit. *Int J Earth Sci* 93: 297-313
- Haas J, Mioč P, Pamić J, Tomljenović B, Árkai P, Bérczi-Makk A, Koroknai B, Kovács S, Rálich-Felgenhauer E (2000). Complex structural pattern of the Alpine-Dinaridic-Pannonian triple junction. *Int J Earth Sci* 89: 377-389
- Hardenbol J, Jacques T, Farley MB, de Graciansky PC, Vail PR (1998): Mesozoic and Cenozoic sequence chronostratigraphic framework of European basins. In: de Graciansky PC, Hardenbol J, Jacquin T, Vail PR (eds): Mesozoic and Cenozoic sequence stratigraphy of European basins. SEPM Special Publication 60:3-13 Tulsa, OK, United States.
- Haq BU, Hardenbol J, Vail PR (1987) The chronology of fluctuating sea level since the Triassic. *Science* 235: 1156-1167
- Horváth F, Bada G, Szafián P, Tari G, Ádám A, Cloetingh S (2005) Formation and deformation of the Pannonian basin: constraints from observational data. *Geol Soc London Spec Publ*, in press.
- Huisman RS, Bertotti G, Ciulavu D, Sanders CAE, Cloetingh S, Dinu C (1997) Structural evolution of the Transylvanian Basin (Romania): a sedimentary basin in the bend zone of the Carpathians. *Tectonophysics* 272: 249-268
- Hurford AJ, Green PF (1983) The zeta age calibration of fission track dating. *Isotope Geoscience* 1: 185-317
- Jipa D (1962) Directii de aport în gresia de Borsa (Maramures). *Com Acad. RPR* 12: 1363-1368
- Kirschvink JL (1980) The least-squares line and plane and the analysis of paleomagnetic data. *Geophysical Journal of the Royal Astronomical Society* 62, 699-718. Kovács S, Haas S, Csazar G, Szederkenyi T, Buda G, Nagymarosy A (2000) Tectonostratigraphic terranes in the pre-Neogene basement of the Hungarian part of the Pannonian area. *Acta Geol Hung* 43/3: 225-328
- Kováč M, Král J, Márton E, Plašienka D, Uher P (1994) Alpine uplift history of the Central West Carpathians: geochronological, paleomagnetic, sedimentary and structural data. *Geologica Carpathica* 45: 83-96
- Kováč M, Kováč P, Marko F, Karoli S, Janočko J (1995) The East Slovakian Basin – a complex back arc basin. *Tectonophysics* 252: 453-466.
- Kovács S, Haas S, Csazar G, Szederkenyi T, Buda G, Nagymarosy A (2000) Tectonostratigraphic terranes in the pre-Neogene basement of the Hungarian part of the Pannonian area. *Acta Geol Hung* 43/3: 225-328
- Kräutner HG, Kräutner F, Szasz L (1982): Geological Map 1:50.000 No 20a Pietrosul Rodnei. Institutul de Geologie si Geofizica, Bucharest.
- Kräutner HG, Kräutner F, Szasz L (1983) Geological Map 1:50.000 No 20b Ineu, Institutul de Geologie si Geofizica, Bucharest

- Lowrie W (1990) Identification of ferromagnetic minerals in a rock by coercivity and unblocking temperature properties. *Geophysical Research Letters* 17, 159–162
- Marret R, Allmendinger RW (1990) Kinematic analysis of fault slip-data. *J Struct Geol* 12: 973-986
- Márton E (1987) Paleomagnetism and tectonics in the Mediterranean region. *Journal of Geodynamics* 7: 33-57
- Márton E, (2000) The Tisza Megatectonic Unit in the light of paleomagnetic data. *Acta Geol Hung* 43/3: 329– 343
- Márton E, (2001): Tectonic implications of Tertiary paleomagnetic results from the PANCARDI area (Hungarian contribution). *Acta Geol Hung* 44: 135-144.
- Márton E, Fodor L (1995) Combination of palaeomagnetic and stress data - a case study from North Hungary. *Tectonophysics* 242: 99–114
- Márton E, Fodor L (2003) Tertiary paleomagnetic results and structural analysis from the Transdanubian Range (Hungary): rotational disintegration of the ALCAPA unit. *Tectonophysics* 363: 201-224
- Márton E, Márton P (1978) On the difference between the palaeomagnetic poles from the Transdanubian Central Mountains and the Villány Mountains respectively (in Hungarian). *Magyar Geofizika* XIX/4: 129-136
- Márton E, Márton P (1996) Large scale rotations in North Hungary during the Neogene as indicated by palaeomagnetic data. In: *Palaeomagnetism and Tectonics of the Mediterranean Region* (edited by Morris, A. & Tarling, D.H.). *Geol. Soc. Spec. Publication* 105: 153-173
- Márton E, Pécskay Z (1998) Correlation and dating of the ignimbritic volcanics in the Bükk foreland, Hungary: complex evaluation of paleomagnetic and K/Ar isotope data. *Acta Geologica Hungarica* 41: 467-476
- Márton E, Márton P, Less G (1988) Paleomagnetic evidence of tectonic rotations in the Southern margin of the Inner West Carpathians. *Physics Earth and Planetary Interiors* 52: 256-266
- Márton E, Mastella L, Tokarski AK (1999) Large counterclockwise rotation of the Inner West Carpathian Paleogene Flysch – evidence from paleomagnetic investigation of the Podhale Flysch (Poland). *Physics and Chemistry of the Earth (A)* 24/8, 645-649
- Márton E, Vass D, Tunyi, I (2000) Counterclockwise rotations of the Neogene rocks in the East Slovak basin. *Geologica Carpathica* 51/3: 159-168
- Márton E, Fodor L, Jelen J, Marton P, Rifej H, Kevric R (2002) Miocene to Quarternary deformation in NE Slovenia: complex paeomagnetic and structural study. *Journal of Geodynamics* 34: 627-651
- Mason PRD, Seghedi I, Szákasc A, Downes H (1998) Magmatic constraints on geodynamic models of subduction in the Eastern Carpathians, Romania. *Tectonophysics* 297: 157-176
- Matenco L, Bertotti G (2000) Tertiary tectonic evolution of the external East Carpathians (Romania). *Tectonophysics* 316: 255-286
- Matenco L, Bertotti G, Cloetingh S, Dinu C (2003) Subsidence analysis and tectonic evolution of the external Carpathian-Moesian Platform during Neogene times. *Sediment Geol* 156: 71-94
- McFadden PL (1990) A new fold test for palaeomagnetic studies. *Geophysical Journal International* 103: 163-169

- Mihailescu N, Panin N (1962) Directii de curent în depozitele Eocen-Oligocene din Regiunea Telciu-Romuli (Maramures). *Com Acad RPR* 12: 1357-1362
- Moiescu V, (1981) Oligocene deposits of Transylvania and their correlation in Parathethys. *Révues Roumanien de Géologie, Géophysique et Géographie*, ser Géologique, 25: 161–169
- Mutti E, Tinterri R, Remacha E, Mavilla N, Angella S, Fava L (1999) An introduction to the analysis of ancient turbidite basins from an outcrop perspective. *AAPG Continuing Education Course Note Series*. 39, Tulsa, OK, United States. pp 1-61
- Mutti E, Ricci Lucci F (1972) Le torbiditi dell'Apennino settentrionale: introduzione all'analisi di facies. *Mem. Soc. Geol. Italy* 11: 161-99
- Mutti E, Normark WR (1987) Comparing examples of modern and ancient turbidite systems; problems and concepts. In: Legget JK, Zuffa GG (eds). *Marine clastic sedimentology; concepts and case studies*, Graham and Trotman. London, pp 1-38
- Nemčok M (1993) Transition from convergence to escape: field evidence from the West Carpathians. *Tectonophysics* 217: 117-142
- Orlický O (1996) Paleomagnetism of neovolcanics of the East-Slovak Lowlands and Zemplínske Vrchy Mts: A study of the tectonics applying the paleomagnetic data (Western Carpathians). *Geologica Carpathica* 47/1, 12-20
- Pamic J (2000) Basic geological features of the Dinarides and South Tisia. In: Pancardi 2000 Fieldtrip Guidebook (eds. Pamic, J. and Tomljeenovic, B.). *Vijesti* 37/2: 9-18
- Pamic J (2000) Basic geological features of the Dinarides and South Tisia. In: Pancardi 2000 Fieldtrip Guidebook (eds. Pamic, J. and Tomljeenovic, B.). *Vijesti* 37/2: 9-18
- Panaiotu C (1998) Paleomagnetic constraints on the geodynamic history of Romania. In: *Monograph of Southern Carpathians* (edited by Ioane, D.). *Reports on Geodesy* 7: 205-216
- Panaiotu C (1999) Paleomagnetic studies in Romania; Tectonophysics implications (in Romanian). PhD thesis University of Bucharest, 265 pp
- Pătrăscu S (1993) Paleomagnetic study of some Neogene magmatic rocks from the Oas – Ignis – Varatec – Tibles Mountains (Romania). *Geophys. J. Int.* 113, 215-224.
- Pătrăscu S, Panaiotu C, Seclaman M., Panaiotu CE (1994): Timing of rotational motion of Apuseni Mountains (Romania): paleomagnetic data from Tertiary magmatic rocks. *Tectonophysics* 233: 163-176
- Pécskay Z, Edelstein O, Kovacs M, Bernád A, Crihan M (1994) K/Ar age determination of Neogene volcanic rocks from the Gutai Mts. (Eastern Carpathians, Romania). *Geol Carp* 45(6): 357-363
- Pécskay Z, Edelstein O, Seghedi I, Szakács A, Kovacs M, Crihan M, Bernád A (1995) K-Ar datings of Neogene-Quaternary calc-alkaline volcanic rocks in Romania. In: Downes H, Vaselli O (eds). *Neogene and related magmatism in the Carpatho-Pannonian Region*. *Acta Vulcanologica* 7: 53-61
- Pettijohn FJ, Potter PE, Siever R (1987) *Sand and Sandstone*. Springer-Verlag, New York, pp 1-533pp
- Pickering KT, Hiscott RN, Hein FJ (1989) *Deep Marine Environments*. Unwin Hyman. London, United Kingdom. pp 1-416
- Pickering KT, Clark JD, Smith RDA, Hiscott RN, Ricci Lucci F, Kenyon NH (1995) Architectural element analysis of turbidite systems, and selected topical problems for sand-prone deep-water systems. In: Pickering KT, Hiscott RN, Kenyon NH, Ricci Lucci F, Smith RDA (eds). *Atlas of deep water environments – Architectural style in turbidite systems*. Chapman and Hall, London, pp 1-10

- Plasienska D, Grecula P, Mutis M, Kováč M, Hovorca D (1997a) Evolution and structure of the Western Carpathians: an overview. In: (Grecula, P. et al. eds) Geological Evolution of the Western Carpathians. Mineralia Slovaca Monograph, Bratislava, pp 1-24
- Plasienska D, Putis M, Kováč M, Sefara J, Hrussecky I (1997b) Zones of Alpidic subduction and crustal underthrusting in the Western Carpathians. In: (Grecula, P. et al. eds) Geological Evolution of the Western Carpathians, Mineralia Slovaca Monograph, Bratislava, pp 35-42
- Pfiffner OA, Burkhard M (1987) Determination of paleo-stress axes orientations from fault, twin and earthquake data. *Annales Tectonicae* 1(1): 48-57
- Popescu BM (1984): Lithostratigraphy of cyclic continental to marine Eocene deposits in NW Transylvania, Romania. In: Popescu BM (ed) The Transylvanian Paleogene Basin. Geneva, pp37-73
- Ratschbacher L, Merle O, Davy P, Cobbold P (1991a) Lateral extrusion in the Eastern Alps; Part 1, Boundary conditions and experiments scaled for gravity. *Tectonics* 10(2): 245– 256
- Ratschbacher L, Frisch W, Linzer HG, Merle O, (1991b) Lateral extrusion in the Eastern Alps; Part 2, Structural analysis. *Tectonics* 10(2): 257– 271
- Ratschbacher L, Linzer HG, Moser F (1993) Cretaceous to Miocene thrusting and wrenching along the Central South Carpathians due to a corner effect during collision and orocline formation. *Tectonics* 12: 855-873
- Rögel, F (1999): Mediterranean and Paratethys. Facts and Hypotheses of an Oligocene to Miocene Paleogeography (Short Overview). *Geologica Carpathica* 50(4): 339-349
- Royden LH (1988) Late Cenozoic Tectonics of the Pannonian Basin System In: Royden LH, Horváth F (eds). The Pannonian Basin; a study in basin evolution. AAPG Mem 45: 27-48
- Rusu A, Balintoni I, Bombita G, Popescu G (1983) Geological Map 1:50.000 No 18c Preluca, Institutul de Geologie si Geofizica, Bucharest
- Rusu A (1989) Problems of correlation and nomenclature concerning the Oligocene formations in NW Transylvania. In: Petrescu (ed) The Oligocene from the Transylvanian basin, Romania. Cluj-Napoca, pp112-147.
- Sanders C (1998) Tectonics and erosion: competitive forces in a compressive orogen. A fission track study of the Romanian Carpathians. Ph.D. thesis, Vrije Universiteit Amsterdam, Amsterdam, pp 1-204
- Săndulescu M (1980) Sur certain problèmes de la corrélation des Carpathes orientales Roumaines avec les Carpathes Ukrainiennes. *D. S. Inst geol geofiz* LXV(5): 163-180
- Săndulescu M, (1984) *Geotectonica Romaniei*. Editura Tehnica, Bucharest, pp1 – 450
- Săndulescu M (1994) Overview of Romanian Geology. In: ALCAPA II field guide book. *Romanian J of Tectonics and Reg Geol*, 75 suppl. 2: 3-15
- Săndulescu M, Micu M (1989) Oligocene Paleography of the east Carpathians. In: The Oligocene from the Transylvanian Basin. Cluj-Napoca, pp 79-86
- Săndulescu M, Kräutner H, Borcos M, Năstăseanu S, Patrulius D, Ștefănescu M, Ghenea C, Lupu M, Savu H, Bercia I, Marinescu F (1978) Geological map of Romania 1:1.000.000. *Inst. Geol. Rom.*, Bucharest

- Săndulescu M, Krätner HG, Balintoni I, Russo-Săndulescu D, Micu M (1981): The Structure of the East Carpathians. (Guide Book B1), Carp-Balk Geol Assoc 12th Congress, Bucharest, pp 1-92
- Săndulescu M, Szasz L, Balintoni I, Russo-Săndulescu D, Badescu D (1991): Geological Map 1:50.000 No 8d Viseu. Institutul de Geologie si Geofizica, Bucharest.
- Săndulescu M, Visarion M, Stanica D, Stanica M, Atanasiu L (1993) Deep Structure of the inner Carpathians in the Maramures-Tisa zone (East Carpathians). Rom J Geophysics 16: 67-76
- Santavy, Vozár J (1999) Electronical Atlas of Deep Reflection Seismic Profiles of the Western Carpathians. CD ROM, GUDS Bratislava ISBN 80-88974-06-2
- Schmid SM, Froitzheim N (1993) Oblique slip and block rotation along the Engadine line. *Eclogae Geologicae Helveticae*. 86; 2:569-593
- Schmid SM, Berza T, Diaconescu V, Froitzheim N, Fügenschuh B (1998) Orogen-parallel extension in the South Carpathians. *Tectonophysics* 297: 209-228
- Schmid SM, Fügenschuh B, Kissling E; Schuster R (2004a) Tectonic map and overall architecture of the Alpine orogen. *Eclogae geologicae Helveticae* 97: 93-117
- Schmid SM, Fügenschuh B, Kissling E; Schuster R (2004b) TRANSMED Transects IV, V and VI: Three lithospheric transects across the Alps and their forelands. In: Cavazza W, Roure FM, Spakman W, Stampfli GM, Ziegler PA (eds). The TRANSMED Atlas: The Mediterranean Region from Crust to Mantle. Springer, Berlin Heidelberg, attached CD (version of the explanatory text available from the first author as a pdf-file upon request)
- Shanmugan G, Moiola RJ (1988) Submarine fans; characteristics, models, classification, and reservoir potential. *Earth Science Reviews*. 24; 6: 383-428
- Soták J, Rudinec R, Spišiak J (1993) The Penninic «pull-apart» dome in the pre-Neogene basement of the Transcarpathian depression (Eastern Slovakia). *Geol. Carpath.* 44/1: 11-16
- Soták J, Spišiak J, Biron A (1994) Metamorphic sequences with Bündnerschiefer lithology in the pre-Neogene basement of the East Slovakian Basin. *Mitt. Österr. Geol. Ges.* 86: 111-120
- Soták J, Biron A, Prokesova R, Spišiak J (2000) Detachment control of core complex exhumation and back-arc extension in the East Slovakian Basin. In: Environmental, structural and stratigraphical evolution of the Western Carpathians (edited by Kováč, M., Vozár, J., Vozárová, A., Michalik, J.). Slovak Geological Magazine (Geological Survey of Slovak Republic. Bratislava, Slovak Republic) 6: 130-132
- Sperner B, Ratschbacher L, Nemčok M (2002) Interplay between subduction retreat and lateral extrusion: tectonics of the Western Carpathians. *Tectonics* 21(6): 1051
- Sperner B, CRC 461 Team (2005) Monitoring of Slab Detachment in the Carpathians. In: Wenzel F (ed). *Perspectives in modern Seismology. Lecture Notes in Earth Sciences* 105: 187-202
- Stampfli GM, Borel G (2004) The TRANSMED transects in space and time: constraints on the paleotectonic evolution of the Mediterranean domain. In: Cavazza W, Roure FM, Spakman W, Stampfli GM, Ziegler PA (eds). The TRANSMED Atlas: The Mediterranean Region from Crust to Mantle. Springer, Berlin and Heidelberg, pp 53-80

- Steiniger FF, Wessely G (2000) From the Thethyan Ocean to the Paratethys Sea: Oligocene to Neogene Stratigraphy, Paleogeography and Paleobiogeography of the circum-Mediterranean region and the Oligocene to Neogene Basin evolution in Austria. *Mitt Österr Geol Ges* 92: 95-116
- Szakács A, Vlad D, Andriessen PAM, Fülöp A, Pécskay Z (2000) Eruption of the «Dej tuff», Transylvanian Basin: when, where and how many. *Vijesti Hrvatskoga geološkog društva, PANCARDI 2000-Special issue, Abstract volume 37/3*, 122.
- Széky-Fux V, Pécskay Z (1991) Covered Neogene volcanic rocks at the eastern and northern areas of the Pannonian basin, Hungary. In: *Geodynamic evolution of the Pannonian basin* (edited by S. Karamata). *Serb. Acad. Sci. Arts, Acad. Conf. 62, Dept. Nat. Math. Sci. 4*, Belgrade: 275-287pp
- Tischler M, Gröger HR, Fügenschuh B, Schmid SM (2006) Miocene tectonics of the Maramures area (Northern Romania) – implications for the Mid-Hungarian fault zone. *Int. J. Earth Sciences*
- Tucker ME (1981) *Sedimentary Petrology: An Introduction to the Origin of Sedimentary Rocks*. Blackwell Sci Publ Oxford, pp 1-260
- Túnyi I, Márton E, Žec B, Vass D (2005) Paleomagnetism of Neovolcanics of the Vihorlatské vrchy Mts. *Mineralia Slovaca* 37, 268-271
- Van der Voo R (1993) *Paleomagnetism of the Atlantic, Tethys and Iapetus Oceans*. Cambridge University Press, Cambridge
- Wissing, F.N, Herrig, E. (1999): *Arbeitsmethoden der Mikropaläontologie: Eine Einführung*. Enke-Verlag Stuttgart, pp 1-191
- Wortel MJR, Spakman W (2000) Subduction and slab detachment in the Mediterranean-Carpathian region. *Science* 290: 1910-1917

Personal Details

Name: Matthias Tischler
Address: Metzgerstr. 35
CH-4056 Basel
Switzerland
Tel.: +41 – (0)61 321 77 26
e-mail: m.tischler@unibas.ch
Date of Birth: 13.08.1974
Marital status: single
Citizenship: german



Recent occupations

- August 2005 - April 2006 Post-Doctoral position:
SNF-Project “Tectono-metamorphic studies in the Alps”
- Geological mapping in the central Alps, northern Italy
 - Structural fieldwork to solve a long-standing structural problem in the Penninic nappes
- May 2001 - April 2005 Assistant at the Geological Institute Basel:
- Assisting during various undergraduate-level courses (structural geology, construction of sections, introduction to ArcGIS)
 - Assisting during excursions in the Alps in 2002 and 2003
 - Maintenance of the institute-internal computer network
 - User support for network and software issues

School and Studies

- May 2001 - June 2005 PhD in Geology (University of Basel, Switzerland)
“A combined structural and sedimentological study of the Inner Carpathians at the northern rim of the Transylvanian basin (N. Romania)”
Supervisors: Prof. S.M. Schmid, Prof. B.Fügenschuh, Prof. A.Wetzel
Degree: Dr. phil.nat. (summa cum laude)
- Structural geology: field work, analysis of mesoscale structures focusing on brittle deformation (Paleostress analysis)
 - Tectonics: mapping and construction of cross sections to unravel the tectonic history (nappe emplacement of fisch nappes and later brittle deformation)
 - Sedimentology: field work, turbidite facies, paleocurrent and provenance studies integrated with seismic data for basin reconstruction.
 - Integration with paleomagnetic data acquired with collaboration partners into a palinspastic restoration of the study area

School and Studies (continued)

- 1994 - February 2001 Studying geology in Giessen, Clausthal and Göttingen (Germany):
Diploma thesis: "K/Ar- und Sm/Nd- Datierungen zur Liefergebietsanalyse varistischer Einheiten in Sachsen".
 Supervisors: Prof. B. Hansen, Dr. H.Ahrendt, Dr. K.Wemmer.
Diploma mapping: „Kartierbericht zur geologischen Karte der Windy-Pass Region im Cascades Crystalline Core, Washington, USA“.
 Supervisors: Prof. K.Weber, Dr. B. Leiss, Dr. H.Lebit.
 Degree: Diplom-Geologe (very good)
- 1993 – 1994 Community service (alternative to military service: care for handicapped persons)
- 1993 Abitur (Liebigsschule Giessen, Germany)

Further fields of experience

- 1998 - 2001 Lab assistant (Radiometric dating group / Göttingen University):
- Mass spectrometry: good knowledge of measuring procedures
 - sample preparation (K/Ar-dating; Illite crystallinity)
- 2000 (four weeks) Internship at GEG Göttingen (GIS-services):
- Creation and layout of maps
 - Creation of a user-manual for the GIS-Software TOPOL

Field work

- 2005 Mapping in the Penninic nappes of the central Alps northern Italy (6Weeks).
- 2001 - 2004 Structural and sedimentological field-work in northern Romania (2,5 months per season).
- 1998 Mapping and structural field-work in the Cascades Crystalline Core, Washington USA (6 Weeks).
- 2006 - 1994 Excursions in Germany, Spain, Italy, Austria, Switzerland, Poland, Sweden.

Computer skills

Very good general computer skills, fast learner regarding new applications, basic hardware and network knowledge.

- Operating platforms:
- Microsoft Windows family
- Applications:
- Microsoft Office package
 - Adobe Photoshop, Illustrator, InDesign
 - CorelDraw, Photo-Paint
 - Sundry applications for processing and visualizing geological data
- GIS:
- Firm knowledge and long experience with GIS applications
- ArcGIS - package, MapInfo, TOPOL

Miscellaneous

- Languages German (native speaker)
English (good written and spoken skills)
- Driving licence yes